ucc

Coláiste na hOllscoile Corcaigh, Éire
University College Cork, Ireland

Acute Hypoxia-Induced Diaphragm Dysfunction is Prevented by Antioxidant Pre-Treatment

Andrew James O'Leary, ***BSc (Hons)***
Department of Physiology

Thesis submitted to ***National University of Ireland, University College Cork*** *for the award of* ***Doctor of Philosophy***

Under the supervision of:

Professor Ken D. O'Halloran (Head of Department)

December 2016

Table of Contents

Declaration

I declare that this thesis is not under consideration for other qualifications in University College Cork or elsewhere, and that the work contained within is original and my own.

Sign: _____ Date: _____

Andrew O'Leary

December 2016

List of Figures

Chapter 1: Introduction

Chapter 2: Materials & Methods

Chapter 3: Acute Hypoxia Induces Respiratory Muscle Dysfunction in Mice and Rats

Chapter 5: N-acetylcysteine Ameliorates Acute Hypoxia-Induced Diaphragm Dysfunction

Chapter 6: Summary & Conclusions

List of Tables

Chapter 2: Materials & Methods

List of Abbreviations

Akt	protein kinase B
ALI	acute lung injury
AMC	7-amino-4-methylcoumarin
ANOVA	analysis of variance
AP-1	activating protein-1
AP	action potential
ARDS	acute respiratory distress syndrome
ATP	adenosine triphosphate
BCA	bicinchoninic acid
BNIP3	BCL2 interacting protein 3
Bpm	breaths per minute
Ca^{2+}	calcium
CDF	critical diaphragm failure
cDNA	complementary DNA
CHF	chronic heart failure
CIH	chronic intermittent hypoxia
CO_2	carbon dioxide
COPD	chronic obstructive pulmonary disease
Cq	quantification cycle
CREB	cyclic AMP-response element-binding protein
CSA	cross sectional area
DHPR	dihydropyridine receptor
DTT	dithiothreitol
ECC	excitation-contraction coupling
EDL	extensor digitorum longus
Egr-1	early growth response-1
Em	emission
ERK1/2	extracellular signal-regulated kinase 1/2
ETC	electron transport chain
Ex	excitation
F_iO_2	fraction of inspired oxygen

F_{max}	peak specific force
FoxO	forkhead box class O
GABARAPL3	GABA(A) receptor-associated protein-like 3
GSH	glutathione
GSK-3	glycogen synthesis kinase 3
H_2O	water
H_2O_2	hydrogen peroxide
Hgb	haemoglobin
HIDD	hypoxia-induced diaphragm dysfunction
HIF	hypoxia inducible factor
HPRT1	hypoxanthine phosphoribosyltransferase 1
HRC	histidine-rich calcium binding protein
HRE	hypoxia response element
HRM or hypoximir	hypoxia-regulated miRNA
HVR	hypoxic ventilatory response
Hz	hertz
ICU	intensive care unit
ICUAW	intensive care unit acquired weakness
I.P.	intraperitoneal
ITPR	inositol 1,4,5-trisphosphate receptor
JNK	c-Jun N-terminal kinase
KCl	potassium chloride
LC3B	microtubule-associated protein 1A/1B-light chain 3
L/L_o	length of shortening per optimal length
L_o	optimum length
L_o/s	optimum length per second
MAP	mitogen-activated protein
MAPK	mitogen-activated protein kinase
MEK1/2	mitogen-activated protein kinase kinase 1/2
$MgSO_4$	magnesium sulfate
MHC	myosin heavy chain
miRNA	microRNA
MKK3/6	mitogen-activated protein kinase kinase 3/6

MKK4/7	mitogen-activated protein kinase kinase 4/7
MnSOD	manganese superoxide dismutase
mRNA	messenger RNA
mTOR	mammalian target of rapamycin
MuRF1	muscle RING-finger 1
N_2	nitrogen
NAC	N-acetylcysteine
NaCl	sodium chloride
NaH_2PO_4	monosodium phosphate
NaOH	sodium hydroxide
NF-IL6	nuclear factor for interleukin 6
NF-κB	nuclear factor κB
NO	nitric oxide
NRF	nuclear respiratory factor
O_2	oxygen
$\cdot O_2^-$	superoxide anions
$\cdot OH$	hydroxyl radicals
OCT	optimal cutting temperature compound
OSA	obstructive sleep apnoea
PaO_2	partial pressure of oxygen in arterial blood
PBS	phosphate buffer saline
PGC	peroxisome proliferator-activated receptor gamma coactivator
PI-3	phosphor-ionositol-3
PiO_2	partial pressure of inspired oxygen
P_{max}	peak specific mechanical power
PO_2	partial pressure of oxygen
PPARα	peroxisome proliferator-activated receptor α
p38	p38 MAP kinase
p70S6K	70 kDa ribosomal protein S6 kinase
RER	respiratory exchange ratio
RIPA	radio-immunoprecipitation assay
ROS	reactive oxygen species
RyR	ryanodine receptor

SaO_2	oxygen saturation of haemoglobin
SD	standard deviation
SDB	sleep disordered breathing
SEM	standard error mean
SEPN1	selenoprotein N 1
SERCA	sarco/endoplasmic reticulum Ca^{2+}-ATPase pump
SIDS	sudden infant death syndrome
S_{max}	peak specific shortening
SOD	superoxide dismutase
SR	sarcoplasmic reticulum
S6RP	ribosomal protein S6
TTP	time to peak
T_{50}	half relaxation time
UCP-3	mitochondrial uncoupling protein – 3
VALI	ventilator associated lung injury
VCO_2	carbon dioxide production
VE/VCO_2	carbon dioxide ventilatory equivalent ratio
VE/VO_2	oxygen ventilatory equivalent ratio
VIDD	ventilator-induced diaphragmatic dysfunction
VILI	ventilator induced lung injury
V_{max}	peak specific shortening velocity
VO_2	oxygen consumption
W_{max}	peak specific mechanical work

Publications and Conference Proceedings

Diaphragm muscle weakness and increased UCP-3 gene expression following acute hypoxic stress in the mouse.
O'Leary AJ, O'Halloran KD.
Respiratory Physiology & Neurobiology, 2016;226:76-80.

Acute hypoxic stress causes diaphragm muscle weakness in mice and rats.
O'Leary AJ, Rieux C, Browne L, O'Halloran KD.
The Physiological Society, 2016 – Proceedings from Physiology 2016 (Dublin, Ire)

An Acute Sustained Hypoxic Stress is Sufficient to Cause Respiratory Muscle Weakness in the Mouse.
O'Leary AJ, O'Halloran KD.
The FASEB Journal, 2016 – Conference proceedings from Experimental Biology 2016 meeting in San Diego

Respiratory muscle remodelling following acute sustained hypoxic stress in the mouse.
O'Leary AJ, O'Halloran KD.
The Physiological Society, 2015 – Proceedings from Physiology 2015 (Cardiff, UK)

Respiratory muscle weakness following acute sustained hypoxic stress in the mouse.
O'Leary AJ, O'Halloran KD.
International Hypoxia Symposium (Lake Louise, Canada), 2015 – Conference Publication

Differential sarcoplasmic reticulum gene expression in mouse respiratory and limb muscle following exposure to acute sustained hypoxia.
O'Leary AJ, O'Halloran KD.
Oxford Conference on the Control of Breathing (Sydney, Australia), 2014 – Conference preceedings

Transcriptional responses of the mouse diaphragm to acute sustained hypoxic stress.

O'Leary AJ, O'Halloran KD.

Royal Academy of Medicine in Ireland Section of Biomedical Sciences Annual Meeting, 2014 – Conference Publication

Presentations

Physiology 2016, Convention Centre, Dublin, Ireland. (2016)

Hypoxia Research Symposium, University College Cork, Cork, Ireland. (2016)

Royal Academy of Medicine in Ireland (RAMI) Biomedical Sciences Meeting, Cork, Ireland. (2016)

Experimental Biology 2016, San Diego Convention Center, San Diego, CA, USA. (2016)

Irish Thoracic Society Scientific Meeting, Cork, Ireland. (2015)

Royal Academy of Medicine in Ireland (RAMI) Biomedical Sciences Meeting, Dublin, Ireland. (2015)

Physiology 2015, Motorpoint Arena, Cardiff, UK. (2015)

International Hypoxia Symposium, Chateau Lake Louise, Alberta, Canada. (2015)

Hypoxia Research Symposium, University of Calgary, Alberta, Canada. (2015)

Oxford Control of Breathing Meeting, Sydney, Australia. (2014)

43rd European Muscle Conference, Salzburg, Austria. (2014)

Royal Academy of Medicine in Ireland (RAMI) Biomedical Sciences Meeting, Dublin, Ireland. (2014)

Manuscripts in Preparation

Acute Hypoxia-Induced Diaphragm Dysfunction is Prevented by Antioxidant Pre-Treatment in the Mouse.
Research article to be submitted to Oxidative Medicine and Cellular Longevity (Special Issue: Oxidative Stress in Muscle Diseases: Current and Future Therapy).

Acute Hypoxia is Sufficient to Cause Sternohyoid Muscle Dysfunction in the Mouse.
Research article to be submitted to Respiratory Physiology & Neurobiology.

Hypoxia Induced Diaphragm Dysfunction: Is oxygen deficiency a HIDDen cost in the ICU?
Review article.

Acknowledgements

First and foremost, I'd like to thank my PhD supervisor Prof. Ken O'Halloran, for the opportunity to take on this project under your tutelage; for providing me with constant training and guidance throughout the course of my scientific training and professional development; for all the enthusiastic chats, advice and ideas, whether over a coffee or a beer, from Manly beach in Sydney to downtown San Diego, from high in the Canadian Rockies to low in the Bagel Box by UCC; and for the many opportunities to present this research all over the world (or "carrots" as it were!). I feel very fortunate to call you a supervisor, a mentor and a friend.

To my fellow postgraduates in the Department of Physiology, UCC, I'd like to thank you for your friendship, camaraderie and support. From the litres of coffee and kilos of burritos we've consumed together to playing footie and tag rugby, frisbee in the park and surfing in west cork, and of course the ridiculous array of music genres we've listened to in the lab! I am very glad and privileged to have worked alongside you all. Shout out to the A-team! #vinowiththegirlos

I'd like to say a special thank you to all of the academic, technical and administrative staff in the Department of Physiology and the BSU for your assistance in, and contributions to, my PhD training and this research project.

To my friends outside of science, I'd like to thank you all for helping me to maintain perspective, and for ensuring I was always able to take my mind off of my research, get away from the lab and reset when needed.

Finally, to my family I would like to say a massive thank you for your unrelenting patience and support throughout this project. I cannot express how important your support was, and I cannot possibly overstate my gratitude to you all. To my parents, without whom my undertaking of this project would not be possible, I dedicate this thesis to you.

Abstract

Introduction:

Diaphragm weakness is a strong predictor of poor outcome in patients. Acute hypoxia is a feature of respiratory conditions such as acute respiratory distress syndrome and ventilator-associated lung injury. However, the effects of acute hypoxia on the diaphragm are largely unknown despite the potential clinical relevance.

Methods:

C57BL6/J mice were exposed to 8hr of acute hypoxia (F_iO_2 = 0.10) or normoxia. A separate group of mice were administered N-acetyl cysteine (NAC; 200mg/kg, I.P.) immediately prior to acute hypoxia exposure. Ventilation was assessed using whole-body plethysmography. Oxygen consumption and carbon dioxide production were measured as indices of metabolism. Diaphragm muscle contractile performance was determined *ex-vivo*. Gene expression was examined at 1, 4, and 8 hrs using quantitative real-time reverse transcription PCR (qRT-PCR). Protein and phosphoprotein content was assessed using a sandwich immunoassay. Proteasome activity was measured using a spectrophotometric assay.

Results:

Acute hypoxia decreased diaphragm peak force, force-frequency relationship, and fatigue. Minute ventilation during acute hypoxia was initially increased during the first 10 minutes, but quickly returned to normoxic levels for the duration of gas exposure. CO_2 production (VCO_2) throughout gas exposure and *post-mortem* body temperature (metabolism) following gas exposure, were reduced by acute hypoxia, and gene expression driving mitochondrial uncoupling was increased. Acute hypoxia increased atrophic gene expression and signalling protein content. However, proteasome activity was unaffected by acute hypoxia. Acute hypoxia increased hypertrophic and hypoxia protein signalling. NAC pre-treatment prevented the acute hypoxia-induced diaphragm weakness.

Conclusions:

Diaphragm weakness is reported in mechanically ventilated patients, which is primarily attributed to inactivity (unloading) of the muscle, although this is controversial. The potential role of hypoxia in the development and/or exacerbation of ICU-related weakness is unclear and perhaps underestimated. Our data reveals that acute hypoxia is sufficient to cause diaphragm muscle weakness, which may relate to atrophy, as evident from increased pro-atrophy signalling. Muscle weakness likely relates to direct hypoxic stress, as there was no persistent change in ventilation (muscle activity) during hypoxic exposure. Moreover, muscle weakness was prevented by antioxidant supplementation, independent of the hypoxia-induced hypometabolic state. These findings highlight a potentially critical role for hypoxia in diaphragm muscle dysfunction observed in patients with acute respiratory diseases. Moreover, the work highlights the potential benefits of NAC in preventing acute hypoxia-induced diaphragm dysfunction.

Chapter 1: Introduction

1.1 Hypoxia

Hypoxia represents an imbalance between oxygen supply and demand, where the oxygen supply to a tissue is outweighed by the metabolic demand for oxygen in that tissue. This can occur in health, upon exposure to high altitude or during endurance exercise. Hypoxia can also occur in disease, in particular respiratory conditions, and it is a feature of chronic respiratory disease that is known to affect skeletal muscle structure and function (Gamboa and Andrade, 2012, 2010; Lewis et al., 2015c; McMorrow et al., 2011).

The normal partial pressure of oxygen in arterial blood (PaO_2) is in the range of 90-100 mmHg, while a drop in PaO_2 below 60mmHg is considered clinically to be hypoxaemic and can lead to tissue hypoxia due to its effect on the oxyhaemoglobin curve (see below), and this can be seen in patients with respiratory diseases. Remarkably PaO_2 as low as 28mmHg has been reported near the summit of Mount Everest (West et al., 1983), and at the summit of Mount Everest, the highest point on the earth's surface (8848 m), the partial pressure of inspired oxygen (PiO_2) is believed to be very close to the limit that is tolerable to acclimatised humans while maintaining functionality (Grocott et al., 2009). From the oxyhaemoglobin curve, we can deduce that once PaO_2 is above 60mmHg the curve is relatively flat and there is little change in the oxygen saturation of haemoglobin (SaO_2). However, once PaO_2 drops below 60mmHg, the curve becomes very steep such that a small change in PaO_2 can translate into a large change in SaO_2.

Hypoxia can be further subdivided into several distinct types based on the etiology. There are primarily 4 categories. (1) Hypoxic hypoxia occurs when there is inadequate O_2 in the inspired environmental air, decreased O_2 partial pressure (PO_2) in the alveolus or insufficient O_2 transfer from the alveoli to the pulmonary capillaries. Situations of hypoxic hypoxia can arise during ascent to high altitude, hypoventilation, gas diffusion abnormalities at the alveoli, pulmonary shunting or a mismatched ventilation/perfusion ratio. (2) Anaemic hypoxia is a situation where the O_2 carrying capacity of the blood is too low. This can occur due to either a lack of sufficient functional haemoglobin (Hgb), as can occur during hypovolaemia, or poor

Hgb-O_2 binding capacity, as can occur during carbon monoxide poisoning. (3) Stagnant/Ischaemic hypoxia can present when blood O_2 is normal but the perfusion of blood in a tissue is reduced or uneven and is insufficient to meet local metabolic demand. This can arise in several cardiovascular conditions which affect blood flow and/or the microcirculation. (4) Histotoxic/Cytopathic hypoxia occurs when blood supply of O_2 may be normal but cells cannot effectively metabolise this O_2. This type of hypoxia can be occur under conditions of poisoning, such as cyanide poisoning (McLellan and Walsh, 2004; Ward, 2006; Wheeler, 2011), as well as being a feature in sepsis (Berdichevsky et al., 2010; Fink, 2002; Fink, 2001; Fink, 2001b; Schwartz et al., 1998; van boxel et al., 2012). As well as these four main categories, genetic hypoxia can also occur due to mutations in genes involved in the regulation of oxygen homeostasis, such as those involved in the degradation of hypoxia-responsive proteins under normoxic conditions, mitochondrial genetic disease and congenital polycythaemia, and can give rise to dysfunctional oxygen utilisation and homeostasis in cells (Cortopassi et al., 2006; Gordeuk et al., 2004). Demand for hypoxia may also supervene when there is over-utilisation of oxygen within the cells. This condition can present in hyperthyroidism, seizures and cases of severe burn (Ash, 1956; Varney et al., 1998).

Sustained hypoxia causes apparently unique adaptations in the muscles of respiration. There remains however a general paucity of information concerning the molecular mechanisms underpinning respiratory muscle remodelling in hypoxia, including the manifestation and progression of these adaptations over time. Aberrant remodelling, and dysfunction of the respiratory muscles, is known to occur in the respiratory muscles of patients with chronic obstructive pulmonary disease (COPD), and it is thought that this may, at least in part, be due to hypoxic adaptation (Barreiro et al., 2005; McMorrow et al., 2011; Nguyen et al., 2005; Ottenheijm et al., 2008), though this is often under-appreciated in the context of disease-related changes in loading and systemic inflammation. Indeed, many studies have reported similar functional and molecular changes in respiratory and limb muscle in animal models of chronic hypoxia to those seen in COPD patients (Gamboa and Andrade, 2012; Lewis et al., 2016, 2015d, 2014; Lewis and O'Halloran, 2016; McMorrow et al., 2011).

1.1.1 Altitude Hypoxia

Pathophysiological conditions aside, hypoxia also occurs during exposure to high altitude. The first ascent to the summit of Mount Everest was achieved by Hillary and Tenzing in 1953 using supplemental oxygen. It was a further quarter century after their ascent before the summit was reached without supplemental oxygen by Messner and Habeler, and less than 4 % of people who climb Mount Everest do so without supplemental oxygen (Grocott et al., 2009), due to the effects of high altitude hypoxia. High altitude/hypobaric hypoxia is known to affect skeletal muscle, including the diaphragm, and the effects of exercise on the diaphragm differ when performed at high altitude or at sea level (Bigard et al., 1992; Levett et al., 2012).

The first written report of high altitude effects on humans was documented in 37-32 B.C., when Chinese official Too Kin wrote of Big Headache Mountain, where he experienced mountain sickness while travelling over the western edge of the Himalayan Karakoram Range, while travelling from Kashi to Kabul (Gilbert, 1983).
Later, in a record breaking attempt in 1875, three French balloonists ascended from Paris in the Zenith balloon to around 8,500 meters. They failed to breathe from bags containing 65% oxygen, which they had brought with them under the advice of French physiologist Paul Bert, due to a feeling of intense hypoxia-induced euphoria before losing consciousness. Two of the men died. The third man, M. Gaston Tissandier, although in a delirium, was able to start a descent and lived to tell the tale. In the same year, Bert published La Pression Barometrique, in which he included the story of the Zenith tragedy and proposed that the reduced partial pressure of oxygen in the air, and thus in the blood, was a vitally important effect of altitude on humans. This sparked the beginning of our understanding of altitude (patho)physiological and respiratory science (Severinghaus, 2016).

1.2 Skeletal Muscle

Skeletal muscle mass alone accounts for 40 – 50 % of total human body weight, making it the largest tissue mass in the body (Sanchez et al., 2014). This combined skeletal muscle mass consumes roughly 20% of available oxygen in the body under

normal resting conditions, and this percentage increases under exercise conditions. Skeletal muscle is a syncytium, and has a variety of roles in the human body such as movement of the skeleton, posture, speech, respiration, and aiding in blood circulation. The motor unit is the functional unit of the skeletal muscle system, and is comprised of a motor neuron and the bundle of muscle fibres which it innervates, which all have similar, if not identical, structural and functional properties (Schiaffino and Reggiani, 2011). Many distinct motor units are assembled together to form a muscle, and selective recruitment of units allows appropriate muscle response to a given functional demand (Schiaffino and Reggiani, 2011). The motor nerve branches in the muscle, with each branch innervating a single muscle fibre. One nerve innervates only a few muscle fibres where fine control is involved, such as the muscles of the eye, whereas in large, strong muscles, such as those involved in posture, hundreds of fibres are innervated per nerve.

1.2.1 Respiratory Muscle

The act of breathing depends on the coordinated activity of many respiratory muscles. The striated muscles involved in breathing are made up of skeletal muscle tissue and can be broadly categorised into two classes; (1) ventilatory pump muscles (the diaphragm being the primary inspiratory pump muscle) and (2) those muscles that modulate upper airway patency and calibre (the sternohyoid muscles are important upper airway dilator muscles). The diaphragm has a mixed muscle fibre type composition (22% type 1, 24% type 2a, 19% type 2b and 28% type 2x), comprising all fibre types grouped together into motor units of common muscle type (McMorrow et al., 2011; Rowley et al., 2005). The sternohyoid muscles are fast glycolytic muscles (77% type 2b) and as such they are very fatigable, which has implications for the control of airway patency (O'Halloran, 2016; O 'Halloran et al., 2016). Respiratory muscles face unique physiological demands due to the continuous rhythmic activity of breathing, making them among the most active skeletal muscles in the human body. Many of these muscles also participate in a variety of other (non-respiratory) functions including swallowing, sneezing, coughing and phonation (Rowley et al., 2005).

1.2.1.1 Sternohyoid Muscles

The upper airway is surrounded by a complex anatomical arrangement of skeletal muscle and soft tissue, allowing the necessary dynamic changes in airway size for varying respiratory patterns as well as a variety of non-respiratory functions such as swallowing, phonation, etc., mentioned above. There are 20 or more upper airway muscles surrounding the airway that play active roles in constriction and dilation of the airway lumen (Ayappa and Rapoport, 2003). The sternohyoid is a primary upper airway dilator muscle involved in maintaining the calibre and patency of the upper airway. It is made up primarily of fast glycolytic type 2b muscle fibres. The sternohyoid muscle is an excellent representative upper airway dilator muscle and one which has been the focus of much of the research into upper airway muscle physiology (Bavis et al., 2007; Bradford et al., 2005; Carberry et al., 2014a; El-Khoury et al., 2012, 2003; Gamboa and Andrade, 2012; Lewis et al., 2015c; McGuire et al., 2002; O'Halloran et al., 2003, 2002, Skelly et al., 2012a, 2012b, 2011, 2010; van Lunteren et al., 2010; Williams et al., 2015).

1.2.1.2 The Diaphragm

The diaphragm is the primary pump muscle of inspiration and, as such, it is active throughout life – due to breathing as well as other activities such as airway clearance manoeuvres and speech. Thus, normal function of the diaphragm muscle, much like that of the heart muscle, is essential to life. The diaphragm is an extremely adaptable and malleable muscle, comprised of a mixed muscle fibre type composition, containing the four major myosin isoform subtypes (McMorrow et al., 2011). This mixed muscle fibre type composition is fundamental to the balance between force generating capacity and endurance necessary for normal diaphragm function.

During quiet breathing, the diaphragm is the primary muscle of respiration. During inspiration the diaphragm contracts and moves downward, lowering pleural pressure, which lowers alveolar pressure, and air is drawn into the expanding lungs. Meanwhile, expiration during quiet breathing is predominantly a passive mechanical process. The diaphragm relaxes and returns to resting position, restoring the thoracic cavity to pre-inspiratory volume, and the elastic lungs return passively to resting volume (functional residual capacity). During exercise or forced/active respiration, many other muscles are involved. During active inspiration, the external intercostal

muscles raise the lower ribs up and out, and the scalene muscles and sternomastoids are recruited, raising and pushing out the upper ribs and sternum. During active expiration, the most important respiratory muscles are those of the abdominal wall, including the rectus abdominus, internal and external obliques, and transverse abdominus, raising intra-abdominal pressure and pushing up the diaphragm, raising pleural pressure and driving air out of the lungs. The internal intercostal muscles also play a role in active expiration, pulling the ribs down and in, decreasing thoracic volume.

The effects of hypoxia on the diaphragm are poorly understood, despite the clinical relevance of such an understanding. Indeed, hypoxia is a feature of many respiratory-related disorders, both acute and chronic. Our laboratory group, and others, have examined some of the effects of chronic hypoxia exposure on the respiratory muscles (Carberry et al., 2014a; Chaudhary et al., 2012; El-Khoury et al., 2012, 2003, Gamboa and Andrade, 2012, 2010, Lewis et al., 2015a, 2015c; McMorrow et al., 2011; Shortt et al., 2014; Skelly et al., 2012a, 2012b), with relevance to certain chronic respiratory conditions in which hypoxia features, such as chronic heart failure (CHF),chronic obstructive pulmonary disease (COPD) and bronchopulmonary dysplasia (Gosker et al., 2000; Testelmans et al., 2010). Indeed hypoxia may also play a prominent role in early life disorders such as sudden infant death syndrome (SIDS), where critical diaphragm failure (CDF) is a postulated cause of SIDS, and early life exposures to hypoxia can have long lasting developmental effects on respiratory muscle (Carberry et al., 2014a; Neary and Breckenridge, 2013; Siren, 2016; Siren and Siren, 2011). Acute hypoxia features in many acute respiratory conditions such as acute lung injury (ALI), ventilator-induced/associated lung injury (VILI/VALI) and hypoxaemic respiratory failure or acute respiratory distress syndrome (ARDS). However, very little to nothing is currently known about the effects of acute hypoxia on the respiratory muscles, and this knowledge gap is one which needs to be addressed, given its clinical relevance.

1.2.2 Hind-limb Muscles

Two muscles of the hind-limb, namely the extensor digitorum longus (EDL) and the soleus muscles, are useful muscles to use as comparators to the respiratory muscles,

the diaphragm and sternohyoid muscles, when aiming to assess whether certain induced effects are respiratory muscle specific or global in skeletal muscle. Both of these muscles have very different functions and fibre type make-ups. The EDL is a fast, powerful, glycolytic muscle (76% type 2b) which lies along the anterolateral side of the hind-leg, deep to the tibialis anterior, and functions in dorsiflexion of the foot. The soleus, however, is composed of slow, highly endurant, oxidative fibres (96% type 1), and is positioned deep in the gastrocnemius muscle, posterior to the leg, and is employed in the maintenance of posture. These two muscles provide two distinct comparative view-points to respiratory muscle adaptations to hypoxia, which may be linked to muscle activity, fibre type composition, or simply muscle specific responses.

1.3 Acute Hypoxia

As stated previously, a knowledge gap exists concerning whether acute hypoxia is implicated in the pathophysiology of conditions in which it features, and this must be addressed. Acute hypoxia can occur as a result of airway obstruction/occlusion, blockage of the alveoli by pulmonary oedema or infectious exudate, or acute haemorrhage (Chapman et al., 1989; Cook and Macdougall-Davis, 2012; Gutierrez et al., 2004; Safar, 1969; Schaible et al., 2010). Acute hypoxia also features in many (acute) respiratory-related disorders, which shall be discussed in greater detail in the next section (1.4 Clinical Relevance). At present, while much work has been conducted in the area of skeletal muscle adaptations to chronic sustained hypoxia, very little is known about the early/acute adaptations of skeletal muscle, including the respiratory and upper airway muscles, to sustained hypoxia (Lundby et al., 2009). This is particularly true in the time frame of a number of hours in humans and animal models. However, it has been reported that mechanisms of gene expression regulation are distinct in acute and chronic exposure to hypoxia and that the cellular response to acute hypoxia is dynamic over time (Koritzinsky et al., 2006). Understanding the temporal effects of hypoxia over both the short- and long-term is essential to understanding the pathophysiological progression of respiratory-related disorders in which hypoxia features. It is also essential to understand how quickly maladaptations

to hypoxia can arise in order to intervene with therapeutic strategies in a timely manner. However, knowledge in this area is currently lacking and underexplored.

Modulation of metabolism attributed to chronic hypoxia has also been reported in skeletal muscle (Hoppeler et al., 2003; Levett et al., 2012; Palma and Ripamonti, 2007), and alterations in mitochondrial content and distribution specific to the diaphragm have been seen in chronic hypoxia (Gamboa and Andrade, 2010). While little work in this area has focused on the acute metabolic or mitochondrial response to hypoxia, mitochondrial UCP-3 messenger RNA (mRNA) and protein expression were found to be increased in rat skeletal muscle after only 30 minutes of hypoxia (Zhou et al., 2000), demonstrating the potential for acute hypoxia to alter skeletal muscle mitochondrial programming in a relatively short period of time, which may have functional outcomes in terms of muscle performance. This evidence further bolsters the argument that there is a need to explore hypoxic effects on the diaphragm within an acute timeframe.

Chronic hypoxia generally leads to a negative regulation of protein balance and an overall loss in skeletal muscle mass, or atrophy (Deldicque and Francaux, 2013), likely contributing to chronic hypoxia induced muscle weakness, while acute hypoxia has been reported to have a positive effect on human skeletal muscle protein balance (D'Hulst et al., 2013), although this area is, as of yet, largely under studied and under explored. This is further evidence of how the effects of hypoxia on skeletal muscle can differ based on the temporal profile of exposure, and how it cannot necessarily be inferred that hypoxia has a defined set of effects on skeletal muscle no matter the length of exposure. Rather, it is emerging to be a dynamic process, which warrants further exploration, particularly in acute timeframes where information is most scarce and the potential role of hypoxia is understated.

1.4 Clinical Relevance

1.4.1 Acute Respiratory-Related Disorders

The effects of acute hypoxia on diaphragm form and function are largely unknown despite the fact that hypoxia is a prominent feature of many respiratory conditions, and while some inroads have been made regarding hypoxia's role in diaphragm dysfunction under chronic conditions, its role in acute respiratory-related disorders is as of yet unexamined. Two acute respiratory conditions often encountered in the intensive care unit (ICU), and in which acute hypoxia features, are VILI and ARDS. These two pathophysiological conditions can give rise to a recognised phenomenon known as ICU acquired weakness (ICUAW). ICUAW includes weakness of the skeletal muscle, and that extends to the respiratory muscles, which is of particular significance due to diaphragm muscle weakness being a strong predictor of poor outcome in patients (Batt et al., 2013; Callahan et al., 2015; Callahan and Supinski, 2013; Sieck, 2015; Supinski and Callahan, 2013). ALI and ARDS are syndromes of acute respiratory failure that result from acute pulmonary oedema and inflammation. The development and/or progression of ALI/ARDS is associated with several clinical disorders including direct pulmonary injury from pneumonia and aspiration as well as indirect pulmonary injury via trauma, sepsis and disorders such as acute pancreatitis and drug overdose (Matthay et al., 2003). Whether hypoxia, which features in these acute respiratory-related disorders, contributes to or causes diaphragm weakness in patients is as of yet unknown.

1.4.2 Acute Lung Injury

ALI is a significant source of morbidity and mortality in critically ill patients, characterised clinically by an acute onset of bilateral pulmonary infiltrates, hypoxaemia and oedema, with an absence of left arterial hypertension, in predominantly young, previously healthy people (Johnson and Matthay, 2010; Parekh et al., 2011). Sepsis, a clinical syndrome caused by systemic inflammation responses to infection and to molecular mechanisms of cell injury, is a common cause of ALI and ARDS (Campos et al., 2012; Matthay et al., 2003; Wheeler and Bernard, 1999).

1.4.3 Acute Respiratory Distress Syndrome

In the United States, patients with ARDS occupy 1 in 10 critical care beds (Powers, 2007). ARDS is a condition of the alveoli characterised by widespread inflammation in the lungs. It is a manifestation of acute lung injury, often due to sepsis, trauma and severe pulmonary infection, characterised clinically by dyspnoea, profound hypoxia, decreased lung compliance, and diffuse bilateral infiltrates on chest radiography (Udobi et al., 2003). Hypoxaemia occurs largely due to pulmonary shunt and ventilation/perfusion mismatch (M. J. Tobin, A. Jubran, 1998). ARDS affects around 200,000 patients annually in the USA (Fuller et al., 2014; Salman et al., 2013). The prevalence rate of ALI/ARDS is around 7.1% of patients admitted to an ICU and 16.1% of all mechanically ventilated patients in the ICU (Fuller et al., 2014; Goyal et al., 2012; Saguil and Fargo, 2012) and the mortality associated with the condition varies based on disease severity, age, and the presence or absence of confounding conditions, but is high at around 40%. Survivors of ARDS exhibit long-term morbidity across a wide range of important clinical outcomes, impacting significantly on public health and quality of life (Bernard, 2005; Fuller et al., 2014; Rubenfeld and Herridge, 2007; Salman et al., 2013). Mechanical ventilation of patients, in conjunction with supplemental oxygen therapy, is a strategy commonly employed in the management of ARDS (Udobi et al., 2003). However, whether hypoxia, featured in this condition, causes diaphragm dysfunction leading to worsened patient prognosis is understudied, which is surprising given the prevalence and severity of the condition and the fact that mechanical ventilation is often a necessary intervention.

1.4.4 Mechanical Ventilation

The use of mechanical ventilators, in the form of negative-pressure ventilation, first appeared early in the 1800s, later followed by positive-pressure devices around 1900, and finally the typical ICU ventilator of today began to be developed in the 1940s (Kacmarek, 2011). Modern positive-pressure mechanical ventilator strategies involve complicated feedback systems, matching ventilation to patient respiratory effort, attempting to provide sufficient ventilation and diaphragm unloading while causing minimal damage to the lungs, controlling for pressure and volume, and maintaining phrenic neural drive to the diaphragm, thus maintaining a level of stimulation of the diaphragm, helping to limit diaphragm atrophy. The number of patients that required

mechanical ventilation in hospital ICUs in the USA in 2005 was estimated at around 800,000 with an estimated national cost of $27 billion, 12% of all hospital costs (Wunsch et al., 2010). The number of patients mechanically ventilated has risen drastically in the past 25 years. Indeed mechanical ventilation is an essential component of general anaesthesia for surgery, and it can be a life-saving intervention, particularly in critically ill patients. However, mechanical ventilation can also have negative influences on the respiratory system, being associated with various short- and long-term complications including lung injury, infection, inflammation, diaphragm atrophy and weakness, and possibly leading to conditions such as VILI/VALI, ARDS and ventilator-induced diaphragmatic dysfunction (VIDD) (Callahan et al., 2015; Jaber et al., 2011a; Petrof et al., 2010; Serpa Neto et al., 2014; Supinski and Callahan, 2013). Mechanical ventilation has also been shown to induce collagen accumulation within two hours in the rat lung (Chen et al., 2015), interestingly, a complication which can be alleviated by pre-treatment with the thiol antioxidant NAC, suggesting that NAC may be useful in aiding the prevention of ventilator-induced lung fibrosis. Problematically, it can often become difficult to wean patients off mechanical ventilators after prolonged periods of time or when complications and confounding factors arise.

Respiratory muscle weakness is reported in ICU patients on mechanical ventilation (Azuelos et al., 2015; Batt et al., 2013; Godoy et al., 2015; Hooijman et al., 2015; Jaber et al., 2011b; Jubran, 2006; Kallet, 2011; Petrof et al., 2010; Powers et al., 2013; Supinski and Callahan, 2013; Watson et al., 2001) and in animal models of VIDD (Mrozek et al., 2012; Powers et al., 2013, 2011, 2009, Smuder et al., 2015, 2012). Indeed, when a hypoxaemic respiratory patient in the ICU is placed on a mechanical ventilator, due to respiratory failure, diaphragm atrophy and dysfunction (VIDD) occurs in a matter of hours (Bruells et al., 2013), and there is recent evidence to suggest that the ubiquitin-proteasome pathway, as well as mitochondrial abnormalities, may be involved (Hooijman et al., 2015; Picard et al., 2015).Whilst inactivity of the diaphragm, due to the mechanical ventilator performing the work of breathing, is widely accepted as a major cause of this weakness (Jaber et al., 2011a; Levine et al., 2008; Supinski and Callahan, 2013), often compounded by infection (Petrof et al., 2010; Supinski and Callahan, 2013), the potential role, if any, that hypoxia may play in the development and/or exacerbation of this weakness is unclear.

Indeed, there now exists some controversy as to whether inactivity *per se* induces diaphragm muscle atrophy, and it has been suggested that other factors such as neurone-derived trophic factors may be at play (Sieck and Mantilla, 2013), which warrants further exploration. Thus, while there is much evidence of VIDD (Azuelos et al., 2015; Jaber et al., 2011a; Petrof et al., 2010; Petrof and Hussain, 2016; Powers et al., 2013), the exact mechanisms by which this weakness manifests are unknown. Acute hypoxia – as a feature of the initial illness which led to a patient requiring mechanical ventilation and/or persistent hypoxaemia – may play a part in the development of this weakness, and this area requires further elucidation.

1.4.5 Ventilator-Induced Diaphragmatic Dysfunction (VIDD)

Diaphragmatic function is a primary determinant of the ability to successfully wean a patient from mechanical ventilation, but animal models have demonstrated that the use of mechanical ventilation itself results in a major reduction in the force-generating capacity of the diaphragm as well as structural injury and atrophy of diaphragm muscle fibres. This leads to the condition termed ventilator-induced diaphragmatic dysfunction, or VIDD (Jaber et al., 2011a). Diaphragm weakness may also increase the risk of fatal airway obstruction incidents, due to the decreased peak force generating capacity limiting the ability of a patient to inspire the volume of air needed to perform the necessary expiratory airway clearance manoeuvre to clear the airway and restore pulmonary ventilation. As well as the other factors which contribute to VIDD, discussed earlier in this chapter, NF-κB signalling contributes to mechanical ventilation-induced diaphragm weakness in the rat. Furthermore, in this model oxidative stress is an upstream activator of NF-κB, and the authors suggest that prevention of mechanical ventilation-induced oxidative stress in the diaphragm could be a useful therapeutic strategy used clinically to prevent VIDD (Smuder et al., 2012). Indeed, it has been demonstrated that targeting of mitochondrial ROS with mitochondrial targeted antioxidants protects against VIDD (Powers et al., 2011), suggesting that mitochondrial ROS may play a causative role in VIDD.

Prolonged mechanical ventilation alters the structure and function of the diaphragm (Powers et al., 2009), primarily manifesting in diaphragmatic atrophy (increased protein breakdown and decreased protein synthesis) and dysfunction. Patients who

undergo prolonged mechanical ventilation have a high mortality rate within the first 12 months post-weaning, with COPD, cardiac and renal failure and respiratory muscle weakness all being factors recognised to contribute to this mortality (Johnson and Johnson, 2012). Interestingly, there may also be a high prevalence of under-recognised sleep-disordered breathing (SDB) conditions such as obstructive sleep apnoea (OSA) in patients who wean from prolonged mechanical ventilation (Diaz-Abad et al., 2011; Johnson and Johnson, 2012), which might relate to weakness in upper airway dilator muscles such as the sternohyoid muscles.

1.4.6 Ventilator-Induced/Associated Lung Injury

VILI and VALI both represent an acute injury to the lung, occurring during mechanical ventilation. VILI is caused by the act of mechanical ventilation itself, with an inadequate ventilator mode used to mechanically ventilate initially healthy lungs, while VALI is an injury to already disease-affected lungs during mechanical ventilation. In both cases, the lung injury primarily results from the differences in transpulmonary pressure, which consequently create an imbalance in lung stress and strain (Kuchnicka and Maciejewski, 2013). The incidence of VALI is around 24% of mechanically ventilated patients who do not have ALI from the outset, with a likely higher incidence in patients also suffering from ARDS/ALI (Gajic et al., 2004). This lung injury may lead to systemic hypoxia which, if it is a cause of diaphragm dysfunction, could exacerbate and perpetuate the need for mechanical ventilation causing further lung injury and the initiation of a vicious circle of ventilation, injury and hypoxia.

1.4.7 Confounding Factors

Through over-distension of the lung, mechanical ventilation induces substantial inflammation that is thought to increase mortality among critically ill patients, and may have relevance for the development of multisystem organ failure (Chiumello et al., 1999; Ranieri et al., 1999; Woods et al., 2015).

Obesity has been suggested to independently increase the risk of developing ARDS (Karnatovskaia et al., 2014). Obese patients display alterations in baseline pulmonary mechanics, including airflow obstruction, decreased lung volumes, and impaired gas

exchange, which can have implications for many diseases including ARDS (Hibbert et al., 2012). However obesity does not, somewhat surprisingly, impact on the length of time a patient is likely to require mechanical ventilation, although it does increase the length of the ICU stay (Boles et al., 2007).

Infection can be a major confounding factor in VIDD. Lower respiratory tract infections often present as severe sepsis or septic shock with respiratory dysfunction in mechanically ventilated patients (Rello et al., 2014). Pneumonia is the second most common nosocomial infection occurring in critically ill patients, presenting in approximately 27% of all critically ill patients (Koenig and Truwit, 2006). Severe sepsis and multiorgan failure invariably leads to muscle dysfunction. Reduced diaphragm muscle force generation, associated with deranged mitochondrial bioenergetics and hypometabolism, was observed in a rodent model of sepsis (Zolfaghari et al., 2015a). Although there was also an increase in UCP-3 expression in this model, these functional and metabolic changes were also present in a UCP-3 knockout version of the same model, suggesting that these alterations are independent of the increase in UCP-3 expression seen in this model, and that reduced mitochondrial coupling efficiency by increased uncoupling (i.e. increased proton leak), potentially limiting mitochondrial ROS production, did not play a role.

Given the prevalence of conditions featuring acute hypoxia discussed above, insight into the acute adaptations of the respiratory muscles to hypoxia may be clinically relevant. Respiratory muscle plasticity is reported in animal models of chronic hypoxia (Carberry et al., 2014; Gamboa and Andrade, 2012, 2010; Lewis et al., 2015a,b; McMorrow et al., 2011); however, very little is known about the effects of an acute hypoxic stress on diaphragm muscle performance.

1.4.8 A Potential Role for Hypoxia

The role of acute hypoxia in the development, progression and exacerbation of acute respiratory related disorders, particularly diaphragmatic dysfunction as a feature of such disorders, is currently under-recognised, despite the clinical relevance of critical diaphragm failure, leading to respiratory failure and poor patient outcomes. In nature, a state of hypoxic tolerance is achieved through the integration of 1) a reduction in

metabolic state, 2) protection against hypoxic cell death/injury and 3) the maintenance of functional integrity (Ramirez et al., 2007). Knowledge of the mechanisms at play in all three of these areas is essential in order to develop novel therapeutic strategies for clinically hypoxic patients. Hypoxia has been shown to significantly decrease diaphragm end-expiratory length in awake canines (Ji et al., 2014), which may exert influence over the force generating capacity of the contracting diaphragm *in vivo*. This may be relevant to respiratory failure patients in an ICU setting and may be another hypoxia-induced factor affecting diaphragm function, as well as those effects exerted at a cellular level. The need to explore whether acute hypoxia contributes to diaphragm muscle weakness is currently most pertinent given the debate as to whether inactivity *per se* causes diaphragm muscle atrophy in mechanically ventilated patients.

1.5 Skeletal Muscle Plasticity

Skeletal muscle fibres are not regarded as fixed units but as highly versatile, adaptable, and malleable tissues. Skeletal muscle has huge capacity for remodelling and shows plasticity to adapt to a variety of stimuli including contractile activity (use and disuse, frequency of activity, etc.), loading conditions, substance supply and environmental conditions, such as hypoxia – the focus of this thesis (Flück and Hoppeler, 2003). Functional adaptations appear to involve alterations in contractile properties of the muscle, metabolic capacity of the mitochondria and regulatory mechanisms/intracellular signalling (Flück and Hoppeler, 2003; Hoppeler et al., 2003; Hoppeler and Fluck, 2003). Adaptations include alterations in muscle fibre size (e.g. hypertrophy, atrophy) and distribution (Bigard et al., 2000; Faucher et al., 2005; McMorrow et al., 2010), oxidative capacity (Faucher et al., 2005), contractile performance (El-Khoury et al., 2003; Faucher et al., 2005), angiogenesis (Deveci et al., 2002) and fibre type (e.g. slow-to-fast fibre type switching) (Pette and Staron, 1997; Schiaffino and Reggiani, 2011). Indeed the diaphragm muscle atrophies in a mere matter of hours when a patient is put on a mechanical ventilator (Levine et al., 2008), demonstrating remarkable structural maladaptive plasticity.

Respiratory muscles continually undergo remodelling as they adapt to the changing demands of respiration e.g. exercise, altitude changes, pathophysiology, etc. Respiratory muscle remodelling is a feature of COPD and may be the result in part of hypoxic adaptation (McMorrow et al., 2011). Dysfunction of respiratory muscle, particularly the diaphragm, is known to occur in patients with severe COPD (Heunks and Dekhuijzen, 2000; Polkey et al., 1996) and muscle oxidative capacity and bioenergetics are disturbed in COPD patients (Hoppeler et al., 2003; Mador & Bozkanat, 2001). However, the exact mechanisms by which skeletal muscle can alter its phenotypic profile are still unclear and under-explored. Furthermore, it is thought that the diaphragm, and other respiratory muscles, may adapt differently than most skeletal muscles due to the fact that, unlike limb skeletal muscle, its activity may be increased in some cases in response to hypoxia, and this needs to be addressed further. Translational animal models of hypoxia allow the examination of the effects of hypoxia on respiratory skeletal muscle without the influence of other confounding factors, which may present in disease states. They also offer an opportunity to explore the underlying molecular mechanisms contributing to adaptation and maladaptation in respiratory muscle. Illumination of such mechanisms could have enormous clinical relevance to conditions in which hypoxia features, and would contribute significantly to this field of research and the development of future therapeutic strategies.

1.5.1 Structural and Function Plasticity in Hypoxia

Some previous studies have looked at various structural and functional changes using animal models of hypoxia, both chronic hypoxia (sustained) and chronic intermittent hypoxia (CIH). McMorrow et al. (2011), using a translational animal model, found that chronic hypoxia decreased diaphragm muscle force and fatigue concomitant with increased sodium-potassium ATPase pump content, which plays a dynamic role in muscle fibre excitability during contractile activity. Moreover, the study suggested that this effect is NO dependent, and also that chronic hypoxia-induced muscle plasticity is time-dependent, further underlining the need to examine the effects of acute hypoxia to determine whether it has a role in diaphragm dysfunction in acute respiratory-related disorders. In another study by Skelly et al. (2010), it was found that CIH caused a significant decrease in sternohyoid muscle force, while chronic hypoxia has been shown to cause both diaphragm and sternohyoid muscle dysfunction

(Lewis et al., 2016, 2014). Fibre size, distribution and oxidative capacity were shown to be altered in hypoxia studies (Faucher et al., 2005; McMorrow et al., 2011), and it was also found that hypoxia induces prolonged angiogenesis in skeletal muscle in the rat (Deveci et al., 2002). The adaptation of skeletal muscle to hypoxia includes the loss of oxidative capacity (mitochondrial content) and a decreased fibre size and cross sectional area. The fatigue resistance of a skeletal muscle is proportional to its mitochondrial content, and so fatigue resistant muscles have a higher mitochondrial content than those with more fatigable fibres. Gamboa & Andrade (2010) stated that chronic hypoxia reduces aerobic capacity, and mitochondrial content, in limb skeletal muscles, and one of the causes seems to be decreased physical activity. Thus, they believed that diaphragm, and other respiratory muscles, may have a different pattern of adaptation as hypoxia may increase the work of breathing and so their activity may increase in response to hypoxia. However, they found that chronic hypoxia was associated with a reduction in mitochondrial volume density (content) in mouse diaphragm. Reduced mitochondrial biogenesis and increased mitophagy seemed to be responsible. Then in 2012, the same group uncovered evidence to suggest that the diaphragm muscle retains its endurance during chronic hypoxia due to a combination of morphometric changes and optimisation of mitochondrial energy production. Changes include reduction in fibre size, increased surface contact between the capillary and fibre, increased mitochondrial complexes IV & V, and reduced mitochondrial uncoupling protein – 3 (UCP-3) content, allowing the muscle to remain highly fatigue resistant (Gamboa and Andrade, 2012). There are also some conflicting results in this area, such as the effects of hypoxia on diaphragm muscle force and endurance in the rat (El-Khoury et al., 2003; McMorrow et al., 2011). McMorrow et al. (2011) found chronic hypoxia decreased force and increased endurance of the diaphragm muscle, while El-Khoury and colleagues found twitch force was increased, tetanic force was unchanged, and there was little effect on endurance in the diaphragm muscle following chronic hypoxia. However, this may relate to differences in protocol, such as muscle bath temperature (30˚C and 25˚C in each set up, respectively) during the *in vitro* muscle function tests (Ranatunga and Wylie, 1983), & barometric pressure of the chambers during CH treatment (380mmHg and 450mmHg respectively), and as such the intensity of the hypoxic stimulus. Indeed, it is clear from work performed by our group that chronic hypoxia (380mmHg or FiO_2 = 0.1) results in substantial diaphragm muscle weakness in rat (McMorrow et al., 2011)

and mouse (Lewis et al., 2016; Lewis and O'Halloran, 2016), presumably a functional trade-off to molecular changes that subserve other apparent advantages such as improved endurance (Gamboa and Andrade, 2012; Lewis et al., 2016; McMorrow et al., 2011) and hypoxic tolerance (Lewis et al., 2015a) .

Recently, the previously unknown function of a protein involved in the cellular response to hypoxia was discovered. When activated by hypoxia, the protein (p75NTR) initiates a cascade of events resulting in increased blood vessel production to replenish oxygen supply in disease (Le Moan et al., 2011). Rowley et al. (2005) stated that muscle plasticity, which occurs following perturbations in the load and/or activity, includes changes in myosin heavy chain (MHC) isoform expression, MHC content per half-sarcomere, fibre cross-sectional area, mitochondrial density, and actomyosin ATPase activity, and that these structural changes are tied to functional plasticity, reflected by changes in some or all of the following: ECC, force, velocity of shortening, and susceptibility to fatigue. The relevance of this is that hypoxia can induce a perturbation of activity in respiratory muscle in humans, and one different to that of other skeletal muscles i.e. altered muscle activity due to increased ventilation. However, it has been demonstrated in humans that hypoxia itself, rather than activity changes, exacerbates diaphragm and indeed abdominal muscle fatigability (Verges et al., 2010).

The mitochondria are the primary location of oxygen consumption and reactive oxygen species (ROS) production, and are becoming recognised as playing a pivotal role in oxygen sensing (Cummins and Taylor, 2005). It is established that in long-term exposure to severe hypoxia there is a decrease in mitochondrial content of skeletal muscle fibres, oxidative muscle metabolism is shifted towards a greater reliance on carbohydrates as fuel, and intramyocellular lipid substrate stores are reduced (Hoppeler et al., 2003). Transcription of genes encoding the mitochondrial proteins involved in beta oxidation can be regulated separately from the genes of the Krebs cycle and the respiratory chain (Hoppeler and Fluck, 2003). Zhou & Lin (2000) demonstrated hypoxia and exercise induced mRNA expression for the mitochondrial transporter protein UCP-3 after only 30minutes in rat EDL muscle, and a corresponding UCP-3 protein increase. Changes in mRNA expression for proteins involved in energy production, as well as muscle structure, function and performance

in response to hypoxia is an important area in understanding hypoxia-induced alterations in respiratory muscle. Muscle fibre mitochondrial function and energy production is clearly a very malleable component contributing to muscle performance and an area that warrants investigation when examining how a stimulus such as hypoxia affects skeletal muscle.

1.6 Skeletal Muscle Signalling

Skeletal muscle is an extremely adaptable and malleable tissue responding functionally, structurally and molecularly to a variety of stimuli and, as such, requires a complex network of signalling pathways to guide these changes. Hypoxia has a profound impact on the cellular transcriptome and triggers a multifaceted cellular response that plays important roles in both normal physiology and pathophysiological disease states. The signalling pathways associated with transcriptional activation in CIH differ from those in chronic hypoxia (Nanduri et al., 2008). Tavi & Westerblad (2011), state that a major part of the activity-dependent plasticity of skeletal muscle relies upon transcriptional alterations controlled by intracellular Ca^{2+} signals. Muscle specific programmes of gene expression that match genetic phenotype with environmental demands are recruited by transcription factors, most of which are affected by Ca^{2+}-dependent signalling cascades (Bassel-Duby and Olson, 2006; Tavi and Westerblad, 2011). However, the activity of these transcription factors is also affected by other factors in the cellular environment and so the result depends on a combination of both Ca^{2+}-dependent and Ca^{2+}-independent signalling (Gundersen, 2011). An understanding of these signalling mechanisms in acute hypoxia is key to understanding how structural and functional changes manifest, and to highlighting targets for therapeutic interventions.

Transcription factors, or transcriptional activators, affected by hypoxia include: hypoxia-inducible factors (HIF-1 & HIF-2), nuclear factor kappa B (NF-κB), cyclic AMP-response element-binding protein (CREB), activating protein-1 (AP-1), p-53, early growth response-1 (Egr-1), nuclear factor for interleukin 6 (NF-IL6), nuclear respiratory factor-1 (NRF-1), among a whole host of others (Cummins and Taylor,

2005; Gutsaeva et al., 2008; Nanduri et al., 2008). NRF-1 mediates expression of multiple nuclear genes encoding for mitochondrial proteins, including subunits of the respiratory chain complexes, among others (Gutsaeva et al., 2008).

1.6.1 Signalling Pathway

Skeletal muscle requires an array of complex signalling pathways in order to function normally and maintain homeostasis in the face of changing demands placed on the muscle. Many of these pathways have both common and distinct targets, and there exists a large amount of interplay between many of them to regulate factors such as growth, fibre type, metabolic activity, contractile performance, etc. in response to various stimuli.

1.6.1.1 Hypertrophy/Atrophy Balance

Atrophy of skeletal muscle can be a major consequence of numerous diseases, mediated via an imbalance between protein synthesis and degradation, or hypertrophy and atrophy, which are regulated by a complex system of signalling pathways (Bodine et al., 2001; Favier et al., 2010; Glass, 2005, 2003). The ubiquitin-proteasome system is a protein degradation system whereby proteins are tagged by poly-ubiquitination for proteasomal degradation. This ubiquitin-proteasome system, along with the autophagy-lysosomal system, is regulated by the FoxO transcriptional network. These two systems are responsible for the majority of protein breakdown in eukaryotes (Altun et al., 2012; Milan et al., 2015a). Diaphragm muscle fibre atrophy signalling, increased proteasome activity and decreased fibre cross-sectional area are features of chronic hypoxia exposure that may contribute to diaphragm muscle weakness in animal models (Lewis et al., 2015b; McMorrow et al., 2011). Diaphragm weakness and atrophy is a recognised consequence of mechanical ventilation in patients, as discussed earlier in this chapter, and the hypertrophy/atrophy balance is an intuitive place to look when examining the cause of muscle weakness, or changes in muscle contractile performance.

1.6.1.1.1 Akt Pathway

Akt is a serine-threonine protein kinase that can act as a modulator of both hypertrophy and atrophy in skeletal muscle, depending on its phosphorylation state. Akt regulates skeletal muscle fibre size and promotes hypertrophy via activation of downstream signalling pathways which are implicated in inducing protein synthesis: those downstream of mammalian target of rapamycin (mTOR) and glycogen synthesis kinase 3 (GSK-3) (Bodine et al., 2001; Léger et al., 2006; Rommel et al., 2001). Indeed, activation of the Akt/mTOR pathway can oppose muscle atrophy induced by muscle disuse *in vivo* (Bodine et al., 2001), and it has been suggested that pharmacological activators of Akt, mTOR or p70S6K (a downstream positively regulated target of Akt/mTOR) may prove beneficial as therapeutic strategies to attenuate muscle atrophy in patients (Rommel et al., 2001). p70S6K exerts its pro-hypertrophic action, partly via activation of S6RP (downstream target), by promoting protein synthesis. GSK-3β becomes inactivated via phosphorylation by Akt, thus suppressing its anti-anabolic effect and aiding pro-hypertrophic mechanisms such as protein synthesis activation.

Activation of the PI3K-Akt-FoxO pathway induces cell growth while inhibition of this pathway reduces cell survival and, in skeletal muscle, causes fibre atrophy. Trim32 is a ubiquitin ligase which reduces PI3K-Akt-FoxO signalling in both normal and atrophying muscle (Cohen et al., 2014). Akt also promotes muscle hypertrophy by blocking the transcriptional upregulation of certain key mediators of skeletal muscle atrophy, namely the E3 ubiquitin ligases muscle RING-finger 1 (MuRF1) and Atrogin-1 (a.k.a. MAFbx), via the phosphorylation, and hence inhibition of nuclear translocation, of the Forkhead box class O (FoxO) family of transcription factors. Upon phosphorylation by Akt, the FoxOs are precluded from entering the nucleus and thus the upregulation of MuRF1 and Atrogin-1 is blocked. MuRF1 and Atrogin-1 mediate their atrophic action via ubiquitination of specific protein targets, tagging them for proteasomal degradation. Targets of MuRF1 include components of the sarcomeric thick filament, including the MHC discussed further in section 1.7.2, which can be broken down under atrophic conditions (Cohen et al., 2009; Glass, 2010). Meanwhile Trim32 catalyses the disassembly and degradation of the desmin cytoskeleton, Z-band and thin filament proteins in muscle atrophy (Cohen et al., 2014, 2012; Sanchez et al., 2014). This targeting of the contractile units, in particular, as

well as others, of skeletal muscle highlights the central role these atrogenes play in skeletal muscle atrophy, and how they may lead to alterations in contractile performance.

1.6.1.1.2 Mammalian Target of Rapamycin (mTOR) Pathway

mTOR, as mentioned above, holds an important position in the regulatory control of skeletal muscle fibre hypertrophy. Downregulation of the Akt/mTOR pathway in skeletal muscle has been shown to occur in response to chronic hypoxia, linked to skeletal muscle fibre atrophy and a negative regulatory effect on skeletal muscle mass (Favier et al., 2010). mTOR is considered to be a central player in the control of skeletal muscle hypertrophy/atrophy balance.

1.6.1.1.3 Mitogen Activated Protein Kinases (MAPK) Pathway

Mitogen-Activated Protein (MAP) kinases are a family of signalling serine/threonine protein kinases which elicit intracellular effects in response to extracellular signals and physical or chemical cellular stresses. They are involved in regulating cell proliferation and differentiation, development, motility, inflammation, cell survival and apoptosis. ERK1/2, p38 and JNK are all MAP kinases, activated by MAPK kinases MEK1/2, MKK3/6 and MKK4/7, respectively (Zhang and Dong, 2005). ERK and p38 MAPK-Activated Protein Kinases are a family of protein kinases with diverse biological functions (Roux and Blenis, 2004). Whether the MAPK pathway is pro-hypertrophic or pro-atrophic depends on the combination of signalling mechanisms converging together. However, ERK1/2 is predominantly pro-hypertrophic, while p38 and JNK are predominantly pro-atrophic.

1.6.1.1.4 FoxOs/FOXO-3a Pathway

FoxO transcription factors, discussed above, are highly conserved, playing important roles in cellular homeostasis, regulating processes such as metabolism, cellular proliferation, stress tolerance and potentially lifespan (Sanchez et al., 2014; van der Horst and Burgering, 2007). The four FoxO members in humans, FoxO1, FoxO3 FoxO4 and FoxO6, are all expressed in skeletal muscle and are involved in the control of skeletal muscle plasticity. FoxO1 and FoxO3 have central roles in energy

homeostasis and mitochondrial metabolism, as well as being key regulators of protein breakdown/atrophy, modulating the activity of certain factors in the ubiquitin-proteasome and the autophagy-lysosome proteolytic pathways (Accili and Arden, 2004; Chung et al., 2013; Mammucari et al., 2007; Milan et al., 2015b; Sanchez et al., 2014). FoxO3 has been shown to be necessary and sufficient for the induction of autophagy in skeletal muscle *in vivo* (Mammucari et al., 2007). FoxO1 and FoxO3 are downstream targets of Akt and the major regulatory transcription factors of the atrogene Atrogin-1 (Milan et al., 2015b; Sandri et al., 2004). FoxO has been shown to be necessary for the activation of key proteolytic mechanisms; ubiquitin-proteasome system, autophagy/lysosomal system and caspase-3, some of these being essential for mechanical ventilation-induced diaphragm atrophy, and contractile dysfunction in the rat diaphragm (Smuder et al., 2015), making FoxO signalling an essential area of interest when examining diaphragm muscle atrophy signalling mechanisms under hypoxia.

1.6.1.1.5 Atrogenes

Development of atrophy from many sources such as fasting, cancer, sepsis, diabetes and kidney failure require or share the transcription and activation of a common programme of atrophy-genes, termed ‘atrogenes’, by FoxO transcription factors, whose activation is sufficient to produce accelerated proteolysis and atrophy (Cohen et al., 2014; Lecker et al., 2004; Sanchez et al., 2014; Sandri et al., 2004). These atrogenes encode proteins which catalyse important steps in autophagy-lysosomal and ubiquitin-proteasome systems, ROS detoxification and mitochondrial function and energy balance. The primary orchestrators of atrogene signalling inducing atrophy in skeletal muscle are muscle-specific ubiquitin ligases; Atrogin-1 and MuRF1 (Milan et al., 2015a). The actions of these ubiquitin ligases are negatively regulated by pro-hypertrophic Akt signalling, via the inhibition of FoxO by Akt, as discussed above. FoxO-1 and FoxO-3 are two of the main transcriptional activators of Atrogin-1.

1.6.1.1.6 Autophagy

Autophagy, or the autophagy-lysosomal system, is a lysosomally mediated proteolytic process which can be activated by oxidative stress, or ROS. As mentioned above, the autophagy-lysosomal system is regulated by FoxO. Autophagy can be induced in the

diaphragm by mechanical ventilation but is not thought of as being a primary cause of diaphragm weakness in VIDD. In fact, autophagy may instead be a possibly beneficial adaptive response in the face of VIDD, working to optimise muscle cellular makeup (Azuelos et al., 2015). Indeed, autophagy allows for cell survival during starvation, via the bulk degradation of proteins and organelles by lysosomal enzymes (Mammucari et al., 2007). LC3B, BNIP3 and GABARAPL3 are key genes positively regulating autophagy and specifically mitophagy (autophagy mediated mitochondrial degradation) signalling (Hamacher-Brady and Brady, 2016; Saito and Sadoshima, 2016), often functioning toward a pro cell survival programme rather than autophagy mediated atrophy. The investigation of autophagy in diaphragm muscle adaptations to hypoxia is therefore pertinent when considering we are dealing with a muscle attempting to maintain or optimise contractile performance in the challenge of a reduced oxygen environment.

1.6.1.2 Hypoxia-Inducible Factor (HIF) Signalling

Hypoxia-inducible factor (HIF) plays a central role in orchestrating the cellular hypoxia response. HIF is a heterodimeric protein belonging to the basic helix-loop-helix PAS family of transcription factors (Lundby et al., 2009) and plays a central role in orchestrating the cellular hypoxia response. HIF-1, the most ubiquitously expressed and the best characterised of the family, is recognised as a master regulator of hypoxia signalling (Cummins and Taylor, 2005; Hoppeler et al., 2003; Semenza, 2004) and is known to play a very general role in hypoxia signalling (Lundby et al., 2009). Its activity is regulated by oxygen-dependent degradation of the dominant HIF-1α subunit (post-translational modification), which occurs at normal oxygen levels (normoxia). However, under hypoxic conditions this degradation rate decreases and HIF-1α stabilises, accumulates, and associates with HIF-1β to form the functional transcription complex, initiating the transcription of an array of hypoxia-inducible genes possessing a hypoxia response element (HRE) (Chi et al., 2006).

Hypoxia in cells and tissues leads to the transcriptional induction of a series of genes that participate in angiogenesis, oxidative metabolism, iron metabolism, glucose metabolism and cell proliferation and survival, and the primary factor mediating this response is HIF-1 (Ke and Costa, 2006; Lundby et al., 2009). There are two other

members of the family, HIF-2 and HIF-3, and transcriptional activation by HIF-2 regulates some target genes in common with HIF-1 as well as other genes uniquely regulated by HIF-2 (Peng et al., 2011), supporting the idea that HIF-1 and HIF-2 have many unique targets (Hu et al., 2003). Indeed, HIF-1α mRNA and protein levels have been found to be constitutively higher in more glycolytic muscles when compared with more oxidative muscles (Pisani and Dechesne, 2005), supporting the hypothesis that the oxygen homeostasis regulation system is fibre type dependent. HIF-1 activation by CIH seems to be linked to increased pro-oxidant(s), while down-regulation of HIF-2 by CIH is coupled to transcriptional down-regulation of antioxidant enzyme(s) (Prabhakar et al., 2009) such as manganese superoxide dismutase (MnSOD). Previous research has shown that mitogen-activated protein kinases (MAPKs) and phosphor-ionositol-3 (PI-3) kinases play a critical role in continuous hypoxia-induced activation of HIF-1 mediated transcription (Nanduri et al., 2008; Sang et al., 2003). Given the central and integral regulatory role of HIF-1α in orchestrating the hypoxia response within muscle fibres it is appropriate to explore how acute hypoxia may alter HIF-1α expression and regulation in respiratory muscle.

MicroRNAs (miRNAs) are small (approx. 19-23 nucleotides long) noncoding RNAs which function in transcriptional and post-transcriptional regulation of gene expression through RNA degradation (Hoppeler et al., 2011). In recent years, studies have established a link between a specific group of miRNAs and hypoxia, known as hypoxia-regulated miRNAs (HRMs or hypoximirs), several of which exhibit induction in response to HIF activation (Kulshreshtha et al., 2008). miR-210 is one of the most hypoxia sensitive miRNAs and has been found to be up-regulated in response to hypoxia and can negatively regulate mitochondrial respiration activity and increase ROS production in cancer cell lines (Chen et al., 2010; Shen et al., 2013). miRNAs have been shown to be critically involved in the regulation of skeletal muscle myogenesis, modulating proliferation and differentiation (Hoppeler et al., 2011).

1.7 Skeletal Muscle Contractile Mechanism

1.7.1 Excitation-Contraction Coupling

Excitation-contraction coupling (ECC) is a term coined by Alexander Sandow in 1952 to describe the physiological process of converting an electrical stimulus (the motor neuron action potential) to a mechanical response (muscle contraction) (Sandow, 1952). In skeletal muscle, when a depolarising action potential (AP) is transmitted along the sarcolemma of the muscle fibre and down the transverse tubules, it is thought to cause a conformational change in the dihydropyridine receptor (DHPR) in the t-tubule membrane which, by means of a protein-protein interaction, opens the ryanodine receptor (RyR), a Ca^{2+} release channel, in the terminal cisternae of the sarcoplasmic reticulum (SR) causing Ca^{2+} to be released into the myoplasm. The SR stores Ca^{2+} at high concentrations, creating a favourable concentration gradient facilitating efflux of Ca^{2+} from the SR into the myoplasm when RyR opens. Calsequestrin is a high capacity, low affinity Ca^{2+} binding protein localised in the lumen of the terminal cisternae of the SR, and is by far the most abundant of such proteins (Beard et al., 2004; Fliegel et al., 1987; Wei & Gallant, 2009). It appears to be anchored near the RyR by intra-membrane/transmembrane proteins including triadin and junctin, which also bind RyR, thereby increasing Ca^{2+} buffering capacity at the site of Ca^{2+} release (Wei et al., 2009). Histidine-rich calcium binding protein (HRC) is another, less abundant, low affinity Ca^{2+} binding protein in the SR and appears to bind triadin in a Ca^{2+} dependent manner, and so could have a role further than Ca^{2+} buffering (Sacchetto et al., 1999). Sarcalumenin is another Ca^{2+} binding protein in the SR and is thought to contribute to Ca^{2+} buffering and maintenance of Ca^{2+} pump proteins (Yoshida et al., 2005).

The rise in intracellular Ca^{2+} concentration, due to SR Ca^{2+} release, promotes actin-myosin interactions and causes a contractile twitch to occur. Ca^{2+} released from the SR binds to Troponin C causing the troponin complex to pull tropomyosin away from the myosin cross-bridge binding sites on the actin filaments. The myosin heads, bound to ADP+Pi, bind actin (cross bridge) at their binding sites. ADP+Pi immediately release, causing cocking of the myosin head and the myosin and actin filaments to slide past each other, known as the power stroke. ATP then binds the

myosin head, causing it to release actin, and ATP is then hydrolysed to ADP+Pi by myosin ATPase in the myosin head. Thus, in the presence of enough ATP and SR released Ca^{2+}, this cycle continues. Relaxation of skeletal muscle occurs as intracellular Ca^{2+} is resequestered by the SR. Uptake of Ca^{2+} into the SR is facilitated by the sarco/endoplasmic reticulum Ca^{2+}-ATPase pumps (SERCAs), which are distributed throughout the longitudinal tubule and terminal cisternae of the SR in skeletal muscle. It is clear that SR Ca^{2+} handling is central to muscle contractile activity, and thus it is logical to examine the expression of some of these key players in SR Ca^{2+} handling, mentioned above, when investigating how a stimulus such as hypoxia may alter contractile performance in respiratory muscle.

1.7.2 Skeletal Muscle Fibre Types

The MHC is the motor protein of the muscle sarcomeric thick filament. MHC isoforms – MHC_{slow}, MHC_{2A}, MHC_{2B} and MHC_{2X} provide a useful marker for muscle fibre types and can be identified by immunoreactivity to specific antibodies or by protein electrophoresis (Rowley et al., 2005; Schiaffino & Reggiani, 2011; Schiaffino et al., 1989). There are four major skeletal muscle fibre types: type I, type IIa, type IIx and type IIb, and these fibre types have varying properties such as fast-/slow-twitch kinetics, fatigue resistance, mitochondrial enzyme activity (oxidative, glycolytic), which influence their contractile and fatigue properties. Type I muscle fibres (red muscle) are slow contractile fibres with high fatigue resistance and low power production. They have a very high mitochondrial density and high capillary density and oxidative capacity, while glycolytic capacity is low. Type IIa fibres (red muscle) produce moderately fast contractions with medium power output and have a fairly high resistance to fatigue. They have a high mitochondrial density and intermediate capillary density with high oxidative and glycolytic capacity. Type IIx fibres are fast contracting fibres with an intermediate fatigue resistance and high power production. They have a medium mitochondrial density, low capillary density, and a high glycolytic capacity and intermediate oxidative capacity. Finally, type IIb muscle fibres (white muscle) produce very fast contraction velocities and have a very high power production, with a low resistance to fatigue. They have a low mitochondrial and capillary density and low oxidative capacity while glycolytic capacity is high in this fibre type. As discussed in section 1.6.1.1.1, MHC can be targeted for

ubiquitination and degradation by MuRF-1 under atrophic conditions in skeletal muscle, directly affecting the contractile unit of the muscle fibre.

1.8 Reactive Oxygen Species (ROS) in Skeletal Muscle

The mitochondria, due to oxidative metabolism, are the primary source of ROS production in skeletal muscle. There is now clear evidence that ROS are not only toxic species but, within certain concentrations, are useful signalling molecules regulating physiological processes (Barbieri and Sestili, 2012). ROS can activate HIFs (Prabhakar and Semenza, 2012), and plasticity of respiratory muscles following chronic hypoxia may be due to the generation of ROS (Bavis et al., 2007). ROS such as hydrogen peroxide (H_2O_2), superoxide anions ($\cdot O_2^-$) and hydroxyl radicals ($\cdot OH$) are chemically reactive, oxygen containing molecules, that are continually produced within skeletal muscle cells as a by-product of oxidative metabolism, and it has been shown previously that components of the contractile machinery are differentially responsive to alterations in the oxidation-reduction balance of muscle fibres (Andrade et al., 1998) and that maximum force production by fast- and slow-twitch skeletal muscles of rats and mice is modified by redox modulation (Plant et al., 2013). In figure 1 below, the baseline (O) muscle redox balance at rest is to the left (slightly reduced state) of the peak redox-balance for force production, and so maximum force production is not optimal. Reduction by Dithiothreitol (DTT) shifts the redox balance further to the left (■), away from the optimal and decreases force production. A slight shift in redox balance to the right (oxidation) of baseline, by a brief exposure to H_2O_2, increases force production to a maximum (▼). However, further oxidation past the optimal redox state and further to the right of the figure (highly oxidised), due to prolonged exposure, decreases force production (▲).

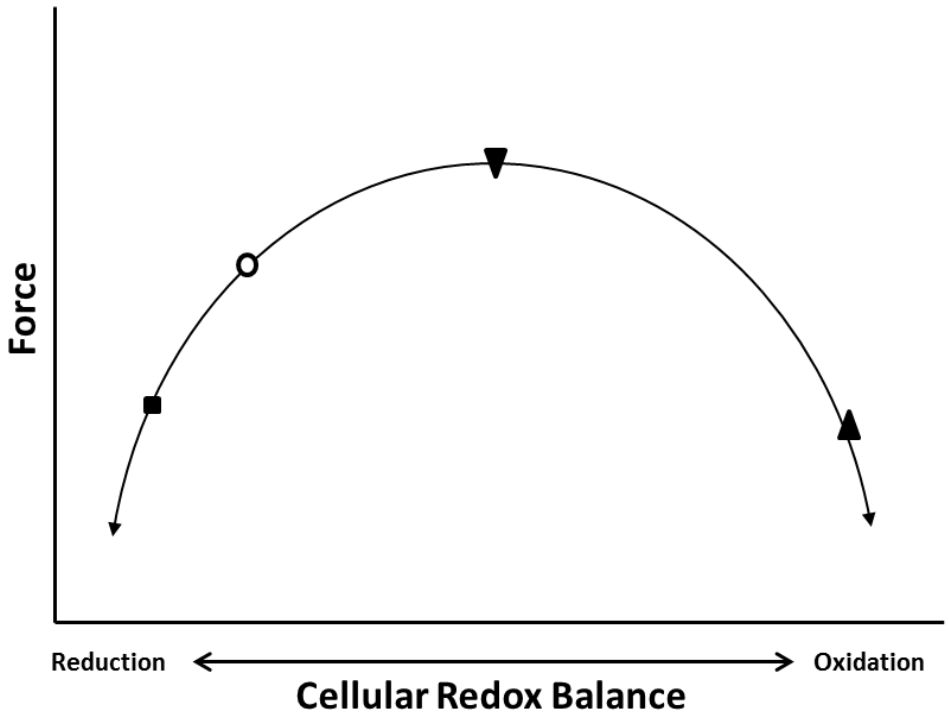

Figure 1. Representative model of maximum isometric force production as a function of cellular redox balance in mouse hind-limb muscle (Figure redrawn from Andrade, et al., 1998).

Xanthine oxidase is a form of the ROS producing enzyme xanthine oxidoreductase, present in human skeletal muscle (Hellsten et al., 1997), and one of its functions is thought to involve purine metabolism (Terada et al, 1990). It catalyses the oxidation of hypoxanthine to xanthine and can further catalyse the oxidation of xanthine to uric acid, and these reactions utilise molecular oxygen as an electron acceptor and form superoxide radicals (Volek et al., 2002). It has thus been shown to be involved in exercise-induced oxidative stress in COPD patients (Heunks, 1999). Giacomo et al. (1993) found evidence to suggest that acetyl-L-carnitine application in rat skeletal muscle, in vitro, reduced lipid peroxidation, and did so by inhibition of XO activity. Catalase is an enzyme that catalyses the decomposition of hydrogen peroxide to water and oxygen, and has a very high rate of turnover. It forms part of the endogenous antioxidant network opposing oxidative stress which also includes, among others, superoxide dismutase (SOD) and glutathione (GSH) peroxidase (Ramirez et al., 2007). Together, these antioxidant enzymes protect cells from the deleterious effects of ROS. GSH is one of the most prevalently expressed and widely studied

antioxidants in this defensive network, and occupies many other cellular roles outside of its antioxidant duties.

Pharmacotherapy for respiratory-related oxidative stress disorders is an attractive option, and antioxidant therapy may prove a viable and beneficial option. Skelly et al. (2012), found that Tempol, a superoxide scavenger, ameliorates pharyngeal dilator muscle dysfunction in a rodent model of CIH, important in the context of antioxidant therapy for respiratory disorders characterised by intermittent hypoxia such as sleep apnoea. Dutta et al. (2008) found that supplementation with L-carnitine, which plays a role in transport of fatty acids from the cytosol into the mitochondria during lipid peroxidation (stimulator of muscle bioenergetics), and is also an antioxidant, attenuated intermittent hypoxia induced oxidative stress and delayed muscle fatigue in rat limb muscle. L-carnitine has also been shown to favourably affect markers of muscle recovery from strenuous exercise by reducing oxidative stress (Volek et al., 2002).

N-acetylcysteine (NAC) is a highly effective free radical scavenger in its own right, but also functions as a major contributor to the maintenance of normal cellular GSH status in skeletal muscle cells (Kerksick and Willoughby, 2005). NAC has been credited with roles in improving skeletal muscle performance, including respiratory muscle, and preventing apoptosis following heavy exercise (Quadrilatero and Hoffman-Goetz, 2005, 2004; Reid et al., 1994; Shindoh et al., 1990; Supinski et al., 1997), suggesting that NAC may be beneficial in cases of hypoxia-induced respiratory muscle weakness. NAC shall be discussed further in section 1.10 Therapeutic Strategies below.

1.9 Metabolism in Skeletal Muscle

The patterns and strategies of lipid and carbohydrate metabolism in skeletal muscle change with muscle type and disease state (van Lunteren et al., 2010; van Lunteren and Moyer, 2013). The mitochondria are a prominent site within skeletal muscle fibres for ROS production (Muller et al., 2007; Murphy, 2009; Zorov et al., 2014).

Indeed, diaphragmatic mitochondrial ROS production is implicated in ventilation-induced diaphragm weakness, and it has been demonstrated that targeting of mitochondrial ROS with specific mitochondrial targeted antioxidants prevents mechanical ventilation-induced increases in diaphragmatic mitochondrial ROS, and protects the diaphragm from mechanical ventilation-induced diaphragm weakness in animal models (Agten et al., 2011; Powers et al., 2011), suggesting that mitochondrial ROS may play a very central role in VIDD by weakening the diaphragm muscle.

It has been suggested that mitochondrial membrane potential regulates the production of mitochondrial ROS. Therefore, uncoupling of oxidative phosphorylation from the electron transport chain in the mitochondrial membrane, dissipating the membrane potential as heat, may decrease mitochondrial superoxide production. Positive regulation of UCP-3 expression may therefore serve a protective role, by diminishing mitochondrial ROS generation in skeletal muscle. Indeed, ROS production is enhanced in UCP-3 knockout mice (Bodrova et al., 1998; Sastre et al., 2003).

In sepsis, muscle dysfunction is observed and bioenergetics dysfunction and oxidative stress are implicated as underlying pathophysiological mechanisms. Increased UCP-3 in sepsis is suggestive of increased proton leak, as described above, limiting ROS production at the cost of mitochondrial coupling and efficiency of ATP production. However, in mouse knockout model, UCP-3 did not appear to play a role in sepsis-induced muscle dysfunction (Zolfaghari et al., 2015b), although mitochondrial bioenergetics were deranged. UCP-3 upregulation may also serve an antioxidant function in protecting muscle mitochondria from exercise-induced oxidative stress, at the compromise of oxidative phosphorylation efficiency in skeletal muscle during exercise (Jiang et al., 2009). It would appear that oxidative stress and ROS, particularly mitochondrial ROS production is an area warranting investigation in situations where muscle weakness occurs and oxygen homeostasis is altered.

1.10 Therapeutic Strategies

1.10.1 Antioxidants and NAC

The use of antioxidants has been suggested as a therapy in the treatment of many respiratory-related disorders such as ALI, sepsis, COPD, lung fibrosis and cystic fibrosis where oxidative stress or imbalance may feature (Campos et al., 2012; Cazzola et al., 2015; Conrad et al., 2015; Day, 2008; Skov et al., 2015; Suter et al., 1994; Víctor et al., 2009). NAC, a thiol containing compound, is one such antioxidant with widespread clinical use and which has been used to treat a variety of respiratory and lung diseases as well as other pharmacological uses, such as the treatment of paracetamol overdose. NAC has been in clinical use for almost 50 years, primarily as a mucolytic but also in conditions characterised by oxidative stress or decreased GSH. It is the acetylated variant of the amino acid L-cysteine, is an excellent source of sulfhydryl groups, and is metabolised in the body into products capable of stimulating the synthesis of GSH, the important endogenous antioxidant, as well as acting directly as a free radical scavenger itself (Kelly, 1998).

NAC has been shown to alleviate mechanical ventilation-induced collagen accumulation in the rat and may be a potential candidate in preventing ventilation-induced lung fibrosis (Chen et al., 2015). Intravenous NAC administration during a 72 hour period has been shown to improve systemic oxygenation and reduce the requirement for ventilator support in patients presenting with mild to moderate ALI subsequent to various underlying conditions. However, in that study, the incidence of ARDS development and mortality were not reduced significantly by this intervention (Suter et al., 1994). In a recent study by Azuelos et al. (2015), using a mouse model of VIDD, they found that treatment with an I.P. injection of NAC immediately after the initiation of 6 hours of mechanical ventilation completely prevented the development of mechanical ventilation-induced diaphragmatic weakness. However, it did not suppress autophagy but rather it augmented autophagosome formation. They suggest that this may elucidate a novel mechanism whereby NAC exerts its beneficial effects on VIDD via stimulation of autophagy (excess ROS can inhibit autophagy), which may in fact be a beneficial adaptive response in the diaphragm, as discussed

previously in section 1.6.1.1.6 Autophagy, to the physiological stress of mechanical ventilation rather than representing a contributing factor to the development of VIDD.

1.10.2 NAC and Muscle Function

Intravenous NAC pretreatment appears to be beneficial in offsetting the rate of development of muscle fatigue in the rabbit diaphragm in situ (Shindoh et al., 1990). Superoxide scavengers have been shown to increase upper airway/pharyngeal dilator muscle (sternohyoid) force under both hyperoxic and hypoxic conditions *ex vivo* and ameliorate sternohyoid muscle dysfunction in a rodent model of CIH, and may be of potential therapeutic value in OSA and central sleep apnoea patients (Skelly et al., 2012b, 2010). Recently, it was found that NAC improved soleus, but not EDL, muscle fatigue resistance in a mouse model of peripheral arterial insufficiency (Roseguini et al., 2015), suggesting that the beneficial effects of NAC may be muscle specific under certain conditions. Finally, chronic antioxidant supplementation has been shown to prevent chronic hypoxia induced sternohyoid and diaphragm muscle weakness, and alter the activation of some of the chronic hypoxia induced signalling mechanisms in these muscles when given concomitantly (Lewis et al., 2015b, 2015c). Taken together these data suggest that NAC may hold great potential in alleviating muscle dysfunction in conditions of oxidative stress, hypoxia or muscle weakness.

Currently, little to no research exists regarding how acute hypoxia exposure may affect the diaphragm. This is surprising given the clinical prominence and relevance of acute hypoxia, alongside the fact that it often presents in conditions concomitant with diaphragm weakness/dysfunction .Weakness, particularly diaphragm muscle weakness, potentially caused/exacerbated by acute hypoxia could accelerate critical diaphragm failure and thus respiratory failure, extend the timeframe in which an acute-respiratory patient may require mechanical ventilation, contribute significantly to an inability to wean patients from mechanical ventilation, and could thus lead to poor prognosis in ICU patients. Investigation of the potential role that hypoxia, as a feature of acute respiratory disorders, may play in the development and/or exacerbation of diaphragmatic dysfunction in acute respiratory-related disorders and mechanically ventilated patients is therefore pertinent and clinically relevant.

1.11 Thesis Aims

The aim of this thesis is to determine if acute hypoxia is sufficient to cause diaphragm muscle dysfunction, to uncover some of the mechanisms by which this process may be occurring, and assess the efficacy of NAC in precluding any acute hypoxia-induced diaphragmatic effects. The sternohyoid muscle is also of interest due to its clinical relevance discussed earlier.

In order to study this, a mouse model was utilised whereby mice were exposed to different durations of acute hypoxia, with and without NAC pretreatment. Mouse diaphragm and sternohyoid muscle contractile function, and rat diaphragm contractile function, are reported in chapter 3. *In vivo* metabolic and respiratory responses to hypoxia of the mouse, as well as diaphragm proteasome activity and gene expression relating to metabolism, atrophy and SR calcium handling in diaphragm, sternohyoid, EDL and soleus (as comparators) muscles are described in chapter 4. Chapter 5 describes the effects of NAC pretreatment on diaphragm muscle contractile function, alongside diaphragm and sternohyoid signalling pathway responses to hypoxia relating to hypertrophy/atrophy and HIF signalling, as well as the effects of NAC pretreatment on these signalling processes in the diaphragm.

Chapter 2: Materials and Methods

2.1 Ethical Approval and Animal Licence

All protocols involving animals described in this study were approved by local ethics committee and were performed under licence from the Irish Government Department of Health and Children in accordance with EU legislation.

2.2 Animal Model

Mouse models of acute hypoxia were generated using adult male C57BL6/J mice (Envigo, formerly known as Harlan, UK). Mice (approximately 14 weeks of age) were placed in environmental plethysmography chambers (BUXCO Ltd, St. Paul, Minneapolis, USA), at room temperature, in which ambient oxygen levels were measured and adjusted to desired levels (Gas Analyzer, ML206, AD Instruments, Fig. 9), (Fig. 1(A)). Mice were exposed to 1, 4 or 8 hours of hypoxia (Fraction of inspired oxygen, F_iO_2 = 0.10) or normoxia (F_iO_2 = 0.21) (n = 8 per group, 4 groups). Reducing the fractional volume of oxygen within the environmental chamber results in a reduction of the fractional volume of oxygen in the inspired air in the mouse airway, alveoli and thus blood, resulting in hypoxaemia for the animals. Exposures to normoxia and hypoxia were performed in parallel, staggered, using a two-chamber set-up. In all instances, mice were in environmental chambers for approximately nine hours, between 0900h and 2100h (daytime) (Fig. 1(B)). For the first thirty minutes the mice were allowed to settle, under room air conditions. The second thirty minute period was used to establish baseline breathing parameters (see methods section 2.8 Whole-Body Plethysmography). Then the animal was exposed to 8 hours of normoxia for the control group, 7 hours of normoxia followed by 1 hour of hypoxia for the 1 hour hypoxia group, 4 hours of normoxia followed by 4 hours of hypoxia for the 4 hour hypoxia group, or 8 hours of hypoxia for the 8 hour hypoxia group. Designing the experiments in this way allowed us to reduce the number of animals needed as we did not need a control group matched to each exposure duration but rather one control group to compare with all groups, as animals in all groups spent the same amount of time in the environmental chambers. During gas exposure animals had access to water.

(A)

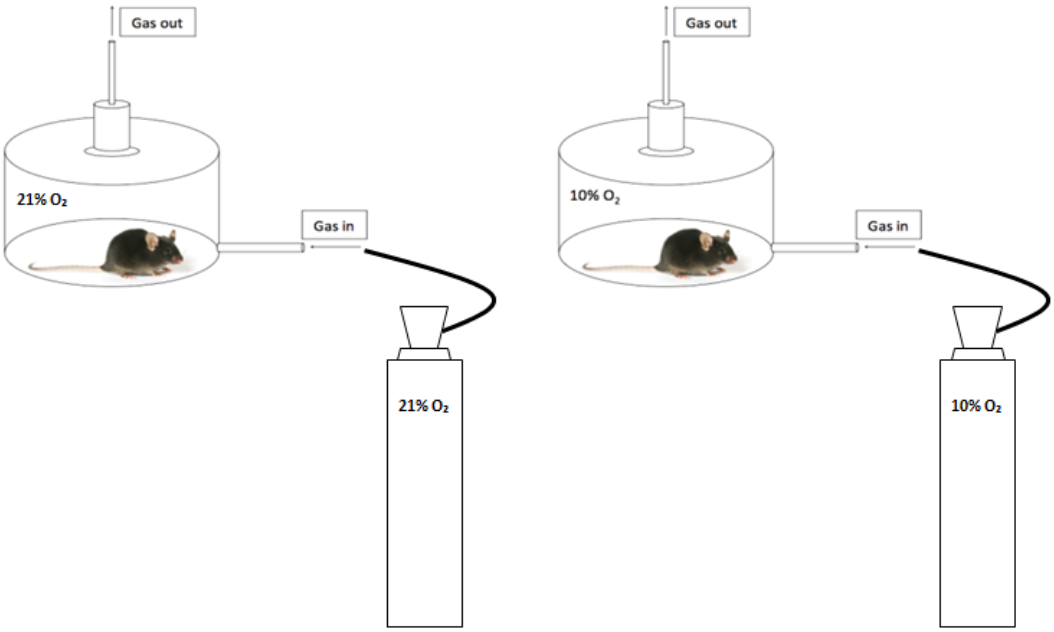

(B)

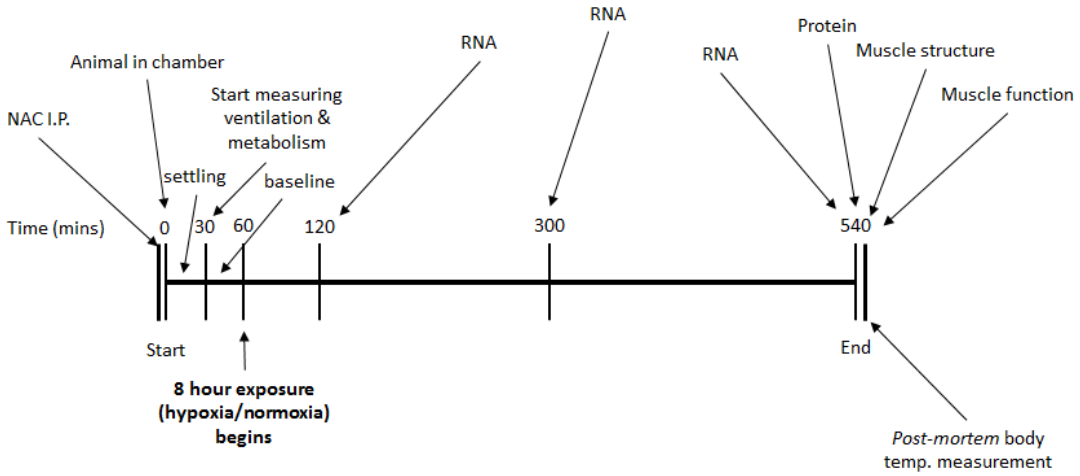

Figure 1: Gas exposure experiments. (**A)** Parallel environmental chamber set up and **(B)** Gas exposure experiments timeline.

2.2.1 Sample Size Calculation

N numbers for each group were based on previously published work by our lab group (McMorrow et al., 2011):

Diaphragm fatigue index (a percentage of force generation, relative to initial force, following a fatigue protocol/repeated stimulation): ~72.5% ± 6% and ~50% ± 6% in hypoxia and control groups respectively (difference to detect = 22.5%), n = 6 per group.
Standard deviation: ~14%
Experimental power desired: 80%
Confidence level: 95%
Sample size required: ~7 (n = 8 was used in case of animal/sample loss during technical experimental procedures)

Calculations

Sample size equation:

Sample size (n) = $(2 \times SD^2) \times (Z^{a/2} + Z^{\beta})^2/(d^2)$

SD = standard deviation = 14
$Z^{a/2} = Z^{0.05/2} = 1.96$ (Z tables) for 5% significance level
$Z^{\beta} = Z^{0.2} = 0.842$ (Z tables) for 80% power
d = effect size to detect = 22.5

$n = (2 \times 14^2) \times (1.96 + 0.842)^2 / (22.5^2) = 6.1$

n = ~7 (n = 8 was used in case of animal/sample loss during technical experimental procedures)

2.2.2 Exposure Groups

Five independent hypoxia exposure trials were carried out over the course of this study. Four of these were conducted on mice while one was conducted on rats, to determine if the phenotype was conserved across species.

2.2.2.1 Mice

Group 1: Thirty-two mice (4 groups; n = 8 per group) were exposed to hypoxia for 1, 4 and 8 hours while mice in the fourth control group were exposed to normoxia (mice in all groups spent the same amount of time in the environmental chambers). Mice in these groups were used to harvest tissue for RNA analysis.

Group 2: Sixteen mice (2 groups; n = 8 per group) were exposed to 8 hours of either hypoxia or normoxia in environmental plethysmography chambers, thus allowing us to monitor breathing in real-time, breath by breath, during gas exposure. Following gas exposure and respiratory analysis, muscles from these animals were excised for functional analysis.

Group 3: Thirty-two mice mice (4 groups; n = 8 per group) were exposed to either hypoxia (sixteen mice, two groups of eight) or normoxia (sixteen mice, two groups of eight) for 8 hours. One control group and one hypoxia group were utilised to monitor breathing, *in vivo* metabolism, *post-mortem* body temperature and muscle contractile function. Muscle samples from these animals were also preserved in cryoprotectant medium (OCT) for future studies to measure muscle fibre cross sectional area. Mice in the remaining hypoxia and normoxia groups were used to harvest tissue for protein analysis. *Post-mortem* body temperatures were also taken from these animals.

Group 4: Eight mice (1 groups; n = 8) were administered a single intraperitoneal (I.P.) injection of NAC immediately prior to entering the environmental chambers and subsequently being exposed to 8 hours of hypoxia. Following gas exposure these mice were used to analyse muscle function, *post-mortem* body temperature, and muscle tissue was snap-frozen for protein analysis.

2.2.2.2 Rats

Group 1: Sixteen male Wistar rats, approximately 14 weeks of age (Envigo, UK) (2 groups; n = 8 per group) were exposed to either hypoxia or normoxia for 8 hours in environmental plethysmography chambers. Breathing parameters, *in vivo* metabolism,

post-mortem body temperature and muscle contractile function were measured in these animals.

2.2.3 I.P Injection of NAC

To prepare the NAC solution for I.P injection, one phosphate buffer saline (PBS) tablet was dissolved to 200ml in deionised H_2O the day before injection. The PBS solution was then sterilised by autoclave and refrigerated until the next morning. NAC was dissolved in the PBS solution, pH adjusted to 7.4 using NaOH and filter (vacuum) sterilised. Mice were then injected with 200mg/kg NAC (Azuelos et al., 2015), at room temperature, via I.P. injection in the lower left quadrant using a sterile syringe.

Following gas exposures, animals were immediately euthanised using a rising concentration of CO_2 until narcosis, followed immediately by cervical dislocation to confirm euthanasia. Care was taken while performing this procedure in order to prevent causing damage to the sternohyoid muscles. Core *post*-mortem body temperature was determined immediately (within 10 seconds of euthanasia), via insertion of a rectal thermometer probe and body weights were recorded. Diaphragm, sternohyoid, EDL and soleus muscles were excised *post-mortem* and either immediately used for functional analysis or immediately preserved in OCT or snap-frozen in liquid nitrogen and stored at -80°C until further processing.

2.3 Gene Expression

2.3.1 RNA Extraction and Preparation

Total RNA was extracted, using Tripure Isolation Reagent (Roche Diagnostics Ltd., West Sussex, UK), from 20 – 70 mg of frozen muscle tissue using a General Laboratory Homogenizer (Omni-Inc., Kennesaw, Georgia, USA) as per the manufacturer's instructions, with an additional chloroform wash step during phase

separation. Following isolation, RNA was treated with TURBO DNA-free Kit (Life Technologies, Bio-Sciences, Dun Laoghaire, Ireland) as per the manufacturer's instructions. RNA quantity and purity was assessed by spectrophotometry with a Nanodrop 1000 (Thermo Scientific, Wilmington, Delaware, USA) (Fig. 2). RNA integrity was assessed using an agarose gel electrophoresis system (E-gel, Life Technologies) and visualisation of clear 18S and 28S ribosomal RNA bands (Fig. 3).

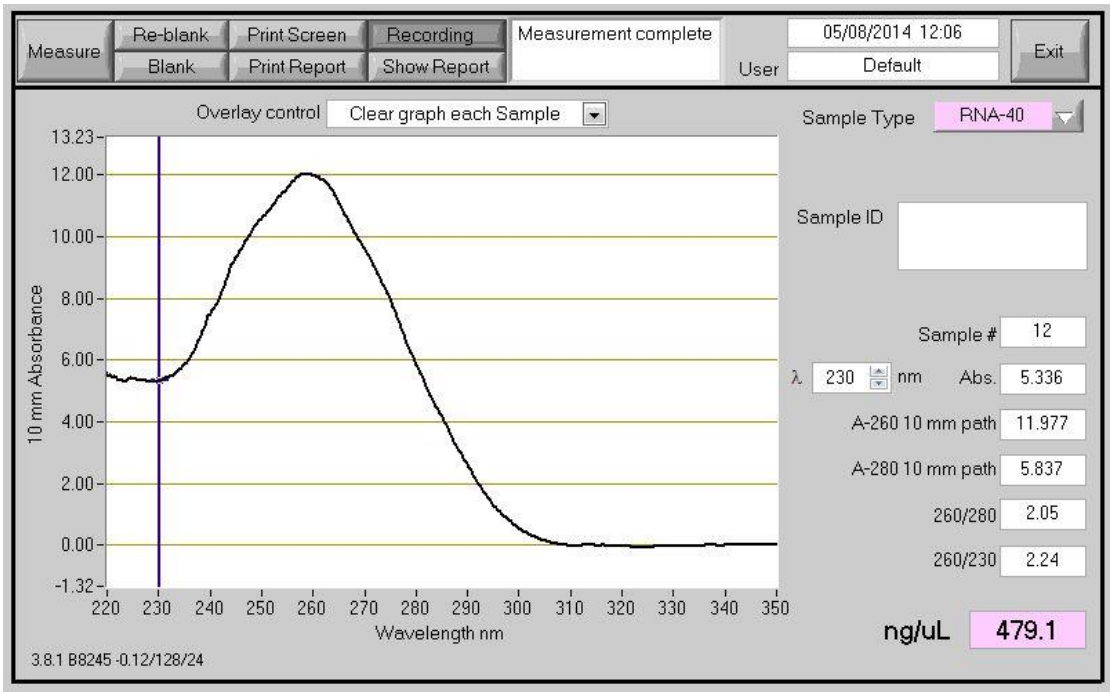

Figure 2: RNA quantity & purity control. Screenshot of the absorbance curve generated during the testing of one of the RNA samples on the Nanodrop 1000 showing the RNA concentration of the sample in the bottom right corner and above that the 260/280 and 260/230 ratios which, along with the single peak on the trace at 260, show that the purity of the sample is good.

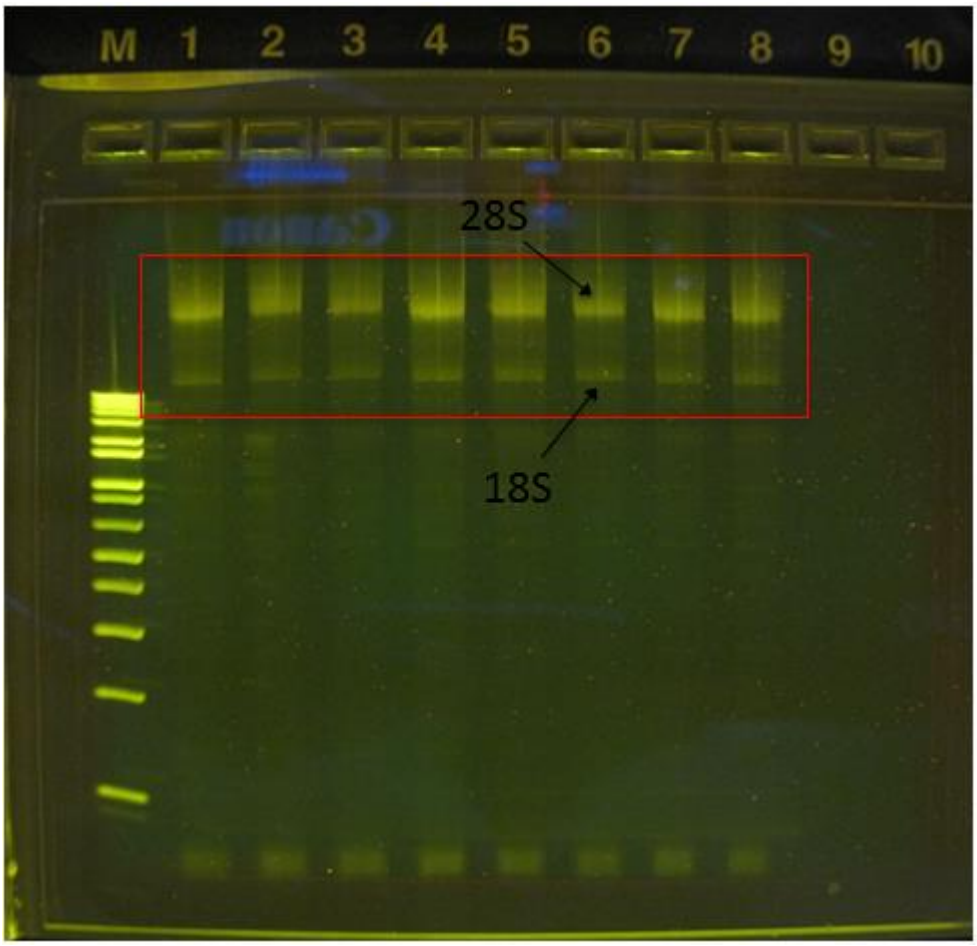

Figure 3: RNA integrity control. A picture of one of some of the RNA samples after being run on the E-gels system, clearly showing the separate 28S and 18S ribosomal RNA bands indicating the RNA integrity is preserved.

2.3.2 Reverse Transcription

RNA was reverse transcribed using Transcriptor First Strand cDNA Synthesis Kit (Roche Diagnostics Ltd.) as per the manufacturer's instructions.

2.3.3 qPCR

cDNA was amplified using Realtime ready Catalog or Custom Assays (Roche Diagnostics Ltd.) (Table 1, below) and Fast Start Essential DNA Probe Master (Roche Diagnostics Ltd.) in 20 µl reactions (5 µl cDNA and 15 µl master mix) as per the manufacturer's instructions, using the LightCycler 96 (Roche Diagnostics Ltd.) on 96-well plates (Fig. 4). All reactions were performed in duplicate and reverse transcriptase negatives, RNA negatives, cDNA negatives (no template) and plate

calibrator controls were used on every plate. Data were normalised to a reference gene, hprt1, to compensate for variations in input RNA/cDNA amounts and efficiency of reverse transcription. Several candidate reference genes were screened and hprt1 was found to be most stable considering tissue type, time and gas exposures. Figure 5 below shows the standard deviations of quantification cycles (Cq) of the best four candidate reference genes screened across muscle type and gas exposure time. A standard deviation of less than or equal to 0.5 was set as an acceptable level. Hprt1 was revealed to be the most stable reference gene for this model, with a standard deviation of 0.39. Relative expression was calculated using the ΔΔCT method to normalise expression of the gene of interest to that of the reference gene with changes in expression displayed as a fold change over the control group.

Gene Title	Gene Symbol	Assay ID	Configuration No.
Transcription Factors			
PGC-1α	Ppargc1a	313427	100067673
PGC-1β	Ppargc1b	313430	100096956
PPARα	Ppara	314790	100096947
NRF1	Nrf1	314790	100067682
NRF2	Gabpa	317384	100097269
NF-κB1	Nfkb1	300085	100067691
Metabolism			
UCP-3	Ucp3	313410	100096965
Calcium Handling			
SERCA1	Atp2a1	308007	100058338
SERCA2	Atp2a2	308005	100058347
Selenoprotein N1	Sepn1	316860	100067664
Junctophilin 1	Jph1	316620	100058374
Junctophilin 2	Jph2	316843	100067646
Ryanodine receptor 1	Ryr1	300626	100058365
Ryanodine receptor 3	Ryr3	316841	100067655
DHPR	Cacna1s	301252	100058383
Calsequestrin 1	Casq1	316619	100058356
Triadin	Trdn	316845	100067637
ITPR1	Itpr1	300435	100067743
Housekeeper gene			
HPRT1	Hprt1	307879	100058310
Hypoxia Signalling			
HIF-1α	Hif1a	300617	100067716
HIF-2α	Epas1	314102	100067707
Atrophy			
FOXO-1	Foxo1	317375	100107968
FOXO-3	Foxo3	317907	100113453
Atrogin-1	Fbxo32	317844	100107940
MuRF-1	Trim63	317843	100107959
Autophagy			
LC3b	Map1lc3b	317920	100115556
NIP3	Bnip3	311465	100115565
GABARAPL1	Gabarapl1	317923	100115574

Table 1: Realtime ready Catalog and Custom Assays used for cDNA amplification.

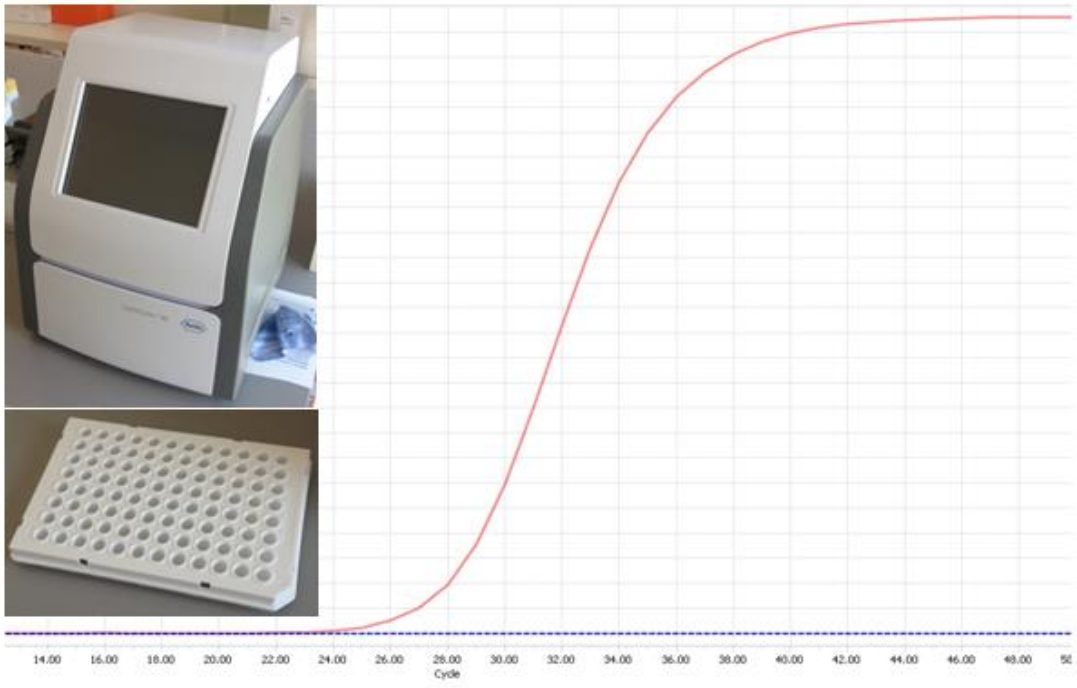

Figure 4: PCR. LightCycler 96 instument, 96-well plate and an example of a single amplification curve created from the reaction in one well on a 96-well plate following PCR.

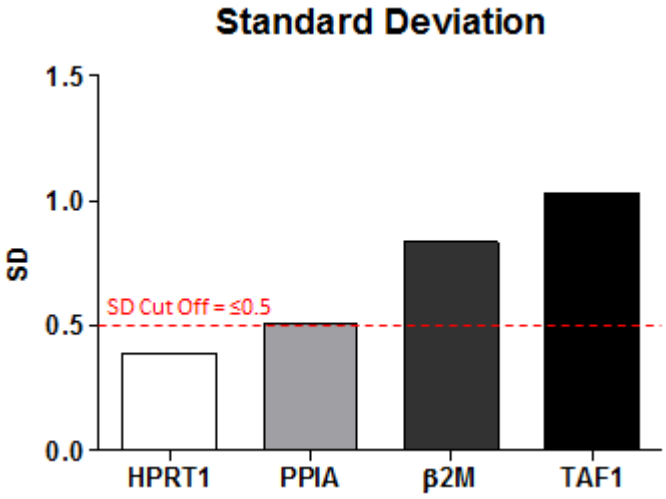

Figure 5: Standard deviation (SD) values of candidate reference genes. Each column represents the SD of that gene across 16 samples – a sample from each muscle (diaphragm, sternohyoid, EDL and soleus) in each treatment group (control, 1 hour, 4 hours and 8 hours of hypoxia).

2.4 Protein Extraction and Quantification

Frozen muscle samples were removed from storage at -80ºC, weighed and homogenised, on ice, in ice-cold 2.5% w/v modified radio-immunoprecipitation assay (RIPA) buffer (1X RIPA, deionised H_2O, 200mM sodium fluoride, 100mM phenylmethylsulfonylfluoride (PMSF), 1X protease inhibitor cocktail, 2X phosphatase inhibitor cocktail) using a General Laboratory Homogenizer (Omni-Inc., Kennesaw, Georgia, USA). Following 20 minutes lyse time on ice, with vortexing every 4 minutes, samples were centrifuged in a U-320R centrifuge (Boeckel + Co, Hamburg, Germany) at 14,000 RPM and at 4ºC for 20 minutes to separate insoluble cellular fractions from the protein homogenates. The protein containing supernatant was separated from the insoluble pellet in each sample and these were stored at -80ºC. The pellets were discarded.

The protein concentration of each sample was determined using a bicinchoninic acid (BCA) protein quantification assay (Pierce Biotechnology, (Fisher Scientific), Ireland) as per the manufacturer's instructions, at a dilution of 1:3.

2.5 Hypertrophy and Atrophy Signalling

2.5.1 Akt Signalling Panel – phospho-Akt, phospho-p70S6K, phospho-S6RP and phospho-GSK-3β

The Akt signalling panel measures the phosphorylated content of four key signalling proteins in the Akt signalling cascade, namely Akt (a.k.a. Protein kinase B), p70S6K, ribosomal protein S6 (S6RP) and glycogen synthesis kinase-3 (GSK-3β). The Mesoscale multiplex format assay (Mesoscale Discovery, Gaithersburg, USA) allows the measurement of all four of these phosphor-proteins in one well. The assay is a sandwich immunoassay. Each well of a 96-well plate is pre-coated with an array of capture antibodies targeted against each different protein of interest adhered to spatially distinct electrodes, or spots, within that well. The assay was carried out in accordance with the manufacturer's instructions. Briefly, samples were loaded onto

the 96-well plate and incubated to allow the proteins of interest to be captured by their specific capture antibodies. Each well was then washed and incubated in a detection antibody solution. The detection antibodies, specific for each protein of interest, are conjugated with an electrochemiluminescent compound, or tag. The detection antibodies bind to the captured proteins of interest, which are bound to their specific capture antibodies, on the distinct spots on the bottom surface of the well. This completes the antibody-protein-antibody sandwich (Fig. 6). The well was then washed again and read buffer was added, creating the correct chemical environment for electrochemiluminescence. The plate was loaded into the MSD SECTOR Imager (a specialised spectrophotometer from Mesoscale) where a voltage is rapidly applied to the distinct working electrodes on the plate spots resulting in the tags conjugated to the antibodies attached to those electrodes emitting light, which is read by the imager at 620nm. The intensity of this emitted light from each spot, separated both temporally and spatially, provided a quantitative measurement for each protein of interest in the sample. This assay was performed on diaphragm samples from control, 8 hours hypoxia and 8 hours hypoxia + NAC groups, and on sternohyoid samples from control and 8 hours hypoxia groups. A series of dilutions of an EDL sample was also assayed to demonstrate increased luminescence with increased protein content added to the well.

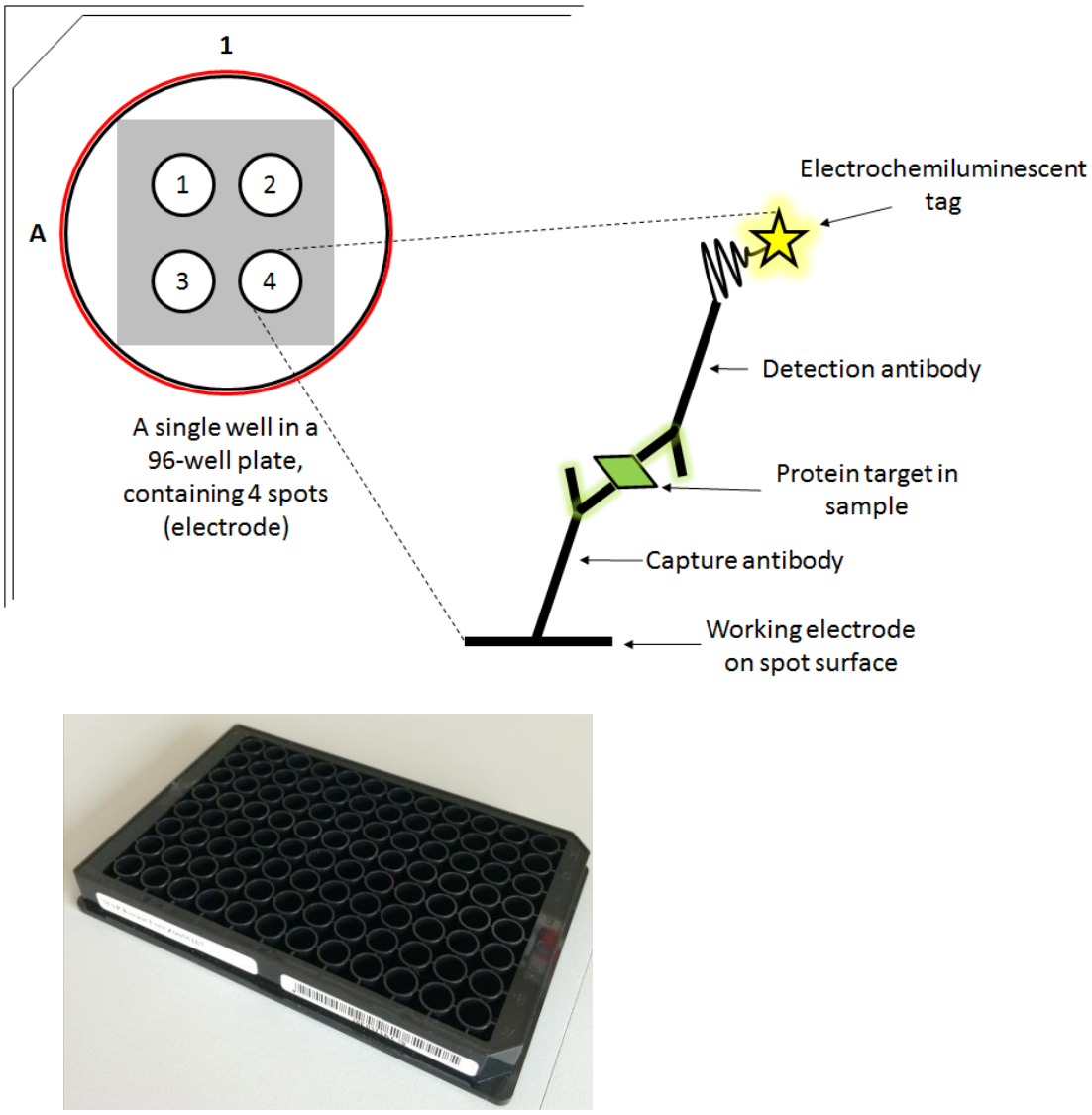

Figure 6: The Mesoscale 96-well plate. Including depiction of how the capture antibodies are laid out in distinct spots in each well and how the antibody-protein-antibody sandwich is formed.

2.5.2 Phospho-/Total mTOR Assay

The Phospho-/Total mTOR Assay allows the measurement of both phosphorylated mammalian Target of rapamycin (mTOR) and total mTOR content on spatially distinct spots as described above for the Akt signalling panel but with some variation to the incubation periods. This assay was performed on diaphragm samples from control, 8 hours hypoxia and 8 hours hypoxia + NAC groups, and on sternohyoid samples from control and 8 hours hypoxia groups. A series of dilutions of an EDL

sample was also assayed to demonstrate increased luminescence with increased protein content added to the well.

2.5.3 Phospho-FOXO3a Assay

The Phospho-FOXO3a Assay is a singleplex version of the assays described above, examining phosphorylated Forkhead box O3a (FOXO3a) only. This assay was performed on diaphragm samples from control, 8 hours hypoxia and 8 hours hypoxia + NAC groups, and on sternohyoid samples from control and 8 hours hypoxia groups. A series of dilutions of an EDL sample was also assayed to demonstrate increased luminescence with increased protein content added to the well.

2.5.4 MAP Kinase Phosphoprotein Assay – phospho-MAP, phospho-ERK1/2, and phospho-JNK

The MAP Kinase Phosphoprotein Assay quantifies at the phosphoprotein content of the Mitogen-Activated Protein (MAP) kinases ERK1/2, p38 and JNK in a multiplex fashion as described above. This assay was performed on diaphragm samples from control, 8 hours hypoxia and 8 hours hypoxia + NAC groups, and on sternohyoid samples from control and 8 hours hypoxia groups. A series of dilutions of an EDL sample was also assayed to demonstrate increased luminescence with increased protein content added to the well.

2.6 Hypoxia Signalling

2.6.1 Total HIF-1α Assay

The Total HIF-1α Assay examines the Hypoxia-Inducible Factor (HIF) 1α protein content in samples. This assay was performed on diaphragm samples from control, 8 hours hypoxia and 8 hours hypoxia + NAC groups, and on sternohyoid samples from control and 8 hours hypoxia groups. A series of dilutions of an EDL sample was also

assayed to demonstrate increased luminescence with increased protein content added to the well.

2.7 Proteasome Activity

Chymotrypsin-like 20S proteasome activity was measured via fluorescence in a spectrophotometric assay as per the manufacturer's instructions (Abcam) and using a Spectramax M3 (Molecular Devices, CA, USA) spectrophotometer (Fig. 7). The assay employs a peptide substrate tagged to AMC. In the presence of proteasome activity the AMC tag is released and fluoresces. The kit includes a positive control in the form of Jurkat cell lysate with high proteasome activity and a specific proteasome inhibitor MG-132 which suppresses all proteolytic activity attributed to proteasomes, thus allowing the differentiation of proteasome activity from other protease activity in the sample. This assay was performed on diaphragm samples from control and 8 hours hypoxia groups on a white 96-well plate and all samples and positive controls were assayed with and without the proteasome inhibitor. The samples, positive controls and standards were added to the 96-well plate. Inhibitor was added to their assigned wells (an equal volume of assay buffer was added to the uninhibited wells) and proteasome substrate was added to all wells except the standards. The plate was then incubated at 37°C in the spectrophotometer (protected from light) for one hour while fluorometric readings were made kinetically over that time at Ex/Em = 350/440 nm. There is a slight nonlinearity to the reaction kinetics at the beginning due to the lag time it takes for the reaction to mix and warm to 37°C. Readings were made from the linear range of the reaction. Non-proteasome activity was then subtracted from total proteasome activity to give proteasome activity. One unit of proteasome activity is defined as the amount of proteasome which generates 1nmol of AMC per minute at 37°C.

Figure 7: Spectromax M3 spectrophotometer.

2.8 Whole-Body Plethysmography

Respiratory recordings were made throughout the period of gas exposure in unrestrained, freely-behaving mice using whole-body plethysmography (Buxco Ltd). This allowed the measurement of breathing parameters on a breath-by-breath basis in real-time (Fig. 8). The technique is based on the measurement of pressure changes within the environmental chamber by a sensitive pressure transducer. These pressure changes are influenced by the animal's breathing. The system allows for the continuous flow of gas, in this instance air or 10% O_2 in N_2, from an external source, through the chamber set-up. The chambers were fitted with screen pneumotachographs which allowed air to pass out of the chamber, so that small changes in pressure within the chamber were directly proportional to flow. The system was calibrated each morning, prior to beginning the experiment, by slowly and steadily injecting a known volume of air (1 ml) into the chamber, such that the volume of gas injected is within defined parameters of deflection along the x axis (time) and y axis (flow), allowing the system to accurately calibrate for determining respiratory parameters in the mouse. The Buxco FinePointe software derives ventilatory parameters from these small flow signals. Mice were introduced to the chamber and allowed to settle and acclimatise to their surroundings while breathing room air (normoxia) for approximately 30 minutes. Next, 30 minutes of baseline recording was then made under room air conditions. Then, respiratory recordings were made over 8 hours under either normoxic or hypoxic conditions depending on

which group the mouse was assigned to. Respiratory rate (frequency) and tidal volume were measured and from these values minute ventilation (the product of respiratory rate and tidal volume) was determined. These values were normalised to animal weight.

(A)

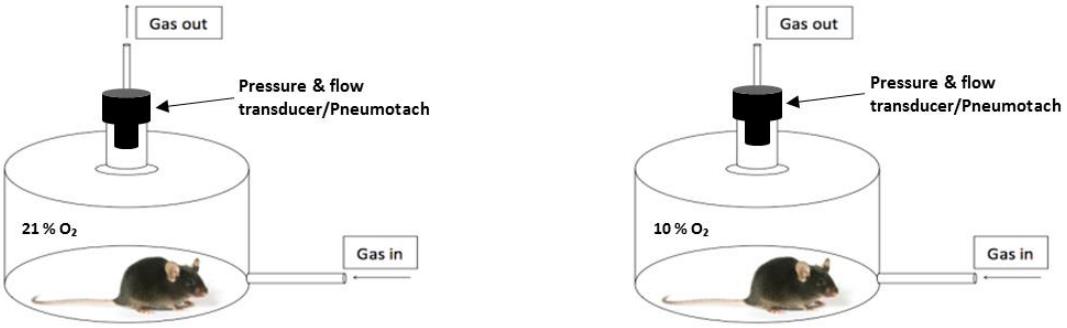

(B)

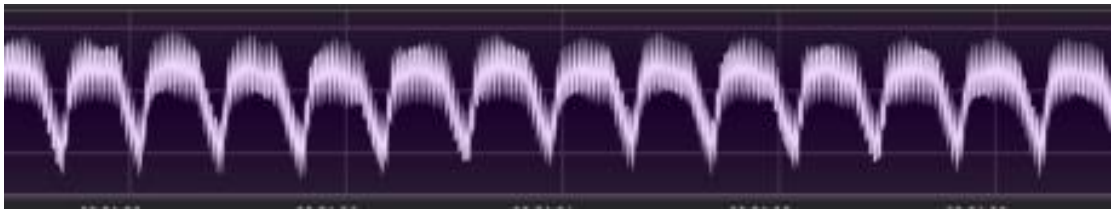

Figure 8: Plethysmography set-up. (A) Two chamber set-up, run in parallel, one containing a mouse under hypoxic conditions and one containing a mouse under normoxic conditions. **(B)** FinePointe software respiratory trace showing respiration in real time breath-by-breath.

2.9 *In-Vivo* Metabolism Measurement

The O_2 consumption and CO_2 production of mice were both monitored over the course of the gas exposure, as an index of *in-vivo* metabolism. This was performed using a Gas Analyzer (ML206, AD Instruments, Fig. 9). The gas analyser allows the measurement of respiratory gas concentrations from mice in the chambers. It uses an

infrared CO_2 transducer, calibrated to output voltages from 0 – 1 V proportional to the CO_2 concentration between 0 – 10% of the sampled gas. The O_2 transducer uses absorption spectroscopy in the visible spectrum whereby narrow band light is supplied by a laser diode, thermally tuned to an emission line in the oxygen spectrum, and is directed through a chamber through which the gas to be sampled flows. The detector on the other side of this sampling chamber then detects any change in the light intensity at the wavelength of interest. The more oxygen in the sample, the less light that the detector receives. Using a damped, micro-vacuum sampling pump, the analyser is used to sample gas from both the chamber input and the chamber output gases for percentage O_2 and CO_2. The analyser was calibrated using calibration gas mixtures. Room air was used to obtain one of the calibration points for each of O_2 (20.95%) and CO_2 (0.039%) and 10% O_2 in nitrogen was used to obtain a second O_2 calibration point (10%) while carbogen (5%CO_2/95%O_2) was used to obtain the second CO_2 calibration point (5%). From these values, incorporating the flow of gas through the chamber and the body weight of the animal (taken *post-mortem*), we are able to calculate the oxygen consumption (VO_2) and carbon dioxide production (VCO_2), which are indices of basal metabolic rate in the animal. These data also allowed us to examine the respiratory exchange ratio and the ventilatory equivalent. As described at the end of section 2.2, *post-mortem* body temperature was also taken as another, albeit less precise, index of metabolic rate.

$$VO_2 = (flow_{in} \times O_2conc_{in}) - (flow_{out} \times O_2conc_{out})$$

$$VCO_2 = (flow_{out} \times CO_2conc_{out}) - (flow_{in} \times CO_2conc_{in})$$

Ventilatory equivalent for $CO_2 = V_E/VCO_2$

Ventilatory equivalent for $O_2 = V_E/VO_2$

$$RER = VCO_2/VO_2$$

(A)

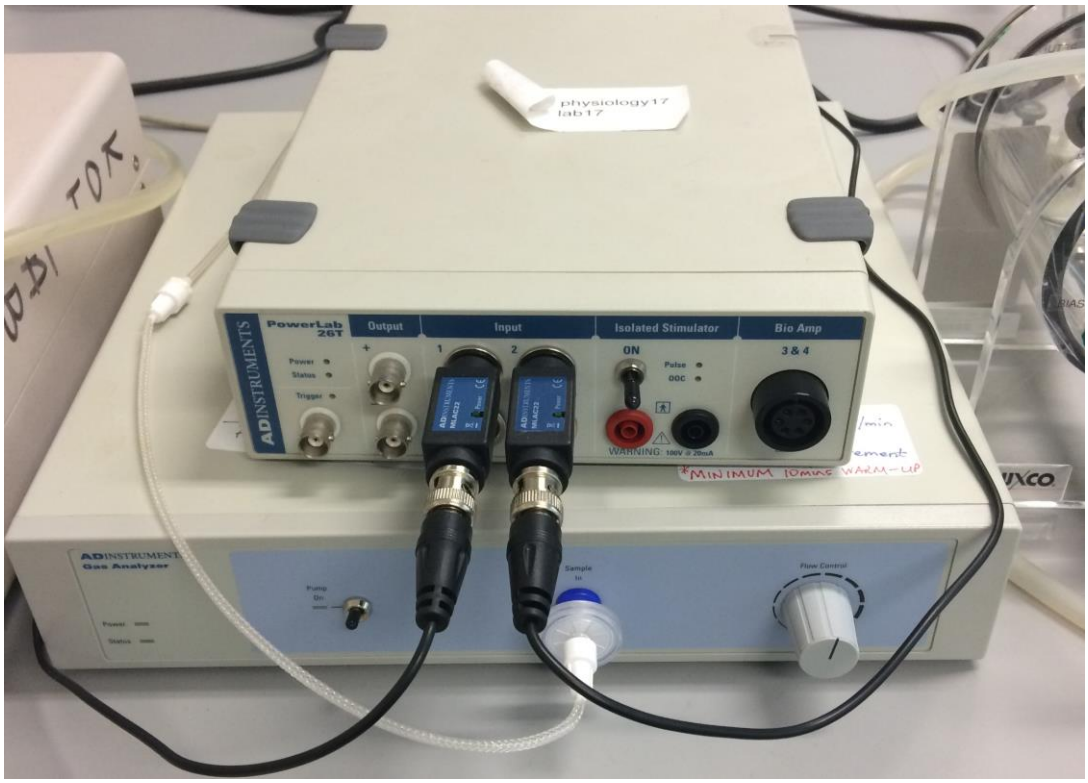

(B)

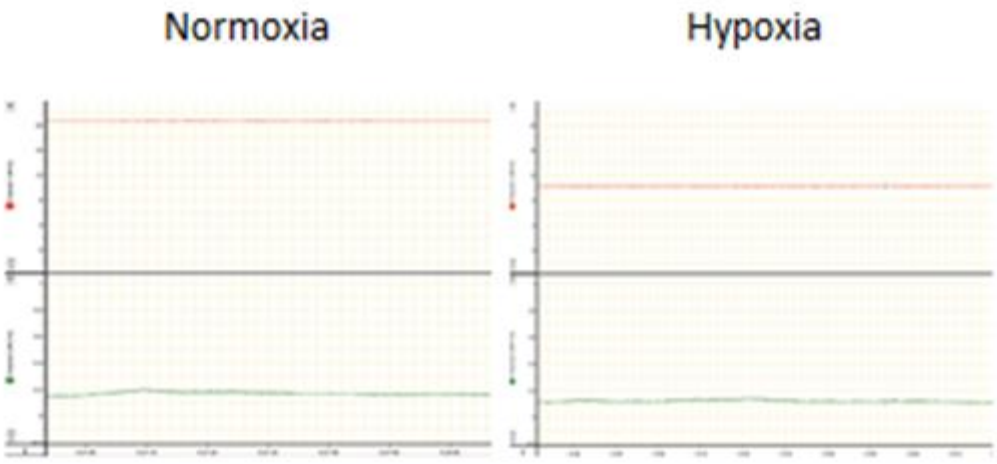

Figure 9: *In-vivo* metabolism measurement. (A) AD Instruments Gas Analyzer (on bottom) running through an AD Instruments PowerLab (on top) before going to a PC. **(B)** Example of O_2 (red) and CO_2 (green) traces under normoxia and hypoxia.

2.10 Muscle Function – Experimental Protocol

2.10.1 Muscle Dissection and Preparation

Following euthanasia, as described above at the end of section 2.2, diaphragm and sternohyoid muscles were excised immediately for functional analysis. During the dissection a ventral incision was made along the midline of the torso from below the ribcage up to the top of the neck. The paired sternohyoid muscles and diaphragm, with central tendon and lower rib attached and intact, were excised and immediately placed in a storage bath containing continuously gassed hyperoxic (95% O_2/5% CO_2) Krebs solution (NaCl 120mM, KCl 5mM, Ca^{2+} gluconate 2.5 mM, $MgSO_4$ 1.2 mM, NaH_2PO_4 1.2 mM, $NaHCO_3$ 25 mM, glucose 11.5 mM and d-tubocurarine 25 μM (a neuromuscular blocking agent)) at room temperature. The sternohyoid muscles were separated and a thin strip (approximately 1mm in diameter) was cut longitudinally from one muscle and returned to the storage bath to recover from the dissection before function was assessed. A strip of diaphragm muscle was taken from the right hemidiaphragm running from the rib, parallel to the long axis of the muscle fibres, to the central tendon (approximately 2mm in diameter at the rib end and slightly narrower at the central tendon end) and the small sections of the rib and central tendon which were attached to the muscle were dissected out with it. The diaphragm strip was then returned to the storage bath to recover from the dissection.

2.10.2 Isolated Muscle Preparation *In-Vitro*

Sternohyoid muscle function was assessed first as the diaphragm is stable in the storage bath for a longer period of time. A single strip of sternohyoid muscle was suspended vertically in a water-jacketed organ bath. The bath was filled with Krebs solution which was bubbled with hyperoxic carbogen (95% O_2/5% CO_2) and the set-up was maintained at 35°C. The strip of sternohyoid muscle was mounted, using non-elastic string, between a stationary hook at the bottom and a dual-mode force transducer (Aurora Scientific, Canada) at the top (Fig. 10), and was flanked by a pair of platinum plate electrodes. For the diaphragm strip, the rib end was mounted on the stationary hook and the central tendon was attached to the transducer. The dual-mode force transducer allowed the measurement of both isometric and isotonic contractions,

be measuring contractile force and shortening distance and velocity respectively, when the muscle was stimulated. The position of the force transducer could be adjusted, using a micro-positioner, to alter the length of the muscle strip. Once mounted in the bath, the muscle strip was left to equilibrate for 10 minutes before initiating the experimental protocol.

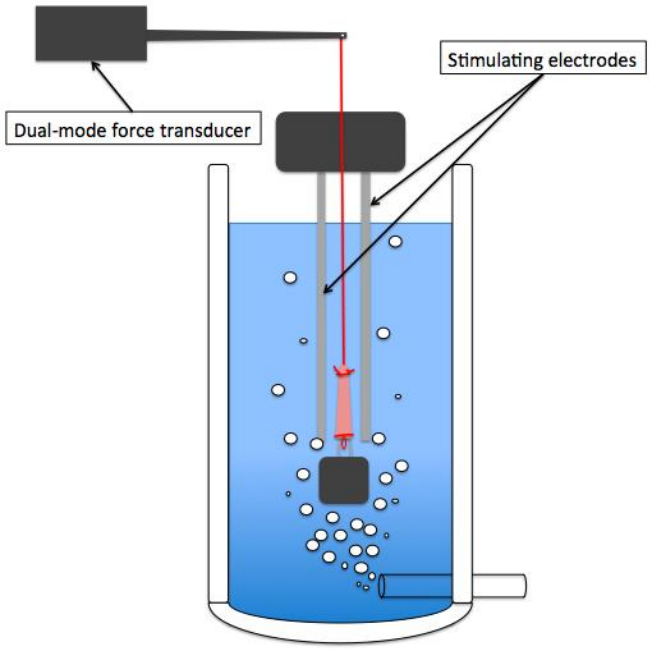

Figure 10: The muscle bath set-up.

2.10.3 Protocol

2.10.3.1 Isometric Protocol

For measurements of isometric contractions, the force transducer was set to maximum rigidity (~500nM; >100% load).

2.10.3.1.1 Optimum Length

The optimum length (L_o – the length at which peak isometric tetanic force is generated in response to a supra-maximal stimulation) of the muscle strip was determined by intermittently stimulating the muscle and adjusting the micro-

positioner, and thus muscle length, between those stimulations. Once L_o was determined, this length was measured and recorded (in mm) and the muscle strip was kept at this length for the entire isometric protocol. The measurement was taken from the knot in the string at the hook end to the knot in the string at the transducer end so as to only include muscle fibres actively contracting between the hook and the force transducer.

2.10.3.1.2 Peak Isometric Twitch and Tetanic Force and Twitch Contractile Kinetics

The peak isometric twitch force was generated by stimulating the muscle strip with a single pulse. Twitch contractile kinetics – time to peak (TTP) and half relaxation time (T_{50}) – were measured from the peak twitch contraction recorded. Peak isometric tetanic force was assessed by stimulating the muscle with a supra-maximal stimulation voltage (previously determined voltage, above which an increase in stimulation voltage will not result in an increase in contractile force, 80 V) at 100 hertz (Hz) for 300ms. Figure 11 below is an example of a diaphragm tetanic contraction. Peak specific force (F_{max}) was calculated in N/cm^2 of muscle cross sectional area (CSA). CSA was calculated by dividing muscle weight (weighted following blotting and air drying for 10 minutes) by the product of L_o and the specific density – assumed to be $1.056 g/cm^3$.

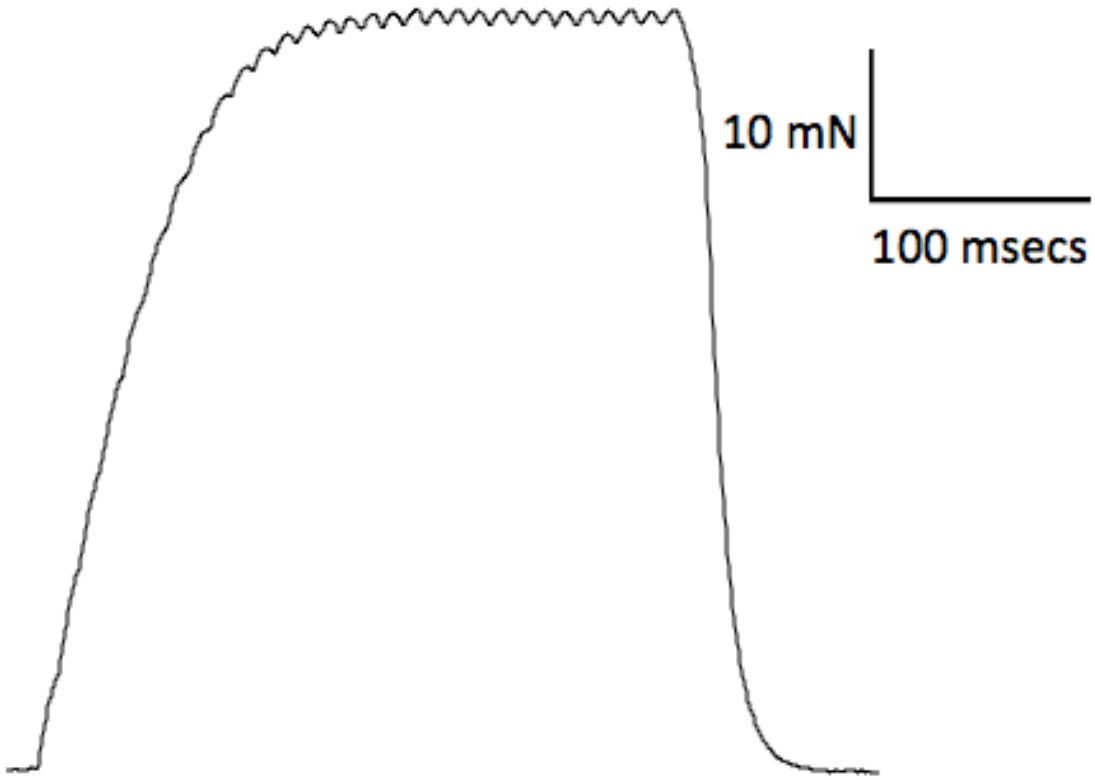

Figure 11: An example of a diaphragm tetanic contraction.

2.10.3.1.3 Force – Frequency Relationship

Next, the relationship between stimulation frequency and force generation was assessed by stimulating the muscle strip at increasing stimulation frequencies from 10 Hz to 160 Hz and recording the force generated at each frequency. Forces recorded as each frequency were then normalised to the muscle strip and expressed as specific forces in N/cm^2 (described above).

2.10.3.2 Isotonic Protocol

For measurements of isotonic contractions, the force transducer was set to varying rigidity (0% to 100% load).

2.10.3.2.1 Step Test

2.10.3.2.1.1 Shortening Length and Velocity

The force transducer was initially set to a minimum rigidity, approximately 0%, and the muscle was stimulated to contract against "0% Load", a load on the muscle that equals approximately 0% of the peak isometric tetanic force of that muscle strip, at L_o. This rigidity, or load on the muscle, was then increased in incremental steps from 0% to 100% of peak isometric tetanic force while eliciting a muscle contraction at each step. Shortening length was defined as the maximum distance of shortening over the duration of the contraction. Shortening velocity was derived from the distance of shortening during the first 30 ms of the shortening phase of the contraction as this is when contraction velocity is greatest. Peak shortening length and velocity were achieved at "0% load". Peak specific shortening (S_{max}) was defined as the length of shortening per optimal length (L/L_o). Peak specific shortening velocity (V_{max}) was defined as L_o/s.

2.10.3.2.1.2 Work and Power

From the protocol described above, work and power could be calculated at each step of the % load protocol as the product of force x shortening length and force x shortening velocity, respectively. From the work-load and power-load relationships achieved through this protocol, peak work and peak power were extrapolated. Peak specific mechanical work (W_{max}) was calculated as Joules/cm^2 and peak specific mechanical power (P_{max}) as Watts/cm^2.

2.10.3.2.1.3 Fatigue

After a 5 minute rest period following the step test, muscle endurance, or resistance to fatigue, was assessed by repeatedly stimulating the muscle strip at 100 Hz for 300 ms trains occurring every 2 seconds for a 5 minute period under isotonic conditions with a 33% load on the force transducer lever. 33% load is approximately the load at which peak power is achieved. Shortening length, shortening velocity, work and power were all extrapolated from each measurement, every 2 seconds, over the 300 second period, with the muscle strip at L_o.

2.11 Data Analysis

GraphPad Prism (GraphPad Software Inc., CA, USA) was used to perform statistical analysis. Tests for normality and equal variance were performed (KS normality test, F test and Bartlett's test where appropriate), Student's t-test was performed for comparisons between two groups, and one-way or two-way ANOVA was utilised for comparisons between multiple groups larger than two and/or those with two different independent variables and appropriate post-hoc tests were used for multiple comparisons –Tukey's test and Bonferroni's test. Statistical significance was taken at the level of $P < 0.05$. All data is expressed as mean ± SEM.

Chapter 3: Acute Hypoxia Induces Respiratory Muscle Dysfunction in Mice and Rats

3.1 Introduction

In this chapter, respiratory muscle contractile performance is assessed following 8 hours of normoxia (Control) or 8 hours of hypoxia (Hypoxia). Muscle contractile function is tested *ex vivo* in this study in order to elucidate functional changes intrinsic to the muscle itself, and not attributed to other influential factors such as: conscious effort, anatomical shape of the diaphragm, neuronal drive – which are eliminated by this method (discussed in chapter 2) of isolating viable muscle strips in the muscle bath set-up and utilising d-tubocurarine as a neuromuscular blocking agent (Lewis et al., 2015a, 2015c, Skelly et al., 2012b, 2012c, 2011, 2010; Williams et al., 2015).

The diaphragm muscle, as discussed in chapter 1, is a highly malleable muscle which has been shown to functionally adapt, or maladapt, to hypoxia in animal models of chronic hypoxia (1 – 6 weeks) (Carberry et al., 2014a; Gamboa and Andrade, 2012, 2010, Lewis et al., 2015a, 2015c; McMorrow et al., 2011). However, as of yet, there is a lack of information concerning how acute hypoxia influences diaphragm and sternohyoid muscle contractile performance.

Acute hypoxia, as discussed in chapter 1, is a prominent feature of acute respiratory conditions such as acute respiratory distress syndrome (ARDS) and ventilator-induced/associated lung injury (VILI/VALI). These conditions can go on to induce ICUAW, including respiratory muscle weakness, a sequela which is a robust predictor of poor outcome in patients (Batt et al., 2013; Sieck and Mantilla, 2013; Supinski and Callahan, 2013). Indeed, patients receiving chronic mechanical ventilation are weak and deconditioned, which can be due to one, or likely a combination, of inactivity, disease processes, infection and sepsis, and they respond to aggressive whole-body and respiratory muscle training with improved strength, weaning outcome and functional status (Martin et al., 2005). Whether or not hypoxia has a role in this weakness is unknown. However it is noteworthy that models of high altitude hypoxia also affects respiratory muscle contractile function (El-Khoury et al., 2012, 2003). Thus, insight into the adaptations of the respiratory muscle to acute hypoxic exposure may have wide-ranging relevance, from the clinic to altitude physiology.

Isometric muscle contractions, contractions of the muscle at a fixed and maintained length (i.e. no muscle shortening), allow the measurement of peak force generating capacity of the muscle at a particular stimulation frequency. This is a useful measure and/or index of muscle strength and performance overall. However, during normal diaphragm contraction during breathing *in vivo*, the expansion of the chest cavity and thus the generation of thoracic pressure changes necessary for breathing requires diaphragm muscle shortening, i.e. isotonic contractions (Goldman et al., 1978; Gorman et al., 2002; Pengelly et al., 1971). Isotonic muscle contraction are contractions of the muscle whereby the muscle length shortens at various speeds against various fixed loads on the muscle between 0 and 100 % load (100% load = F_{max} of the muscle). Due to the variety of diaphragm functional activity necessary to maintain life, from the rhythmic activity of breathing to airway clearance manoeuvres, it is essential to review the broader scope of diaphragm contractile performance when examining how acute hypoxia potentially affects diaphragm function.

The sternohyoid muscle, unlike the mixed muscle fibre type of the diaphragm, is composed of fast twitch muscle fibres and functions to maintain upper airway calibre during inspiration. Similarly to the diaphragm, while work has been carried out examining how chronic hypoxia affects the sternohyoid muscle (Lewis et al., 2015c), nothing is known about how (8 hours) acute hypoxia affects sternohyoid muscle performance. Clinically, the effects of acute hypoxia on the sternohyoid may have relevance to patients with acute respiratory diseases who also present with upper airway dysfunction and/or OSA – which is most prevalent among obese individuals. Indeed, obesity or body mass index is associated with ARDS development (Gong et al., 2010; Karnatovskaia et al., 2014). Moreover, persistent upper airway muscle weakness increases the risk of obstructive airway events during sleep, such that acute hypoxia could conceivably increase risk of subsequent sleep apnoea, which gives rise to further exposure to hypoxia and the establishment of a perpetual vicious cycle (O'Halloran, 2016; O'Halloran et al., 2016).

Animal models are useful in that they afford the examination of the effects of acute hypoxia on respiratory muscle without the influence of other confounding factors which may be present in disease states. The reason for repeating the assessment of

diaphragm muscle contractile function in the rat following acute hypoxia is that the mouse and rat adopt slightly different metabolic strategies under hypoxic conditions (Haouzi et al., 2009). Therefore it was important to confirm that the muscle weakness observed in the mouse was also seen in the rat, and therefore more likely related to hypoxic stress *per-se*, rather than being solely due to the metabolic strategy adopted by the mouse (discussed further in chapter 4).

Given the effects of chronic hypoxia on diaphragm and sternohyoid muscle contractile function (Lewis et al., 2016, 2015d; Lewis and O'Halloran, 2016), in this chapter we assessed whether an acute bout of sustained hypoxia would be sufficient to cause respiratory muscle dysfunction. Given that chronic hypoxia has been shown to weaken respiratory muscle, it would be interesting to determine whether an acute bout of hypoxia would be sufficient to cause respiratory muscle dysfunction, notwithstanding that the mechanisms at play may be quite different between respiratory muscle responses to acute and chronic hypoxia.

Diaphragm muscle performance in the mouse is reported first, in section 3.2.1, followed by mouse sternohyoid muscle performance in section 3.2.2 and finally diaphragm isometric characteristics in the rat are reported in section 3.2.3. Assessment of EDL muscle function was attempted following respiratory muscle assessment, but a stable, repeatable preparation was not attained, possibly due to deterioration of the preparation while it was being kept in the storage bath during assessment of respiratory muscle performance. This period of time, between dissection and testing, was evidently too long.

Chapter Aims

The primary aims of this chapter are: 1) to assess the effects of an acute bout of sustained hypoxia on respiratory muscle function, primarily the diaphragm, in the mouse and 2) to determine if this effect is conserved in another mammalian species, the rat.

Methods Summary

Respiratory muscle contractile function was examined *ex vivo* in a muscle bath set-up as described in more detail in Chapter 2 Materials and Methods, Section 2.10.

Briefly, a strip of sternohyoid or diaphragm muscle from the mouse, or diaphragm muscle from the rat, was fixed between a stationary hook and a dual mode force transducer in an organ bath, filled with hyperoxic Krebs solution maintained at 30°C, allowing contractile performance to be assessed when the muscle strip was stimulated to contract.

When assessing muscle isometric contractile performance, the length of the muscle strip was fixed to the length at which the muscle produced the highest force – optimum length (L_o). Under isometric conditions, peak force generating capacity, isometric twitch kinetics and the relationship between force generation and stimulation frequency of the muscle strip were measured.

When assessing muscle isotonic contractile performance, the muscle strip was allowed to shorten when contracting against a fixed load (% Load) on the muscle strip, expressed as a percentage of the maximum force generating capacity of the muscle (F_{max}). This allowed the measurement of shortening distance, velocity, work and power at various loads on the muscle.

Finally, when measuring muscle fatigue, the muscle strip was repeatedly stimulated to contract every 2 seconds for a 5 minute period under isotonic conditions at a 33% load on the force transducer lever, allowing the measurement of shortening distance, velocity, work and power over repeated stimulation.

These data were normalised to muscle cross sectional area.

3.2 Chapter Results

3.2.1 Mouse Diaphragm

Diaphragm isometric peak tetanic force, peak twitch force and twitch kinetics are shown in Fig. 1. There was a statistically significant reduction in diaphragm peak tetanic force (Fig.1A) (29.5 ± 3.2 vs. 20.8 ± 2.0 mean ± SEM N/cm^2; Control vs. Hypoxia; n = 8 per group; p = 0.0334; unpaired t-test) of ~30% following 8 hours of hypoxia compared with control. There was no statistically significant change in diaphragm peak twitch force (Fig.1B) (4.4 ± 0.5 vs. 3.3 ± 0.4 mean ± SEM N/cm^2; Control vs. Hypoxia; n = 8 per group; p = 0.1160; unpaired t-test) after 8 hours of hypoxia. There was no statistically significant change in diaphragm TTP (Fig.1C) (14.2 ± 0.4 vs. 14.4 ± 0.4 mean ± SEM N/cm^2; Control vs. Hypoxia; n = 8 per group; p = 0.6676; unpaired t-test) after 8 hours of hypoxia. There was no statistically significant change in diaphragm T50 (Fig.1D) (14.3 ± 0.5 vs. 14.4 ± 0.6 mean ± SEM N/cm^2; Control vs. Hypoxia; n = 8 per group; p = 0.8737; unpaired t-test) after 8 hours of hypoxia. Although 8 hours of hypoxia did not affect diaphragm twitch kinetics, it did reduce the peak force-generating capacity of the diaphragm muscle by ~30%.

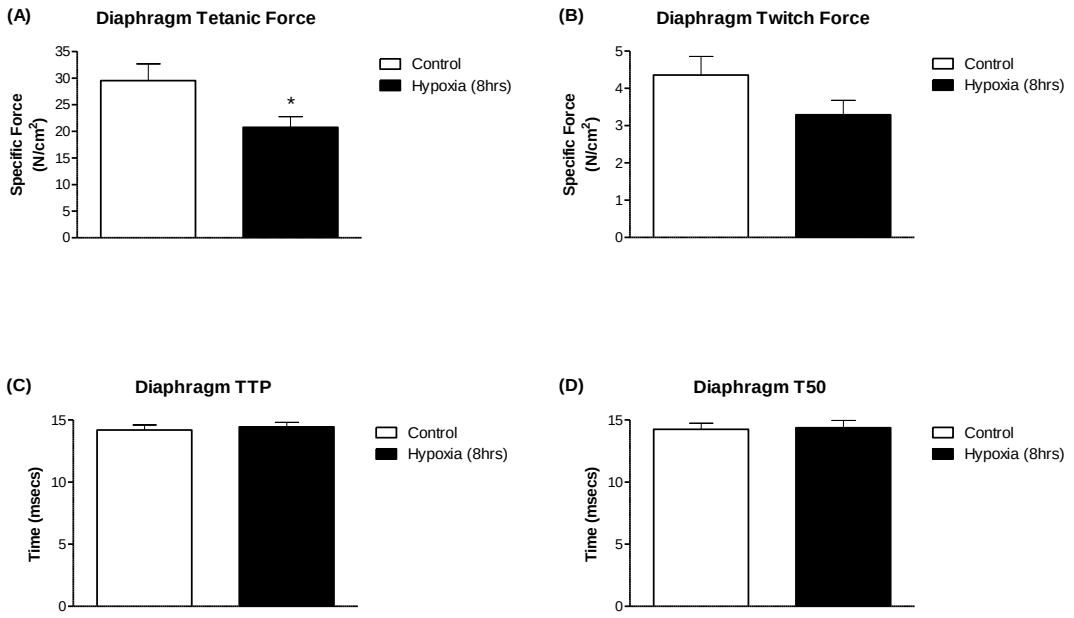

Figure 1: Diaphragm isometric peak tetanic force, peak twitch force and twitch kinetic parameters. (A) Diaphragm peak tetanic force (mean ± SEM) expressed as force per unit CSA (N/cm^2); n = 8 per group. (B) Diaphragm peak twitch force (mean ± SEM) expressed as force per unit CSA (N/cm^2); n = 8 per group. (C) Diaphragm time to peak twitch tension (TTP) (mean ± SEM) expressed as time (msecs); n = 8 per group. (D) Diaphragm twitch half relaxation time (T50) (mean ± SEM) expressed as time (msecs); n = 8 per group. *$p < 0.05$, unpaired t-test.

The mouse diaphragm force–frequency relationship in a separate cohort of animals is displayed in Fig. 2. As one would expect, the specific force-generating capacity of the diaphragm muscle increased as the stimulation frequency is increased, from 10 to 160 Hz, and this effect of stimulation frequency on muscle contractile force was statistically significant ($p< 0.0001$, two-way ANOVA). More importantly however, hypoxia caused a significant reduction in force generation over the range of stimulation frequencies tested ($p = 0.0112$, two-way ANOVA) compared with normoxia. The weakness was most prominent at higher frequencies. The hypoxia group was 37% weaker than the control group at maximum stimulation frequencies. There was no interaction (gas x stimulation; $p = 0.8634$). Bonferroni's multiple comparisons test did not reveal any statistically significant differences at individual stimulation frequencies.

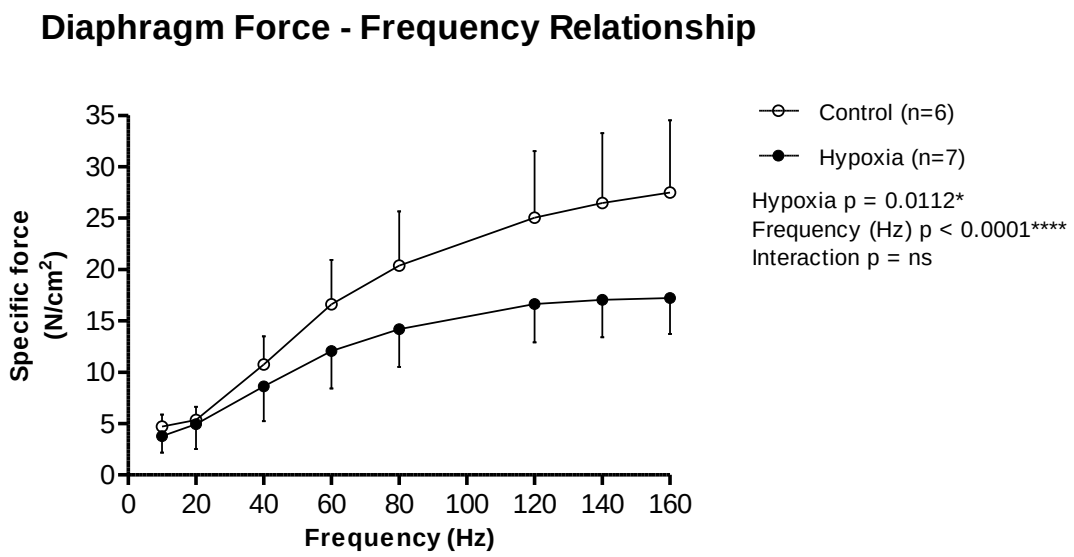

Figure 2: Diaphragm muscle force–frequency relationship in the mouse.

Diaphragm specific force (mean ± SEM) expressed as force per unit CSA (N/cm^2) as a function of stimulation frequencies ranging between 10 and 160 Hz.

Diaphragm muscle peak power, peak work, maximum shortening velocity and maximum shortening are displayed in Fig. 3. There were no statistically significant changes to (A) peak power (15.0 ± 2.1 vs. 12.1 ± 1.5 mean ± SEM Watts/cm^2; Control vs. Hypoxia; n = 8 per group; p = 0.2780; unpaired t-test), (B) work (2.1 ± 0.3 vs. 1.9 ± 0.2 mean ± SEM Joules/cm^2; Control vs. Hypoxia; n = 8 per group; p = 0.6; unpaired t-test), (C) velocity (4.0 ± 0.2 vs. 4.1 ± 0.3 mean ± SEM L_o/s; Control vs. Hypoxia; n = 8 per group; p = 0.6932; unpaired t-test) or (D) shortening (0.4 ± 0.02 vs. 0.4 ± 0.02 mean ± SEM L/L_o; Control vs. Hypoxia; n = 8 per group; p = 0.1464; unpaired t-test) between control and hypoxia groups.

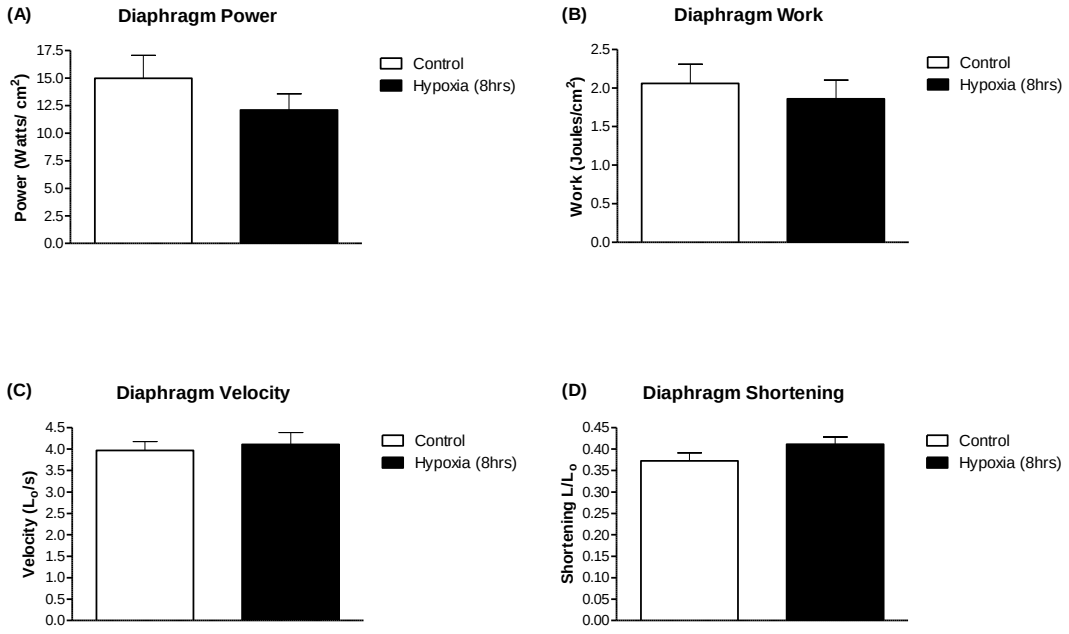

Figure 3: Diaphragm muscle peak power, peak work, maximum shortening velocity and maximum shortening. (A) Diaphragm peak power (mean ± SEM) expressed as power/CSA (Watts/cm^2); n = 8 per group. (B) Diaphragm peak work (mean ± SEM) expressed as work/CSA (Joules/cm^2); n = 8 per group. (C) Diaphragm peak shortening velocity (mean ± SEM) expressed as optimal lengths/time (L_o/s); n = 8 per group. (D) Diaphragm peak shortening distance (mean ± SEM) expressed as length/optimal length (L/L_o); n = 8 per group.

Diaphragm muscle power–load relationship is shown in Fig. 4. This is specific power generated by the muscle at incremental loads on the muscle from 0-100% of the peak force generation capacity of the muscle strip. Two-way ANOVA revealed significant effects of both % load ($p < 0.0001$) and hypoxia ($p = 0.0011$) on power generation over the full range of loads tested; there was no interaction ($p = 0.6829$). The load on the muscle when it contracts, as one would expect, affects the power output of the muscle in a classic bell-shaped fashion, peaking at a load of around 40% of the maximum force generation capacity of the muscle. Hypoxia diminished the power–load curve, reducing diaphragm power output over the range of loads as a whole, although not at every individual % load.

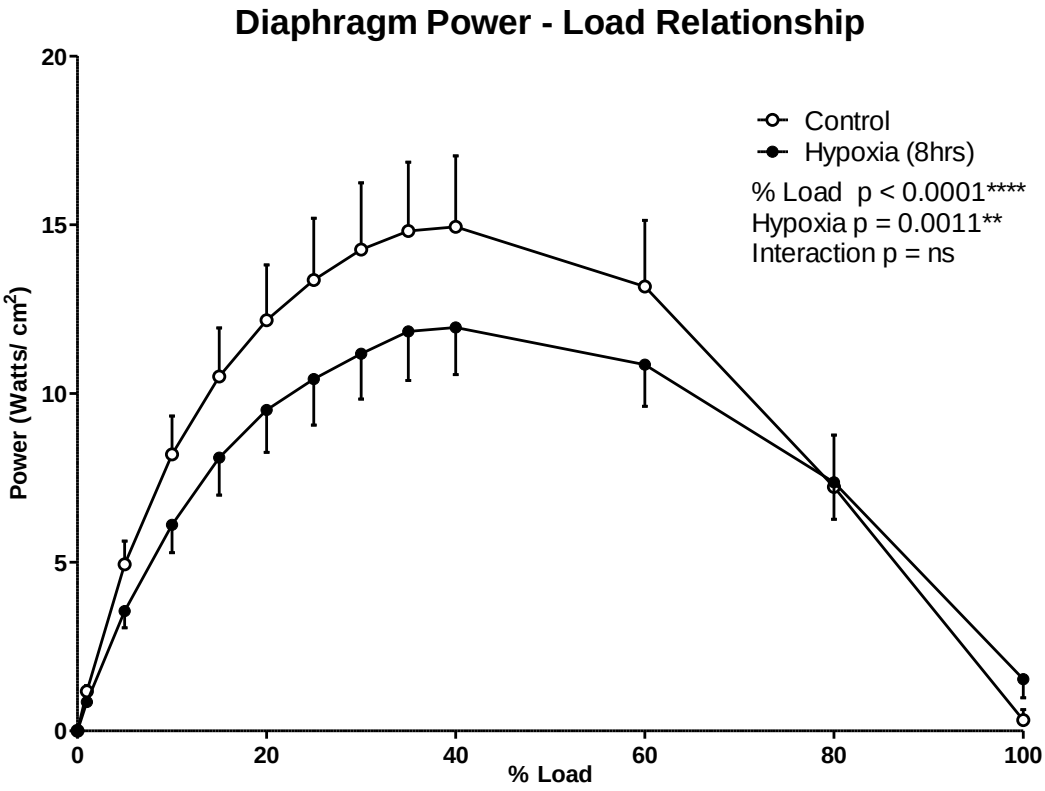

Figure 4: Diaphragm muscle power–load relationship. Diaphragm power (mean ± SEM) expressed as power per unit CSA (Watts/cm^2) as a function of the load on the muscle expressed as a percentage of peak force (force/peak force*100); n = 8 per group.

The diaphragm muscle work–load relationship is shown in Fig. 5. This is work generated by the muscle at incremental loads on the muscle from 0-100% of the peak force generation capacity of the muscle strip. Two-way ANOVA revealed a significant effect of % load ($p < 0.0001$), but not hypoxia ($p = 0.0820$) on work over the full range of loads tested; there was no interaction ($p = 0.8096$). Although hypoxia did not significantly reduce the mechanical work over the range of loads, a slight rightward shift is observed in the hypoxia curve.

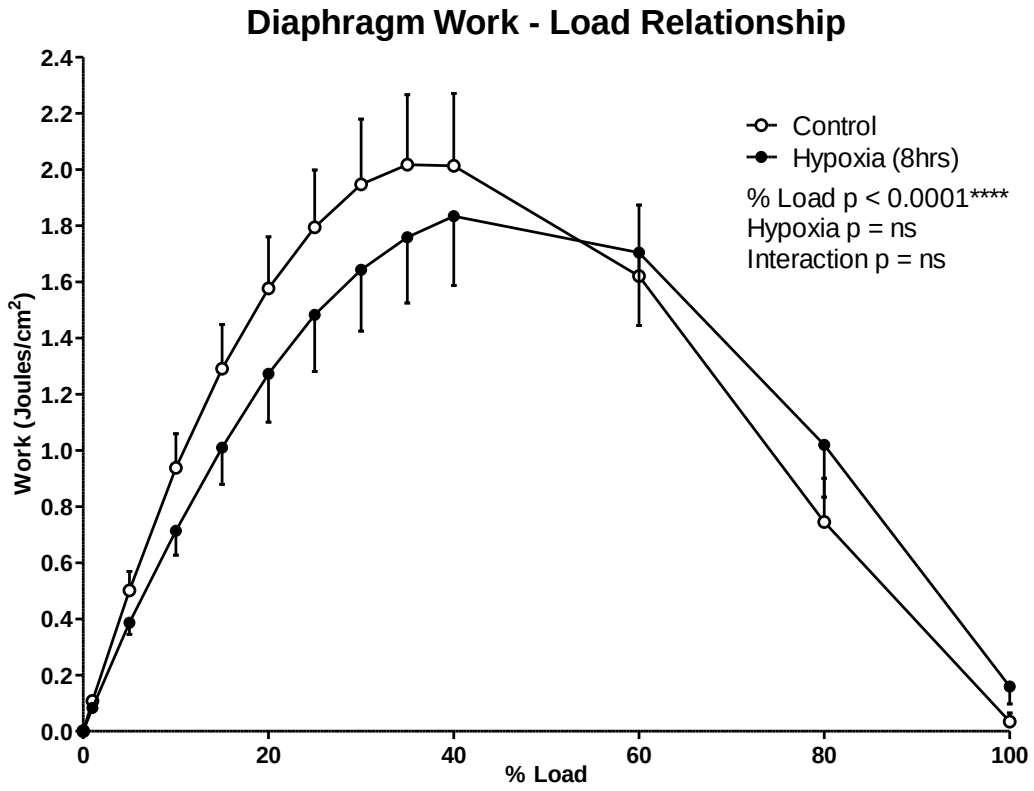

Figure 5: Diaphragm muscle work–load relationship. Diaphragm work (mean ± SEM) expressed as work per unit CSA (Joules/cm^2) as a function of the load on the muscle expressed as a percentage of peak force (force/peak force*100); n = 8 per group.

The diaphragm muscle shortening velocity–load relationship is shown in Fig. 6. This is shortening velocity of the muscle at incremental loads on the muscle from 0-100% of the peak force generation capacity of the muscle strip. Two-way ANOVA revealed a significant effect of % load ($p < 0.0001$) and hypoxia ($p = 0.003$) on velocity over the full range of loads tested; there was no interaction ($p = 0.9996$). Shortening velocity was reduced in both groups as % load increased, and the hypoxia group produced a slightly elevated velocity over the range of loads in comparison with the control group.

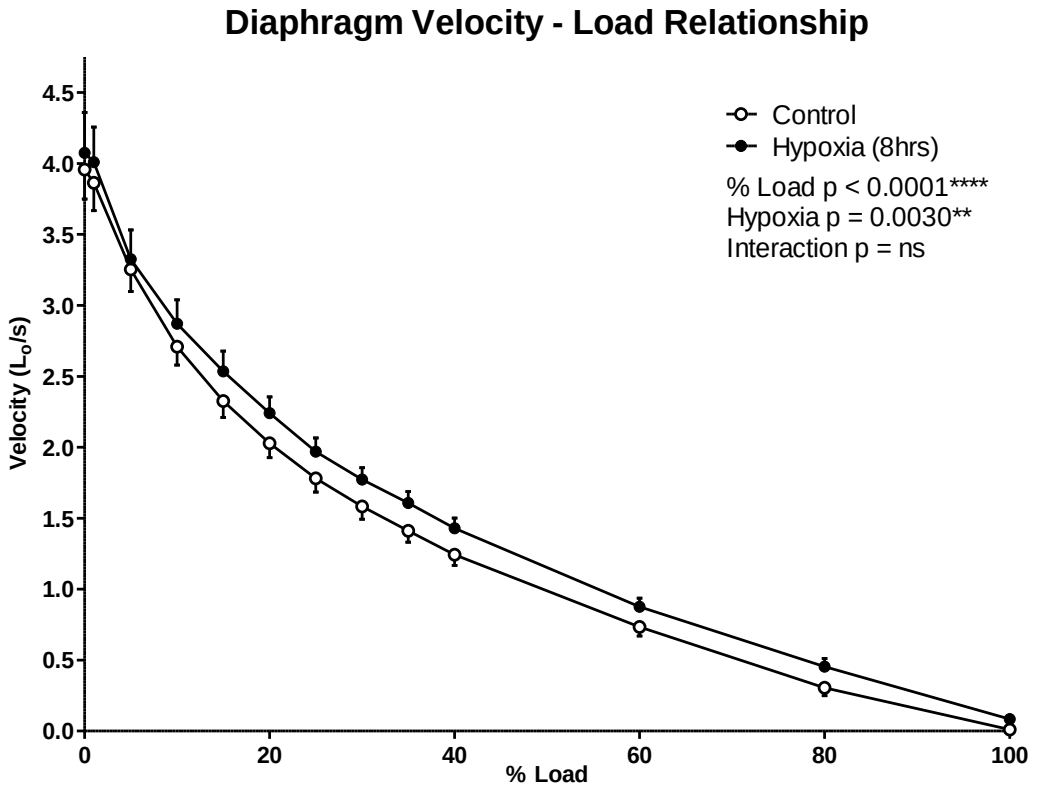

Figure 6: Diaphragm muscle velocity–load relationship. Diaphragm shortening velocity (mean ± SEM) expressed as optimal lengths per unit time (Lo/s) as a function of the load on the muscle expressed as a percentage of peak force (force/peak force*100); n = 8 per group.

The diaphragm muscle shortening–load relationship is shown in Fig. 7. This is specific shortening of the muscle at incremental loads on the muscle from 0-100% of the peak force generating capacity of the muscle strip. Two-way ANOVA revealed a significant effect of % load ($p < 0.0001$) and hypoxia ($p < 0.0001$) on shortening over the full range of loads tested; there was no interaction ($p = 0.4155$). Shortening distance was reduced in both groups as % load increased, and the hypoxia group shortened by a greater distance over the range of loads on the muscle compared with the control group.

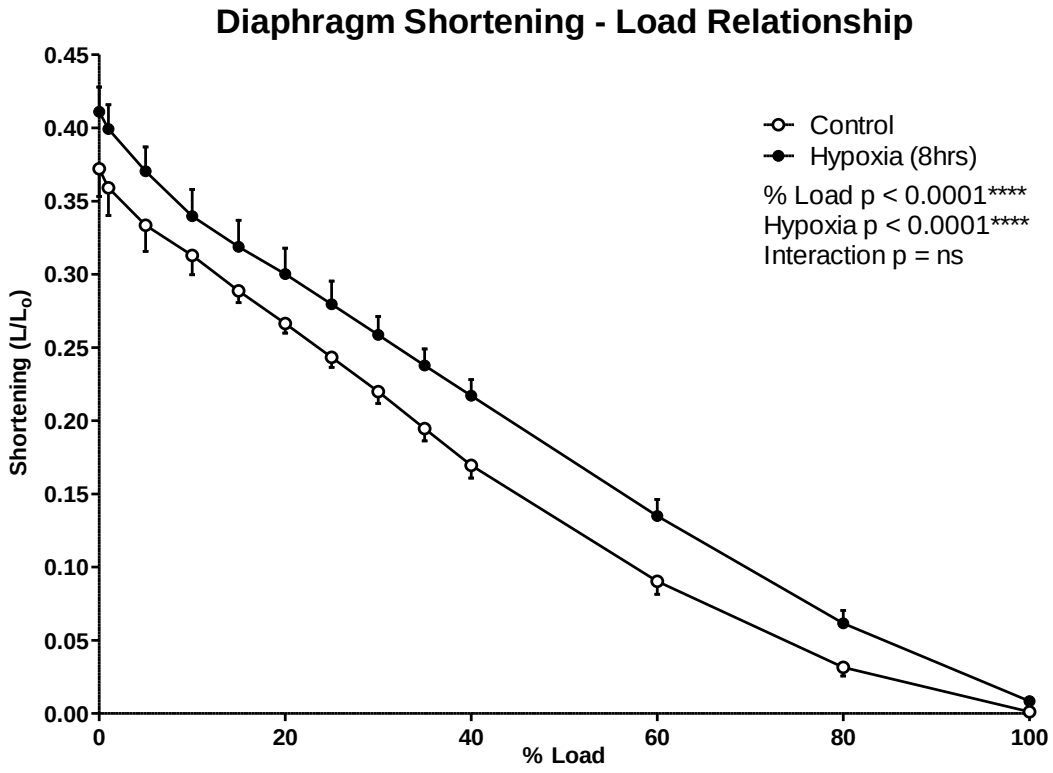

Figure 7: Diaphragm muscle shortening–load relationship. Diaphragm shortening (mean ± SEM) expressed as length per unit optimal length (L/L_o) as a function of the load on the muscle expressed as a percentage of peak force (force/peak force*100); n = 8 per group.

Fatigue

Diaphragm muscle fatigue parameters are displayed below. Fig. 8 shows diaphragm fatigue in terms of power output over time during repeated fatiguing stimulation every 2 seconds for a 300 second period (the power–time fatigue relationship). Data is displayed in (A) absolute power values and (B) the fall off in power over time relative to initial power production at the beginning of the fatigue protocol. For both approaches, two-way ANOVA revealed a significant effect of time ($p < 0.0001$) and hypoxia ((A) $p < 0.0001$ & (B) $p < 0.0001$) on diaphragm specific power (fatigue); there was no interaction ($p = 1.0$). The data reveal that the diaphragm muscle was weaker (although not with statistical significance) at the beginning of the fatigue protocol in the hypoxia group compared with control, producing a lower power

output. However, as the protocol progresses, the power produced by the hypoxia diaphragm did not fall off to the same extent as the power output of the control diaphragm, such that both groups produced the same power output by the end of the protocol (i.e. an apparent fatigue tolerance).

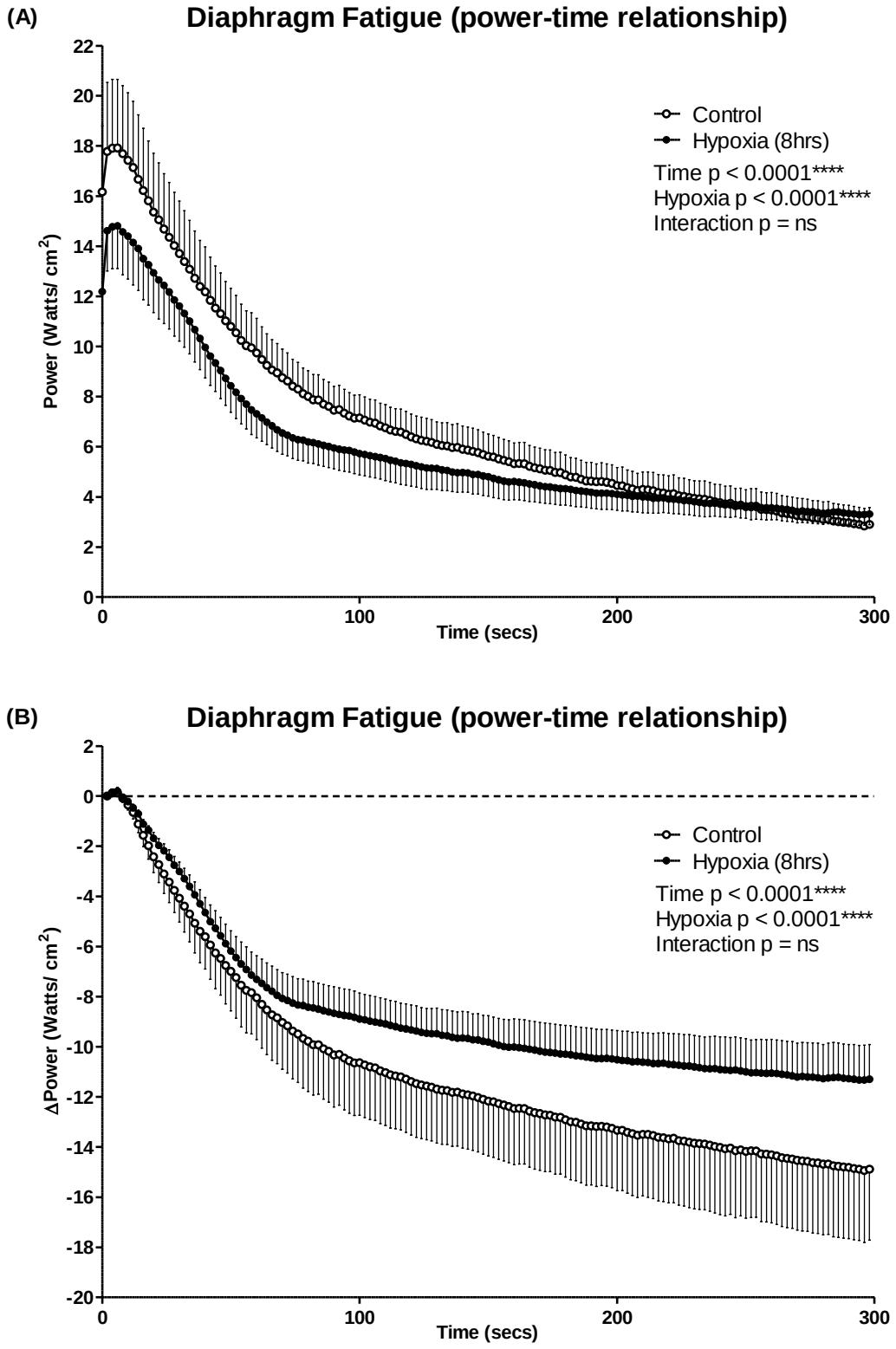

Figure 8: Diaphragm muscle fatigue (power–time relationship). Diaphragm muscle power (mean ± SEM) expressed as (A) power per unit CSA (Watts/cm^2) as a function of time (secs) over a 300sec period of repeated stimulation every 2 seconds and as (B) the change (Δ) in power (Watts/cm^2) relative to the initial power of that

muscle upon the first contraction of the fatigue protocol as a function of time over the 300sec fatiguing period of repeated stimulation every 2 seconds; n = 7-8 per group.

Fig. 9 shows diaphragm fatigue in terms of work over time during repeated stimulation (the work–time relationship). Two-way ANOVA revealed a significant effect of time ($p < 0.0001$) and hypoxia ($p < 0.0001$) on diaphragm work (fatigue) over time; there was no interaction ($p = 1.0000$). Again, similar to observations in the power fatigue data, the hypoxia group produced less work than the control group at the beginning of the protocol but did not fall off to the same extent, producing the same amount of work as the control group by the end of the protocol (i.e. an apparent fatigue tolerance).

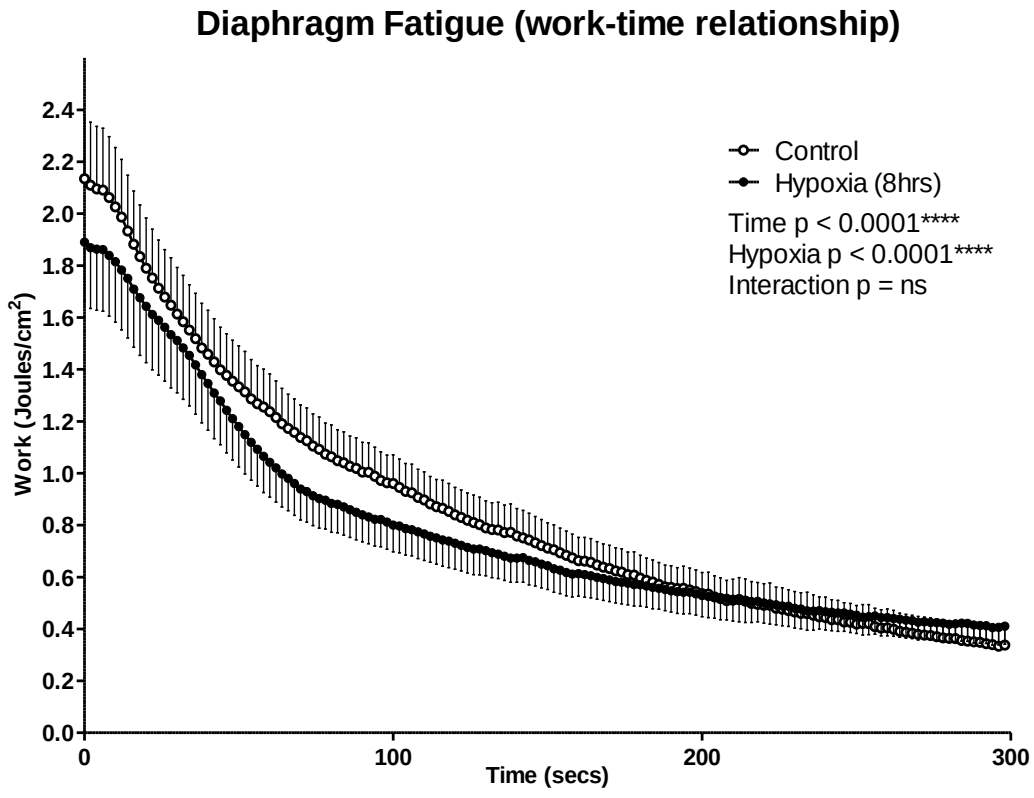

Figure 9: Diaphragm muscle fatigue (work–time relationship). Diaphragm muscle work (mean ± SEM) expressed as work per unit CSA (Joules/cm^2) as a function of time (secs) over a 300sec fatiguing period of repeated stimulation every 2 seconds; n = 7-8 per group.

Fig. 10 shows diaphragm muscle fatigue in terms of muscle shortening velocity over time during repeated stimulation (the velocity–time relationship). Two-way ANOVA revealed a significant effect of time ($p < 0.0001$) and hypoxia ($p < 0.0001$) on diaphragm muscle specific shortening velocity over time; there was no interaction ($p = 1.0000$). The hypoxia group produced a faster shortening velocity over the course of the fatigue protocol compared with the control group.

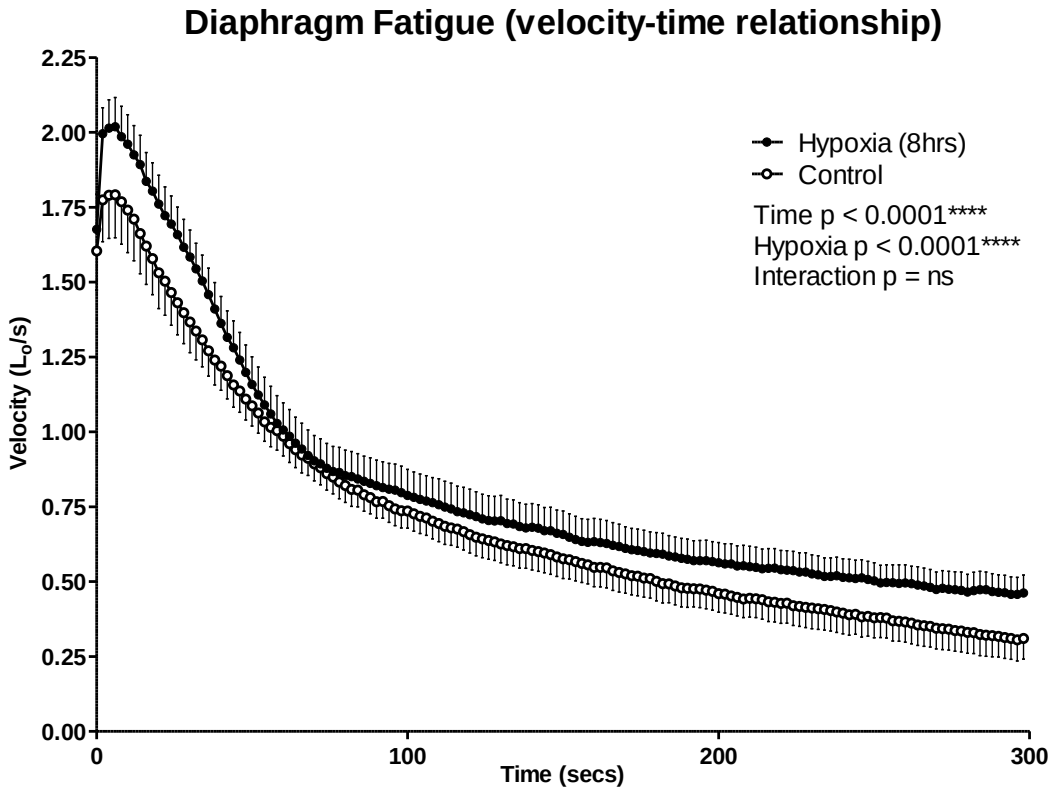

Figure 10: Diaphragm muscle fatigue (velocity–time relationship). Diaphragm muscle specific shortening velocity (mean ± SEM) expressed as optimal lengths per unit time (L_o/s) as a function of time (secs) over a 300sec fatiguing period of repeated stimulation every 2 seconds; n = 7-8 per group.

Fig. 11 shows diaphragm muscle fatigue in terms of muscle shortening over time during repeated stimulation (the shortening–time relationship). Two-way ANOVA

revealed a significant effect of time ($p < 0.0001$) and hypoxia ($p < 0.0001$) on diaphragm muscle shortening over time; there was no interaction ($p > 0.9999$). The hypoxia group produced a greater shortening distance than the control group over the duration of the fatigue protocol.

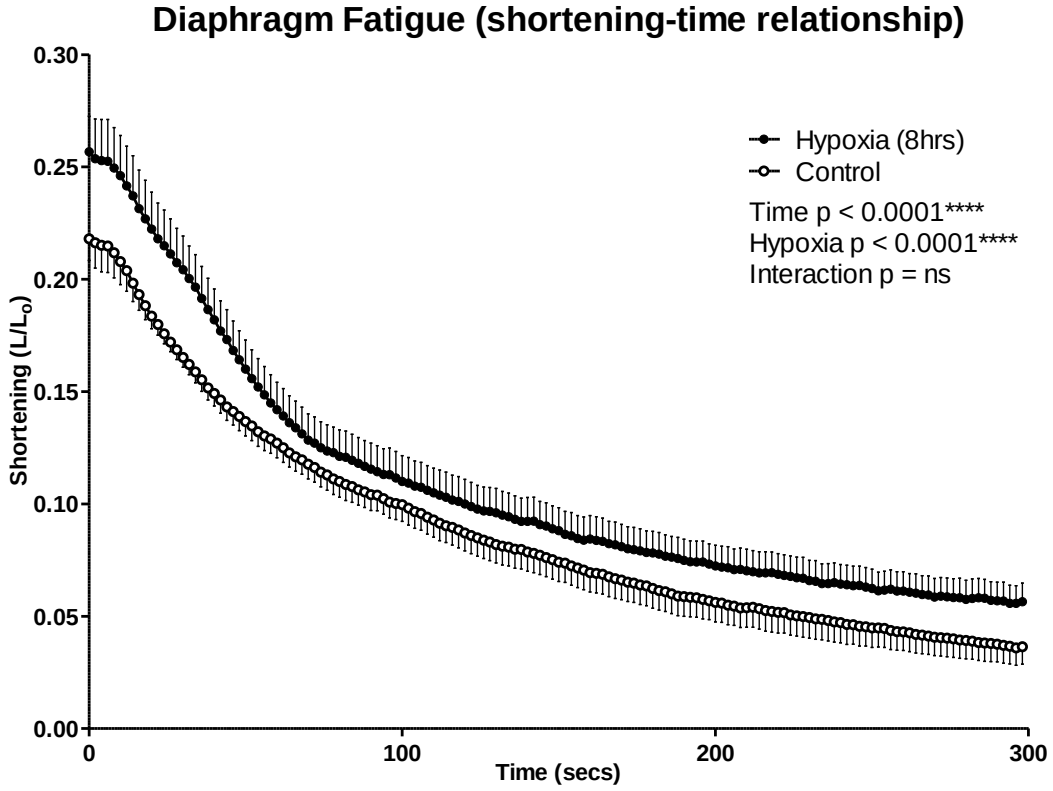

Figure 11: Diaphragm muscle fatigue (shortening–time relationship). Diaphragm muscle shortening (mean ± SEM) expressed as length per unit optimal length (L/L_o) as a function of time (secs) over a 300sec fatiguing period of repeated stimulation every 2 seconds; n = 7-8 per group.

3.2.2 Mouse Sternohyoid

Sternohyoid isometric peak tetanic force, twitch force and twitch kinetics are shown in Fig. 12. There was no statistically significant change in sternohyoid peak specific tetanic force (Fig. 12A) (12.8 ± 1.2 vs. 9.7 ± 1.1 mean ± SEM N/cm^2; Control vs. Hypoxia; n = 8 per group; p = 0.0683; unpaired t-test) after 8 hours of hypoxia,

although there was a non-statistically significant reduction in peak tetanic force generating capacity by ~25%. There was no statistically significant change in sternohyoid peak twitch force (Fig. 12B) (1.9 ± 0.2 vs. 1.5 ± 0.2 mean ± SEM N/cm^2; Control vs. Hypoxia; n = 8 per group; p = 0.1658; unpaired t-test) after 8 hours of hypoxia. There was no statistically significant change in sternohyoid TTP (Fig. 12C) (10.6 ± 0.5 vs. 10.1 ± 0.2 mean ± SEM N/cm^2; Control vs. Hypoxia; n = 8 per group; p = 0.3426; unpaired t-test) after 8 hours of hypoxia. There was no statistically significant change in sternohyoid T50 (Fig. 12D) (16.6 ± 1.5 vs. 13.1 ± 0.9 mean ± SEM N/cm^2; Control vs. Hypoxia; n = 8 per group; p = 0.0636; unpaired t-test) after 8 hours of hypoxia, although there was a non-statistically significant reduction in T50. Hypoxia appears to weaken the sternohyoid muscle in terms of peak force generating capacity, with modest alterations to the twitch kinetics – namely the T50 which was reduced to near statistical significance (p = 0.0636).

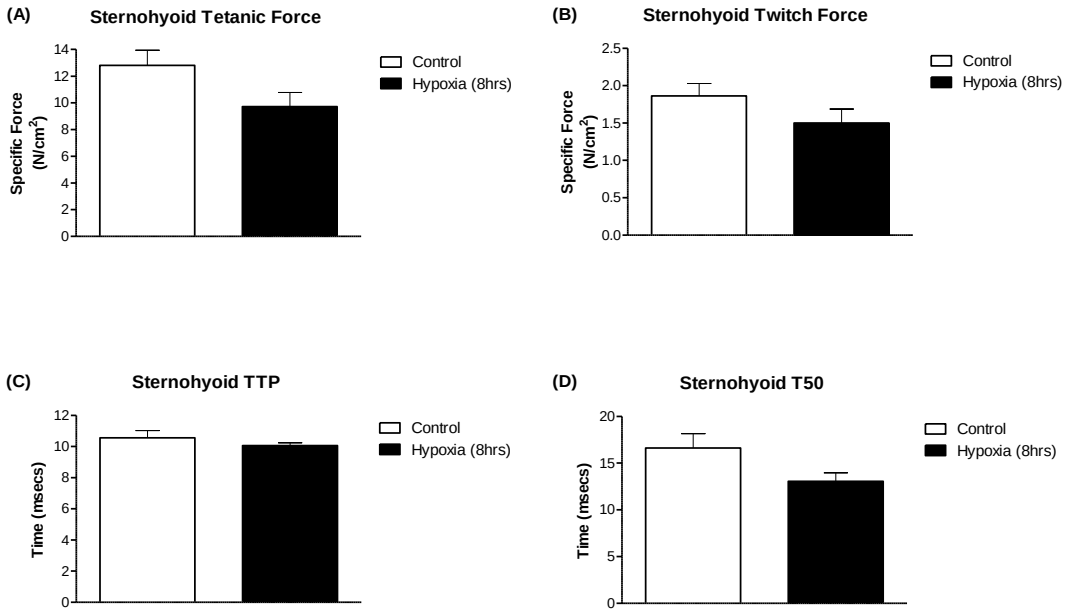

Figure 12: Sternohyoid isometric peak tetanic force, twitch force and twitch kinetic parameters. (A) Sternohyoid peak tetanic force (mean ± SEM) expressed as Force per unit CSA (N/cm^2); n = 8 per group. (B) Sternohyoid peak twitch force (mean ± SEM) expressed as Force per unit CSA (N/cm^2); n = 8 per group. (C) Sternohyoid time to peak twitch tension (TTP) (mean ± SEM) expressed as time

(msecs); n = 8 per group. (D) Sternohyoid twitch half relaxation time (T50) (mean ± SEM) expressed as time (msecs); n = 8 per group.

Sternohyoid muscle peak power, peak work, maximum shortening velocity and maximum shortening are displayed in Fig. 13. There were no statistically significant changes to (A) peak power (5.8 ± 0.8 vs. 4.4 ± 0.6 mean ± SEM Watts/cm^2; Control vs. Hypoxia; n = 8 per group; p = 0.1900; unpaired t-test), (B) work (0.6 ± 0.1 vs. 0.5 ± 0.1 mean ± SEM Joules/cm^2; Control vs. Hypoxia; n = 8 per group; p = 0.1152; unpaired t-test), (C) velocity (3.1 ± 0.2 vs. 3.1 ± 0.3 mean ± SEM L_o/s; Control vs. Hypoxia; n = 8 per group; p = 0.9853; unpaired t-test) or (D) shortening (0.2 ± 0.01 vs. 0.2 ± 0.01 mean ± SEM L/L_o; Control vs. Hypoxia; n = 8 per group; p = 0.7647; unpaired t-test) between control and hypoxia groups.

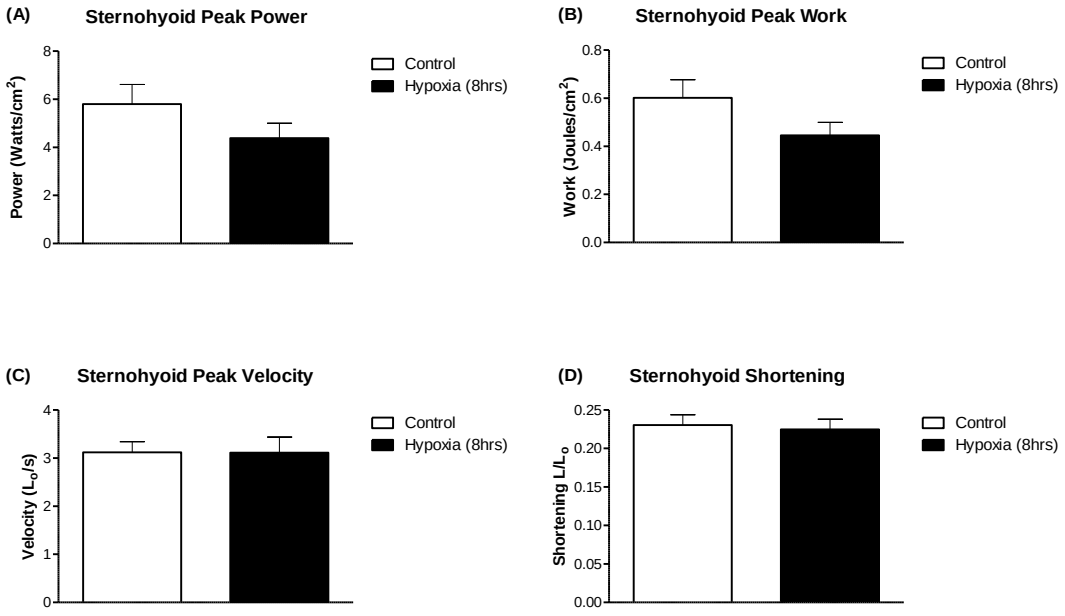

Figure 13: Sternohyoid muscle peak power, work, shortening velocity and shortening. (A) Sternohyoid peak power (mean ± SEM) expressed as power per unit CSA (Watts/cm^2); n = 8 per group. (B) Sternohyoid peak work (mean ± SEM) expressed as work per unit CSA (Joules/cm^2); n = 8 per group. (C) Sternohyoid peak shortening velocity (mean ± SEM) expressed as optimal lengths per unit time (L_o/s); n

= 8 per group. (D) Sternohyoid peak shortening distance (mean ± SEM) expressed as length per unit optimal length (L/L_o); n = 8 per group.

The sternohyoid muscle power–load relationship is shown in Fig. 14. This is power generated by the muscle at incremental loads on the muscle from 0-100% of the peak force generation capacity of the muscle strip. Two-way ANOVA revealed significant effects of% load ($p < 0.0001$) and hypoxia ($p = 0.0009$) on power generation over the full range of % loads tested; there was no interaction ($p = 0.9695$). The load on the muscle when it contracts, as expected, affected the power output of the muscle in a classic bell-shaped fashion, peaking at a load of around 35% of the maximum force generation capacity of the muscle. Hypoxia diminished the sternohyoid power–load curve, reducing sternohyoid power output over the range of loads as a whole, although not at the lowest % load.

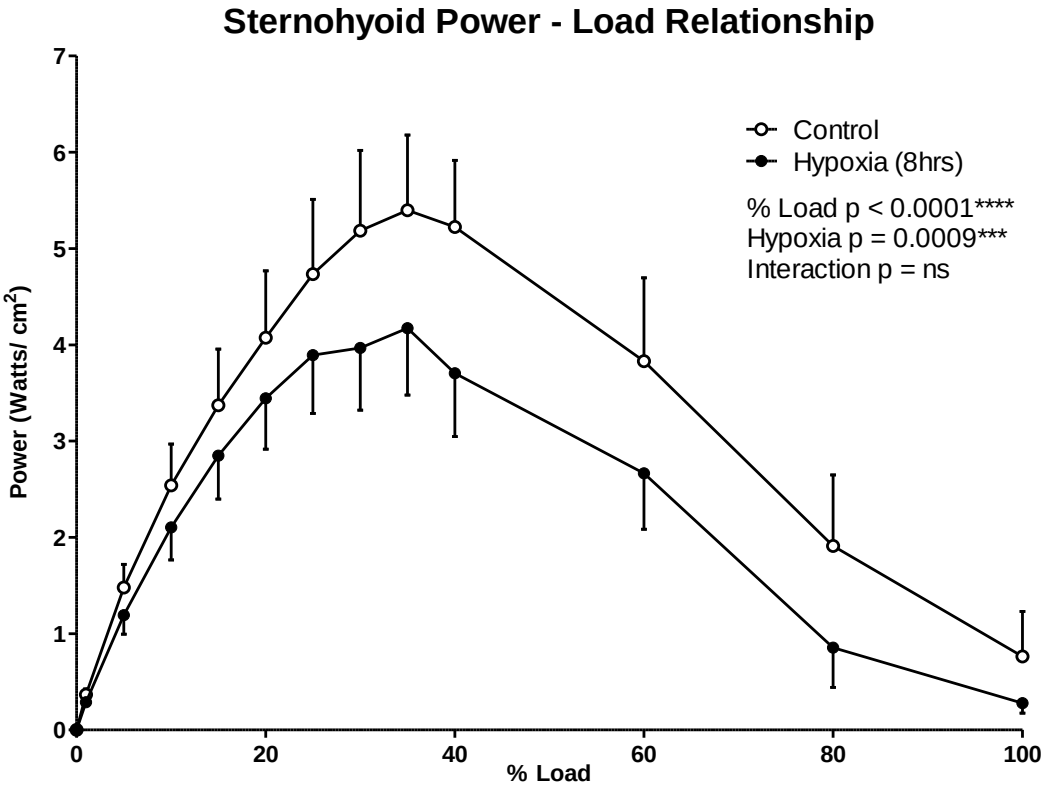

Figure 14: Sternohyoid muscle power–load relationship. Sternohyoid power (mean ± SEM) expressed as power per unit CSA (Watts/cm^2) as a function of the load

on the muscle expressed as a percentage of peak force (force/peak force*100); n = 8 per group.

The sternohyoid muscle work–load relationship is shown in Fig. 15. This is work generated by the muscle at incremental loads on the muscle from 0-100% of the peak force generation capacity of the muscle strip. Two-way ANOVA revealed a significant effect of % load ($p < 0.0001$) and hypoxia ($p < 0.0001$) on work over the full range of % loads tested; there was no interaction ($p = 0.3788$). Bonferroni's post-hoc multiple comparisons test also revealed significant differences in work at 60% and 80% load between control and hypoxia groups ($p < 0.05$). The load on the muscle when it contracts affected the work output of the muscle in a manner similar to its effect on power above. Here, hypoxia diminished the sternohyoid work output over the range of loads as a whole, except at the lowest load (~0% load), with most significant reductions in work seen at 60% and 80% load.

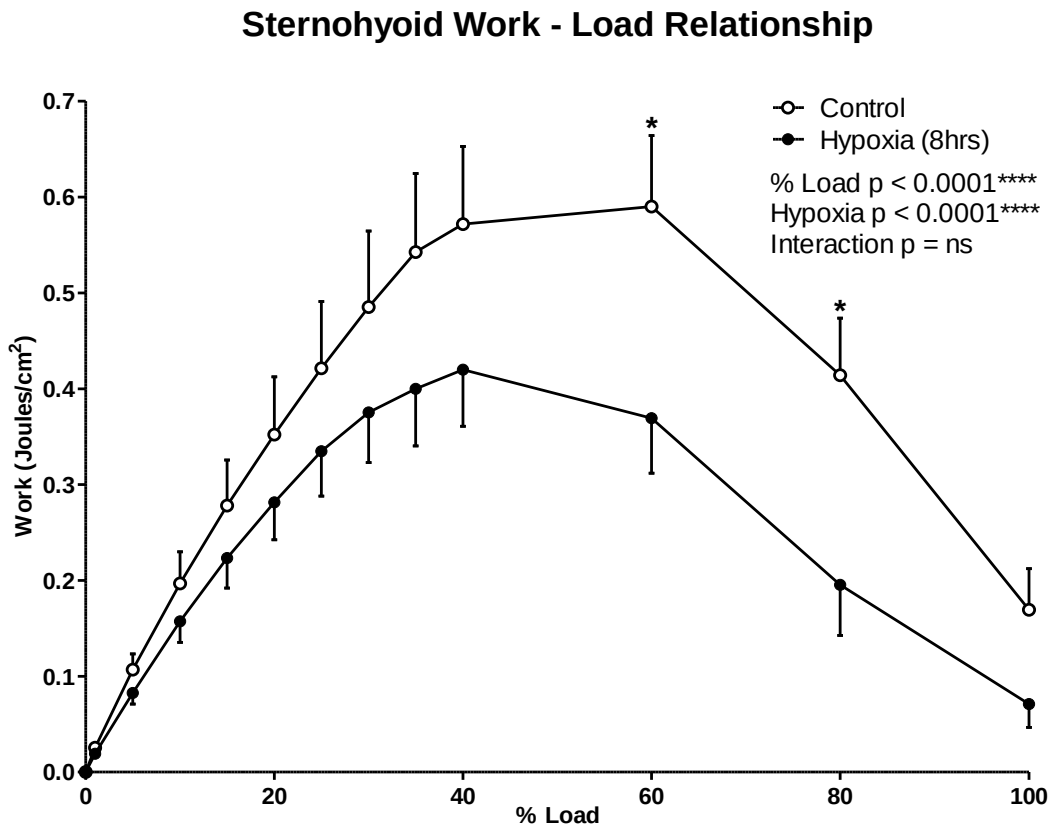

Figure 15: Sternohyoid muscle work–load relationship. Sternohyoid work (mean

± SEM) expressed as work per unit CSA (Joules/cm^2) as a function of the load on the muscle expressed as a percentage of peak force (force/peak force*100); n = 8 per group; *p < 0.05.

The sternohyoid muscle shortening velocity–load relationship is shown in Fig. 16. This is shortening velocity of the muscle at incremental loads on the muscle from 0-100% of the peak force generating capacity of the muscle strip. Two-way ANOVA revealed a significant effect of % load (p < 0.0001), but not hypoxia (p = 0.6577) on velocity over the full range of % loads tested; there was no interaction (p = 0.9997). Shortening velocity was reduced as expected in both groups as % load increased.

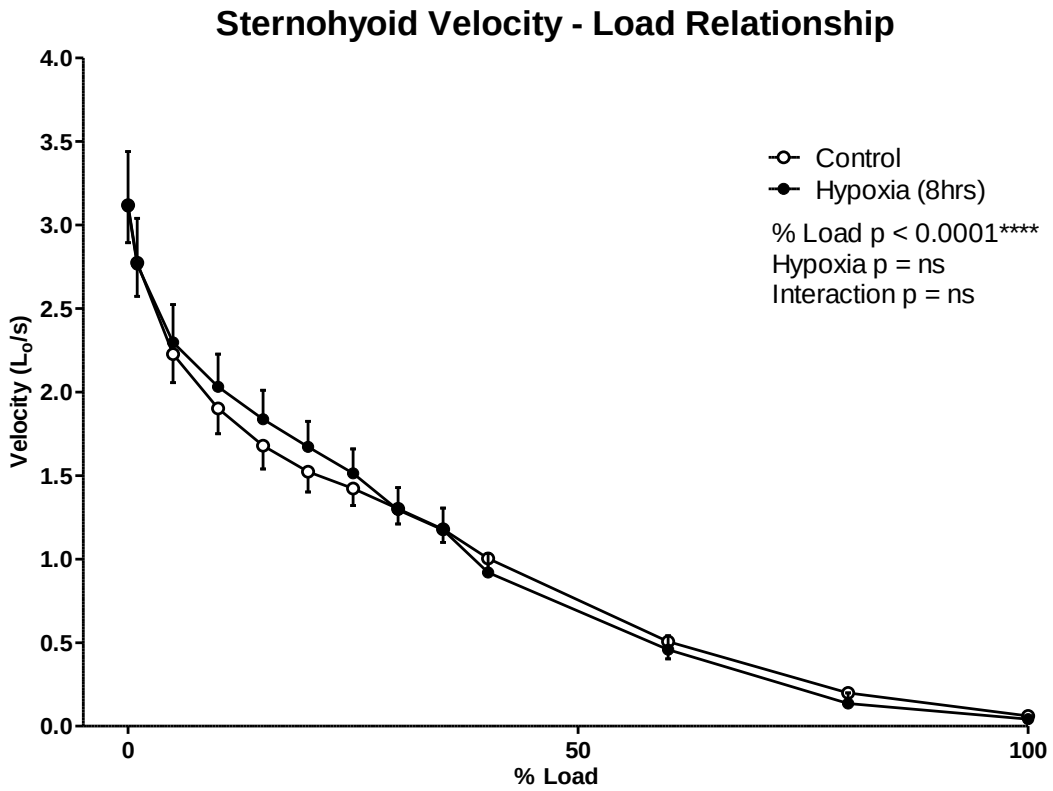

Figure 16: Sternohyoid muscle velocity–load relationship. Sternohyoid shortening velocity (mean ± SEM) expressed as optimal lengths per unit time (Lo/s) as a function of the load on the muscle expressed as a percentage of peak force (force/peak force*100); n = 8 per group.

The sternohyoid muscle shortening–load relationship is shown in Fig.17. This is shortening of the muscle at incremental loads on the muscle from 0-100% of the peak force generating capacity of the muscle strip. Two-way ANOVA revealed a significant effect of % load ($p < 0.0001$), but not hypoxia ($p = 0.7574$) on shortening over the full range of % loads tested; there was no interaction ($p = 0.9986$). Shortening distance was reduced as expected in both groups as % load increased.

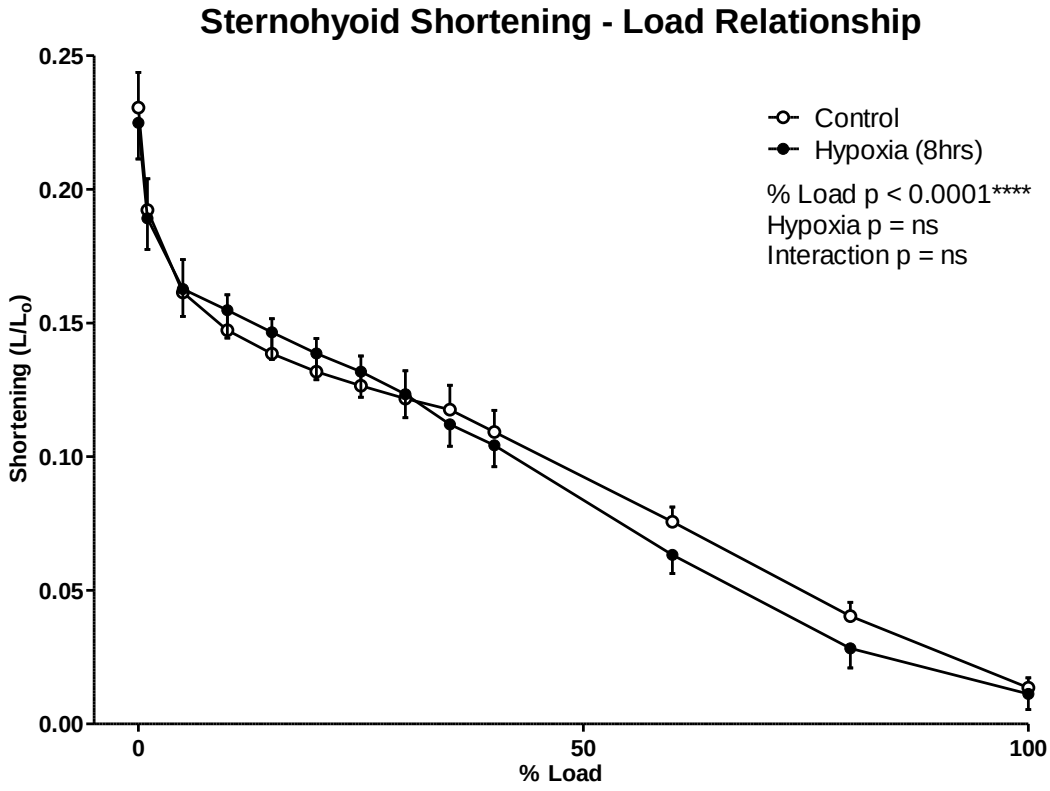

Figure 17: Sternohyoid muscle shortening–load relationship. Sternohyoid shortening (mean ± SEM) expressed as length per unit optimal length (L/L_o) as a function of the load on the muscle expressed as a percentage of peak force (force/peak force*100); n = 8 per group.

Fatigue

Sternohyoid muscle fatigue parameters are displayed below. Fig. 18 shows sternohyoid fatigue in terms of power output over time during repeated fatiguing

stimulation every 2 seconds for a 300 second period (the power–time relationship). Data is displayed in (A) absolute power values and (B) the fall off in power over time relative to initial power production at the beginning of the fatigue protocol. When data was analysed in terms of absolute power values (A), two-way ANOVA revealed a significant effect of time ($p < 0.0001$), but not hypoxia ($p = 0.9868$) on sternohyoid power (fatigue); there was no interaction ($p = 0.9985$). However, when analysing the fall off in power relative to the initial power (B), two-way ANOVA revealed a significant effect of both time ($p < 0.0001$) and hypoxia ($p < 0.0001$) on sternohyoid specific power (fatigue); there was no interaction ($p = 1.0000$). The data reveal that the sternohyoid muscle was weaker at the beginning of the fatigue protocol in the hypoxia group compared with control, producing a lower power output. However as the protocol progressed, the power produced by the sternohyoid from hypoxic animals does not fall off to the same extent as the power output of the sternohyoid from control animals, and both groups were producing the same power output by the end of the protocol (i.e. an apparent fatigue tolerance).

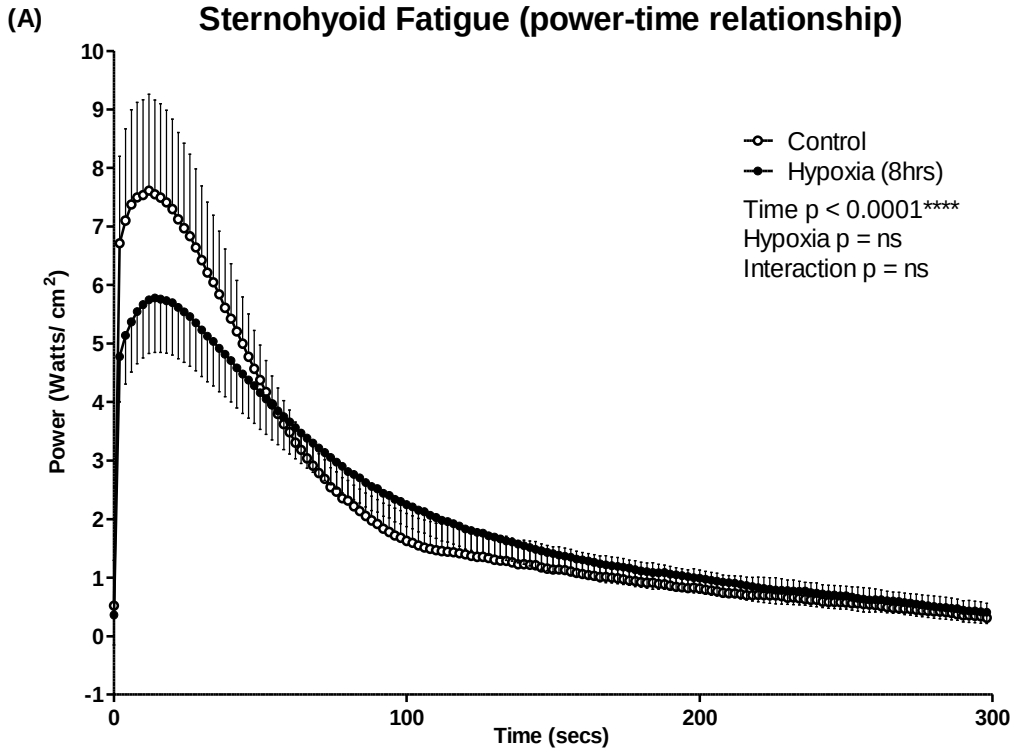

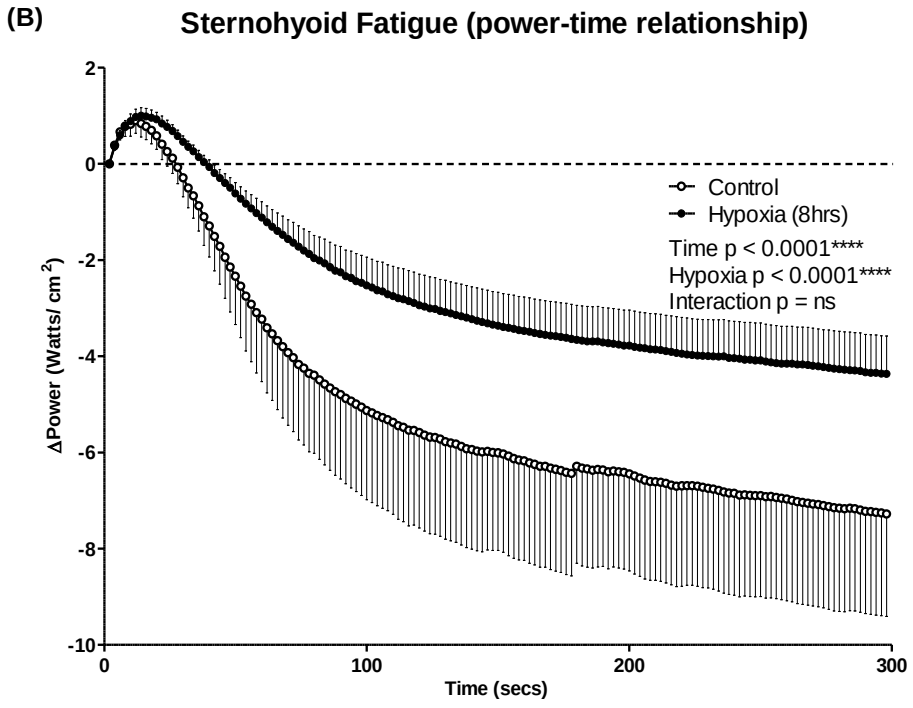

Figure 18: Sternohyoid muscle fatigue (power–time relationship). Sternohyoid muscle power (mean ± SEM) expressed as (A) power per unit CSA (Watts/cm^2) as a function of time (secs) over a 300sec period of repeated stimulation every 2 seconds and as (B) the change (Δ) in power (Watts/cm^2) relative to the initial power of that

muscle upon the first contraction of the fatigue protocol as a function of time over the 300sec fatiguing period of repeated stimulation every 2 seconds; n = 7 per group.

Fig. 19 shows sternohyoid fatigue in terms of work over time during repeated stimulation (the work–time relationship). Two-way ANOVA revealed a significant effect of time ($p < 0.0001$) and hypoxia ($p = 0.0292$) on sternohyoid work (fatigue); there was no interaction ($p > 0.9999$). Again, similar to observations in the power fatigue data, the hypoxia group produced less work than the control group at the beginning of the protocol, but work did not fall off to the same extent, producing the same amount of work as the control group by the end of the protocol (i.e. an apparent fatigue tolerance).

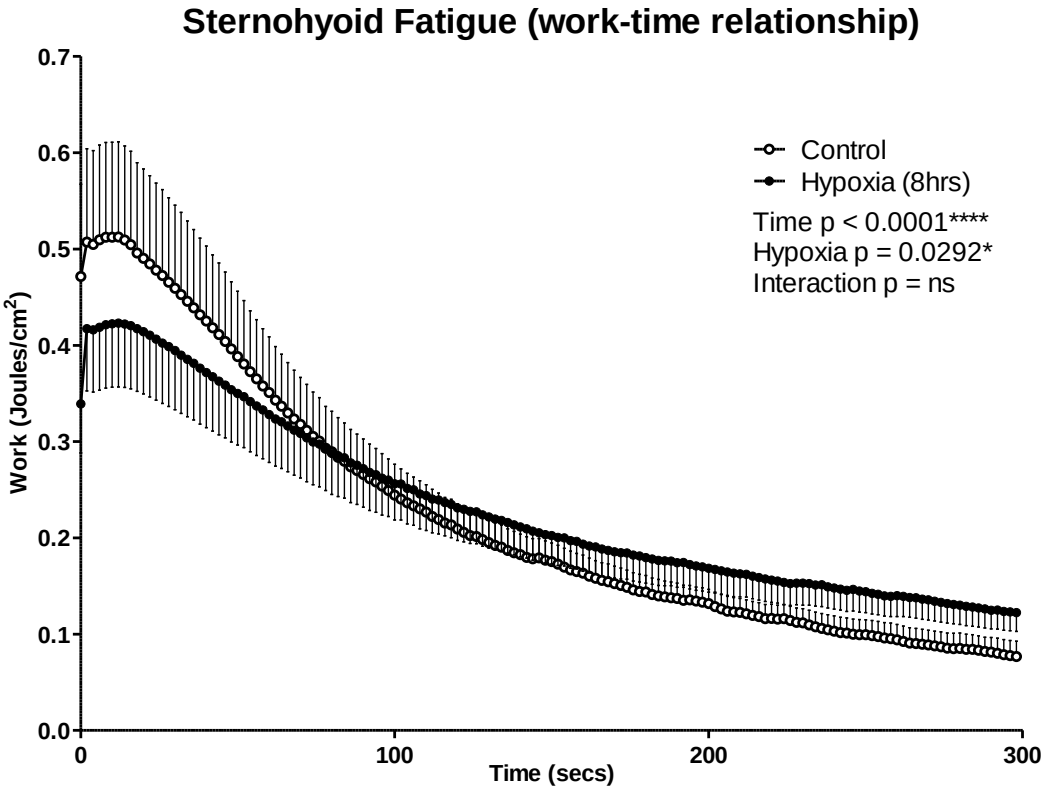

Figure 19: Sternohyoid muscle fatigue (work – time relationship). Sternohyoid muscle work (mean ± SEM) expressed as work per unit CSA (Joules/cm^2) as a function of time (secs) over a 300sec fatiguing period of repeated stimulation every 2 seconds; n = 7 per group.

Fig. 20 shows sternohyoid muscle fatigue in terms of muscle shortening velocity over time during repeated stimulation (the velocity–time relationship). Two-way ANOVA revealed a significant effect of time ($p < 0.0001$) and hypoxia ($p < 0.0001$) on sternohyoid muscle specific shortening velocity; there was no interaction ($p = 1.0000$). The hypoxia group produced a faster shortening velocity over the course of the fatigue protocol than the control group.

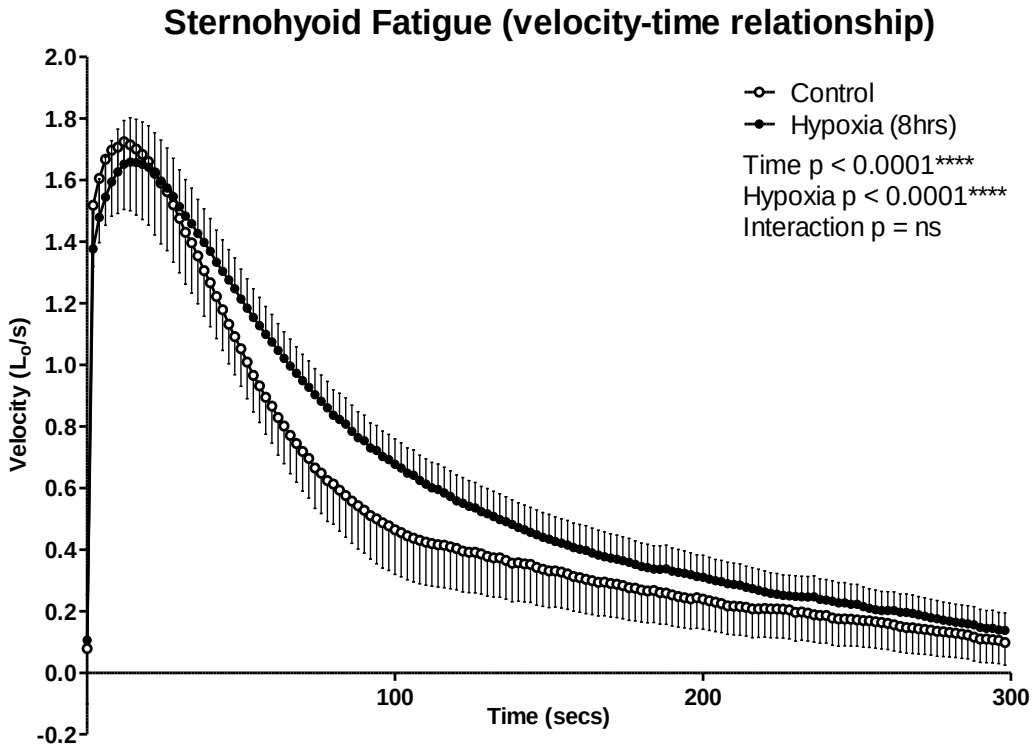

Figure 20: Sternohyoid muscle fatigue (velocity – time relationship). Sternohyoid muscle shortening velocity (mean ± SEM) expressed as optimal lengths per unit time (L_o/s) as a function of time (secs) over a 300sec fatiguing period of repeated stimulation every 2 seconds; n = 7 per group.

Fig. 21 shows sternohyoid muscle fatigue in terms of muscle shortening over time during repeated stimulation (the shortening–time relationship). Two-way ANOVA revealed a significant effect of time ($p < 0.0001$) and hypoxia ($p < 0.0001$) on sternohyoid muscle specific shortening; there was no interaction ($p = 1.0000$). The

hypoxia group produced a greater shortening distance than the control group over the duration of the fatigue protocol.

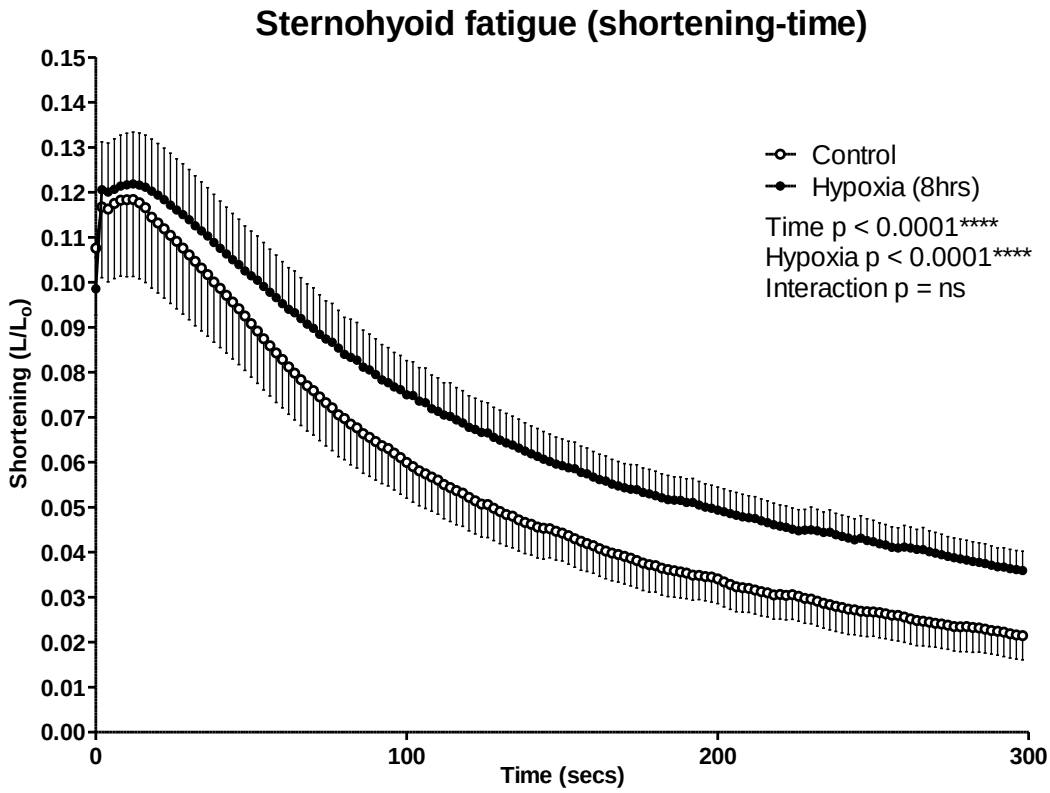

Figure 21: Sternohyoid muscle fatigue (shortening–time relationship).
Sternohyoid muscle shortening (mean ± SEM) expressed as length/optimal length (L/L_o) as a function of time (secs) over a 300sec fatiguing period of repeated stimulation every 2 seconds; n = 7 per group.

3.2.3 Rat Diaphragm

The force–frequency relationship of the rat diaphragm muscle is shown in Fig. 22. As one would expect, the force-generating capacity of the diaphragm muscle increased as the stimulation frequency is increased, from 10 to 160 Hz, and this effect of stimulation frequency on muscle contractile force was statistically significant ($p < 0.0001$, two-way ANOVA). Importantly, hypoxia caused a significant reduction in force generation over the range of stimulation frequencies ($p < 0.0001$, two-way

ANOVA) and Bonferroni's multiple comparisons test revealed statistically significant comparisons between the force generating capacity of control and hypoxia groups at 40, 60, 80, 120, 140, and 160 Hz. There was no interaction (p = 0.0791). Consistent with observations in mice, the rat diaphragm was significantly weakened by exposure to 8 hours of hypoxia.

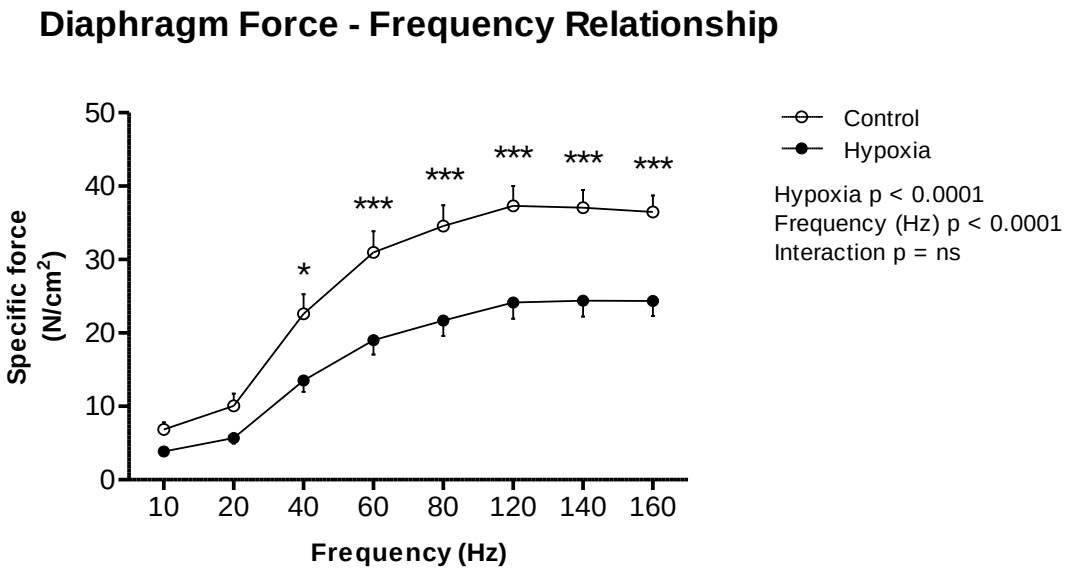

Figure 22: Rat diaphragm force–frequency relationship. Diaphragm force (mean ± SEM) expressed as force per unit CSA (N/cm^2) as a function of stimulation frequencies ranging between 10 and 160 Hz (n = 8 per group).

3.3 Chapter Discussion

The main findings of this chapter are:

1. 8 hours of hypoxia weakens the diaphragm significantly in terms of peak force generating capacity, the force – frequency relationship and power generating capacity.

2. 8 hours of hypoxia significantly improved diaphragm resistance to fatigue, although this may be a bottoming out effect due to the hypoxic diaphragm being weaker at the beginning of the fatigue protocol.

3. 8 hours of hypoxia weakens the sternohyoid significantly in terms of power & work generating capacity.

4. 8 hours of hypoxia significantly improved sternohyoid resistance to fatigue, although this may be a bottoming out effect due to the hypoxic sternohyoid being weaker at the beginning of the fatigue protocol.

5. 8 hours of hypoxia also weakens the rat diaphragm significantly in terms the force – frequency relationship, demonstrating conservation of the phenotype across both species despite notable differences in metabolic strategies in the face of hypoxia.

3.3.1 Mouse Diaphragm

There were no changes in the peak contractile kinetics of the diaphragm muscle following 8 hours of hypoxia when compared with control. This is also the case in studies examining the contractile kinetics of the diaphragm muscle following exposure of both mice and rats to chronic hypoxia (El-Khoury et al., 2003; Lewis et al., 2015b; McMorrow et al., 2011). While no change in peak contractile kinetics would suggest that Ca^{2+} handling, i.e. release and reuptake, at the SR is unaffected – T_{50} may be determined by SERCA activity (McMorrow et al., 2011), although there

exists some controversy in this matter (Hill et al., 2001) –, certain gene expression patterns revolving around Ca^{2+} handing at the SR that are uncovered in chapter 4, potentially suggest otherwise. This will be discussed further in chapter 4. However, while peak contractile kinetics were unaffected, diaphragm shortening and shortening velocity over the range of loads on the muscle from 0 – 100% load were both slightly, yet significantly, increased following hypoxia.

8 hours of hypoxia was sufficient to weaken the diaphragm by 30% compared with control. Interestingly, this degree of weakness is reminiscent of the weakness induced in diaphragm muscle following 6 weeks of chronic hypoxia (Lewis et al., 2015b). The mechanism at play during diaphragm muscle remodelling – ultimately leading to muscle weakness – in response to chronic hypoxia are likely quite distinct from those inducing muscle weakness in this acute hypoxia model. Indeed, 6 weeks of chronic hypoxia induces diaphragm muscle fibre atrophy, reducing muscle fibre CSA (McMorrow et al., 2011) with evidence of increased proteolysis (Lewis and O'Halloran, 2016), likely contributing to chronic hypoxia induced diaphragm weakness. Diaphragm atrophy is also a likely factor contributing to diaphragm muscle weakness in VILI/VALI patients, leading to VIDD, due to unloading and inactivity of the diaphragm while the mechanical ventilator performs the work of breathing (Bruells et al., 2013; Jaber et al., 2011a; Supinski and Callahan, 2013), although there exists some controversy in this area and it is debated as to whether inactivity *per se* induced diaphragm muscle atrophy (Sieck and Mantilla, 2013). However, this is an unlikely factor contributing to diaphragm muscle weakness in acute hypoxia (see chapter 4). Similarly, in the second exposure study on separate groups of mice, diaphragm weakness was again observed, demonstrating the repeatability and reproducibility of the finding, with evidence that force production was reduced over a range of stimulation frequencies. In particular, the weakness is most strongly evident at the higher stimulation frequencies, with the hypoxia group diaphragms being 37% weaker than the control group diaphragms at the highest frequency of 160Hz.

Diaphragm work output was unaffected by hypoxia, although there was a slight rightward shift in the work–load relationship, indicating an altered load at which peak work generation was achieved. However, while peak power generating capacity of the diaphragm was not significantly reduced, diaphragm muscle power output over the

range of loads on the muscle from 0 – 100% load was significantly reduced by hypoxia. During normal, healthy breathing the diaphragm is contracting against a relatively low load. Therefore there is a large reserve of power generating capacity remaining in the diaphragm. This power reserve can become a critical factor if airway clearance is required or indeed if the airway becomes blocked or obstructed. As such, the hypoxia induced reduction in the power–load relationship could make hypoxic respiratory patients more susceptible to a negative outcome if these complications arise.

Diaphragm endurance, or resistance to fatigue, was tested by repeated stimulation every 2 seconds for 300 seconds, contracting against 33% load. The initial power generating capacity of the control diaphragm was significantly higher than that of the hypoxic diaphragm. As the protocol progressed, however, the control diaphragm power output fell off to a greater extent than that of the hypoxic group, and by the end of the 300 second protocol the power output was identical in the two groups. When these data were expressed as fall off in power output relative to the initial power output of each group at the beginning of the protocol, it became evident how significant this difference in fatigue was. There are two potential explanations for this. Firstly, the hypoxic diaphragm is, in fact, more endurant than the control diaphragm and is thus more resistant to fatigue over repeated stimulation. Secondly, it was a bottoming out effect, whereby repeatedly stimulating the diaphragm at 33% load could only fatigue the diaphragm so far, and as the hypoxic diaphragm was weaker to begin with then it did not have as far to fall in terms of reduction in power output. Both groups appeared to have the same profile in terms of rate of fatigue during the protocol, with power output falling off at the greatest rate, and at a similar rate in both groups, during the first 70 seconds of the protocol. Then, from 70 seconds onward, the rate of reduction in power output slowed in both groups, although it remained slightly faster in the control group, leading to both groups producing the same power output by the end of the protocol. Indeed, it has previously been postulated that chronic hypoxia increases diaphragm endurance in the rat (McMorrow et al., 2011). A potential method of allowing the weakened diaphragm to recover is to rest the muscle using controlled mechanical ventilation. However this then introduces another problem, namely disuse atrophy which can weaken the muscle further (Vassilakopoulos et al., 2006). Difficulty weaning patients from ventilators can be

attributed to three primary causes: hypoxaemia, psychological issues and respiratory muscle dysfunction (Tobin, Jubran, 1998; Tobin et al., 1998). This chapter demonstrates that hypoxia itself can be a factor causing respiratory muscle dysfunction, and places hypoxia as a potential candidate for being a major contributor to diaphragm weakness following acute respiratory failure induced by acute respiratory-related disorders. Although hypoxia has been shown here to weaken the diaphragm, it has also been shown to increase fatigue resistance of the diaphragm. However, due to the muscle being weaker to begin with, this perceived increase in endurance of the muscle still ultimately leads to lower power generation capacity sooner during repeated stimulation. The power output by both muscles at 300 seconds was at about 3 Watts/cm^2, a significant drop from the initial power outputs generated by the diaphragm under control and hypoxic conditions – 18 and 15 Watts/cm^2 respectively. However, the control diaphragm did not reach 6 Watts/cm^2 (arbitrary value, for example purposes) of power output until 134 seconds into the fatigue protocol, while the hypoxic diaphragm reached a power output of 6 Watts/cm^2 by 88 seconds into the fatigue protocol. Approximately 20% of all mechanically ventilated patients fail their first attempt to wean (Eskandar and Apostolakos, 2007) However, diaphragm fatigue is not a common cause of this failure. In a study aiming to determine if weaning failure is caused by low-frequency fatigue of the diaphragm, it was discovered that weaning failure was not accompanied by low-frequency diaphragmatic fatigue, but that many of the weaning failure patients displayed diaphragm muscle weakness (Laghi et al., 2003), therefore diaphragmatic strength rather than fatigue properties may be of greater importance when determining the functional integrity of this pump muscle in mechanically ventilated patients. It is important to note, however, that diaphragm strength is not a primary predictor of whether a patient will or will not wean from mechanical ventilation successfully, often the reason behind weaning failure can be due to upper airway collapse, respiratory loading, neuropsychological/neuromuscular complications, and metabolic disorders.

3.3.2 Mouse Sternohyoid

Similar to the diaphragm, there were no changes in the peak contractile kinetics of the sternohyoid muscle following 8 hours of hypoxia when compared with control, with the exception of peak T_{50} which was reduced to near significance at $p = 0.0636$. This is also the case for contractile kinetics of the sternohyoid muscle following exposure of mice to chronic hypoxia (Lewis et al., 2015c). While no change in contractile kinetics would suggest that Ca^{2+} handling, i.e. release and reuptake, at the SR is unaffected, certain gene expression patterns revolving around Ca^{2+} handing at the SR that are elucidated in chapter 4 suggest otherwise, and this evidence for alterations in the regulation in SR Ca^{2+} handing is stronger for the sternohyoid than the diaphragm (chapter 4). Sternohyoid muscle shortening and shortening velocity over the range of loads on the muscle from 0 – 100% load were also unaffected by hypoxia.

8 hours of hypoxia was sufficient to weaken the sternohyoid muscle. Peak tetanic force generating capacity of the sternohyoid muscle was reduced by hypoxia to near statistical significance ($p = 0.0683$), while both power & work outputs of the sternohyoid muscle was significantly reduced by hypoxia over the range of loads on the muscle from 0 – 100% load.

In terms of sternohyoid fatigue resistance, similar to the diaphragm the initial power generating capacity of the control sternohyoid was significantly higher than that of the hypoxic sternohyoid. As the protocol progresses, however, the control sternohyoid power output fell off to a greater extent than that of the hypoxic group, and by the end of the 300 second protocol the power output was identical in the two groups. When these data were then expressed as fall off in power output relative to the initial power output of each group at the beginning of the protocol, it was evident how significant this difference in fatigue was, with a greater fall off in power production in the control sternohyoid. As with the diaphragm, there are two potential explanations for this, as discussed above – the sternohyoid muscle was either more endurant than the control sternohyoid or it was a bottoming out effect. The profiles of the two groups in terms of the rate of fatigue during the protocol were slightly different between the control and hypoxic group. In the control sternohyoid, although initially producing more power at the beginning of the protocol, the power output diminished quickly and at a faster rate than did the power output from the weaker hypoxic sternohyoid, and by 50

seconds into the protocol both control and hypoxic sternohyoid muscles were producing the same power output. For the remainder of the 300 second protocol the power output of both control and hypoxic sternohyoid muscles was the same at each stimulation, leading to both groups producing the same power output by the end of the protocol.

In both the diaphragm and the sternohyoid, if this is evidence of a true fatigue resistance, as opposed to a bottoming out effect, one potential mechanism for this fatigue resistance would be an increased oxidative capacity of the muscles. The data is not included in this thesis, and is as of yet unpublished, but recent findings in our laboratory demonstrate that citrate synthase enzyme activity is increased by 8 hours of hypoxia in both diaphragm and sternohyoid, which is a marker for increased oxidative capacity in skeletal muscle.

As discussed in the introduction to this chapter, OSA is most prevalent in obese individuals, and obesity increases the risk of the development of ARDS in surgical patients. While the type of hypoxia experienced by OSA patients is primarily intermittent hypoxia during sleep, due to intermittent occlusion of the upper airway, the effects of acute hypoxia discussed in this thesis may have relevance to patients with acute respiratory diseases who also present with upper airway dysfunction and/or OSA. The sternohyoid muscle is an important upper airway dilator muscle and one which is the focus of much research on the deleterious effects of intermittent hypoxia on upper airway muscle with relevance to OSA (Shortt et al., 2014; Skelly et al., 2012b, 2012c; Williams et al., 2015). The acute hypoxia induced sternohyoid weakness and dysfunction presented in this chapter could exacerbate and perpetuate the pathophysiology of OSA, as dysfunction of the pharyngeal dilator muscles of the upper airway, including the sternohyoid muscles, increases the susceptibility of patients to collapse and occlusion of the upper airway.

3.3.3 Rat Diaphragm

8 hours of hypoxia also caused diaphragm muscle weakness in the rat when exposed to hypoxia under the same conditions. Force production was reduced over the range

of stimulation frequencies tested. In particular, the weakness was most strongly evident at the higher stimulation frequencies. The relevance of this diaphragm weakness to human conditions is discussed in section 3.3.1 above. The implication of this hypoxia induced weakness being present in the rat as well as the mouse, however, is that the mouse and rat adopt slightly different metabolic strategies under hypoxic conditions, with the rat closer to the human response i.e. hyperventilation. These data confirm that the muscle weakness observed in the mouse was also present in the rat suggesting, importantly, that the hypoxia induced diaphragm weakness was most likely related to hypoxic stress *per se*, rather than being solely due to the metabolic strategy adopted by the mouse, or indeed the rat. These metabolic strategies will be discussed further in chapter 4.

3.4 Chapter Conclusions

Acute hypoxia (8 hours) is sufficient to cause diaphragm muscle weakness, in both mice and rats. Acute hypoxia primarily weakens and limits diaphragm force generating capacity, which in turn leads to reduced power generating capability of the diaphragm muscle. Acute hypoxia also reduces mouse sternohyoid power and work production, which is likely due to acute hypoxia effects on sternohyoid force generating capacity.

Acute hypoxia appears to lead to dysfunction of both the diaphragm and sternohyoid muscles, and in both cases this dysfunction appears to stem from acute hypoxia induced muscle weakness. In the case of the diaphragm, this weakness has clinical relevance to a range of acute respiratory-related disorders in which hypoxia features, such as ARDS ALI, VILI/VALI/VIDD, acute respiratory failure and mechanical ventilation in patients, including attempts to wean patients from mechanical ventilatory support. In the case of the sternohyoid, the acute hypoxia induced muscle weakness has clinical relevance to patients with acute respiratory diseases who also present with risk of upper airway dysfunction and/or OSA. Respiratory muscle weakness could prove particularly problematic when the diaphragm is required to perform tasks other than quiet breathing, such as airway clearance manoeuvres and/or

ventilation through a narrowed airway, increasing the load on the muscle and in the context of upper airway muscle weakness may present problems for recovery of a collapsed upper airway during sleep.

Diaphragm weakness can exacerbate and perpetuate respiratory morbidity in respiratory patients, prolonging the process of weaning a patient from mechanical ventilation and ultimately predisposing a patient to a poorer clinical outcome (Supinski and Callahan, 2013). Elucidating the mechanisms of acute hypoxia induced respiratory muscle dysfunction will pave the way for the development of suitable therapeutic strategies, that may be used as adjunct therapies, in a clinical setting, for respiratory patients, in which acute hypoxia features, in order to enhance respiratory muscle performance and increase the likelihood of positive outcomes for patients.

Chapter 4: Metabolic, Respiratory and Atrophic Mechanisms That May Underpin Acute Hypoxia Induced Respiratory Muscle Dysfunction in Mice

4.1 Introduction

In this chapter, respiratory and limb muscle gene expression relating to metabolism and mitochondrial function, hypoxic signalling and inflammation, sarcoplasmic reticulum calcium handling, release and re-uptake, and atrophy and autophagy, is assessed following normoxia (control), 1 hour of hypoxia, 4 hours of hypoxia and 8 hours of hypoxia. Given the potential contribution of muscle fibre atrophy to diaphragm weakness in models of chronic hypoxia and in VIDD (discussed in chapter 1 and chapter 3), proteasome activity is assessed in this chapter following 8 hours of hypoxia compared with control. Respiration is assessed *in vivo* to determine if ventilatory activity is altered in hypoxia and *in vivo* metabolism is examined to give further insight into the metabolic strategy adopted by the mouse in an acute hypoxic environment.

As previously stated, in chapter 1 and elsewhere, the effects of acute hypoxia on respiratory muscle are relatively unknown. Therefore, in attempting to uncover the mechanisms leading to diaphragm and sternohyoid muscle weakness highlighted in chapter 3, in the absence of previous literature in this area, previous work on chronic hypoxia and hypoxic (mal-)adaptation provided guidance and direction. In nature, a state of hypoxic tolerance is achieved through the integration of 1) a reduction in metabolic state; 2) protection against hypoxic cell death/injury; and 3) the maintenance of functional integrity (Ramirez et al., 2007). Mitochondrial effects of, and metabolic adaptations to, chronic hypoxia in diaphragm and sternohyoid muscle have been reported previously (Lewis et al., 2016, 2015c) and attributed to redox modulation. Indeed, muscle function, hypoxia and metabolism are intrinsically linked via HIF signalling as well as other transcription factors regulating metabolism and mitochondrial function being hypoxia responsive (Cummins and Taylor, 2005; Gutsaeva et al., 2008; Kim et al., 2006; Nanduri et al., 2008; Semenza et al., 1994; Vogt et al., 2001).

Calcium handling at the SR is a key factor in ECC, ultimately affecting muscle contraction (discussed in chapter 1) and contractile kinetics (mentioned in chapter 3). Therefore, in a situation whereby muscle function is perturbed, calcium handling at

the SR is one of many logical processes to examine in attempting to unveil the cause of contractile dysfunction.

Diaphragm muscle fibre atrophy occurs during exposure to chronic hypoxia and is a likely contributing factor to diaphragm dysfunction following chronic hypoxia (Lewis et al., 2016; McMorrow et al., 2011). As discussed in chapter 1, the diaphragm is an extremely adaptable and malleable muscle and can atrophy within a matter of hours under certain conditions such as mechanical ventilation. Combining this information it is pertinent to examine atrophy signalling in a model of acute hypoxia where diaphragm weakness occurs, and further to this, examine proteasome enzyme activity and autophagy signalling, given that autophagy can be induced in the diaphragm by mechanical ventilation, where it may limit VIDD, as well as being an atrophy inducing factor in mouse diaphragm following intermittent hypoxia, which can be activated by oxidative stress (Azuelos et al., 2015; Giordano et al., 2015).

Study Aims

Given the acute hypoxia induced respiratory muscle weakness and dysfunction uncovered in chapter three, the primary aims of this chapter are: 1) to examine gene expression changes in diaphragm and sternohyoid muscle, in order to elucidate certain molecular mechanisms relating to metabolism and mitochondrial function, hypoxic signalling and inflammation, sarcoplasmic reticulum calcium handling, release and re-uptake, and atrophy and autophagy, that may be underpinning this respiratory muscle dysfunction, and to compare some of these responses to limb muscles (EDL & Soleus) in order to determine if certain acute hypoxia induced transcriptional changes are respiratory muscle specific; 2) to determine if proteasome activity is increased by acute hypoxia in the diaphragm, which could contribute to muscle weakness; and 3) to determine the *in-vivo* respiratory and metabolic remodelling strategy adopted by the mouse during acute hypoxic exposure, to see how these interact with each other, to further understand molecular changes. Furthermore, examining *in vivo* respiration informs whether diaphragm muscle activity is altered under acute hypoxia, as an increase in ventilation would mean an increase in respiratory muscle activity, which is a potential confounding factor with regards to muscle function in a hypoxic environment.

Methods Summary

Gene expression in respiratory and limb muscle, diaphragm proteasome activity, *in vivo* respiration and *in vivo* metabolism were measured in mice, as described in more detail in Chapter 2 Materials and Methods, Sections 2.3, 2.7, 2.8 and 2.9.

Briefly, gene expression data was obtained via qRT-PCR experiments, expressing changes in gene expression as a fold change over the control group. Genes were examined based on their involvement in the following cellular processes: metabolism and metabolic regulation, SR calcium handling, atrophy, autophagy and hypoxia signalling.

Proteasome activity was measured via a fluorometric assay, whereby the presence of proteasome activity in a sample leads to the cleavage of a peptide substrate, releasing a fluorescent AMC tag. The level of fluorescence detected is relative to the proteasome activity in the sample.

In vivo respiration was monitored using unrestrained whole body plethysmography in mice during gas exposure. This allowed the measurement of respiratory frequency, tidal volume and, from these values, minute ventilation.

In vivo metabolism was measured by monitoring O_2 consumption and CO_2 production in the mice during gas exposure. *Post-mortem* core body temperature was also recorded immediately (within 10 seconds) following euthanasia of the mouse via insertion of a rectal thermometer probe, as a crude index of metabolism in rodents.

4.2 Chapter Results

4.2.1 Gene Expression and Proteasome Activity

4.2.1.2 Diaphragm

The gene expression data for the mouse diaphragm is displayed below. These data are expressed as fold changes in mRNA levels, relative to the control (normoxia) group, following 1, 4 and 8 hours of sustained hypoxia. The expression of genes related to energy metabolism and mitochondrial function and biogenesis in the diaphragm are displayed in Fig. 1. PGC-1α mRNA expression was significantly increased ($p<0.05$, one-way ANOVA & Tukey's post hoc test) at 1 hour of hypoxia compared with control, however expression returned to control levels by 8 hours (Fig. 1(A)). PGC-1β mRNA expression was not significantly affected compared with the control group, although there was a significant difference between the 8 hour and 4 hour hypoxia groups ($p<0.05$, one-way ANOVA & Tukey's post hoc test) (Fig. 1(B)). NRF1 mRNA expression was not significantly different between groups, although there was a trend toward decreased expression at 4 and 8 hours of hypoxia compared with control (Fig. 1(C)). Neither NRF2 nor PPARα displayed any significant changes in expression across groups (one-way ANOVA & Tukey's post hoc test) (Fig. 1(D) & (E)). UCP-3 mRNA expression increased progressively with increased hypoxic exposure time compared with control; following 8 hours of hypoxic exposure, UCP-3 mRNA levels were significantly increased compared with the control group ($p<0.01$, one-way ANOVA & Tukey's post hoc test), and the 1 hour of hypoxia group ($p<0.05$) (Fig. 1(F)).

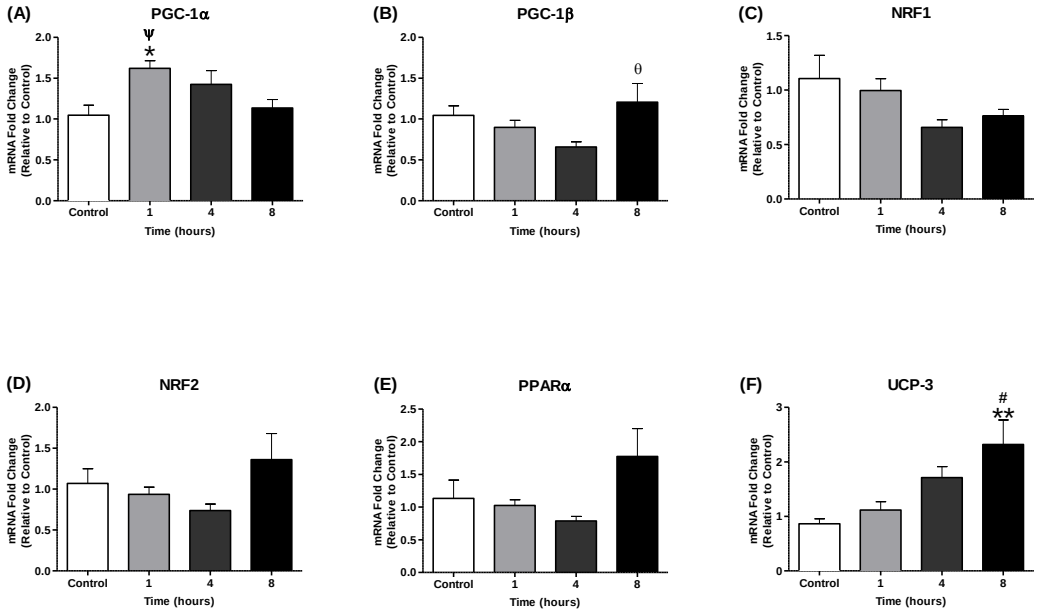

Figure 1: Diaphragm muscle gene expression related to metabolism and mitochondrial function. Fold changes in mRNA expression (relative to the control group) for (A) PGC-1α; (B) PGC-1β; (C) NRF1; (D) NRF2; (E) PPARα; and (F) UCP-3 (mean ± SEM, n = 7-8 per group) (*$p < 0.05$ vs. control, **$p < 0.01$ vs. control, #$p < 0.05$ vs. 1 hour, ψ$p < 0.05$ vs. 8 hours, θ$p < 0.05$ vs. 4 hours, one-way ANOVA and Tukey's post hoc test) following 1, 4 and 8 hours of hypoxia or control (normoxia).

Fig.2 shows the diaphragm expression data for genes related to hypoxic signalling and inflammation. There was no significant change in HIF-1α mRNA expression (one-way ANOVA & Tukey's post hoc test) across groups (Fig. 2(A)). There was no significant change in HIF-2α mRNA expression (one-way ANOVA & Tukey's post hoc test) across groups (Fig. 2(B)). NF-κB1 mRNA expression displayed a trend toward decreased expression at 4 and 8 hours of hypoxia compared with control, with expression in the 4 hours hypoxia group significantly lower than expression in the control and 1 hour hypoxia groups ($p<0.05$ in both cases, one-way ANOVA & Tukey's post hoc test) (Fig. 2(C)).

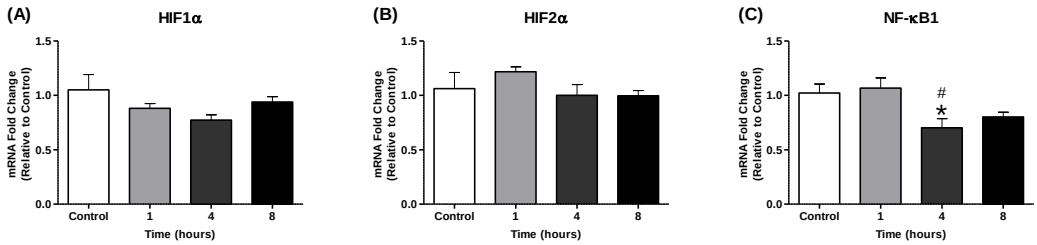

Figure 2: Diaphragm muscle gene expression related to hypoxic signalling and inflammation. Fold changes in mRNA expression (relative to the control group) for (A) HIF1α; (B) HIF2α; and (C) NF-κB1 (mean ± SEM, n = 7-8 per group) (*$p < 0.05$ vs. control, #$p < 0.05$ vs. 1 hour, one-way ANOVA and Tukey's post hoc test) following 1, 4 and 8 hours of hypoxia or control (normoxia).

Fig.3 shows the diaphragm expression data for genes related to sarcoplasmic reticulum calcium handling, release and re-uptake. There were no significant changes in SERCA 1, SERCA 2a, Junctophilin 1, Junctophilin 2, Calsequestrin 1, Triadin, Ryanodine Receptor 1, Ryanodine receptor 3, Dihydropyridine Receptor or Inositol Trisphosphate Receptor 1 mRNA expression (one-way ANOVA & Tukey's post hoc test) across groups (Fig. 3A-H, J & K). Selenoprotein N1 mRNA expression displayed a trend toward decreased expression at 1, 4 and 8 hours of hypoxia compared with control, with expression in the 4 hours hypoxia group significantly lower than expression in the control group ($p<0.05$, one-way ANOVA & Tukey's post hoc test) (Fig. 3(I)).

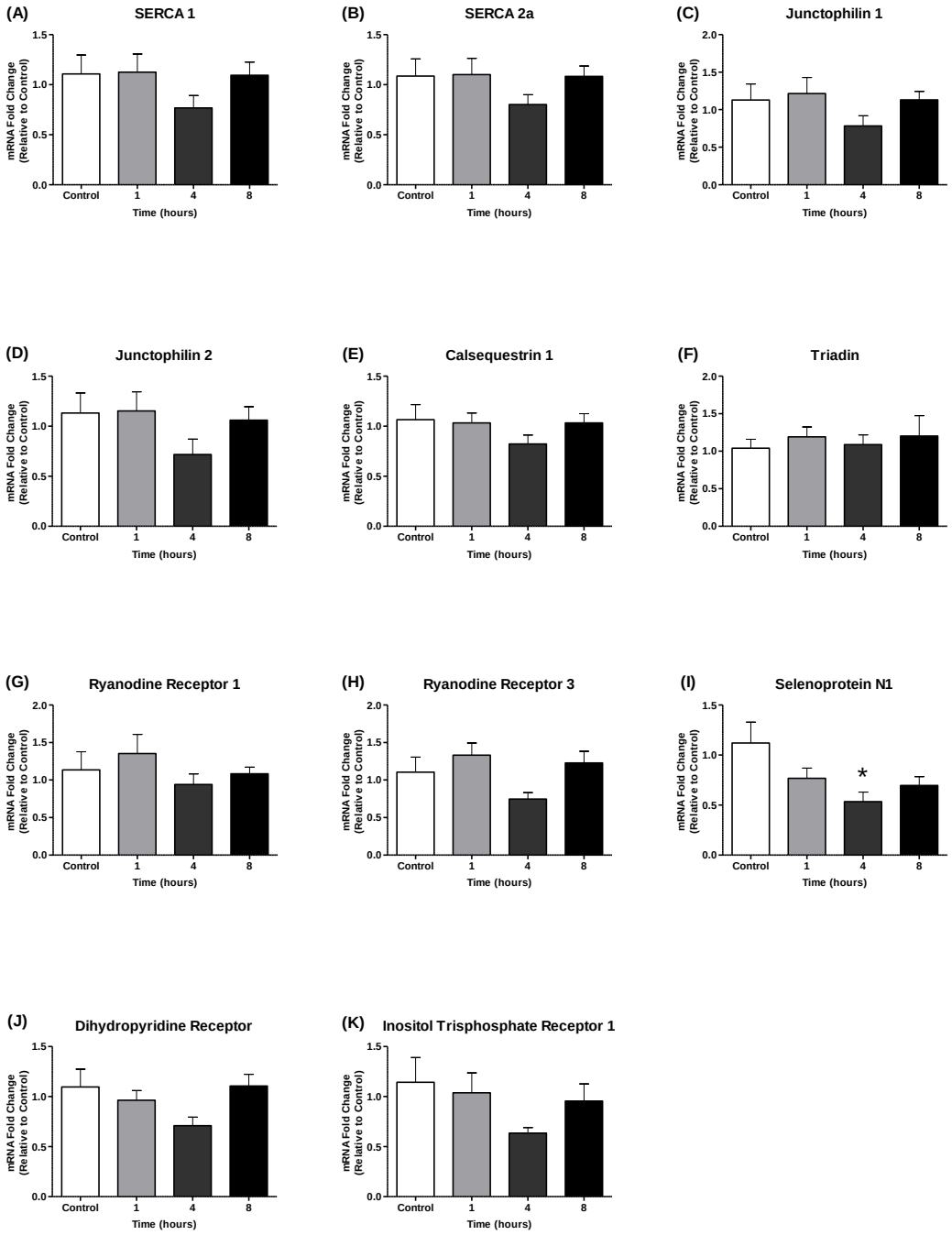

Figure 3: Diaphragm muscle gene expression related to sarcoplasmic reticulum calcium handling, release and re-uptake. Fold changes in mRNA expression (relative to the control group) for (A) SERCA 1; (B) SERCA 2a; (C) Junctophilin 1; (D) Junctophilin 2; (E) Calsequestrin 1; (F) Triadin; (G) Ryanodine Receptor 1; (H) Ryanodine Receptor 3; (I) Selenoprotein N1; (J) Dihydropyridine Receptor; and (K) Inositol Triphosphate Receptor 1 (mean ± SEM, n = 7-8 per group) (*$p < 0.05$ vs. control, one-way ANOVA and Tukey's post hoc test) following 1, 4 and 8 hours of hypoxia or control (normoxia).

Fig.4 shows diaphragm expression data for genes related to atrophy and autophagy. There were no significant changes in Foxo-1, Atrogin-1, LC3B, BNIP3, or GABARAPL3 mRNA expression (one-way ANOVA & Tukey's post hoc test) across groups (Fig. 4(A), (C), (E), (F), and (G) respectively). Foxo-1, Atrogin-1, and BNIP3 displayed non-significant trends toward increased expression levels following increasing durations of hypoxic exposure. Both Foxo-3 and MuRF-1 mRNA expression was significantly increased following 8 hours of hypoxic exposure compared with control ($p<0.05$, one-way ANOVA & Tukey's post hoc test) (Fig. 4B) and (D) respectively).

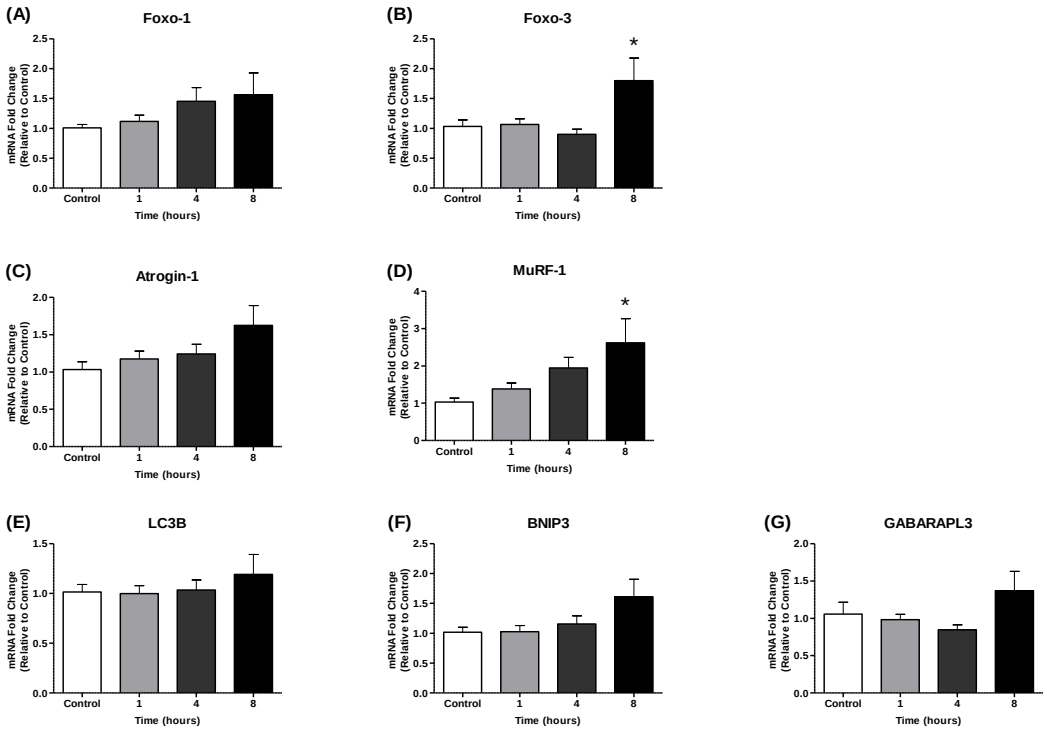

Figure 4: Diaphragm muscle gene expression related to atrophy and autophagy. Fold changes in mRNA expression (relative to the control group) for (A) Foxo-1; (B) Foxo-3; (C) Atrogin-1; (D) MuRF-1; (E) LC3B; (F) BNIP3; and (G) GABARAPL3 (mean ± SEM, n = 7-8 per group) (*$p < 0.05$ vs. control, one-way ANOVA and Tukey's post hoc test) following 1, 4 and 8 hours of hypoxia or control (normoxia).

Fig. 5 is a heat map depicting the diaphragm expression data for all of the genes examined, as discussed above.

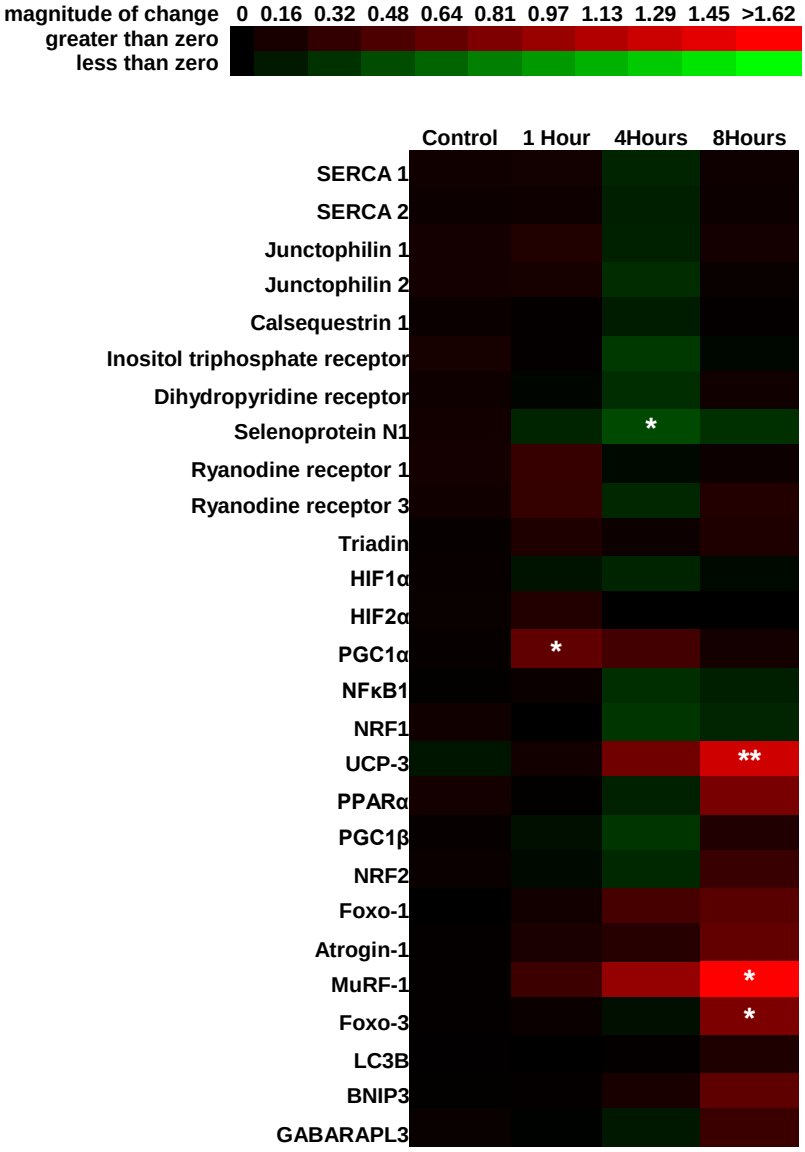

Figure 5: Diaphragm muscle gene expression data expressed in a heat map. Heat map depicting the fold changes in mRNA expression (relative to the control group) for genes related to metabolism and mitochondrial function, hypoxic signalling and inflammation, sarcoplasmic reticulum calcium handling, release and re-uptake, and atrophy and autophagy (mean ± SEM, n = 7-8 per group) (*$p < 0.05$ vs. control, **$p < 0.01$ vs. control, one-way ANOVA and Tukey's post hoc test) following 1, 4 and 8 hours of hypoxia or control (normoxia). Red represents an increase in expression; green represents a decrease in expression.

Fig. 6 shows diaphragm muscle chymotrypsin-like proteasome activity in control (normoxia) and hypoxia (8 hours) groups. There was no significant difference in chymotrypsin-like proteasome activity between the two groups (0.36 ± 0.03 vs. 0.35 ± 0.01 mean ± SEM pmol/min/mg protein; Control vs. Hypoxia; n = 8 per group; p = 0.9084; unpaired t-test).

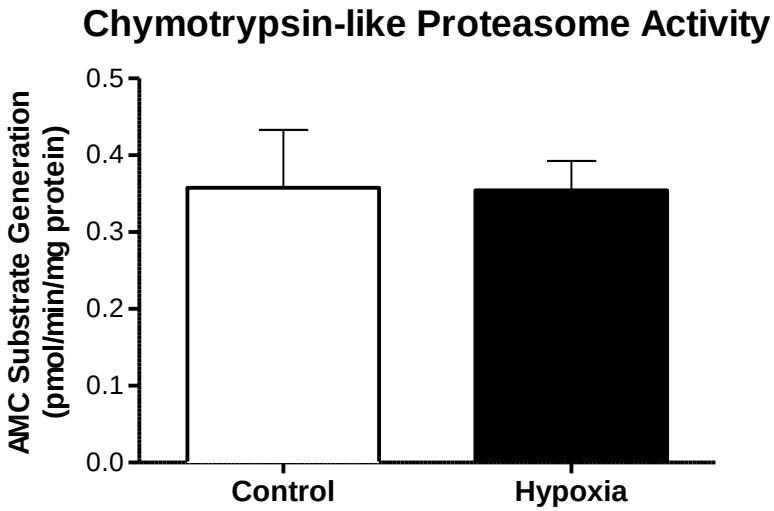

Figure 6: Diaphragm muscle chymotrypsin-like proteasome activity.
Chimotrypsin-like proteasome activity in diaphragm muscle from control (normoxia) and (8 hours) hypoxia groups (mean ± SEM, n = 8 per group, unpaired t-test) expressed as rate of AMC tag release from peptide substrate (pmol/min/mg of protein).

4.2.1.3 Sternohyoid

The expression of genes related to energy metabolism and mitochondrial function and biogenesis in the sternohyoid muscle are displayed in Fig. 7. PGC-1α mRNA expression was unaffected by hypoxia across all time points (one-way ANOVA & Tukey's post hoc test) (Fig. 7(A)). PGC-1β mRNA expression was not significantly affected compared with the control group, although there was a slight trend towards decreased expression levels in hypoxia (one-way ANOVA & Tukey's post hoc test) (Fig. 7(B)). NRF1 mRNA expression was significantly decreased at 4 hours compared with control and 1 hour groups ($p < 0.05$ and $p < 0.01$ respectively, one-way ANOVA

& Tukey's post hoc test) and decreased at 8 hours of hypoxia, non-significantly compared to the control group, but significantly compared with the one hour group ($p< 0.05$, one-way ANOVA & Tukey's post hoc test) (Fig. 7(C)). Neither NRF2 nor PPARα displayed any significant changes in expression across groups (one-way ANOVA & Tukey's post hoc test) (Fig. 7(D) & (E)). UCP-3 mRNA expression increased progressively with increased duration of hypoxic exposure compared with control; following 8 hours of hypoxic exposure, UCP-3 mRNA levels were significantly increased compared with the control (normoxia) group ($p<0.01$, one-way ANOVA & Tukey's post hoc test), and the 1 hour of hypoxia group ($p<0.05$) (Fig. 7(F)).

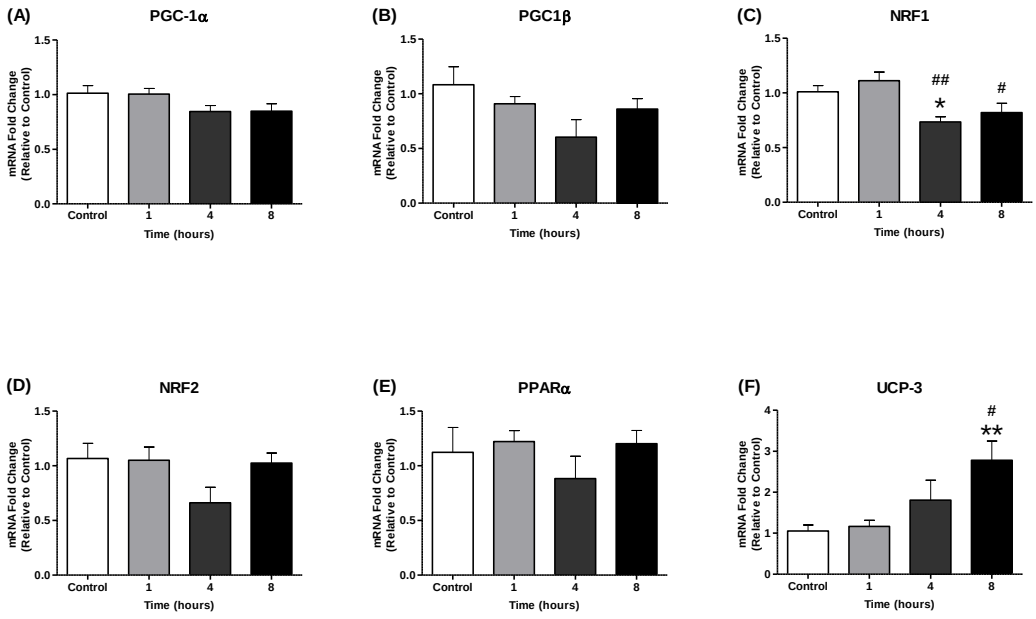

Figure 7: Sternohyoid muscle gene expression related to metabolism and mitochondrial function. Fold changes in mRNA expression (relative to the control group) for (A) PGC-1α; (B) PGC-1β; (C) NRF1; (D) NRF2; (E) PPARα; and (F) UCP-3 (mean ± SEM, n = 7-8 per group) (*$p < 0.05$ vs. control, **$p < 0.01$ vs. control, #$p < 0.05$ vs. 1 hour, ##$p < 0.001$ vs, 1 hour, one-way ANOVA and Tukey's post hoc test) following 1, 4 and 8 hours of hypoxia or control (normoxia).

Fig. 8 shows sternohyoid muscle expression data for genes related to hypoxic signalling and inflammation. There was no significant change in HIF-1α mRNA expression in hypoxia at any time point (one-way ANOVA & Tukey's post hoc test) compared with control, although there was a decreased expression after 4 hours of hypoxia compared with the 1 hour hypoxia group (Fig. 8(A)). There was no significant change in HIF-2α mRNA expression (one-way ANOVA & Tukey's post hoc test) across groups (Fig. 8(B)). NF-κB1 mRNA expression showed significantly decreased expression at 4 and 8 hours of hypoxia compared with both control and 1 hour groups ($p<0.01$ 4 hours vs. control, $p < 0.001$ 8 hours vs. control, $p< 0.05$ 4 hours vs. 1 hour, $p <0.01$ 8 hours vs. 1 hour, one-way ANOVA & Tukey's post hoc test) (Fig. 8(C)).

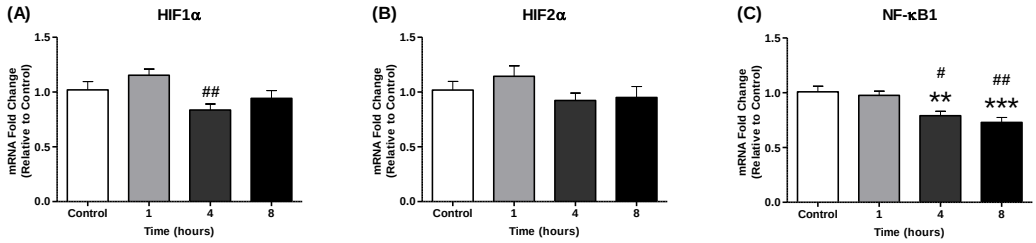

Figure 8: Sternohyoid muscle gene expression related to hypoxic signalling and inflammation. Fold changes in mRNA expression (relative to the control group) for (A) HIF1α; (B) HIF2α; and (C) NF-κB1 (mean ± SEM, n = 7-8 per group) (*$p < 0.05$ vs. control, **$p < 0.01$ vs. control, ***$p < 0.001$ vs. control, #$p < 0.05$ vs. 1 hour, ##$p < 0.01$ vs. 1 hour, one-way ANOVA and Tukey's post hoc test) following 1, 4 and 8 hours of hypoxia or control (normoxia).

Fig. 9 shows sternohyoid muscle expression data for genes related to sarcoplasmic reticulum calcium handling, release and re-uptake. There were no significant changes in SERCA 1, SERCA 2a, Triadin, Ryanodine receptor 3, or Inositol Trisphosphate Receptor mRNA expression (one-way ANOVA & Tukey's post hoc test) across groups (Fig. 9 (A), (B), (F), (H) and (K) respectively). Junctophilin 1 mRNA expression was significantly decreased at 4 hours compared with control and 1 hour groups ($p < 0.05$ and $p < 0.01$ respectively, one-way ANOVA & Tukey's post hoc

test) (Fig. 9(C)). Junctophilin 2 mRNA expression was significantly decreased at 4 hours compared with control ($p < 0.05$, one-way ANOVA & Tukey's post hoc test) (Fig. 9(D)). Calsequestrin 1 mRNA expression was significantly decreased at 4 hours compared with control and 1 hour groups ($p < 0.01$ and $p < 0.05$ respectively, one-way ANOVA & Tukey's post hoc test) (Fig. 9(E)). Ryanodine Receptor 1 mRNA expression was significantly decreased at 4 hours compared with the 1 hour groups ($p < 0.05$, one-way ANOVA & Tukey's post hoc test), but not compared with the control group (Fig. 9(G)). Dihydropyridine Receptor mRNA expression was significantly decreased at 4 hours compared with control and 1 hour groups ($p < 0.05$ in both cases, one-way ANOVA & Tukey's post hoc test) (Fig. 9(J)). Selenoprotein N1 mRNA expression displayed a trend toward decreased expression at 1, 4 and 8 hours of hypoxia compared with control, with expression in the 4 hours and 8 hours hypoxia groups significantly lower than expression in the control group ($p<0.05$ in both cases, one-way ANOVA & Tukey's post hoc test) (Fig. 3(I)).

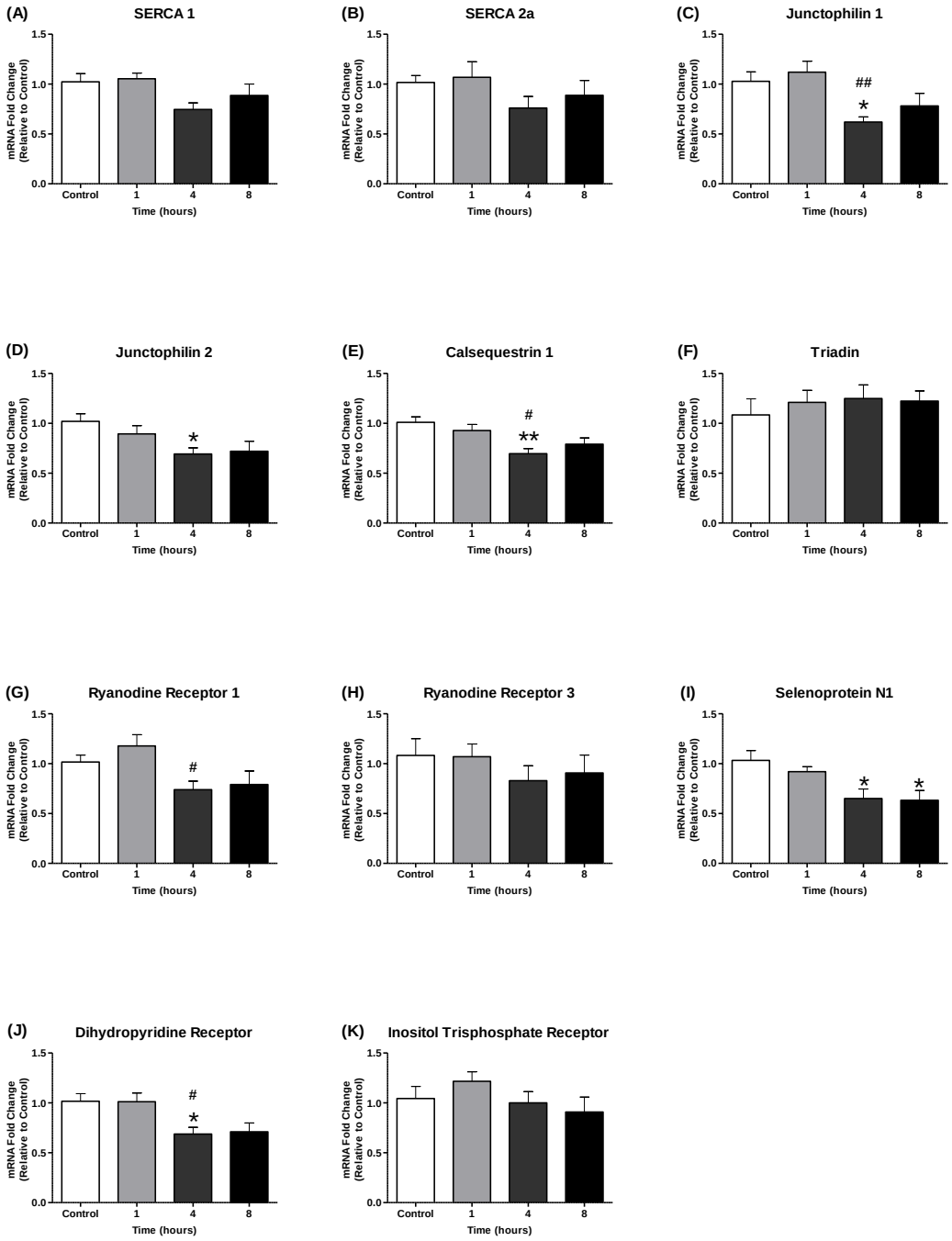

Figure 9: Sternohyoid muscle gene expression related to sarcoplasmic reticulum calcium handling, release and re-uptake. Fold changes in mRNA expression (relative to the control group) for (A) SERCA 1; (B) SERCA 2a; (C) Junctophilin 1; (D) Junctophilin 2; (E) Calsequestrin 1; (F) Triadin; (G) Ryanodine Receptor 1; (H) Ryanodine Receptor 3; (I) Selenoprotein N1; (J) Dihydropyridine Receptor; and (K) Inositol Triphosphate Receptor 1 (mean ± SEM, n = 7-8 per group) (*$p < 0.05$ vs. control, **$p < 0.01$ vs. control, #$p < 0.05$ vs. 1 hour, ##$p < 0.01$ vs. 1 hour, one-way

ANOVA and Tukey's post hoc test) following 1, 4 and 8 hours of hypoxia or control (normoxia).

Fig. 10 shows sternohyoid muscle expression data for genes related to atrophy. There were no significant changes in Foxo-1, Atrogin-1, or MuRF-1 mRNA expression (one-way ANOVA & Tukey's post hoc test) across groups (Fig. 4 (A), (B) and (C) respectively). Foxo-1 and Atrogin-1 displayed non-significant trends toward increased expression levels following increasing durations of hypoxic exposure.

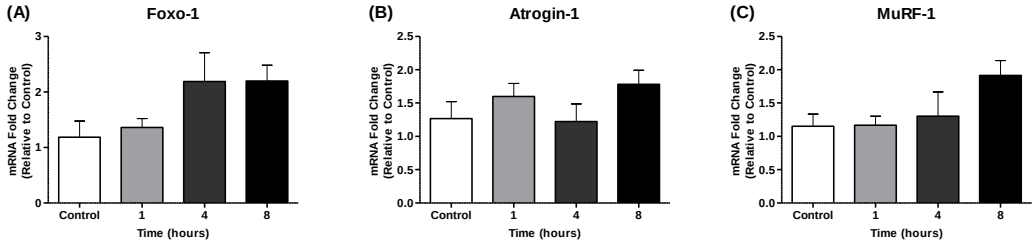

Figure 10: Sternohyoid muscle gene expression related to atrophy. Fold changes in mRNA expression (relative to the control group) for (A) Foxo-1; (B) Atrogin-1; and (C) MuRF-1 (mean ± SEM, n = 7-8 per group) (one-way ANOVA and Tukey's post hoc test) following 1, 4 and 8 hours of hypoxia or control (normoxia).

Fig.11 is a heat map depicting the sternohyoid muscle expression data for all of the genes examined, as discussed above.

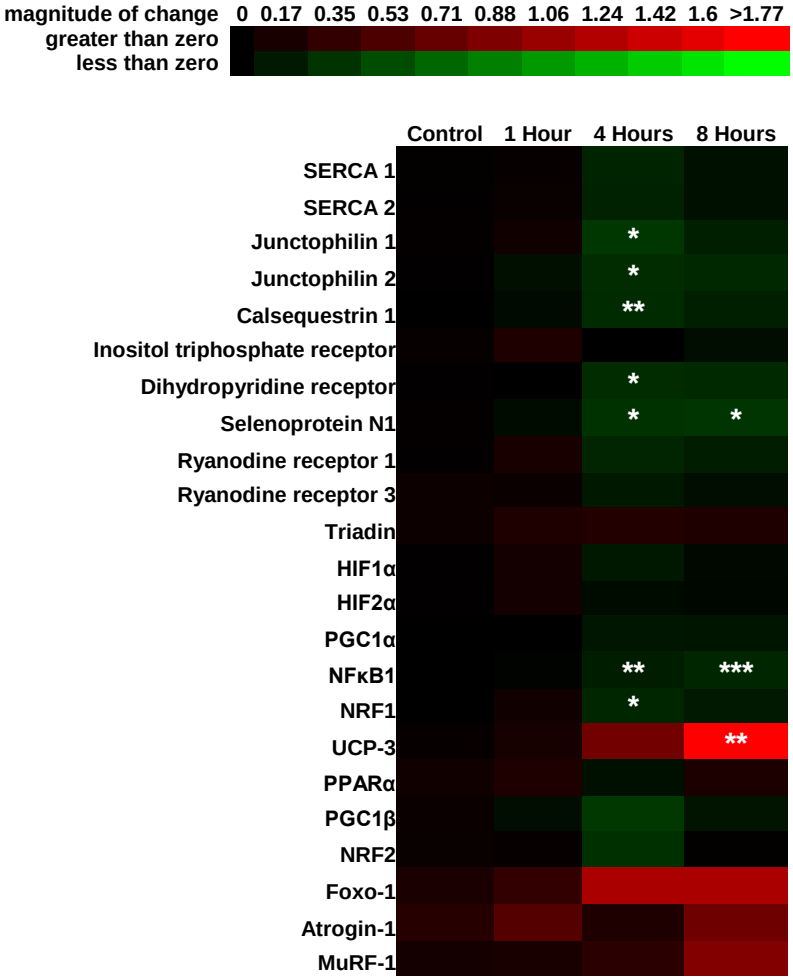

Figure 11: Sternohyoid muscle gene expression data expressed in a heat map. Heat map depicting the fold changes in mRNA expression (relative to the control group) for genes related to metabolism and mitochondrial function, hypoxic signalling and inflammation, sarcoplasmic reticulum calcium handling, release and re-uptake, and atrophy and autophagy (mean ± SEM, n = 7-8 per group) (*$p < 0.05$ vs. control, **$p < 0.01$ vs. control, ***$p < 0.001$ vs. control, one-way ANOVA and Tukey's post hoc test) following 1, 4 and 8 hours of hypoxia or control (normoxia). Red represents an increase in expression; green represents a decrease in expression.

4.2.1.4 Limb Muscles

4.2.1.4.1 EDL

The expression of genes related to energy metabolism and mitochondrial function and hypoxia signalling in the EDL muscle are displayed in Fig. 12. PGC-1α mRNA expression was unaffected by hypoxia across all time points (one-way ANOVA & Tukey's post hoc test) (Fig. 12(A)). NRF1 mRNA expression was also unaffected by hypoxia across all time points (one-way ANOVA & Tukey's post hoc test) (Fig. 12(B)), as was the expression of NFκB1, HIF1α, and HIF2α (one-way ANOVA & Tukey's post hoc test) (Fig. 12 (C), (D) and (E)). UCP-3 mRNA expression increased with increased duration of hypoxic exposure compared with control. Following 4 hours of hypoxic exposure, UCP-3 mRNA levels were significantly increased compared with the control (normoxia) group ($p<0.01$, one-way ANOVA & Tukey's post hoc test), and the 1 hour of hypoxia group ($p<0.05$) (Fig. 12(F)); following 8 hours of hypoxic exposure UCP-3 mRNA levels were increased significantly compared with the control group ($p<0.05$, one-way ANOVA & Tukey's post hoc test).

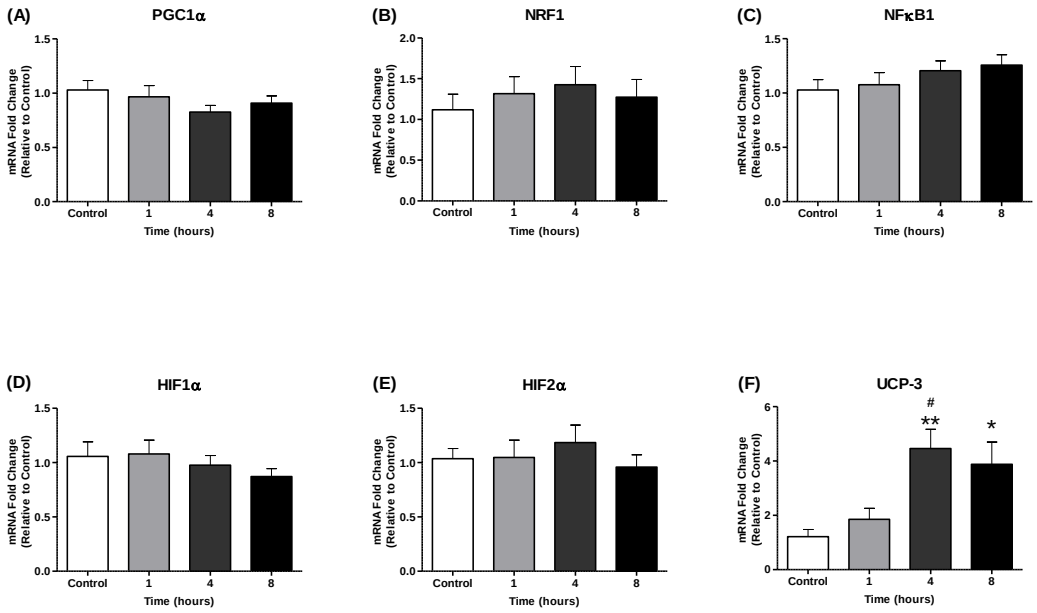

Figure 12: EDL muscle gene expression related to metabolism and mitochondrial function, and hypoxia signalling. Fold changes in mRNA expression (relative to the

control group) for (A) PGC-1α; (B) NRF1; (C) NFκB1; (D) HIF1α; (E) HIF2α; and (F) UCP-3 (mean ± SEM, n = 7-8 per group) (*$p < 0.05$ vs. control, **$p < 0.01$ vs. control, #$p < 0.05$ vs. 1 hour, one-way ANOVA and Tukey's post hoc test) following 1, 4 and 8 hours of hypoxia or control (normoxia).

Fig. 13 shows EDL muscle expression data for genes related to sarcoplasmic reticulum calcium handling, release and re-uptake. There were no significant changes in SERCA 1, SERCA 2a, Calsequestrin 1, Junctophilin 1, Junctophilin 2, Triadin, Ryanodine Receptor 1, Ryanodine receptor 3, Selenoprotein N1, Dihydropyridine Receptor or Inositol Trisphosphate Receptor mRNA expression (one-way ANOVA & Tukey's post hoc test) across groups (Fig. 13A-K).

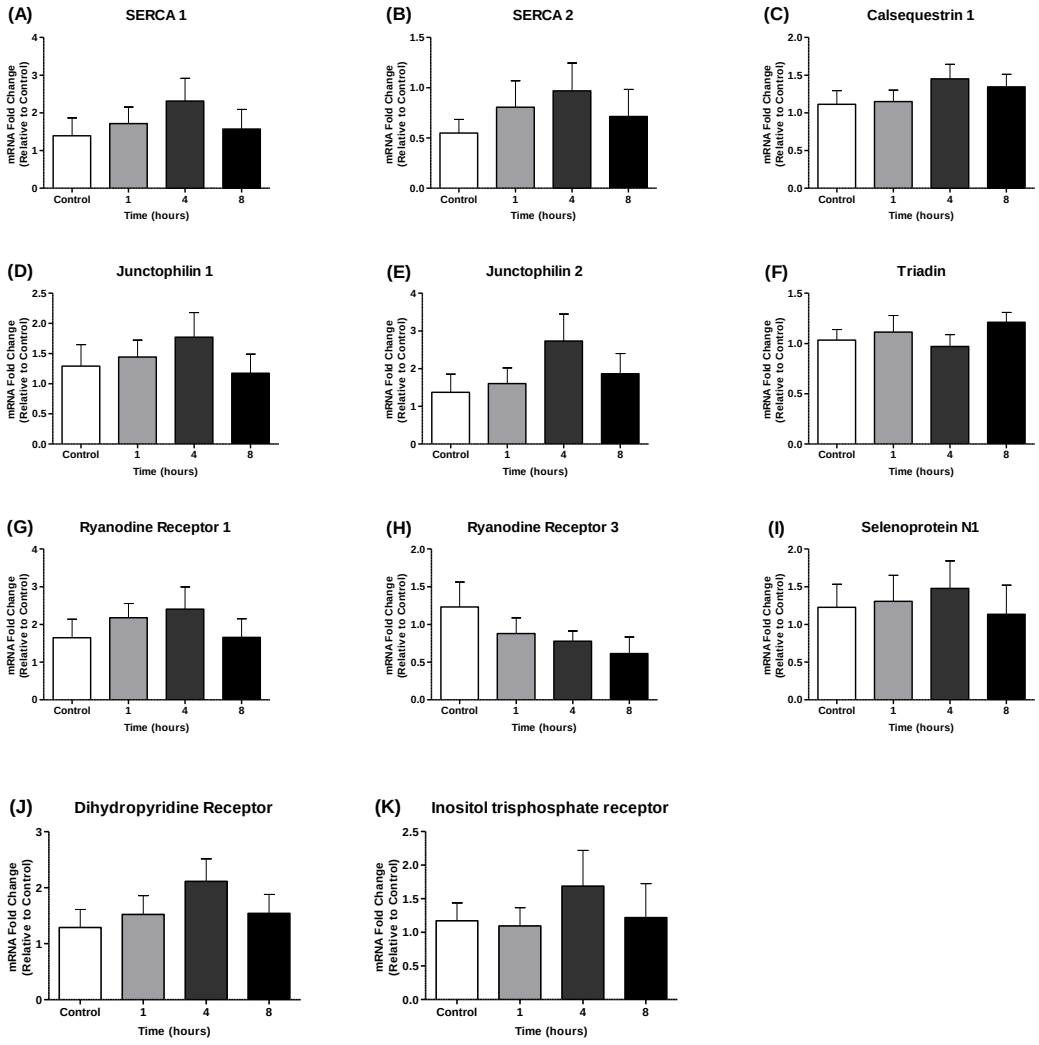

Figure 13: EDL muscle gene expression related to sarcoplasmic reticulum calcium handling, release and re-uptake. Fold changes in mRNA expression (relative to the control group) for (A) SERCA 1; (B) SERCA 2; (C) Calsequestrin 1; (D) Junctophilin 1; (E) Junctophilin 2; (F) Triadin; (G) Ryanodine Receptor 1; (H) Ryanodine Receptor 3; (I) Selenoprotein N1; (J) Dihydropyridine Receptor; and (K) Inositol Triphosphate Receptor 1 (mean ± SEM, n = 7-8 per group) (one-way ANOVA and Tukey's post hoc test) following 1, 4 and 8 hours of hypoxia or control (normoxia).

Fig. 14 shows EDL muscle expression data for genes related to atrophy. MuRF-1 gene expression in the EDL was significantly increased following 4 and 8 hours of hypoxic exposure compared with the control group ($p < 0.05$ in both cases, one-way ANOVA & Tukey's post hoc test) (Fig. 14 (A)). FOXO-1 gene expression in the EDL

was significantly increased following 4 hours of hypoxic exposure compared with the control and 1 hour hypoxia groups ($p < 0.01$ in both cases, one-way ANOVA & Tukey's post hoc test) and expression was also elevated in the 8 hours hypoxia group although not to statistical significance (Fig. 14 (B)). Atrogin-1 mRNA expression in the EDL was significantly increased following 4 hours of hypoxic exposure compared with the control group and the 1 hour group ($p < 0.01$ and $p < 0.05$ respectively, one-way ANOVA & Tukey's post hoc test) and expression was also increased significantly in the 8 hours group compared with the control group ($p < 0.05$, one-way ANOVA & Tukey's post hoc test) (Fig. 14 (C)).

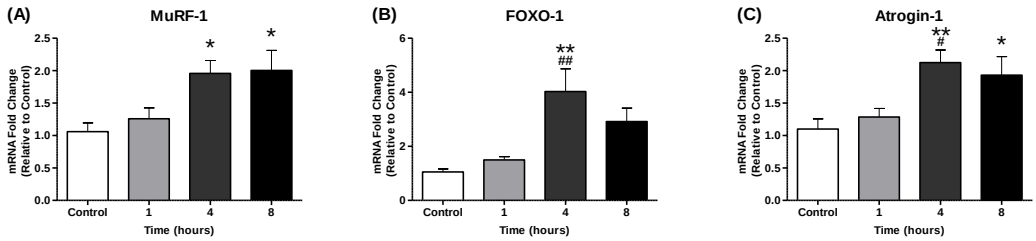

Figure 14: EDL muscle gene expression related to atrophy. Fold changes in mRNA expression (relative to the control group) for (A) MuRF-1; (B) FOXO-1; and (C) Atrogin-1 (mean ± SEM, n = 7-8 per group) (one-way ANOVA and Tukey's post hoc test) following 1, 4 and 8 hours of hypoxia or control (normoxia).

Fig.15 is a heat map depicting the EDL muscle expression data for all of the genes examined, as discussed above.

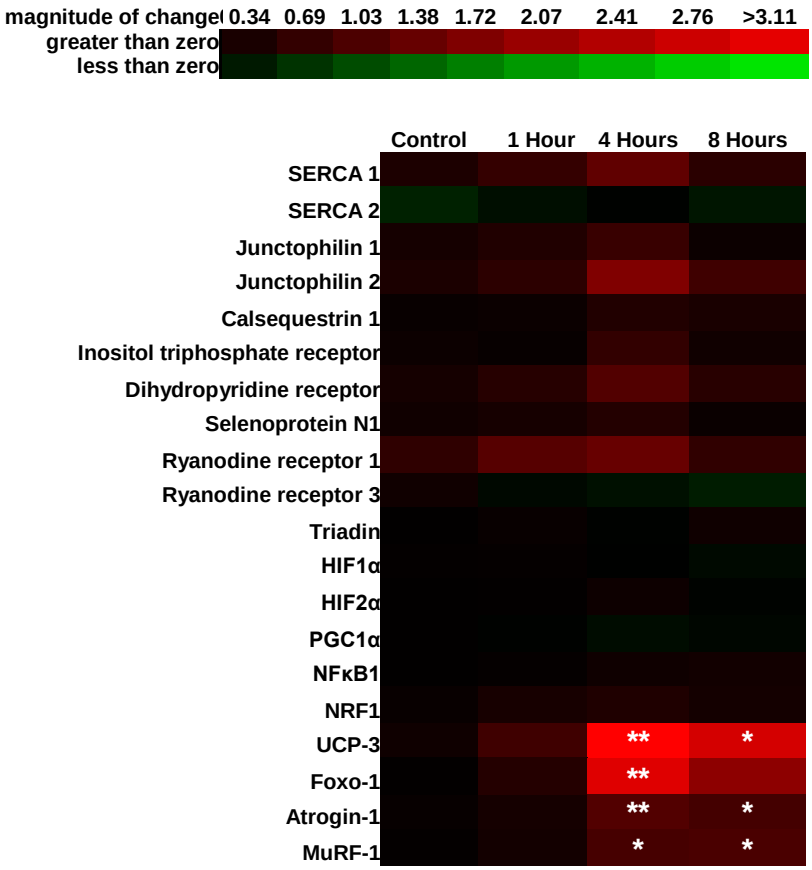

Figure 15: EDL muscle gene expression data expressed in a heat map. Heat map depicting the fold changes in mRNA expression (relative to the control group) for genes related to metabolism and mitochondrial function, hypoxic signalling and inflammation, sarcoplasmic reticulum calcium handling, release and re-uptake, and atrophy and autophagy (mean ± SEM, n = 7-8 per group) (*$p < 0.05$ vs. control, **$p < 0.01$ vs. control, one-way ANOVA and Tukey's post hoc test) following 1, 4 and 8 hours of hypoxia or control (normoxia). Red represents an increase in expression; green represents a decrease in expression.

4.2.1.4.2 Soleus

The expression of genes related to energy metabolism and mitochondrial function and hypoxia signalling in the soleus muscle are displayed in Fig. 16. PGC-1α mRNA expression was unaffected by hypoxia across all time points (one-way ANOVA & Tukey's post hoc test) (Fig. 16(A)). NRF1 mRNA expression was also unaffected by hypoxia across all time points (one-way ANOVA & Tukey's post hoc test) (Fig. 16(B)), as was the expression of NFκB1, HIF1α, and HIF2α (one-way ANOVA & Tukey's post hoc test) (Fig. 16 (C), (D) and (E)). UCP-3 mRNA expression increased with increased hypoxic exposure compared with control. Following 8 hours of hypoxic exposure, UCP-3 mRNA levels were significantly increased compared with the control (normoxia) group ($p<0.05$, one-way ANOVA & Tukey's post hoc test), and the 1 hour of hypoxia group ($p<0.05$) (Fig. 15(F)).

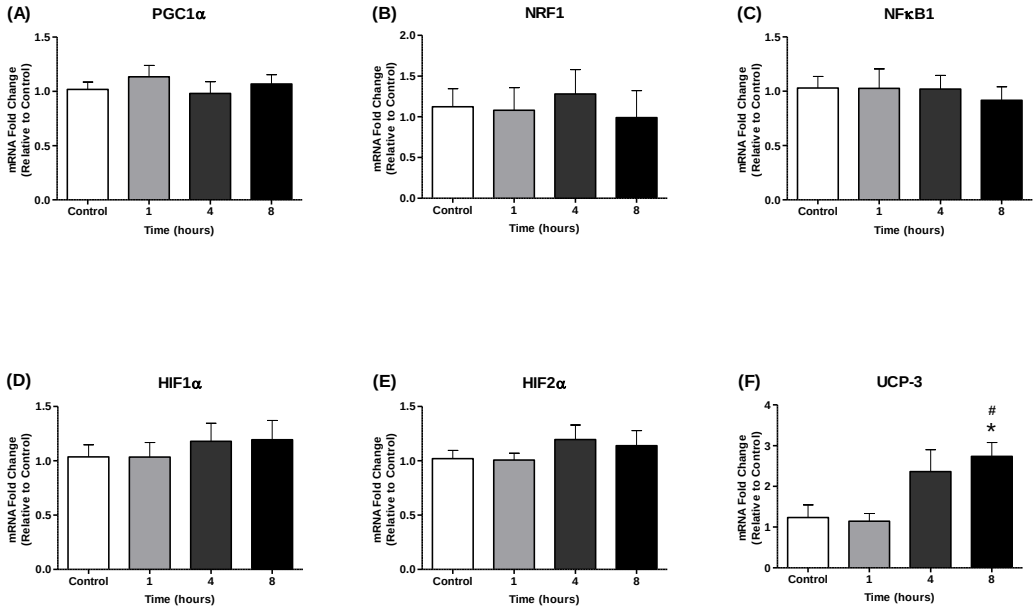

Figure 16: Soleus muscle gene expression related to metabolism and mitochondrial function, and hypoxia signalling. Fold changes in mRNA expression (relative to the control group) for (A) PGC-1α; (B) NRF1; (C) NFκB1; (D) HIF1α; (E) HIF2α; and (F) UCP-3 (mean ± SEM, n = 7-8 per group) (*$p < 0.05$ vs. control, #$p < 0.05$ vs. 1 hour, one-way ANOVA and Tukey's post hoc test) following 1, 4 and 8 hours of hypoxia or control (normoxia).

Fig. 17 shows soleus muscle expression data for genes related to sarcoplasmic reticulum calcium handling, release and re-uptake. There were no significant changes in SERCA 1, SERCA 2a, Calsequestrin 1, Junctophilin 1, Junctophilin 2, Triadin, Ryanodine Receptor 1, Ryanodine receptor 3, Selenoprotein N1, Dihydropyridine Receptor or Inositol Trisphosphate Receptor mRNA expression (one-way ANOVA & Tukey's post hoc test) across groups (Fig. 17 A-K).

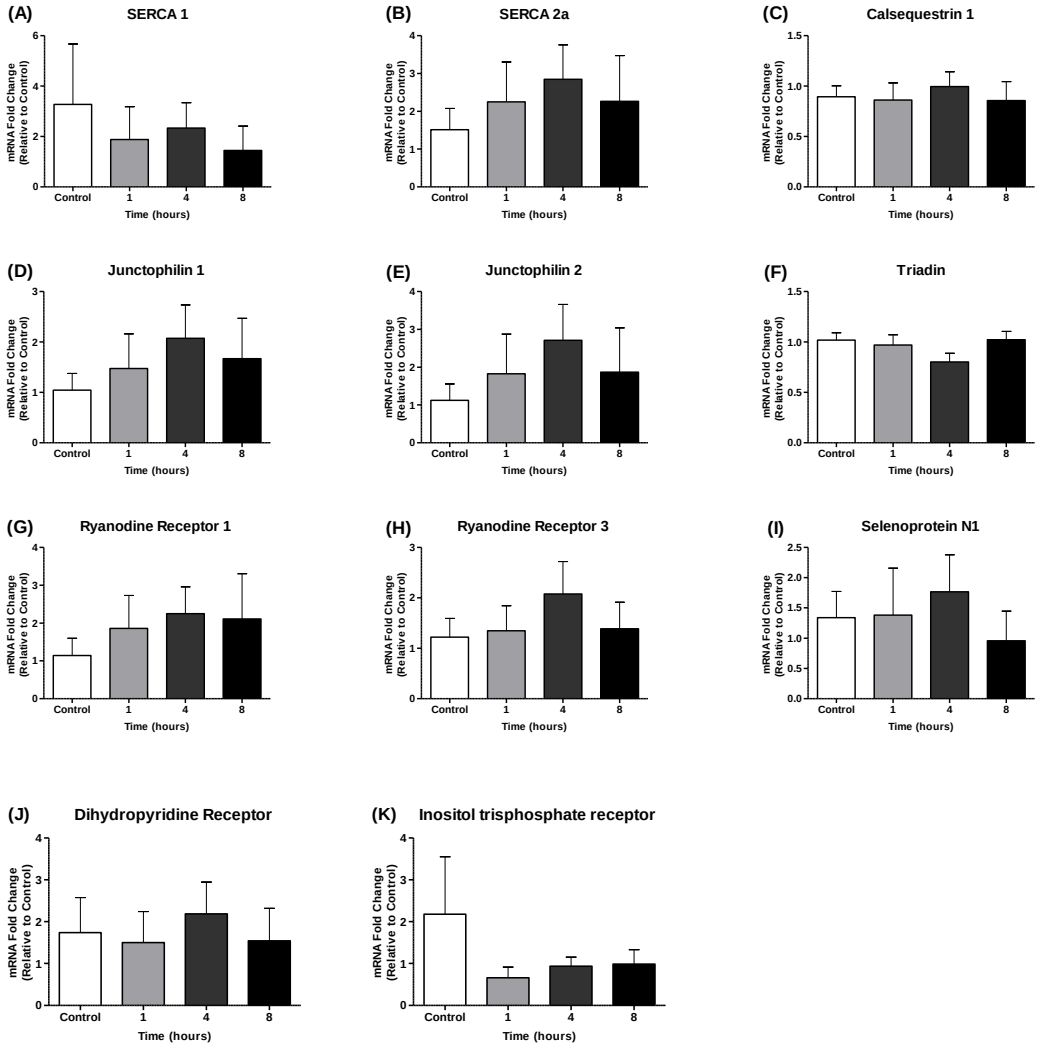

Figure 17: Soleus muscle gene expression related to sarcoplasmic reticulum calcium handling, release and re-uptake. Fold changes in mRNA expression (relative to the control group) for (A) SERCA 1; (B) SERCA 2a; (C) Calsequestrin 1; (D) Junctophilin 1; (E) Junctophilin 2; (F) Triadin; (G) Ryanodine Receptor 1; (H)

Ryanodine Receptor 3; (I) Selenoprotein N1; (J) Dihydropyridine Receptor; and (K) Inositol Triphosphate Receptor 1 (mean ± SEM, n = 7-8 per group) (one-way ANOVA and Tukey's post hoc test) following 1, 4 and 8 hours of hypoxia or control (normoxia).

Fig. 18 shows soleus muscle expression data for genes related to atrophy. FOXO-1 gene expression in the soleus muscle was significantly increased following 4 hours of hypoxic exposure compared to the control group ($p < 0.05$, one-way ANOVA & Tukey's post hoc test) (Fig. 18 (A)). FOXO-1 expression was also increased in the 8 hours of hypoxia group, although not to statistical significance. Atrogin-1 gene expression was not significantly affected by hypoxia in any group compared with control, although there was a trend towards increased atrogin-1 mRNA expression as the duration of hypoxic exposure increased (Fig. 18 (B)). MuRF-1 mRNA expression in the soleus muscle was significantly increased following 8 hours of hypoxic exposure compared with the control group and the 1 hour group ($p < 0.05$ in both cases, one-way ANOVA & Tukey's post hoc test) (Fig. 18 (C)).

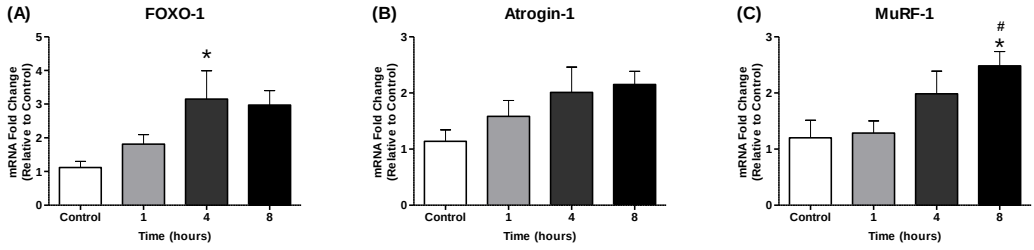

Figure 18: Soleus muscle gene expression related to atrophy. Fold changes in mRNA expression (relative to the control group) for (A) FOXO-1; (B) Atrogin-1; and (C) MuRF-1 (mean ± SEM, n = 7-8 per group) (*$p < 0.05$ vs. control, #$p < 0.05$ vs. 1 hour, one-way ANOVA and Tukey's post hoc test) following 1, 4 and 8 hours of hypoxia or control (normoxia).

Fig.19 is a heat map depicting the Soleus muscle expression data for all of the genes examined, as discussed above.

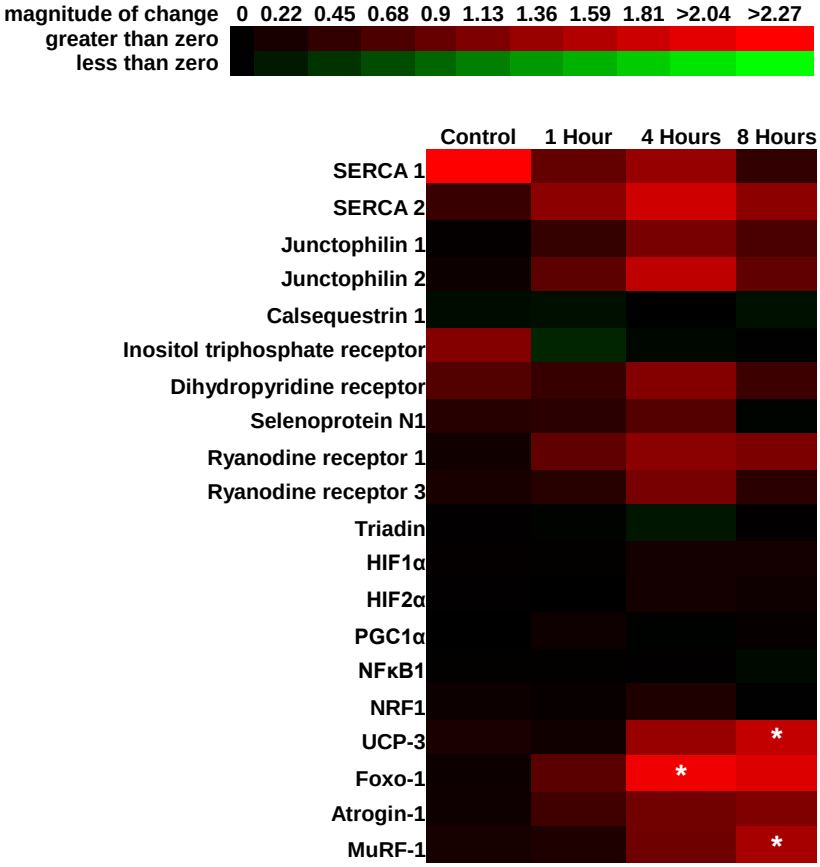

Figure 19: Soleus muscle gene expression data expressed in a heat map. Heat map depicting the fold changes in mRNA expression (relative to the control group) for genes related to metabolism and mitochondrial function, hypoxic signalling and inflammation, sarcoplasmic reticulum calcium handling, release and re-uptake, and atrophy and autophagy (mean ± SEM, n = 7-8 per group) (*$p < 0.05$ vs. control, one-way ANOVA and Tukey's post hoc test) following 1, 4 and 8 hours of hypoxia or control (normoxia). Red represents an increase in expression; green represents a decrease in expression.

4.2.2 Breathing and Metabolism

4.2.2.2 Breathing

Fig. 20 shows mouse respiratory rate over 8 hours of normoxia (control) and hypoxia exposure. Respiratory frequency was increased ($p<0.01$, two-way ANOVA & Bonferroni post hoc test) after 10 mins of hypoxia compared with normoxia, but returned to levels equivalent to normoxia by 20mins, and then dropped significantly below normoxic levels at 2 hours ($p<0.05$, two-way ANOVA & Bonferroni post hoc test), before returning to levels equivalent to normoxic levels, and remaining similar to normoxia for the remainder of the 8 hour hypoxia exposure.

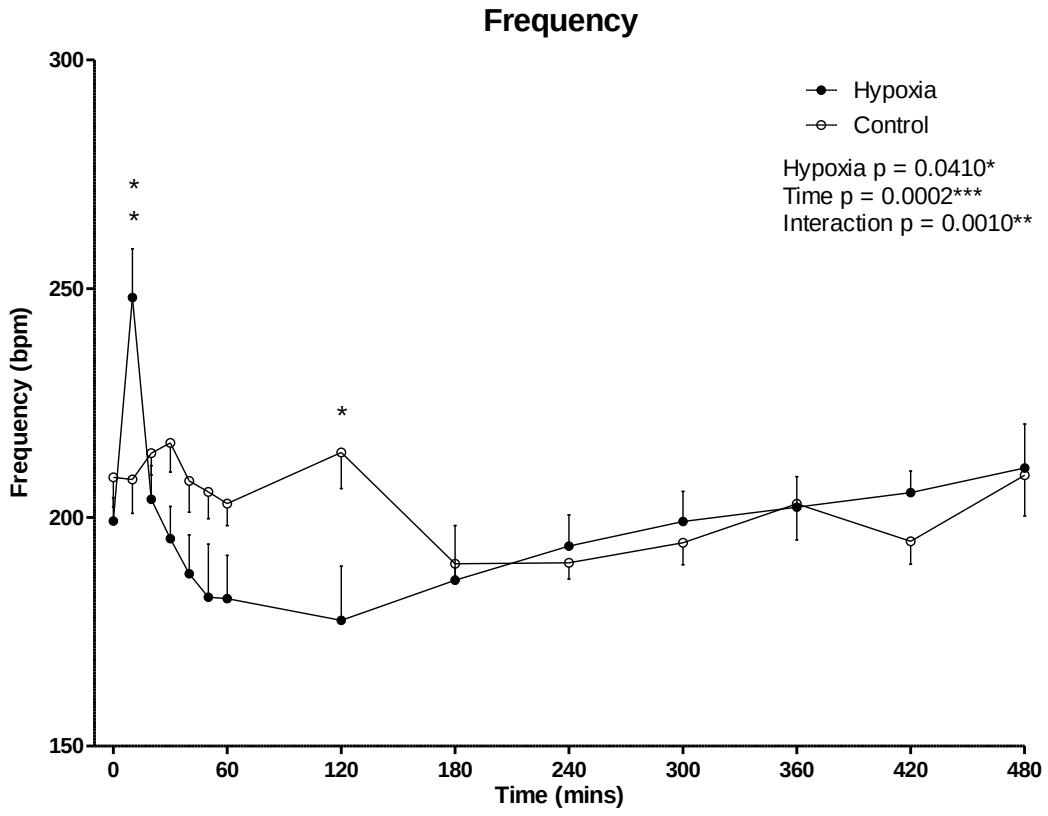

Figure 20: Mouse respiratory frequency during 8 hour exposure to either a normoxic (Control) or hypoxic (Hypoxia) environment. Mouse respiratory frequency (mean ± SEM) expressed as breaths per minute (bpm) over the 480 minute

(8 hour) period of exposure to gases (n = 6-7 per group) (*p < 0.05, **p < 0.01, two-way ANOVA and Bonferroni's multiple comparisons test).

Fig. 21 shows mouse tidal volume over 8 hours of normoxia (control) and hypoxia. Tidal volume was increased significantly (p<0.001, two-way ANOVA & Bonferroni post hoc test) after 10 mins of hypoxia compared with normoxia, but returned to levels equivalent to normoxia by 20mins and remained at levels similar to normoxia for the remainder of the 8 hour hypoxia exposure.

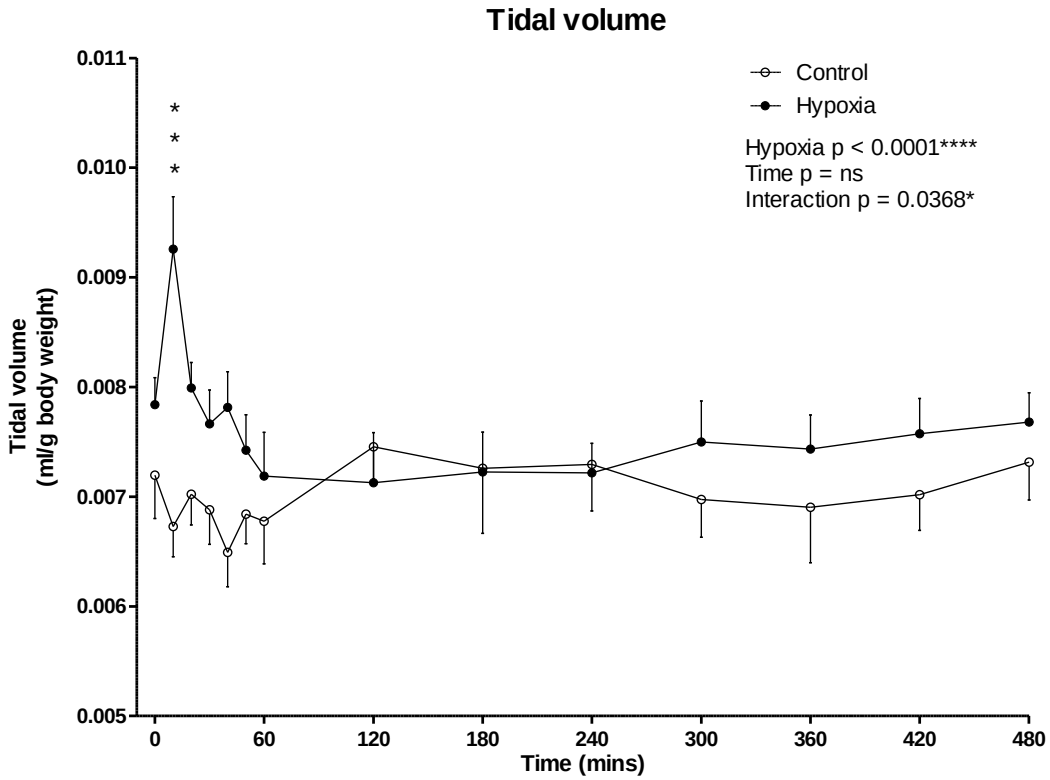

Figure 21: Mouse tidal volume during 8 hour exposure to either a normoxic (Control) or hypoxic (Hypoxia) environment. Mouse tidal volume (mean ± SEM) expressed as ml per gram of body weight (ml/g) over the 480 minute (8 hour) period of exposure to gases (n = 6-7 per group) (***p < 0.001, two-way ANOVA and Bonferroni's multiple comparisons test).

Fig. 22 shows mouse minute ventilation, a product of respiratory frequency and tidal volume, over 8 hours of normoxia (control) and hypoxia. Minute ventilation was increased significantly ($p<0.001$, two-way ANOVA & Bonferroni post hoc test) after 10 mins of hypoxia compared with normoxia, but returned to levels equivalent to normoxia by 20mins and remained at levels similar to normoxia for the remainder of the 8 hour hypoxia exposure.

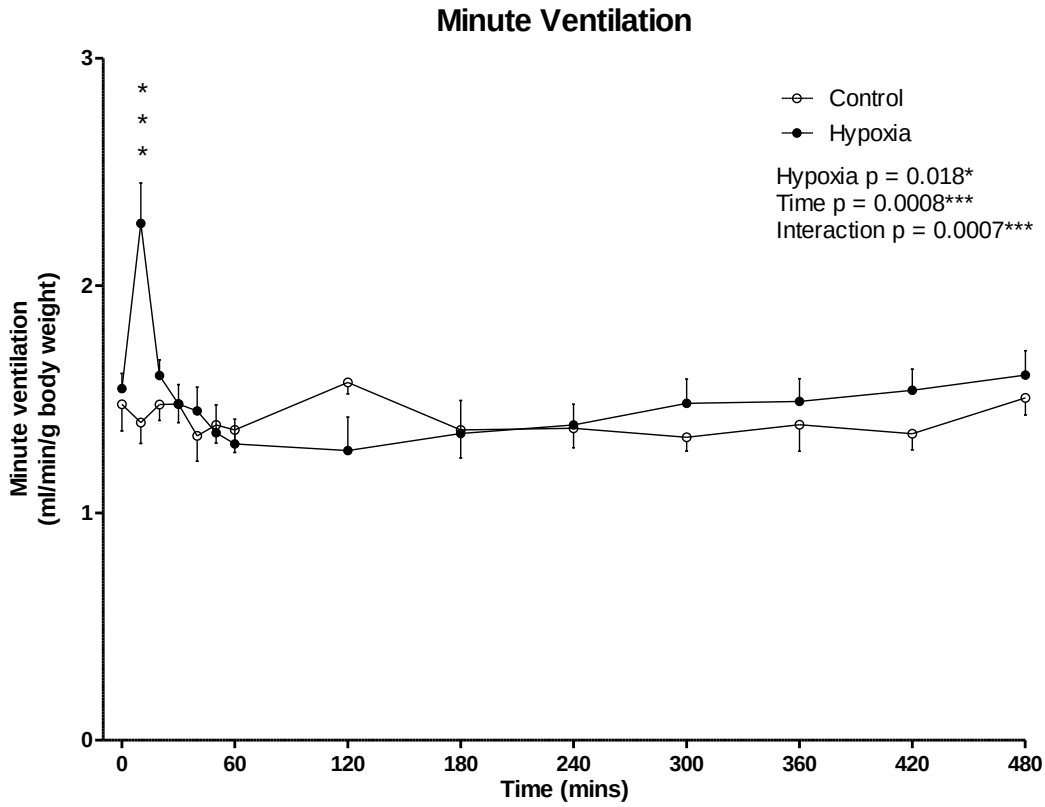

Figure 22: Mouse minute ventilation during 8 hour exposure to either a normoxic (Control) or hypoxic (Hypoxia) environment. Mouse minute ventilation (mean ± SEM) expressed as ml per minute per gram of body weight (ml/min/g) over the 480 minute (8 hour) period of exposure to gases (n = 6-7 per group) (***$p < 0.001$, two-way ANOVA and Bonferroni's multiple comparisons test).

4.2.2.3 Metabolism

Fig. 23 displays mouse *post-mortem* body temperature following 8 hours of exposure to hypoxia or normoxia. Fig. 23(A) shows data for mice that were housed individually during gas exposure for the purpose of measuring breathing and metabolic parameters during gas exposure, whereas Fig. 23(B) shows data for mice that were housed in groups of 4 during gas exposure and subsequently used for tissue harvest for molecular analysis. In both instances, mice exposed to hypoxia had consistently lower body temperatures by ~ 2°C following hypoxia in comparison to mice in the control group that were exposed to normoxia (**$p = 0.0021$ for individually exposed mice; ****$p < 0.0001$ for grouped mice, unpaired t-test).

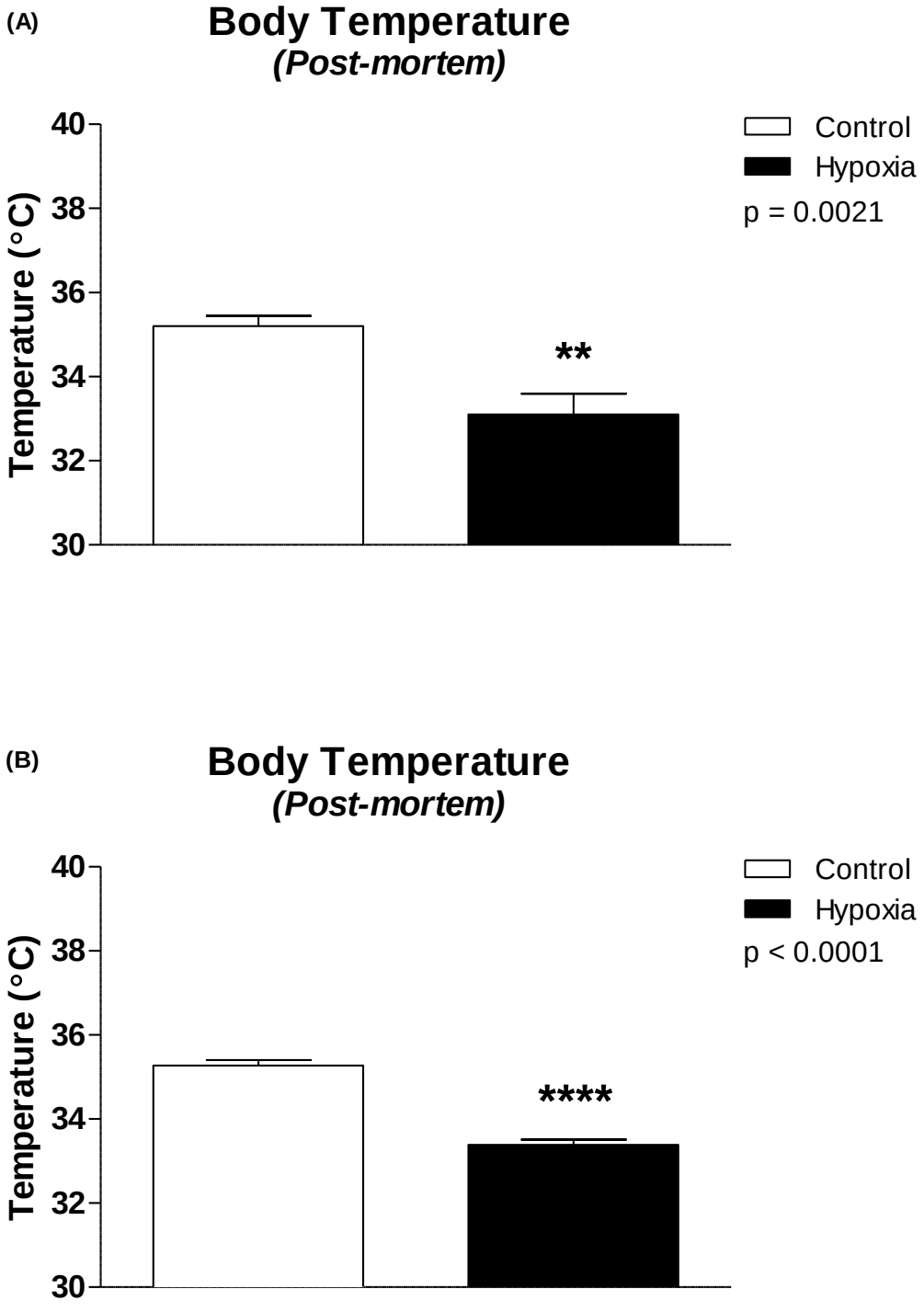

Figure 23: Mouse post-mortem body temperature. *Post-mortem* rectal temperatures (mean ± SEM) of mice exposed to hypoxia or normoxia, either (A) individually or (B) in groups following 8 hours of exposure to hypoxia or normoxia (n = 6-8 per group) (**p = 0.0021, ****p < 0.0001, unpaired t-test).

Fig. 24 displays mouse *post-mortem* body temperature following 8 hours of hypoxia and normoxia. Fig. 24(A) shows data comparing control mice that were individually exposed to normoxic gas to control mice that were grouped during normoxic gas exposure, whereas fig. 24(B) shows data from hypoxic mice that were individually exposed to hypoxic gas compared with hypoxic mice that were grouped during hypoxic exposure. In both instances, there are no differences for temperature values between mice exposed to either gas individually or in groups (unpaired t-test).

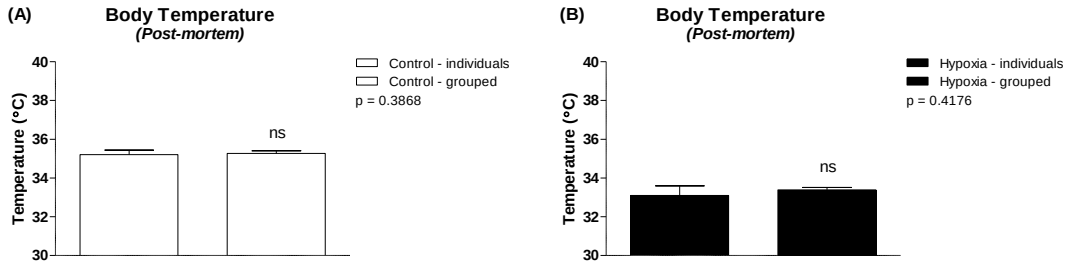

Figure 24: Mouse post-mortem body temperature. *Post-mortem* rectal temperatures (mean ± SEM) of mice exposed to hypoxia or normoxia displayed as (A) Control (normoxia) mice exposed individually vs. those exposed in groups and (B) Hypoxia mice exposed individually vs. those exposed in groups, following 8 hours of hypoxia or normoxia (n = 6-8 per group) (unpaired t-test).

Fig. 25 shows mouse oxygen consumption over 8 hours of exposure to either a normoxic (Control) or hypoxic (Hypoxia) environment. Oxygen consumption showed an initial spike in the first 5–10 minutes of hypoxia and then dropped below the oxygen consumption level of the control group, over the course of the 8 hours of exposure. Hypoxia thus significantly affected oxygen consumption (***p = 0.0008, two-way ANOVA and Bonferroni's multiple comparisons test), predominantly decreasing it over the 8 hours of gas exposure.

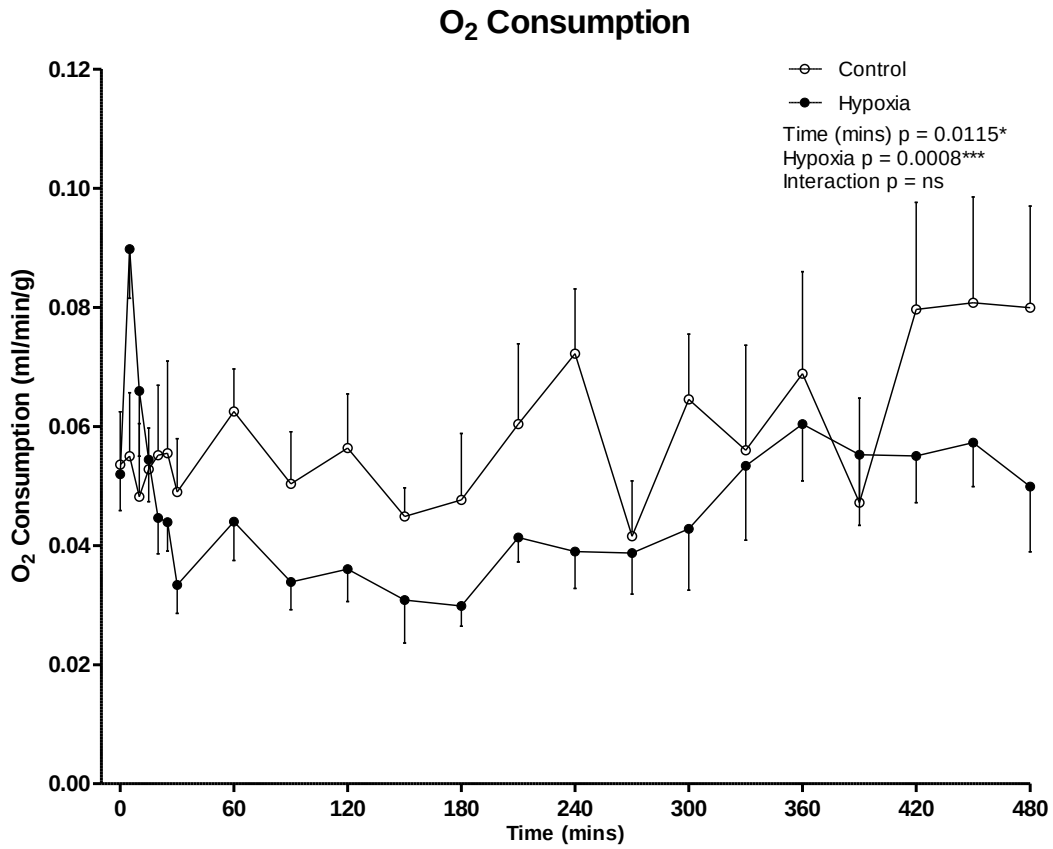

Figure 25: Mouse oxygen consumption during 8 hour exposure to either a normoxic (Control) or hypoxic (Hypoxia) environment. Oxygen consumption (mean ± SEM) in the mouse expressed as ml per minute per gram of body weight (ml/min/g) over the 480 minutes (8 hour) period of exposure to either hypoxia or normoxia (n = 6-7 per group) (two-way ANOVA and Bonferroni's multiple comparisons test).

Fig. 26 shows mouse carbon dioxide production over 8 hours of exposure to either a normoxic (Control) or hypoxic (Hypoxia) environment. Carbon dioxide production began to drop upon hypoxic exposure and dropped below the carbon dioxide production level of the control group, over the course of the 8 hours of gas exposure. Carbon dioxide production was significantly lower in the hypoxia group at 15, 20 and 60 minutes of gas exposure ($p < 0.01$, $p < 0.05$, and $p < 0.01$ respectively, two-way ANOVA and Bonferroni's multiple comparisons test), and hypoxia significantly reduced carbon dioxide production (****$p < 0.0001$, two-way ANOVA and

Bonferroni's multiple comparisons test) over the duration of the 8 hours of gas exposure.

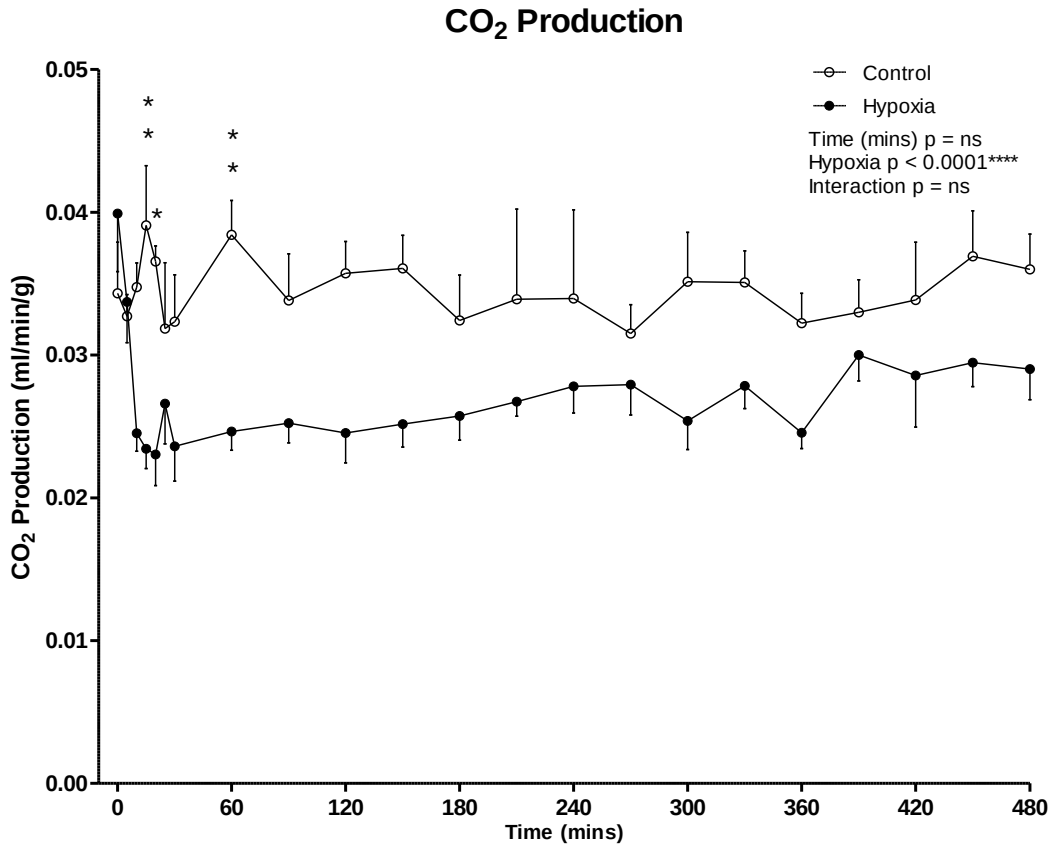

Figure 26: Mouse carbon dioxide production over 8 hours of breathing in either a normoxic (Control) or hypoxic (Hypoxia) environment. Carbon dioxide production (mean ± SEM) in the mouse expressed as ml per minute per gram of body weight (ml/min/g) over the 480 minutes (8 hour) period of exposure to either hypoxia or normoxia (n = 6-7 per group) (two-way ANOVA and Bonferroni's multiple comparisons test).

Fig. 27 shows the mouse carbon dioxide ventilatory equivalent ratio (ventilation/CO_2 production) over 8 hours of exposure to either a normoxic (Control) or hypoxic (Hypoxia) environment. The carbon dioxide ventilatory equivalent ratio was significantly increased in the hypoxic group upon gas exposure compared with the control group with significance reached at 10 and 20 minutes ($p < 0.001$ and $p < 0.01$

respectively, two-way ANOVA and Bonferroni's multiple comparisons test), and remained elevated over the course of the 8 hours of gas exposure (****p < 0.0001, two-way ANOVA and Bonferroni's multiple comparisons test).

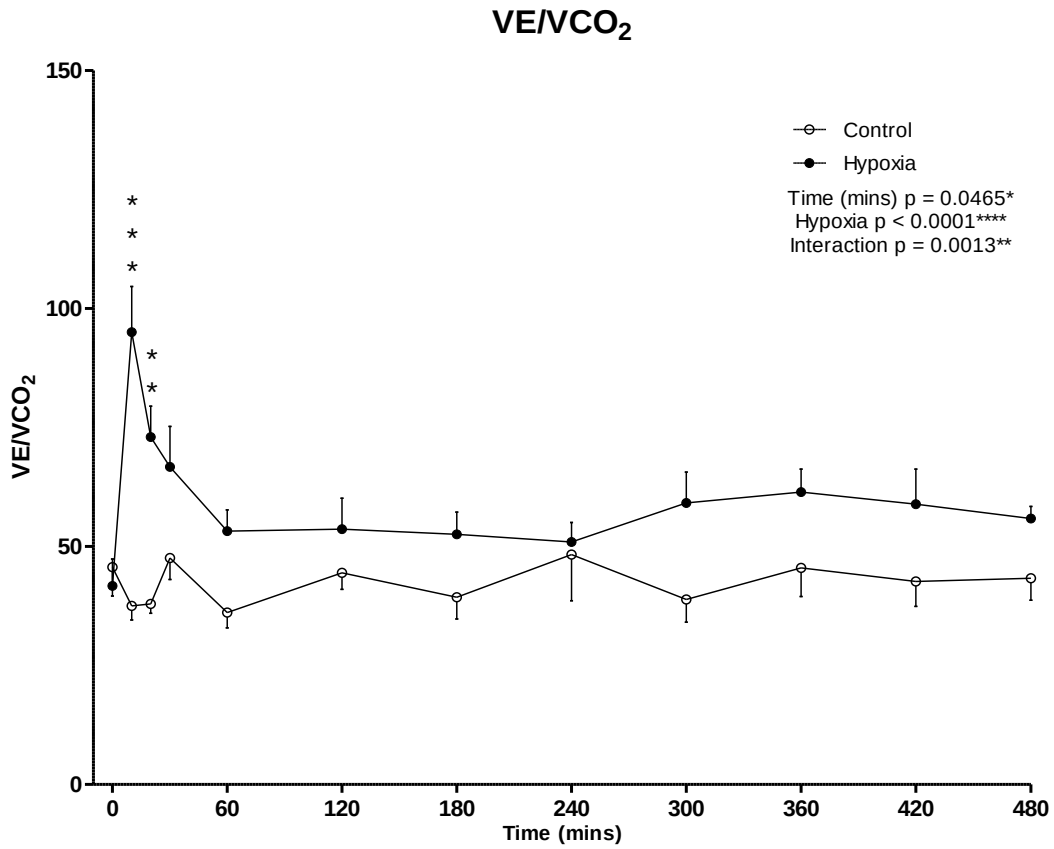

Figure 27: Mouse ventilatory equivalent ratio over 8 hours of exposure to either a normoxic (Control) or hypoxic (Hypoxia) environment. Ventilatory equivalent ratio (mean ± SEM) in the mouse over the 480 minutes (8 hour) period of exposure to either hypoxia or normoxia (n = 6-7 per group) (two-way ANOVA and Bonferroni's multiple comparisons test).

Fig. 28 shows mouse ventilatory equivalent ratio over 8 hours of breathing in either a normoxic (Control) or hypoxic (Hypoxia) environment comparing ventilation to oxygen consumption. The oxygen ventilatory equivalent ratio was significantly increased in the hypoxic group upon gas exposure compared with the control group

and remained elevated over the course of the 8 hours of gas exposure (**p = 0.013, two-way ANOVA and Bonferroni's multiple comparisons test).

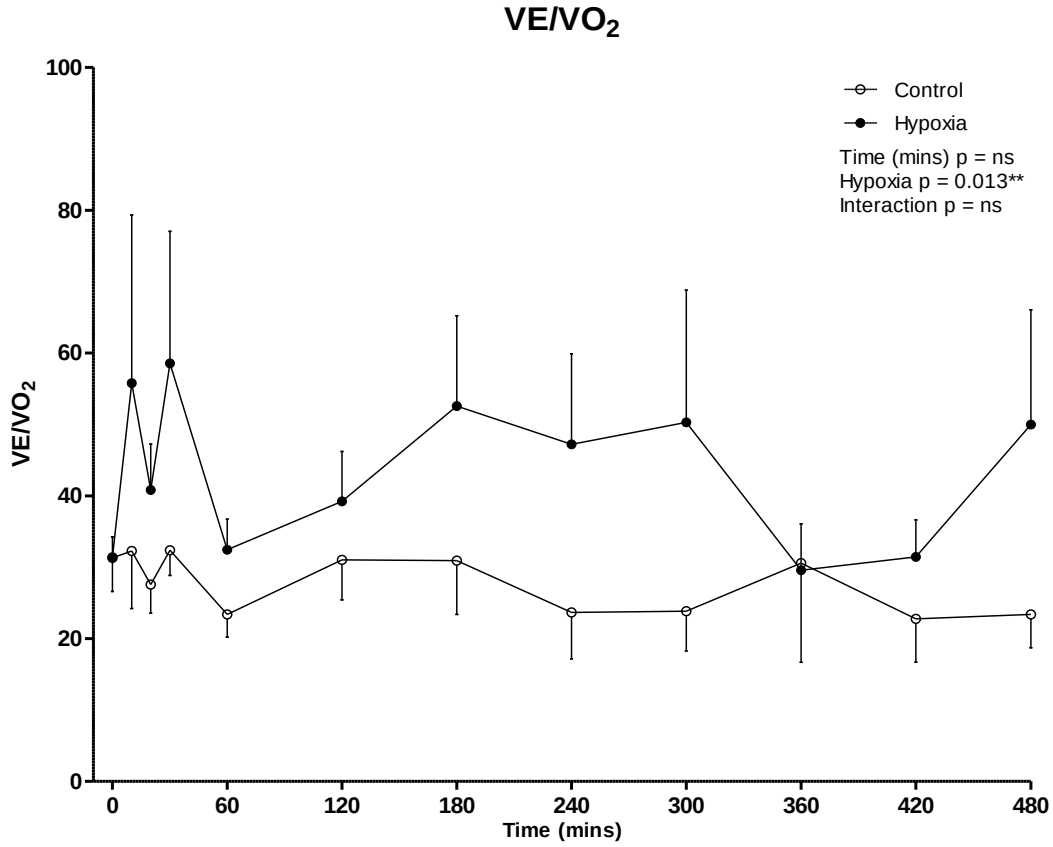

Figure 28: Mouse oxygen ventilatory equivalent ratio over 8 hours of exposure to either a normoxic (Control) or hypoxic (Hypoxia) environment. Oxygen ventilatory equivalent ratio (mean ± SEM) in the mouse over the 480 minutes (8 hour) period of exposure to either hypoxia or normoxia (n = 6-7 per group) (two-way ANOVA and Bonferroni's multiple comparisons test).

Fig. 29 shows mouse respiratory exchange ratio (oxygen consumption/carbon dioxide consumption) over 8 hours of breathing in either a normoxic (Control) or hypoxic (Hypoxia) environment. There was no effect of hypoxia on the respiratory exchange ratio over the course of the 8 hours of gas exposure compared with control (two-way ANOVA and Bonferroni's multiple comparisons test).

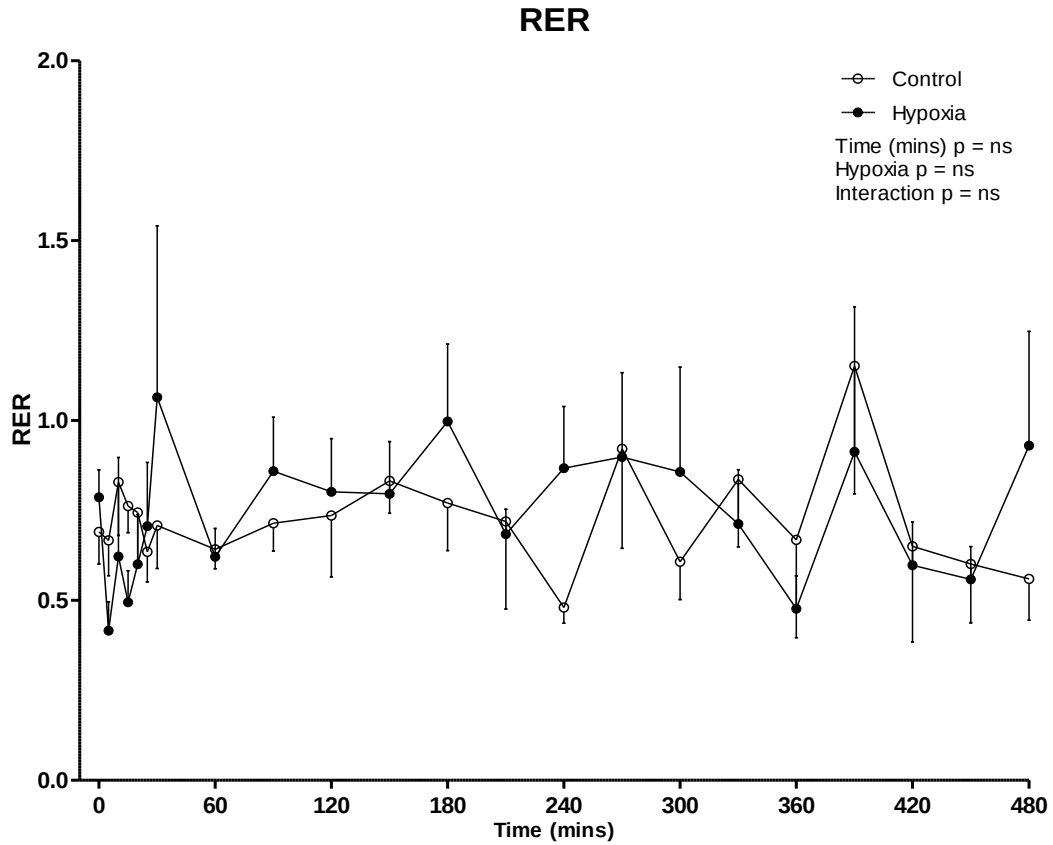

Figure 29: Mouse respiratory exchange ratio over 8 hours of exposure to either a normoxic (Control) or hypoxic (Hypoxia) environment. Respiratory exchange ratio (mean ± SEM) in the mouse over the 480 minutes (8 hour) period of exposure to either hypoxia or normoxia (n = 6-7 per group) (two-way ANOVA and Bonferroni's multiple comparisons test).

Fig. 30 shows the average mouse respiratory exchange ratio (oxygen consumption/carbon dioxide consumption) over 8 hours of breathing in either a normoxic (Control) or hypoxic (Hypoxia) environment. There was no effect of hypoxia on the respiratory exchange ratio over the course of the 8 hours of gas exposure compared with control (0.7 ± 0.1 vs. 0.7 ± 0.1 mean ± SEM RER; Control vs. Hypoxia; n = 6-7 per group; p = 0.5836; unpaired t-test).

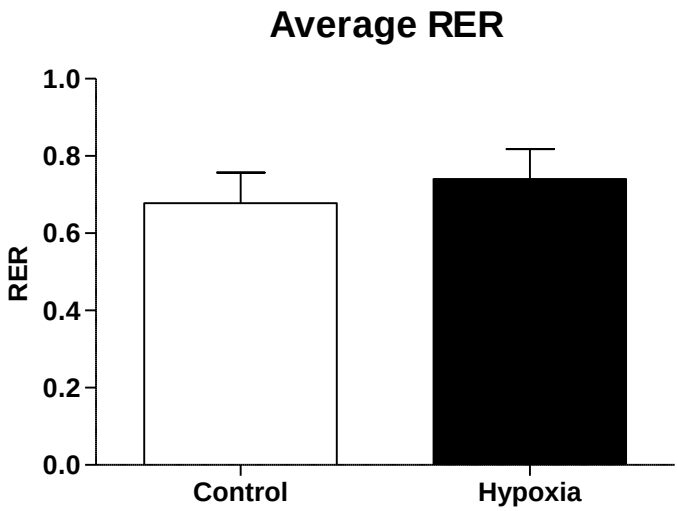

Figure 30: Average mouse respiratory exchange ratio over 8 hours of exposure to either a normoxic (Control) or hypoxic (Hypoxia) environment. Respiratory exchange ratio (mean ± SEM) in the mouse over the 480 minutes (8 hour) period of exposure to either hypoxia or normoxia (n = 6-7 per group) (p = 0.5836, unpaired t-test).

4.3 Chapter Discussion

The main findings of this chapter are:

1. 4-8 hours of hypoxia significantly increases mitochondrial UCP-3 mRNA expression across all 4 muscle types, suggestive of an increased reliance on fatty acid metabolism in skeletal muscle around the body, and potentially uncoupling of oxidative phosphorylation reducing ROS production.

2. Differential and dynamic changes in mRNA expression of transcription factors involved in the regulation of mitochondrial biogenesis & energy metabolism are observed in respiratory, but not limb, muscle following 1, 4 & 8 hours of hypoxia.

3. Pro-atrophy signalling mRNA expression is induced by hypoxia across all 4 muscle types, although not with significance in sternohyoid muscle. There is no change in autophagy related gene expression, or proteasome enzymatic activity in the diaphragm.

4. 4 hours of hypoxia caused a certain level of perturbation in SR calcium handling related gene expression in respiratory muscle, the sternohyoid in particular.

5. Hypoxia did not cause any persistent change in ventilation (muscle activity), therefore muscle weakness and molecular changes are likely directly hypoxia-dependent.

6. Hypoxia decreased metabolism and body temperature, meaning that although ventilation is unaltered, there is in fact a relative hyperventilation when considering the corresponding metabolic rate.

7. The Respiratory Exchange Ratio (RER) is unaffected by hypoxia, suggesting there is no detectable switch in metabolic energy source. An RER of 0.7

suggests that fatty acids are the primary substrate for oxidative metabolism and energy production, over glucose/carbohydrates in normoxia and hypoxia.

4.3.1 Gene Expression and Proteasome Activity

4.3.1.1 Mitochondrial Uncoupling

UCP-3 encodes a protein that functions to uncouple oxidative phosphorylation from the electron transport chain (ETC), and dissipates the proton gradient generated by the ETC as heat, thus preventing ATPase from using that gradient to generate ATP (see fig. 31).

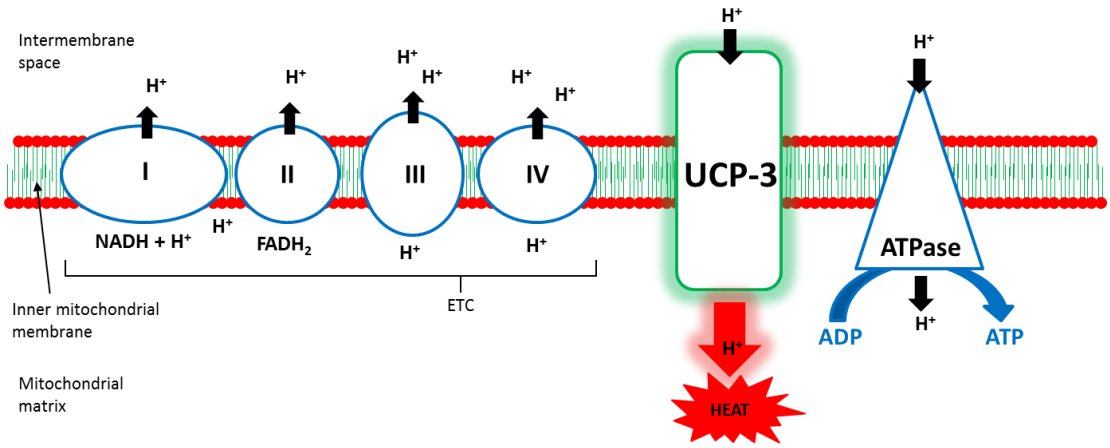

Figure 31: Mitochondrial uncoupling protein 3 (UCP-3). UCP-3 dissipated the proton gradient set up by the ETC as heat, preventing ATPase from using that gradient to generate ATP.

An increase in UCP-3 expression is suggested to be a marker for an increased reliance on fatty acid/lipid metabolism for energy production (Aguer et al., 2013; Giordano et al., 2015). An increased utilisation of fatty acids as metabolic substrate for energy production has been reported in the mouse diaphragm following exposure to 6 weeks of chronic hypoxia (Lewis et al., 2014). Here, UCP-3 mRNA levels are significantly

increased following 8 hours of hypoxia in the diaphragm, sternohyoid and soleus muscles, and at 4 and 8 hours in the EDL muscle. The fact that UCP-3 expression is increased in hypoxia across all 4 muscles, suggests that the effect is not respiratory muscle specific and is a 'global' phenomenon across skeletal muscle in general. The way in which expression increases incrementally across 1, 4 and 8 hours of hypoxia also suggests that the increase in UCP-3 mRNA expression under hypoxic conditions is temporally dependent, and positively correlated with the duration of hypoxic exposure, at least over this acute timeframe. If this increase in gene expression translates into an increase in UCP-3 protein, then this would suggest a decrease in ATP production via oxidative phosphorylation, due to UCP-3 dissipating the ETC proton gradient, which could contribute to diaphragm muscle weakness. This is somewhat surprising, as one would think that it would be more beneficial to the muscle to tighten coupling of the ETC and ATP production by reducing UCP-3 expression and thus increase the efficiency of ATP production from available oxygen (Gamboa and Andrade, 2012). It may also indicate a metabolic state whereby fatty acids are preferred over glucose or carbohydrates as a metabolic substrate for energy production. Mitochondrial membrane potential has been posited to regulate the production of mitochondrial ROS. Therefore, mitochondrial uncoupling may decrease superoxide production by dissipating the membrane potential as heat, and so an increase in UCP-3 expression may serve a protective role by diminishing mitochondrial ROS generation in skeletal muscle. Indeed, ROS production is enhanced in UCP-3 knockout mice (Bodrova et al., 1998; Sastre et al., 2003). Others have reported increased UCP-3 expression in limb skeletal muscle in response to acute hypoxic stress (Zhou et al., 2000). Contrary to these finding in acute hypoxia, chronic hypoxia has been shown to decrease UCP-3 expression in the diaphragm, an adaptive mechanism thought to increase the efficacy of ATP production from available oxygen by tightening coupling, while UCP-3 content did not change in limb muscle (Gamboa and Andrade, 2012). This is further suggestive that the adaptive mechanisms of respiratory muscle to sustained hypoxia differ between acute and chronic exposures and compared with responses in limb muscles.

4.3.1.2 Regulation of Metabolism and Mitochondrial Function

PGC-1α is a transcriptional co-activator involved in the regulation of mitochondrial biogenesis and energy metabolism in skeletal muscle, and it can interact with, and regulate the activity of, NRF1 and FoxO1 (Finck and Kelly, 2006; Levett et al., 2012; Liang and Ward, 2006). Expression of PGC-1α is known to be increased in endurance exercise (Safdar et al., 2011), and the increased expression of PGC-1α mRNA observed in the diaphragm following 1 hour of hypoxia in this chapter may have been induced as a result of the initial hypoxic ventilatory response (HVR) observed in mice during the first 10 minutes of hypoxic exposure. This HVR requires an increase in diaphragm muscle activity to increase respiratory rate, tidal volume and thus minute ventilation. Consistent with the timing of this increased diaphragm activity is the observation that elevated PGC-1α expression is short lived, already declining toward control levels after 4 and 8 hours of hypoxia. There were no changes in PGC-1α mRNA expression levels in sternohyoid, EDL or soleus muscles. PGC-1β is another transcriptional co-activator, believed to control mitochondrial oxidative energy metabolism and lead to the activation of NRF1 (Sonoda et al., 2007). However, its mRNA expression was unaffected by acute hypoxia in the diaphragm. PPARα is transcriptionally co-activated by PGC-1α, involved in mitochondrial plasticity in response to exercise and linked to increased fatty acid oxidation in endurance training (Hoppeler and Fluck, 2003; Horowitz et al., 2000). PPARα mRNA expression was unaffected by acute hypoxia in the diaphragm.

NRF1 is a transcription factor that regulates the expression of certain genes involved in oxidative stress and metabolic genes regulating cell proliferation, and proteins of the ETC. NRF1 also targets genes encoding enzymes involved in glutathione biosynthesis, as well as other oxidative stress defense enzymes (Biswas and Chan, 2010; Liang and Ward, 2006). NRF2 is also crucial in the activation of genes which are regulated by the antioxidant response element, including glutathione synthesis proteins and NAD(P)H; quinone oxidoreductase 1, which it activates under oxidative stress conditions. Both NRF1 and NRF2, as well as having independent roles, such as those involved in the activation of antioxidant response element-dependent genes (Ohtsuji et al., 2008), also interact. Indeed, NRF2 upregulated the mRNA and protein levels of NRF1 (Ohtsuji et al., 2008; Piantadosi et al., 2008; Vomhof-DeKrey and Picklo, 2012). There was no significant change in NRF1 expression in the diaphragm,

although there was a trend toward decreased expression following 4 and 8 hours of hypoxia. NRF1 expression was significantly reduced in the sternohyoid muscle following 4 hours, but not 8 hours, of hypoxia relative to control. There were no changes in NRF1 expression in limb muscle following hypoxia. NRF2 expression is unaffected by hypoxia in all 4 muscles. NRF1 and NRF2 therefore do not appear to play a major role in diaphragm muscle dysfunction under acute hypoxic stress. The short lived reduction in NRF1 expression at 4 hours, but not 8 hours, may indicate some transient alterations in the cellular redox state.

4.3.1.3 Inflammation and Hypoxic Signalling

NF-κB1 mRNA expression is reduced by 4, but not 8 hours of hypoxia in the diaphragm, and reduced in the sternohyoid muscle following 4 and 8 hours of hypoxia, while NF-κB1 mRNA levels are unaffected by hypoxia in the limb muscles. NF-κB1 is a transcription factor which is involved in regulating cell survival and inflammation signalling, and which is responsive to oxidative stress, and hypoxia via HIF-1α (Carbia-Nagashima et al., 2007; Rius et al., 2008). NF-κB1, although classically associated with inflammation, is also linked to induction of skeletal muscle atrophy when activated, and NF-κB1 can mediate the upregulation of MuRF-1 (Glass, 2005; Hunter and Kandarian, 2004; Jackman and Kandarian, 2004; Mourkioti and Rosenthal, 2008). The hypoxia induced reduction in NF-κB1 mRNA expression in respiratory muscle reported in this chapter may indicate a reduction in NF-κB1-mediated atrophy and/or inflammation signalling in respiratory muscle following acute hypoxia.

HIF2α but not HIF1α mRNA expression is increased by PGC-1α in exercise, while PGC-1α is linked to HIF1α dependent gene expression by increasing mitochondrial oxygen consumption in skeletal muscle (O'Hagan et al., 2009; Rasbach et al., 2010). HIF1α and HIF2α and their physiological roles are discussed in more depth in chapter 1 and HIF1α is discussed further in chapter 5. Neither HIF1α nor HIF2α mRNA expression are affected by acute hypoxia in the diaphragm, sternohyoid, EDL or soleus muscles compared with respective controls. However, as HIF is post-translationally modified (as discussed in chapter 1), HIF1α protein levels are assessed in diaphragm and sternohyoid in chapter 5.

4.3.1.4 SR Calcium Handling, Release and Re-uptake

The roles of the proteins encoded by the various genes examined which are related to calcium handling at the SR are discussed in detail in chapter 1. Selenoprotein N1 (SEPN1) was decreased after 4 hours of hypoxia in diaphragm, and 4 and 8 hours of hypoxia in the sternohyoid. SEPN1 was the only SR calcium handling related gene to show significant changes in expression in the diaphragm, while there were trends toward decreased mRNA expression of genes encoding proteins involved in SR calcium handling/release: Junctophilin 1, Junctophilin 2, Ryanodine receptor 3, Dihydropyridine receptor, and Calsequestrin 1 after 4 hours of hypoxia. Meanwhile Junctophilin 1, Junctophilin 2, Calsequestrin 1, Ryanodine Receptor 1 and Dihydropyridine receptor were all significantly reduced in the sternohyoid following 4 hours of hypoxia, but not 8 hours. No SR calcium handling related gene expression changes were observed in the limb muscles. SEPN1 is essential for ryanodine receptor activity (possibly through controlling its redox state), and thus calcium release from the SR, which is fundamental to normal contractile function and calcium homeostasis in human muscle (Jurynec et al., 2008; Shchedrina et al., 2010). Indeed, SEPN1-related myopathy, a human disorder whose symptoms include muscle weakness leading to respiratory insufficiency, is associated with defects in the SEPN1 gene (Kasaikina et al., 2012). The hypoxia induced reduction of SEPN1 mRNA expression in respiratory but not limb muscle, if translated to a reduction in SEPN1 protein, could alter calcium release from the SR during contraction in respiratory muscle, likely affecting muscle contractile performance. Although, it is pertinent to note that in the diaphragm this hypoxia induced reduction in expression is not maintained following 8 hours of hypoxia. These data suggest that SR calcium handling may be altered following acute hypoxic stress. Of note, however, diaphragm peak contractile kinetics (chapter 3) were unaffected by 8 hours of sustained hypoxia compared with control, although diaphragm shortening velocity was increased over the range of loads tested, which could be affected by altered calcium release or altered sensitivity to calcium. However sternohyoid contractile kinetics (chapter 3) were unaffected by 8 hours of sustained hypoxia compared with control, and although T_{50} was reduced to near significance, this would be influenced by calcium uptake not release, and neither SERCA 1 nor SERCA 2a mRNA expression was significantly affected by hypoxia in sternohyoid, or diaphragm. It is plausible that perhaps some of the gene expression changes related to SR calcium handling discussed here are compensatory responses in

the muscle fibres to re-establish a state of functional homeostasis in the face of hypoxia, rather than being detrimental effects of hypoxia acting to perturb muscle contractile function.

4.3.1.5 Atrophy

Muscle fibre atrophy, and decreased fibre cross sectional area, is a factor contributing to muscle weakness in chronic hypoxia (Deldicque and Francaux, 2013; Favier et al., 2010; Lewis et al., 2015d; McMorrow et al., 2011). Diaphragm muscle atrophy and dysfunction occurs within a matter of hours in mechanically ventilated hypoxaemic respiratory patients in the ICU (Powers et al., 2009; Bruells et al., 2013), and there is evidence to suggest that the ubiquitin-proteasome pathway, as well as mitochondrial abnormalities, may be involved (Hooijman et al., 2015; Picard et al., 2015), while the supposedly dominant role of diaphragm inactivity in VIDD is debated (Jaber et al., 2011a, 2011b; Petrof et al., 2010; Petrof and Hussain, 2016; Sieck and Mantilla, 2013; Supinski and Callahan, 2013).

Muscle atrophy requires the transcription and activation of atrogenes (Cohen et al., 2014; Lecker et al., 2004; Sanchez et al., 2014; Sandri et al., 2004). Here, Foxo-1, Foxo-3, Atrogin-1 and MuRF-1 atrogene expression is reported following control, 1, 4 and 8 hours of hypoxia in the diaphragm. There were trends toward increased expression of Foxo-1 and Atrogin-1 mRNA expression in hypoxia, while there were significant increases in the expression of Foxo-3 and MuRF-1 following 8 hours of hypoxia. Some of these atrogenes were also examined in the sternohyoid, EDL and soleus muscles. There are no significant changes in the sternohyoid, but Foxo-1 and Atrogin-1 display non-significant trends toward increased expression levels following increasing durations of hypoxic exposure. While in the limb muscles, EDL MuRF-1 expression was increased following 4 and 8 hours of hypoxia, Foxo-1 expression was increased following 4 hours of hypoxia, and non-significantly after 8 hours, and Atrogin-1 expression was increased following 4 and 8 hours, and in the soleus Foxo-1 expression is increased following 4 hours of hypoxia, and non-significantly after 8 hours, Atrogin-1 displays trends toward increased expression with increased hypoxia exposure, and MuRF-1 expression is increased following 8 hours of hypoxia. These data suggest that atrophy signalling via atrogene activation was induced in the

diaphragm, as well as skeletal muscle in general, in this model of acute hypoxia. The lack of significant increases in the sternohyoid, although there were trends toward increased expression, do not appear to be type 2b muscle fibre type specific as the EDL muscle, also predominantly type 2b (Soukup et al., 2002), showed significant increases in atrogene expression following acute hypoxia. This increase in atrophy signalling, if it leads to fibre atrophy would give us a plausible cause for diaphragm muscle weakness following acute hypoxia. However, although atrophy signalling is induced, we cannot definitively conclude from this that atrophy is occurring.

In mammals, and indeed eukaryotes in general, most protein degradation occurs via the ubiquitin-proteasome system or the autophagy-lysosome system (Milan et al., 2015b). We thus determined diaphragm muscle chymotrypsin-like proteasome activity following 8 hours of hypoxia and control. There was no acute hypoxia induced change in proteasome activity. This would suggest that although atrophy signalling is indeed increased, protein degradation and actual fibre atrophy was not occurring, at least not via the ubiquitin-proteasome system.

4.3.1.6 Autophagy

The expression of key genes relating to autophagy signalling - LC3B, BNIP3 and GABARAPL3 - was also examined in the diaphragm of control mice and those exposed to 1, 4 and 8 hours of hypoxia. There were no changes in the expression profiles of any of these genes, other than a slight, non-significant, trend toward increased expression of BNIP3 following 8 hours of hypoxia. It is therefore unlikely that muscle fibre atrophy was occurring within 8 hours of hypoxia via the autophagy-lysosome system.

4.3.2 Breathing

The diaphragm is the primary pump muscle of inspiration. Therefore, a change in ventilation requires, and is mediated via, a change in diaphragm muscle activity. An increase in diaphragm muscle activity due to hyperventilation under hypoxic conditions would be a confounding factor which could affect diaphragm muscle contractile ability and influence the cellular milieu. It would therefore be misleading to attribute altered diaphragm characteristics to hypoxic stress *per se* if the activity of

the muscle is also altered during hypoxic exposure. However, in this mouse model ventilation is unchanged for the majority of the 8 hours of hypoxic exposure. Respiratory rate, or frequency, (the number of breaths an animal breathes per minute) and tidal volume (the volume of gas that passes in an out of the lung with each breath) were both measured over the course of the 8 hours of hypoxia. The initial increase in respiratory frequency, which manifests during the first 10 minutes of hypoxic exposure, is a reflex hyperventilation, due to the HVR of the animal (Palmer et al., 2013; Powell et al., 1998), and is short lived, with frequency returning to levels equivalent to normoxia within 20 minutes of hypoxic exposure. Respiratory frequency then actually drops slightly below normoxic levels for a short time before returning to levels equivalent to normoxia for the remainder of the 8 hours. Tidal volume follows a similar profile, increasing in the first 10 minutes and then returning to levels equivalent to normoxia for the remainder of the 8 hours. The product of respiratory frequency and tidal volume is minute ventilation (the volume of gas passing in and out of the lungs per minute), an index of overall ventilation. Minute ventilation, staying true to its components, mirrors the profile described above with an initial increase during the initial 10 minutes of hypoxia and then returning to levels equivalent to normoxia by 20 minutes into hypoxia, remaining equivalent to normoxia for the remainder of the 8 hours of hypoxia. The implication of this observation is that the activity of the diaphragm is therefore likely unchanged in hypoxia compared with normoxia over the 8 hours, as the work of ventilation is not different between the two groups. Therefore, although the influence of the initial increase in ventilation during hypoxic exposure cannot be discounted, it is likely that increased muscle activity due to hyperventilation is not likely a confounding factor in this model and thus the muscle weakness and molecular changes reported herein are likely due to direct effects of hypoxic stress *per se*.

The decline of minute ventilation from the peak HVR returning toward normoxic levels is likely partly due to hypocapnia, resulting from hyperventilation in a non-isocapnic hypoxic environment. Hypocapnia (and the resultant effects on acid-base balance) can affect the diaphragm (Shee and Cameron, 1990) and there is evidence that molecular CO_2, independent of pH, can cause alterations in gene expression (Cummins et al., 2010). Although ventilation is equivalent in normoxia and hypoxia, there is a relevant hyperventilation in mice exposed to hypoxia compared with

normoxia, owing to the elaboration of a hypometabolic state in the mouse in response to hypoxia.

4.3.3 Metabolism

Hypometabolism is an adaptive mechanism in hypoxia-tolerant animals (Gamboa and Andrade, 2012; Ramirez et al., 2007; St-Pierre et al., 2000). Hypoxic hypometabolism is a general characteristic of the mammalian response to hypoxia, and one whose magnitude is inversely proportional to the resting or basal VO_2 of the species, making it more prominent in smaller mammals (with higher VO_2) and less prominent in larger mammals (with lower VO_2) (Frappell et al., 1992). Here, 8 hours of hypoxia decreased metabolic measurements and *post-mortem* body temperature by approx. 2°C compared with control. Hypoxia may decrease metabolic rate by decreasing thermogenesis (Frappell et al., 1992) and body temperature can be considered a crude index of *in vivo* metabolism. Importantly, there was no difference in *post-mortem* body temperature between the mice that were exposed to hypoxia individually (for muscle function studies) and those mice that were exposed to hypoxia in groups of 4 (for tissue harvest), suggesting that isolating mice had no effect on their metabolic strategy to hypoxic exposure compared with the grouped response.

It is clear from the significant effect of hypoxia to reduce O_2 consumption (VO_2) and CO_2 production (VCO_2) that the hypoxic group adopted a hypoxic hypometabolic state. Interestingly, the time-scale of the drop off in VCO_2 matches closely with the cessation of the HVR in the minute ventilation, further bolstering the notion that this return of breathing to normoxic levels is prompted by a hypometabolic state rather than hypocapnic alkalosis.

The ventilatory equivalents for both CO_2 and O_2 (VE/VCO_2 & VE/VO_2, respectively) are increased in hypoxia, due to minute ventilation remaining at normoxic levels while VCO_2 and VO_2 are reduced, leading to a relative hyperventilation for the prevailing level of metabolism, in comparison with the control group. Although VE/VCO_2 is increased in hypoxia, following the large increase during the first 20-30 minutes of hypoxia (due to the HVR and the drop in VCO_2) the increased VE/VCO_2 in hypoxia is only modestly higher than the VE/VCO_2 in control for the remainder of

the 8 hours. It is worth noting, however, that this slightly elevated VE/VCO_2 could lead to hypocapnia (respiratory alkalosis), due to normal CO_2 blow off via respiration while CO_2 production is reduced.

Finally, the respiratory exchange ratio is unaffected by hypoxia, suggesting that there is no global change in metabolic substrate for energy production. An RER of 0.7 in both groups suggests that fatty acids are the primary substrate for oxidative metabolism and energy production, over glucose/carbohydrates (Marvyn et al., 2016). The increase in UCP-3 mRNA expression in skeletal muscle discussed earlier is suggested as a marker for an increased reliance on fatty acids as a metabolic energy source. Here the RER of the control group suggests that these mice are already in a metabolic state whereby they are utilising fatty acids as their primary substrate for energy production.

4.4 Chapter Conclusions

In conclusion, hypoxia did not cause any persistent change in ventilation (muscle activity) and therefore muscle weakness and molecular changes are likely directly related to hypoxia *per se*. Hypoxia induces a hypometabolic state in the mouse, and although ventilation is unaltered, there is in fact a relative hyperventilation when metabolism is accounted for. This hypometabolic state could potentially impact diaphragm performance. Therefore, in chapter 5, when examining how NAC pre-treatment may affect acute hypoxia-induced diaphragm dysfunction, we will also examine how NAC pre-treatment impacts *post-mortem* body temperature as an index of metabolism. The UCP-3 findings suggest that skeletal muscle signals, at least at an mRNA level, drive toward an increased reliance on fatty acid metabolism in skeletal muscle around the body. Given that the RER is unaffected by hypoxia, suggesting there is no switch in metabolic energy source, perhaps the effects of this mRNA signal do not manifest within 8 hours. Or perhaps the effect is not observed because the RER in both groups is 0.7, suggestive that fatty acids are already the primary substrate for oxidative metabolism and energy production, over glucose/carbohydrates, in normoxia in these mice. The increase in UCP-3 may, however, be a compensatory mechanism to reduce oxidative stress and ROS

production in the muscle. The differential and dynamic changes in mRNA expression of transcription factors regulating mitochondrial biogenesis & energy metabolism in respiratory, but not limb, muscle are complex and somewhat inconclusive. However there are obviously certain metabolic shifts occurring in the mitochondria, evident from the UCP-3 data and the hypoxic hypometabolic state observed. Acute hypoxia perturbs SR calcium handling related gene expression in respiratory muscle, the sternohyoid in particular, which may be a contributing factor to muscle dysfunction, or may be a compensatory mechanism acting to bring about a homeostatic state. It is interesting to note, however, that SEPN1 is redox sensitive and so alterations in its expression may relate to redox changes in the muscle (Jurynec et al., 2008; Shchedrina et al., 2010). Finally, pro-atrophy signalling is induced by hypoxia across all 4 muscle types, although not with significance in sternohyoid muscle. However, there is no change in autophagy related gene expression, or proteasome enzymatic activity in the diaphragm, suggesting that protein catabolism is not occurring, at least not within 8 hours of hypoxia, which suggests that muscle weakness in hypoxia is not likely related to muscle atrophy.

Chapter 5: N-acetylcysteine Ameliorates Acute Hypoxia-Induced Diaphragm Dysfunction

5.1 Introduction

In this chapter, diaphragm muscle contractile performance is assessed following 8 hours of normoxia (Control), 8 hours of hypoxia (Hypoxia) or 8 hours of hypoxia with N-acetylcysteine (NAC) pre-treatment (NAC + Hypoxia). Signalling pathways associated with hypertrophy-atrophy balance and hypoxia signalling are also examined, to determine how hypoxia influences these mechanisms and if NAC treatment prior to hypoxia alters the response of these mechanisms to hypoxia. Signalling pathways associated with hypertrophy-atrophy balance and hypoxia signalling are also examined in the sternohyoid following 8 hours of normoxia (Control) and 8 hours of hypoxia (Hypoxia).

Diaphragm muscle weakness can be an important determinant of poor outcome in patients, particularly those respiratory patients requiring mechanical ventilation (Supinski and Callahan, 2013). If it is possible to prevent, dampen or delay the onset of diaphragm muscle weakness in hypoxaemic respiratory patients, this could have substantially positive effects on the outcome of patients with acute respiratory diseases. The potential role of acute hypoxia in the development of diaphragm muscle weakness has been overlooked, despite hypoxaemia being a hallmark of ARDS and other acute respiratory conditions, with evidence of severe hypoxaemia in up to 30% of ARDS patients, and evidence that hypoxia alters skeletal muscle physiology, including mitochondrial derangement, in humans (Murray 2009). As highlighted in this thesis, chapter 3, for the first time acute hypoxia is sufficient to weaken the mouse diaphragm by 30%. Given that acute hypoxia features in many acute respiratory conditions (discussed in chapter 1), if this acute hypoxia induced diaphragm weakness translates to humans, avoiding the potential onset and progression of acute hypoxia induced diaphragm dysfunction could substantially improve patient outcome, removing an as of yet overlooked factor which may be contributing to diaphragm weakness in patients.

NAC, as discussed in chapter 1, is an antioxidant, both in its own right as a free radical scavenger as well as by way of boosting synthesis of the endogenous antioxidant GSH and other antioxidant systems. NAC already has a widespread

clinical use, going back almost 50 years, as a treatment for a variety of conditions (chapter 1). Chronic antioxidant supplementation has been shown to prevent chronic hypoxia induced sternohyoid and diaphragm muscle weakness in animal models (Lewis et al., 2015b, 2015c). Indeed, patients with ARDS are in a dysfunctional oxidant to antioxidant ratio and this balance can be improved by NAC supplementation, via increasing GSH, thiol molecules and antioxidant defences (Soltan-Sharifi et al., 2007). Redox balance is known to affect muscle contractile function (Lewis et al., 2015b, 2014; Magalhães et al., 2005; Smith and Reid, 2006). If a single I.P. injection of NAC could alleviate acute hypoxia induced diaphragm dysfunction, similarly to how chronic NAC treatment prevents chronic hypoxia induced diaphragm dysfunction in the mouse, either by a similar mechanism or otherwise, this could prove extremely valuable to hypoxaemic patients with acute respiratory diseases in the clinic. However, it is worth noting here that NAC was administered immediately prior to onset of the bout of acute hypoxia, and it is uncertain whether NAC would be beneficial were it administered after the onset of acute hypoxia, which is more closely aligned to a clinical situation where patients can present with already worsening O_2 levels due to exacerbation of disease.

HIF1α is a master regulator of hypoxia signalling, playing a central role in orchestrating the cellular response to hypoxia via the induction of transcriptional programmes comprising an array of hypoxia-inducible genes. Although HIF1α mRNA expression was unaltered by acute hypoxia in chapter 4, HIF1α is post-translationally regulated by oxygen dependent degradation (discussed in chapter 1) and so it is pertinent to examine HIF1α protein content in the diaphragm and sternohyoid muscles from these animals to determine if HIF1α signalling is occurring in respiratory muscle following acute hypoxia.

The balance between hypertrophy/cell survival and atrophy/cell death signalling is a fundamental aspect of cellular signalling when discussing muscle weakness. In chapter 4, we observe an increase in atrogene mRNA expression across skeletal muscle, including diaphragm and sternohyoid muscle. However, there is no change in proteasome activity following 8 hours of hypoxia. It may be that acute adaptations to hypoxia do not include protein breakdown, but that if hypoxia persists then the acute hypoxia induced increases in atrogene expression translate to muscle atrophy, as

atrophy and increased proteasome activity are observed the diaphragm following chronic hypoxia (Lewis et al., 2016, 2014; McMorrow et al., 2011). It may be that the diaphragm staves off atrophy for a time in an attempt to preserve functional performance, as the diaphragm muscle is perpetually active due to spontaneous breathing. However, as hypoxia persists, protein turnover and amino acid dependent ATP generation may be a favourable use of resources within the muscle for energy homeostasis at the expense of force generating capacity. Many of the signalling pathways that influence the hypertrophy/atrophy balance, such as Akt, mTOR, MAPK, FoxO ultimately influence, via hypertrophy and atrophy, the balance between cell survival/development/proliferation/growth and cell death/catabolism/anti-anabolism/inflammation. These pathways are complex and interact with each other to achieve desirable cellular outcomes. Therefore, when a muscle like the diaphragm is stressed, by oxygen deprivation for example, the ultimate goal is not simply hypertrophy or atrophy, but rather muscle optimisation for the maintenance of functional integrity.

Study Aims

The primary aims of this chapter are: 1) to determine if pre-treatment with the antioxidant N-acetylcysteine (NAC) prior to hypoxic exposure can prevent acute hypoxia-induced diaphragm dysfunction; and 2) to further examine and elucidate signalling mechanisms and pathways associated with hypertrophy-atrophy balance and hypoxia signalling affected by acute hypoxia, in both diaphragm and sternohyoid muscle, and to determine how NAC pre-treatment prior to hypoxia affects these pathways in the diaphragm.

Methods Summary

Diaphragm muscle *ex vivo* contractile function, *post-mortem* body temperature and signalling protein/phosphoprotein levels were examined in control, hypoxia and hypoxia + NAC groups as described in more detail in Chapter 2 Materials and Methods, Sections 2.10, 2.5, 2.6 and 2.2. Signalling protein/phosphoprotein levels were also examined in sternohyoid muscle from mice in both control and hypoxia groups. Mice in the hypoxia + NAC group were given a single I.P. injection of NAC immediately prior to hypoxia exposure.

Briefly, a strip of mouse diaphragm muscle, was fixed between a stationary hook and a dual mode force transducer in an organ bath, filled with hyperoxic Krebs solution maintained at 30°C, allowing contractile performance to be assessed when the muscle strip was stimulated to contract.

When assessing muscle isometric contractile performance, the length of the muscle strip was fixed to the length at which the muscle produced the highest force – optimum length (L_o). Under isometric conditions, force generation capacity was assessed over a range of stimulation frequency in the muscle strip.

Core *post-mortem* body temperature was measured immediately (within 10 seconds) following euthanasia of the mouse via insertion of a rectal thermometer probe.

Protein/Phosphoprotein levels were assessed using sandwich immunoassays targeted for signaling proteins involved in hypoxia signalling and hypertrophy/atrophy balance signalling. These signaling pathways were chosen for their relevance to skeletal muscle strength and responses to hypoxia. Atrophy is a likely factor contributing to chronic hypoxia induced diaphragm weakness, and it is therefore pertinent to examine hypertrophy/atrophy balance signalling following acute hypoxia, given how quickly the diaphragm can atrophy in certain conditions. These assays were performed in sternohyoid muscle from Control and Hypoxia groups, and diaphragm muscle from Control, Hypoxia and Hypoxia + NAC groups.

5.2 Chapter Results

5.2.1 Diaphragm Function

The mouse diaphragm force–frequency relationship following 8 hours of normoxia, hypoxia, and NAC + Hypoxia is displayed in Fig. 1. As one would expect, the specific force generating capacity of the diaphragm muscle increases as the stimulation frequency is increased, from 10 to 160 Hz, and this effect of stimulation frequency on muscle contractile force is statistically significant ($p < 0.0001$, two-way ANOVA). Force generation over the range of stimulation frequencies tested was lower in the hypoxia group compared with the control group, and this weakness was most prominent at higher frequencies (as discussed in chapter 3). A single I.P. injection of NAC prior to hypoxic exposure prevented this hypoxia induced diaphragm weakness from manifesting and the NAC + Hypoxia group actually developed the highest forces over the range of stimulation frequencies tested ($p < 0.0001$, two-way ANOVA). Bonferroni's multiple comparisons test revealed statistically significant differences between the Hypoxia and NAC + Hypoxia groups at 120, 140 and 160 Hz. There was no interaction (p = ns) between treatment and stimulation frequency.

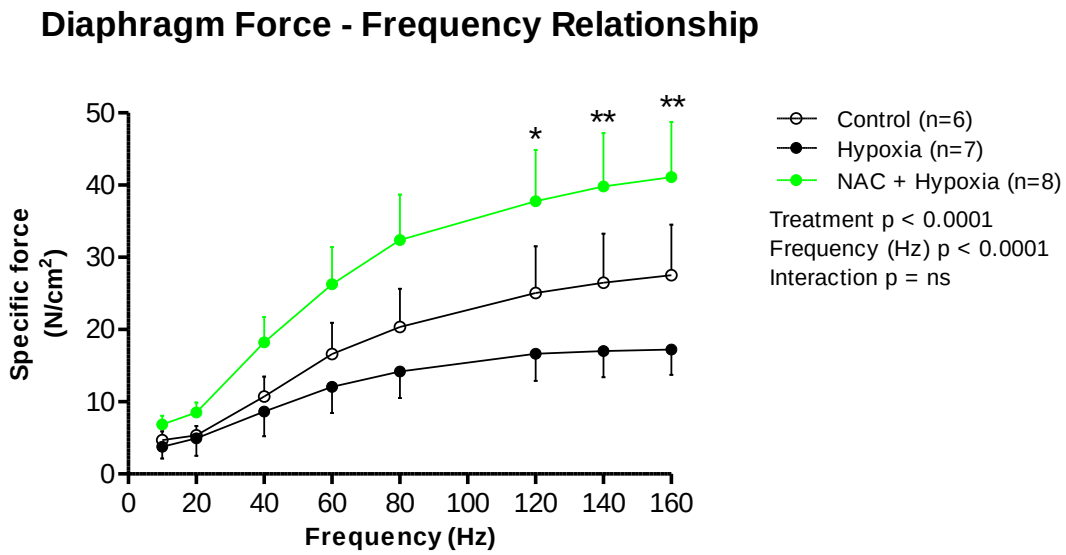

Figure 1: Diaphragm muscle force – frequency relationship in the mouse.

Diaphragm specific force (mean ± SEM) expressed as force/CSA (N/cm^2) as a

function of stimulation frequencies ranging between 10 and 160 Hz (n = 6-8 per group; *p < 0.05, **p<0.01, Bonferroni's post-hoc multiple comparisons test NAC + Hypoxia vs. Hypoxia).

Figure 2 displays diaphragm isometric peak tetanic force generation capacity following 8 hours of normoxia, hypoxia, or NAC + Hypoxia. There was a statistically significant reduction in diaphragm peak tetanic force (29.5 ± 3.2 vs. 20.8 ± 2.0 mean ± SEM N/cm^2; Control vs. Hypoxia; n = 8 per group; p = 0.0334; unpaired t-test) of ~30% following 8 hours of hypoxia compared with control. This hypoxia-induced diaphragm weakness did not appear in the NAC + Hypoxia group and peak force generation capacity was even slightly elevated in this group, although not quite to statistical significance (34.5 ± 6.5 vs. 20.8 ± 2.0 mean ± SEM N/cm^2; NAC + Hypoxia vs. Hypoxia; n = 8 per group; p = 0.0782; unpaired t-test with Welch's correction).

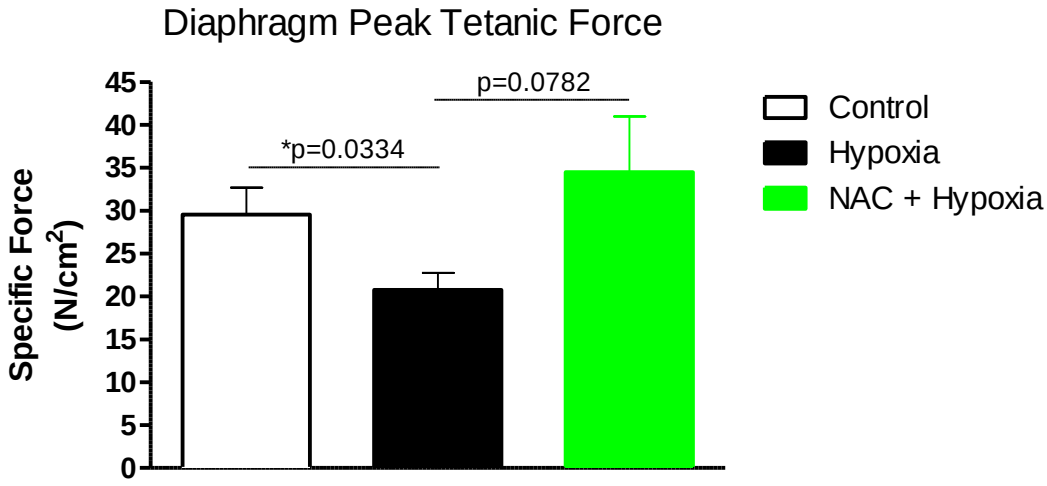

Figure 2: Diaphragm isometric peak tetanic force. Diaphragm peak tetanic force (mean ± SEM) expressed as force/CSA (N/cm^2); n = 8 per group. *p = 0.0334, unpaired t-test, p = 0.0782, unpaired t-test with Welch's correction.

5.2.2 Temperature

Fig. 3 shows mouse *post-mortem* body temperature following 8 hours of normoxia (Control), 8 hours of hypoxia, and 8 hours of hypoxia with NAC pretreatment. Mice exposed to hypoxia, and hypoxia following NAC pretreatment had lower *post-mortem* body temperatures following gas exposure compared with mice in the control group that were exposed to normoxia (****p < 0.0001 for Hypoxia vs. Control, unpaired t-test, and *p = 0.0105 for NAC + Hypoxia vs. Control, unpaired t-test with Welch's correction). There was no difference in *post-mortem* body temperature between Hypoxia and NAC + Hypoxia.

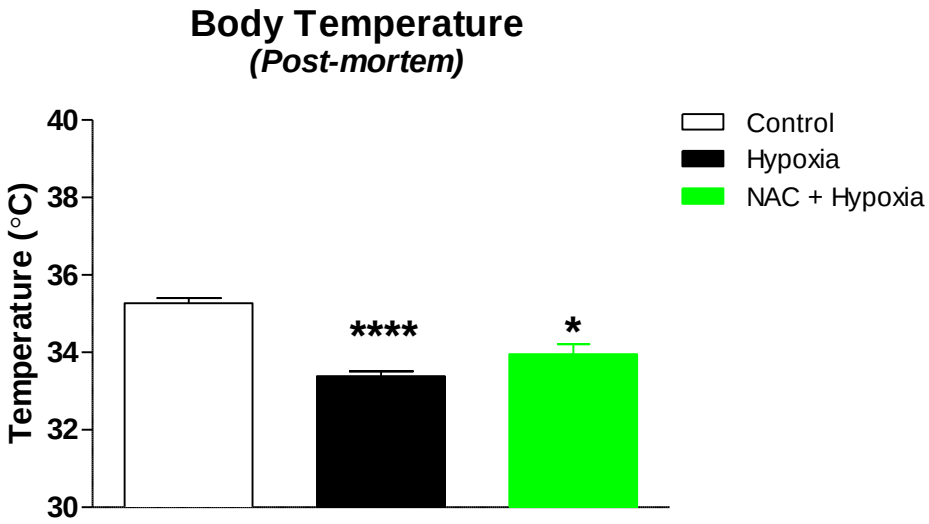

Figure 3: Mouse post-mortem body temperature. *Post-mortem* body temperatures (mean ± SEM) of mice exposed to 8 hours of normoxia, 8 hours of hypoxia or 8 hours of hypoxia with NAC pretreatment (n = 4-8 per group) (****p < 0.0001, unpaired t-test, *p = 0.0105, unpaired t-test with Welch's correction).

5.2.3 Diaphragm Signalling

5.2.3.1 HIF Signalling

Figure 4 shows HIF1α protein content in diaphragm muscle from mice exposed to 8 hours of normoxia, hypoxia, or hypoxia with NAC pretreatment. Hypoxia

significantly increased HIF1α protein content compared with the control group (**p = 0.0019; unpaired t-tests). Hypoxia with NAC pretreatment increased HIF1α protein content further still compared with the control group (****p < 0.0001; unpaired t-tests) and significantly higher than the Hypoxia group (*p = 0.0332; unpaired t-tests).

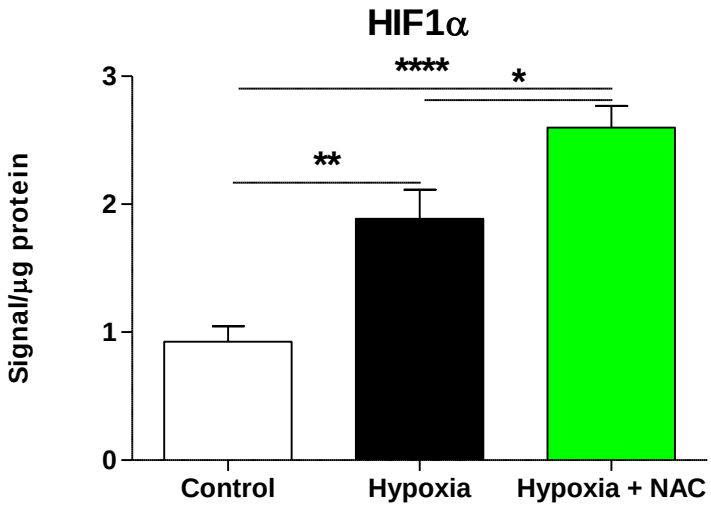

Figure 4: Diaphragm HIF1α protein content following 8 hours of normoxia, hypoxia, and hypoxia + NAC pre-treatment. Diaphragm HIF1α protein content (mean ± SEM) expressed as signal/µg of total protein (corrected for background signal); n = 6-8 per group. *p = 0.0332, **p = 0.0019, ****p < 0.0001; separate unpaired t-tests.

5.2.3.2 Pro-Hypertrophy/Cell Survival Signalling

5.2.3.2.1 Akt Pathway

Figure 5 shows phospho-Akt protein content in diaphragm muscle from mice exposed to 8 hours of normoxia, hypoxia, or hypoxia with NAC pretreatment. Hypoxia significantly increased phospho-Akt protein content compared with the control group (*p = 0.0109; unpaired t-tests). Hypoxia with NAC pretreatment increased phospho-Akt protein content further still compared with the control group (****p = 0.0001;

unpaired t-tests) and significantly higher than the Hypoxia group (***p = 0.0004; unpaired t-tests).

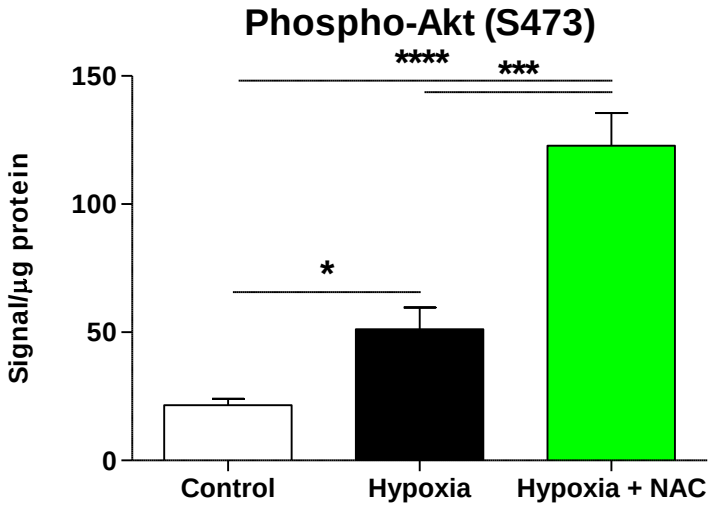

Figure 5: Diaphragm phospho-Akt (S473) protein content following 8 hours of normoxia, hypoxia, and hypoxia + NAC pre-treatment. Diaphragm phospho-Akt (S473) protein content (mean ± SEM) expressed as signal/µg of total protein (corrected for background signal); n = 8 per group. *p = 0.0109, ****p = 0.0001, ***p = 0.0004; separate unpaired t-tests.

Figure 6 shows phospho-p70S6K protein content in diaphragm muscle from mice exposed to 8 hours of normoxia, hypoxia, or hypoxia with NAC pretreatment. Hypoxia has no significant effect on phospho-p70S6K protein content compared with the control group (unpaired t-tests). However, Hypoxia with NAC pretreatment increased phospho-p70S6K protein content compared with the control group (**p = 0.0019; unpaired t-tests) and increases phospho-p70S6K protein content above the level of the Hypoxia group, but not quite to statistical significance (p = 0.0616; unpaired t-tests).

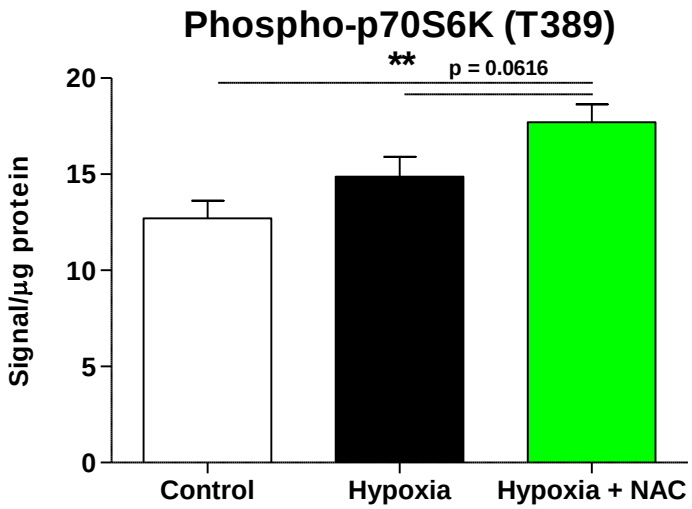

Figure 6: Diaphragm phospho-p70S6K (T389) protein content following 8 hours of normoxia, hypoxia, and hypoxia + NAC pre-treatment. Diaphragm phospho-p70S6K (T389) protein content (mean ± SEM) expressed as signal/µg of total protein (corrected for background signal); n = 8 per group. **p = 0.0019; separate unpaired t-tests.

Figure 7 shows phospho-S6RP protein content in diaphragm muscle from mice exposed to 8 hours of normoxia, hypoxia, or hypoxia with NAC pretreatment. Hypoxia significantly increased phospho-S6RP protein content compared with the control group (*p = 0.0434; unpaired t-tests). The Hypoxia with NAC pretreatment group also increased phospho-S6RP protein content compared with the control group (**p = 0.0099; unpaired t-tests), but there is no difference between the Hypoxia and Hypoxia + NAC groups (unpaired t-tests).

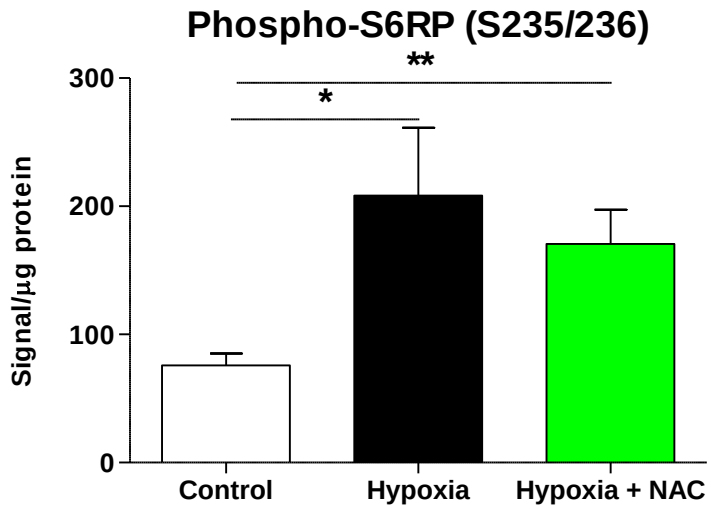

Figure 7: Diaphragm phospho-S6RP (S235/236) protein content following 8 hours of normoxia, hypoxia, and hypoxia + NAC pre-treatment. Diaphragm phospho-S6RP (S235/236) protein content (mean ± SEM) expressed as signal/µg of total protein (corrected for background signal); n = 8 per group. *p = 0.0434, **p = 0.0099; separate unpaired t-tests.

Figure 8 shows phospho-GSK-3β protein content in diaphragm muscle from mice exposed to 8 hours of normoxia, hypoxia, or hypoxia with NAC pretreatment. Hypoxia significantly increased phospho-GSK-3β protein content compared with the control group (***p = 0.0009; unpaired t-tests). Hypoxia with NAC pretreatment increased phospho-GSK-3β protein content further still compared with the control group (****p = 0.0006; unpaired t-tests), and there is no difference between the Hypoxia and Hypoxia + NAC groups (unpaired t-tests).

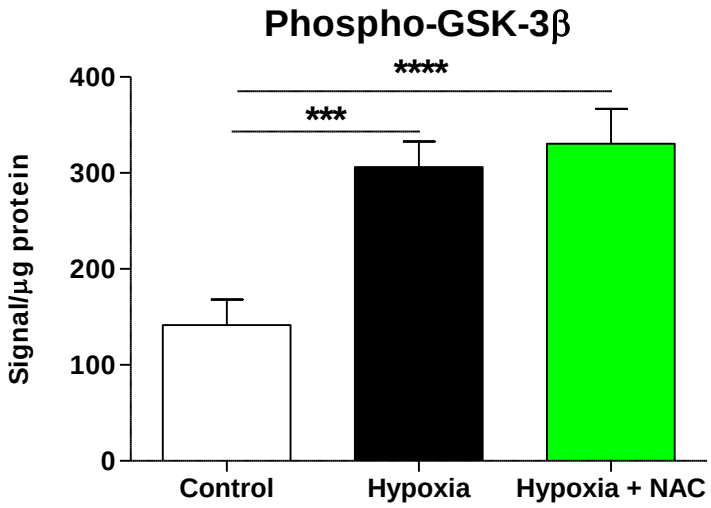

Figure 8: Diaphragm phospho-GSK-3β protein content following 8 hours of normoxia, hypoxia, and hypoxia + NAC pre-treatment. Diaphragm phospho-GSK-3β protein content (mean ± SEM) expressed as signal/µg of total protein (corrected for background signal); n = 8 per group. ****p = 0.0006, ***p = 0.0009; separate unpaired t-tests.

5.2.3.2.2 mTOR Pathway

Figure 9 shows mTOR protein content in diaphragm muscle from mice exposed to 8 hours of normoxia, hypoxia, or hypoxia with NAC pretreatment. Hypoxia significantly increased mTOR protein content compared with the control group (*p = 0.0107; unpaired t-tests). Hypoxia with NAC pretreatment, however, did not increase mTOR protein content compared with the control group (unpaired t-tests) and mTOR protein content was significantly lower in the Hypoxia + NAC group than the Hypoxia group (**p = 0.0020; unpaired t-tests).

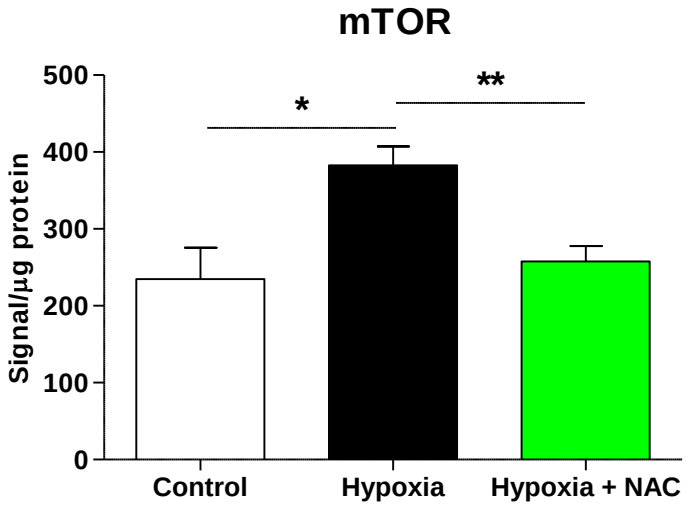

Figure 9: Diaphragm mTOR protein content following 8 hours of normoxia, hypoxia, and hypoxia + NAC pre-treatment. Diaphragm mTOR protein content (mean ± SEM) expressed as signal/µg of total protein (corrected for background signal); n = 7-8 per group. *p = 0.0107, **p = 0.0020; separate unpaired t-tests.

Figure 10 shows phospho-mTOR protein content in diaphragm muscle from mice exposed to 8 hours of normoxia, hypoxia, or hypoxia with NAC pretreatment. Hypoxia significantly increased phospho-mTOR protein content compared with the Control group (*p = 0.0123; unpaired t-tests). Hypoxia with NAC pretreatment increased phospho-mTOR protein content further still compared with the control group (***p = 0.0001; unpaired t-tests) and significantly higher than the Hypoxia group (**p = 0.0067; unpaired t-tests).

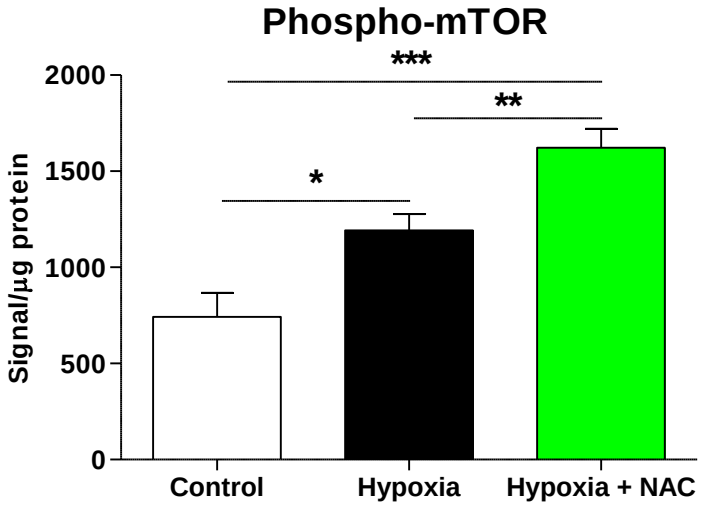

Figure 10: Diaphragm phospho-mTOR protein content following 8 hours of normoxia, hypoxia, and hypoxia + NAC pre-treatment. Diaphragm phospho-mTOR protein content (mean ± SEM) expressed as signal/µg of total protein (corrected for background signal); n = 7-8 per group. *p = 0.0123, **p = 0.0067, ***p = 0.0001; separate unpaired t-tests.

5.2.3.2.3 MAPK Pathway

Figure 11 shows phospho-ERK1/2 protein content in diaphragm muscle from mice exposed to 8 hours of normoxia, hypoxia, or hypoxia with NAC pretreatment. Hypoxia significantly increased phospho-ERK1/2 protein content compared with the Control group (*p = 0.0406; unpaired t-tests). Hypoxia with NAC pretreatment increased phospho-ERK1/2 protein content further still compared with the control group (***p = 0.0020; unpaired t-tests) and significantly higher than the Hypoxia group (**p = 0.0046; unpaired t-tests).

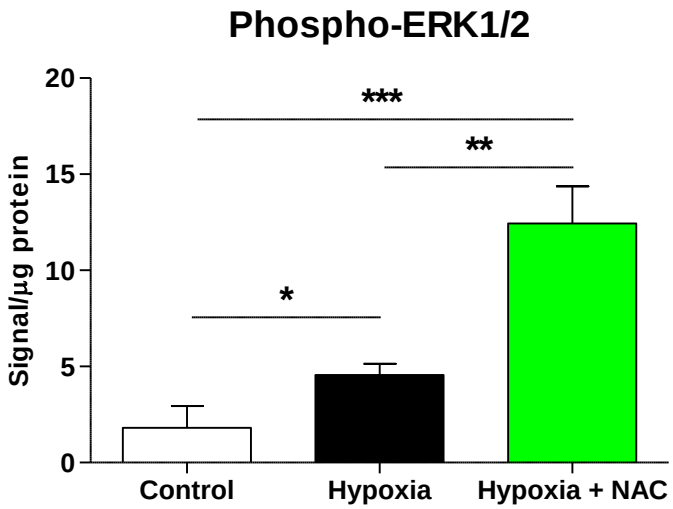

Figure 11: Diaphragm phospho-ERK1/2 protein content following 8 hours of normoxia, hypoxia, and hypoxia + NAC pre-treatment. Diaphragm phospho-ERK1/2 protein content (mean ± SEM) expressed as signal/µg of total protein (corrected for background signal); n = 5-8 per group. *p = 0.0406, ***p = 0.0020, **p = 0.0046; separate unpaired t-tests.

5.2.3.2.4 FoxO3a Pathway

Figure 12 shows phospho-FOXO-3a protein content in diaphragm muscle from mice exposed to 8 hours of normoxia, hypoxia, or hypoxia with NAC pretreatment. Hypoxia significantly increased phospho-FOXO-3a protein content compared with the Control group (***p = 0.0002; unpaired t-tests). Hypoxia with NAC pretreatment increased phospho-FOXO-3a protein content further still compared with the control group (****p < 0.0001; unpaired t-tests) and significantly higher than the Hypoxia group (**p = 0.0024; unpaired t-tests).

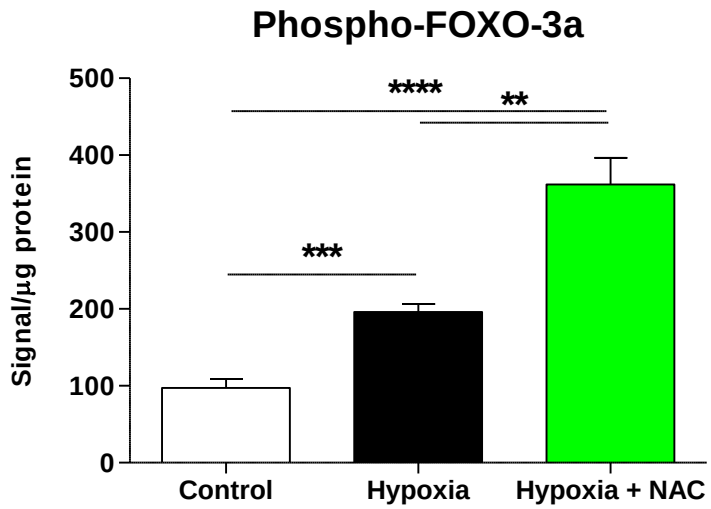

Figure 12: Diaphragm phospho-FOXO-3a protein content following 8 hours of normoxia, hypoxia, and hypoxia + NAC pre-treatment. Diaphragm phospho-FOXO-3a protein content (mean ± SEM) expressed as signal/µg of total protein (corrected for background signal); n = 7-8 per group. **p = 0.0024, ***p = 0.0002, ****p < 0.0001; separate unpaired t-tests.

5.2.3.3 Pro-Atrophy/Cell Death Signalling

5.2.3.3.1 MAPK Pathway

Figure 13 shows phospho-JNK protein content in diaphragm muscle from mice exposed to 8 hours of normoxia, hypoxia, or hypoxia with NAC pretreatment. Hypoxia significantly increased phospho-JNK protein content compared with the Control group (*p = 0.0120; unpaired t-tests). Hypoxia with NAC pretreatment increased phospho-JNK protein content further still compared with the control group (***p = 0.0058; unpaired t-tests) and significantly higher than the Hypoxia group (**p = 0.0108; unpaired t-tests).

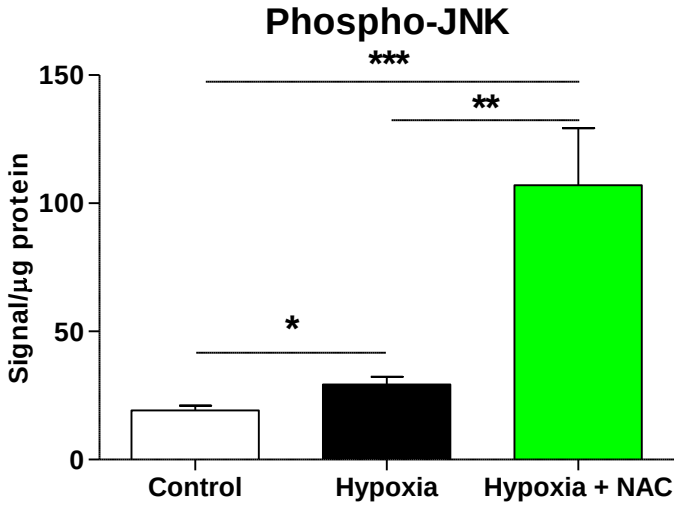

Figure 13: Diaphragm phospho-JNK protein content following 8 hours of normoxia, hypoxia, and hypoxia + NAC pre-treatment. Diaphragm phospho-JNK protein content (mean ± SEM) expressed as signal/µg of total protein (corrected for background signal); n = 8 per group. *p = 0.0120, **p = 0.0108, ***p = 0.0058; separate unpaired t-tests.

Figure 14 shows phospho-p38 protein content in diaphragm muscle from mice exposed to 8 hours of normoxia, hypoxia, or hypoxia with NAC pretreatment. Hypoxia increased phospho-p38 protein content compared with the Control group but not quite to statistical significance (p = 0.0515; unpaired t-tests). Hypoxia with NAC pretreatment increased phospho-p38 protein content further still compared with the control group (***p = 0.0030; unpaired t-tests) and significantly higher than the Hypoxia group (**p = 0.0092; unpaired t-tests).

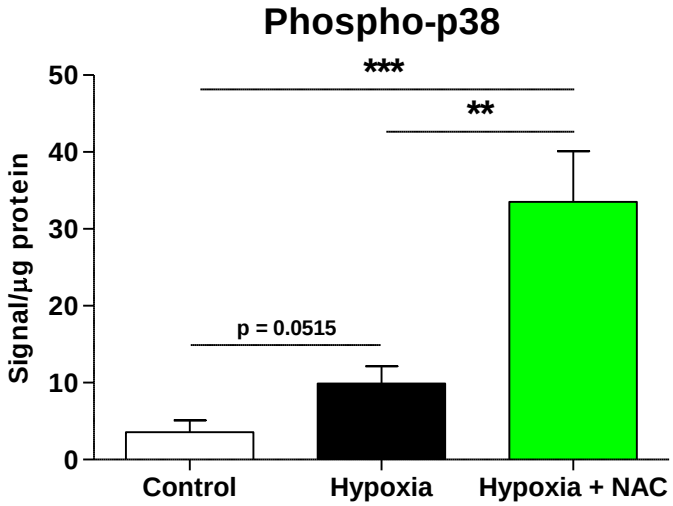

Figure 14: Diaphragm phospho-p38 protein content following 8 hours of normoxia, hypoxia, and hypoxia + NAC pre-treatment. Diaphragm phospho-p38 protein content (mean ± SEM) expressed as signal/µg of total protein (corrected for background signal); n = 6-8 per group. **p = 0.0092, ***p = 0.0030; separate unpaired t-tests.

5.2.4 Sternohyoid Signalling

5.2.4.1 HIF Signalling

Figure 15 shows HIF1α protein content in sternohyoid muscle from mice exposed to 8 hours of normoxia or hypoxia. Hypoxia significantly decreased HIF1α protein content compared with the Control group (*p = 0.0269; unpaired t-tests) in the sternohyoid muscle.

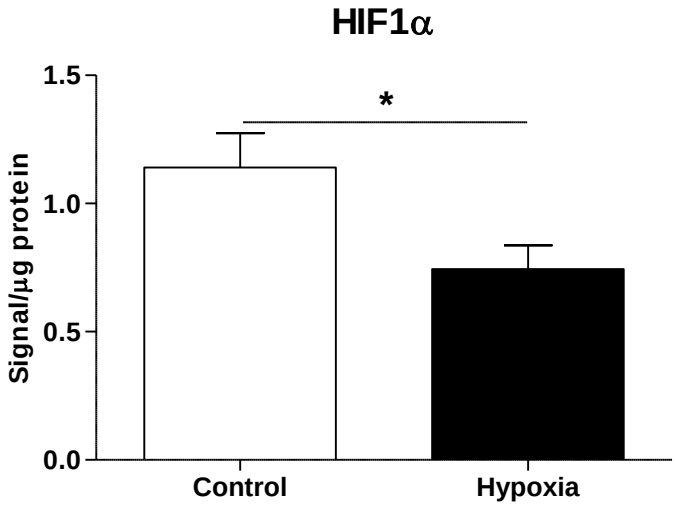

Figure 15: Sternohyoid HIF1α protein content following 8 hours of normoxia, and hypoxia. Sternohyoid HIF1α protein content (mean ± SEM) expressed as signal/µg of total protein (corrected for background signal); n = 7-8 per group. *p = 0.0269; unpaired t-test.

5.2.4.2 Pro-Hypertrophy/Cell Survival Signalling

5.2.4.2.1 Akt Pathway

Figure 16 shows phospho-Akt protein content in sternohyoid muscle from mice exposed to 8 hours of normoxia or hypoxia. Hypoxia significantly decreased phospho-Akt protein content compared with the Control group (**p = 0.0028; unpaired t-tests) in the sternohyoid muscle.

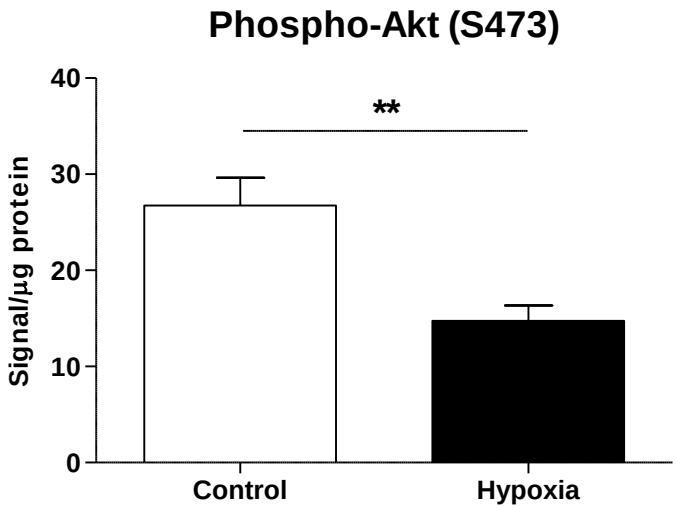

Figure 16: Sternohyoid phospho-Akt (S473) protein content following 8 hours of normoxia, and hypoxia. Sternohyoid phospho-Akt (S473) protein content (mean ± SEM) expressed as signal/µg of total protein (corrected for background signal); n = 8 per group. **p = 0.0028; unpaired t-test.

Figure 17 shows phospho-p70S6K protein content in sternohyoid muscle from mice exposed to 8 hours of normoxia or hypoxia. Hypoxia had no statistically significant effect on phospho-p70S6K protein content compared with the Control group, although there was a slight decrease in expression in the Hypoxia group (p = 0.0776; unpaired t-tests) in the sternohyoid muscle.

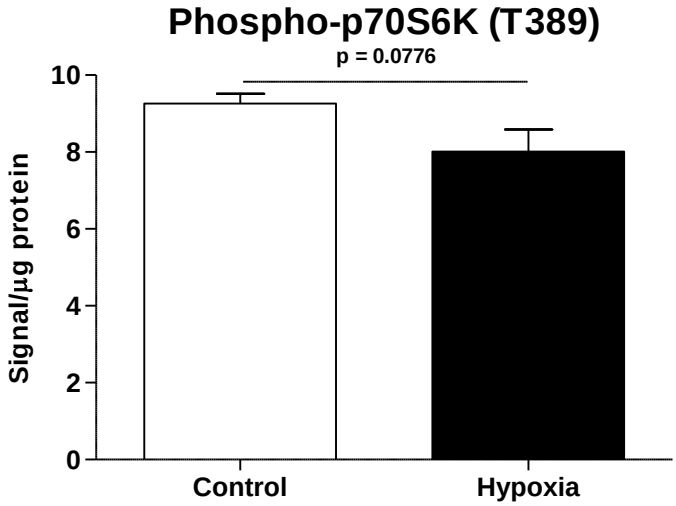

Figure 17: Sternohyoid phospho-p70S6K (T389) protein content following 8 hours of normoxia, and hypoxia. Sternohyoid phospho-p70S6K (T389) protein content (mean ± SEM) expressed as signal/µg of total protein (corrected for background signal); n = 8 per group. Unpaired t-test.

Figure 18 shows phospho-S6RP protein content in sternohyoid muscle from mice exposed to 8 hours of normoxia or hypoxia. Hypoxia significantly increased phospho-S6RP protein content compared with the Control group (*p = 0.0232; unpaired t-tests) in the sternohyoid muscle.

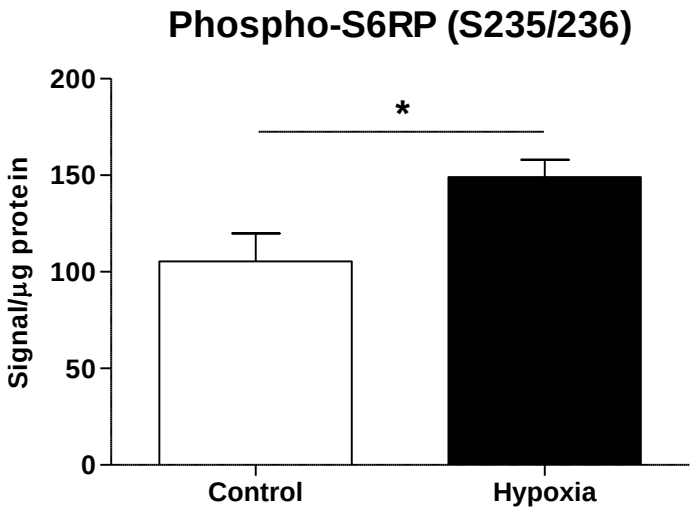

Figure 18: Sternohyoid phospho-S6RP (S235/236) protein content following 8 hours of normoxia, and hypoxia. Sternohyoid phospho- S6RP (S235/236) protein content (mean ± SEM) expressed as signal/µg of total protein (corrected for background signal); n = 8 per group. *p = 0.0232; unpaired t-test.

Figure 19 shows phospho-GSK-3β protein content in sternohyoid muscle from mice exposed to 8 hours of normoxia or hypoxia. Hypoxia had no statistically significant effect on phospho-GSK-3β protein content compared with the Control group (unpaired t-tests) in the sternohyoid muscle.

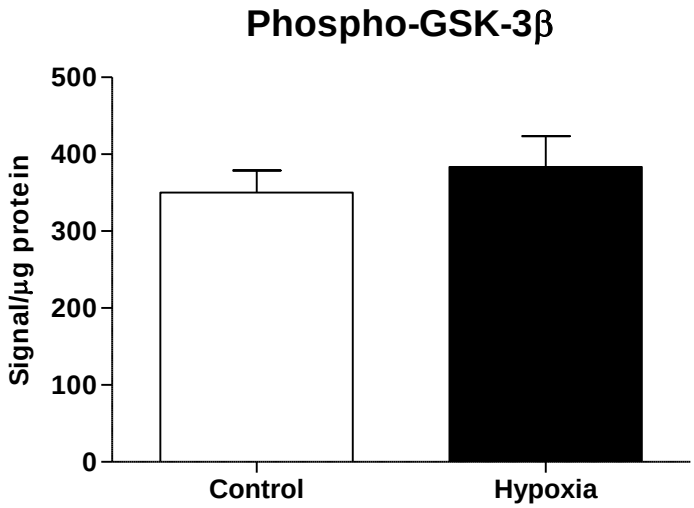

Figure 19: Sternohyoid phospho-GSK-3β protein content following 8 hours of normoxia, and hypoxia. Sternohyoid phospho-GSK-3β protein content (mean ± SEM) expressed as signal/µg of total protein (corrected for background signal); n = 8 per group. Unpaired t-test.

5.2.4.2.2 mTOR Pathway

Figure 20 shows mTOR protein content in sternohyoid muscle from mice exposed to 8 hours of normoxia or hypoxia. Hypoxia had no statistically significant effect on mTOR protein content compared with the Control group (unpaired t-tests) in the sternohyoid muscle.

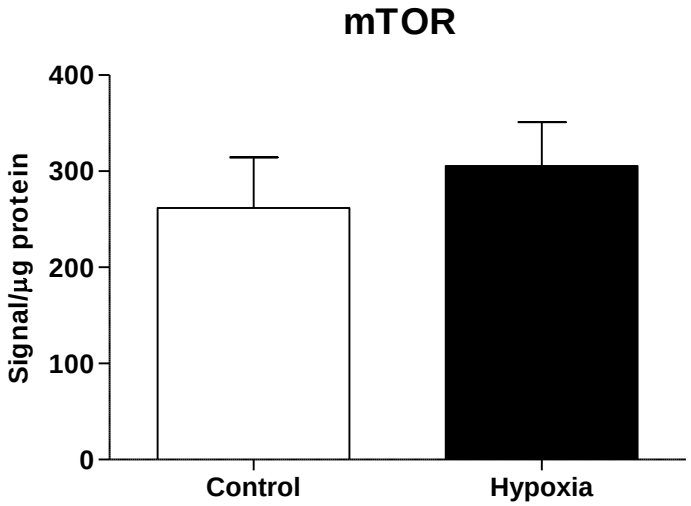

Figure 20: Sternohyoid mTOR protein content following 8 hours of normoxia, and hypoxia. Sternohyoid mTOR protein content (mean ± SEM) expressed as signal/µg of total protein (corrected for background signal); n = 8 per group. Unpaired t-test.

Figure 21 shows phospho-mTOR protein content in sternohyoid muscle from mice exposed to 8 hours of normoxia or hypoxia. Hypoxia had no statistically significant effect on phospho-mTOR protein content compared with the Control group (unpaired t-tests) in the sternohyoid muscle.

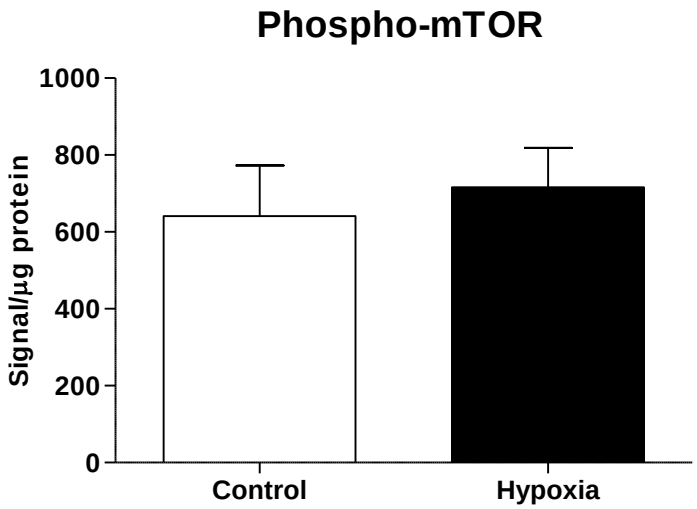

Figure 21: Sternohyoid phospho-mTOR protein content following 8 hours of normoxia, and hypoxia. Sternohyoid phospho-mTOR protein content (mean ± SEM) expressed as signal/µg of total protein (corrected for background signal); n = 8 per group. Unpaired t-test.

5.2.4.2.3 MAPK Pathway

There were not enough numbers available for phospho-ERK1/2 due to low signal in sternohyoid muscle samples.

5.2.4.2.4 FoxO3a Pathway

Figure 22 shows phospho-FOXO-3a protein content in sternohyoid muscle from mice exposed to 8 hours of normoxia or hypoxia. Hypoxia had no statistically significant effect on phospho-FOXO-3a protein content compared with the Control group (unpaired t-tests) in the sternohyoid muscle.

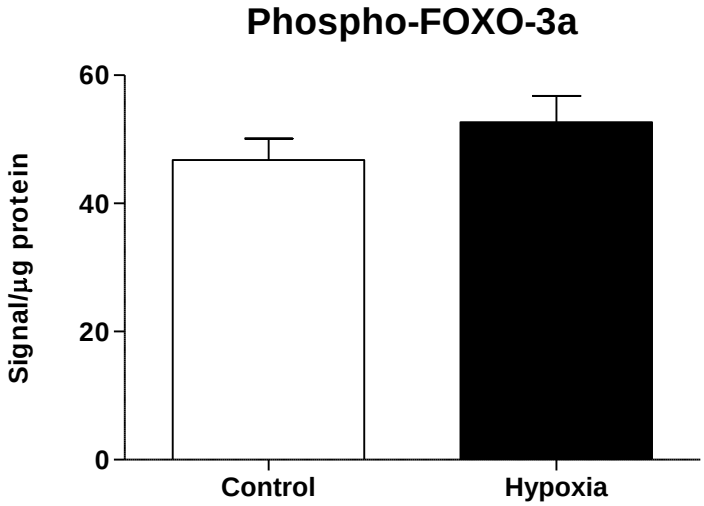

Figure 22: Sternohyoid phospho-FOXO-3a protein content following 8 hours of normoxia, and hypoxia. Sternohyoid phospho-FOXO-3a protein content (mean ± SEM) expressed as signal/µg of total protein (corrected for background signal); n = 8 per group. Unpaired t-test.

5.2.4.3 Pro-Atrophy/Cell Death Signalling

5.2.4.3.1 MAPK Pathway

Figure 23 shows phospho-JNK protein content in sternohyoid muscle from mice exposed to 8 hours of normoxia or hypoxia. Hypoxia had no statistically significant effect on phospho-JNK protein content compared with the Control group (unpaired t-tests) in the sternohyoid muscle.

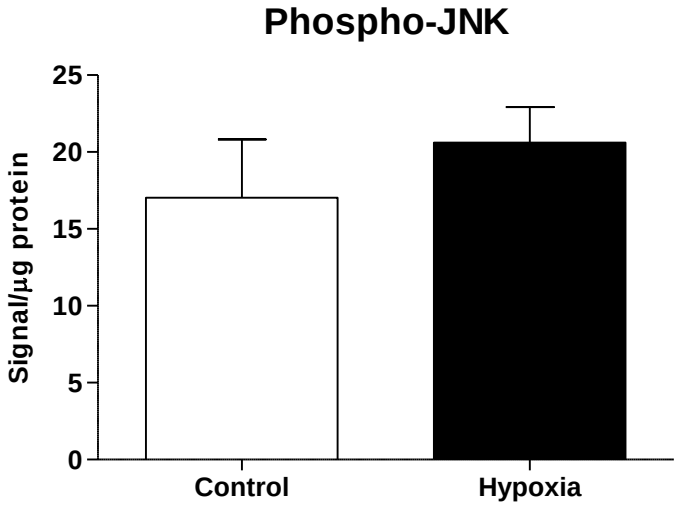

Figure 23: Sternohyoid phospho-JNK protein content following 8 hours of normoxia, and hypoxia. Sternohyoid phospho-JNK protein content (mean ± SEM) expressed as signal/µg of total protein (corrected for background signal); n = 8 per group. Unpaired t-test.

Figure 24 shows phospho-p38 protein content in sternohyoid muscle from mice exposed to 8 hours of normoxia or hypoxia. Hypoxia had no statistically significant effect on phospho-p38 protein content compared with the Control group (unpaired t-tests) in the sternohyoid muscle.

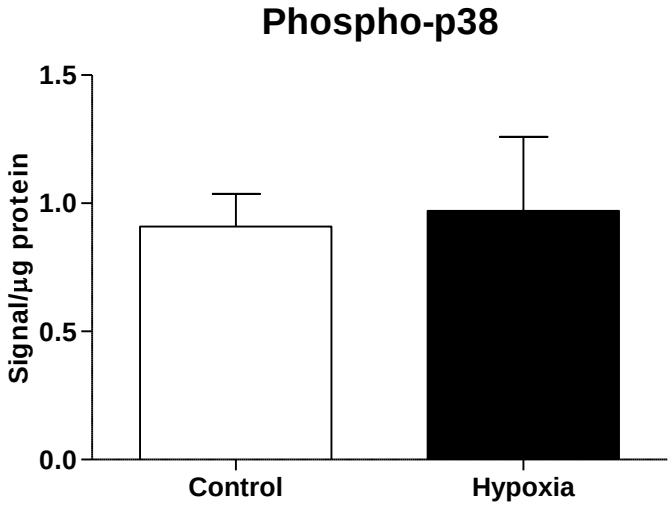

Figure 24: Sternohyoid phospho-p38 protein content following 8 hours of normoxia, and hypoxia. Sternohyoid phospho-p38 protein content (mean ± SEM) expressed as signal/µg of total protein (corrected for background signal); n = 5-7 per group. Unpaired t-test.

5.3 Chapter Discussion

The main findings of this chapter are:

1. The antioxidant NAC ameliorates acute hypoxia induced diaphragm dysfunction.

2. Acute hypoxia induces both pro-atrophic and pro-hypertrophic signalling pathways and HIF signalling in the diaphragm, while reducing HIF signalling in the sternohyoid.

3. A single I.P. injection of NAC prior to hypoxic exposure appears to bolster many of these endogenous signalling responses to acute hypoxia in the diaphragm.

5.3.1 Muscle Function

NAC pre-treatment prior to hypoxic exposure rescues the diaphragm from acute hypoxia induced diaphragm weakness, both in terms of the peak tetanic force generating capacity of the muscle and the force frequency relationship. Not only does NAC prevent the hypoxia induced diaphragm dysfunction, but it actually appears to enhance muscle performance slightly following hypoxia, above control levels. Oxidative stress is a feature of many respiratory conditions and indeed animal models of chronic hypoxia, and as discussed in chapter 1 section 1.8, ROS levels within muscle cells can influence muscle contractile force. Given this positive influence of the antioxidant NAC, preventing acute hypoxia induced diaphragm dysfunction/weakness, it is plausible that oxidative stress due to increased levels of ROS could be a factor leading to this observed muscle weakness. Increased mitochondrial ROS production is a potential source for this increase in oxidative stress.

In a recent study by Azuelos et al. (2015), using a mouse model of VIDD, they found that treatment with an I.P. injection of NAC immediately after the initiation of 6 hours

of mechanical ventilation completely prevented the development of mechanical ventilation-induced diaphragmatic weakness. However, it did not suppress autophagy but rather it augmented autophagosome formation. Autophagy is a lisosomally mediated catabolic and proteolytic process. They suggest that this may elucidate a novel mechanism whereby NAC exerts its beneficial effects on VIDD via stimulation of autophagy (excess ROS can inhibit autophagy), which may in fact be a beneficial adaptive response in the diaphragm to the physiological stress of mechanical ventilation rather than representing a contributing factor to the development of VIDD (Azuelos et al., 2015). In the mouse model of acute hypoxia discussed in this thesis, NAC prevented the development of acute hypoxia induced diaphragm weakness, and although there were no significant hypoxia induced changes in the mRNA expression of the genes related to autophagy which were examined in this model, whether or not NAC, concomitant with hypoxia, influenced autophagy was not examined. This is one potential mechanism by which NAC could be exerting a beneficial effect on the hypoxic diaphragm, acting to streamline cellular processes and optimise performance. Indeed, under conditions of nutrient deprivation, autophagy augments cellular energy production, and functions to maintain cellular homeostasis via degradation of dysfunctional proteins and damaged mitochondria (mitophagy), so here autophagy may exert beneficial effects via bolstering amino acid dependent ATP generation and improving mitochondrial efficiency by removal of damaged mitochondria.

As well as the potential benefits of using NAC as an adjunct therapy in patients with acute respiratory diseases to prevent acute hypoxia induced diaphragm dysfunction, elucidated in this chapter, NAC has also been shown to protect the diaphragm from the damaging effects of controlled mechanical ventilation such as diaphragmatic oxidative stress and proteolysis, as well as controlled mechanical ventilation induced contractile dysfunction (Agten et al., 2011).

5.3.2 Metabolism

Interestingly, the *post-mortem* body temperature was still reduced by hypoxia in the hypoxia + NAC group compared to control. This suggests that the beneficial effects of NAC on hypoxic diaphragm performance are unlikely to be influencing the

hypoxic hypometabolic/hypothermic state (and any associated alkalosis caused by the reduction in CO_2 production, concomitant with maintained ventilation – relative hyperventilation) adopted by the mouse in hypoxia. Thus NAC is likely exerting its benefits on muscle performance via an independent mechanism, or set of mechanisms. This is encouraging, as humans do not adopt this pronounced hypometabolic state when hypoxic.

5.3.3 Respiratory Muscle Hypoxia Signalling

HIF1α protein content was increased in the diaphragm following 8 hours of hypoxia. This is not altogether surprising given that HIF1α protein accumulation is indirectly proportional to cytosolic oxygenation. ROS can induce HIF1α expression, but this effect can be dependent on exposure time, and ROS can exert the opposite effect over prolonged periods, thus creating some uncertainty regarding how swings in cellular redox balance affect HIF1α expression (Bonello et al., 2007; Jusman et al., 2010; Niecknig et al., 2012; Schieber and Chandel, 2014). One might expect that NAC, being an antioxidant, would prevent this hypoxia induced increase in HIF1α protein content. However, HIF1α is responsive to redox balance within the intracellular environment and reducing conditions can stabilise HIF1α, and NAC induced increases in cellular GSH could elevate HIF1α expression (Jin et al., 2011; Nikinmaa et al., 2004; Sceneay et al., 2013; Zhang et al., 2014). Here, pre-treatment with NAC prior to hypoxic exposure enhances HIF1α protein content in diaphragm muscle compared with hypoxia alone, enhancing the HIF1α signalling response in hypoxia + NAC. Indeed, it has been reported that HIF1 contributes to the neuroprotective effect of NAC in an ischaemic stroke model of transient cerebral ischaemia in rats (Zhang et al., 2014). In contrast to these findings regarding diaphragm HIF1α protein content in acute hypoxia and acute hypoxia following NAC pre-treatment in diaphragm, chronic hypoxia induced increases in HIF1α protein content in the diaphragm were attenuated, rather than being augmented, by chronic antioxidant treatment (administered orally) concomitant with chronic hypoxia (Lewis et al., 2015b). In the current study, HIF1α protein content accumulated further still in hypoxia + NAC due to being stimulated on two fronts; induction by hypoxia and induction by altered cellular redox state.

Interestingly, and rather unexpectedly, HIF1α protein content was significantly reduced in the sternohyoid following 8 hours of hypoxia. This may have been due to muscle fibre type differences or muscle activity difference. These differences could give rise to differential redox states in each of the two muscles following acute hypoxia, leading to differential HIF1α protein responses. Indeed, chronic hypoxia has also been shown to have differential effects on HIF1α protein content in sternohyoid and diaphragm (Lewis et al., 2015d). This data suggests that HIF1α signalling in the sternohyoid is unaffected by acute hypoxia.

5.3.4 Respiratory Muscle Hypertrophy/Atrophy Signalling

Finally, we examined the protein and/or phosphoprotein content of various key proteins (fig. 25) associated with signalling pathways involved in the balance between cell survival and death and protein balance, or hypertrophy/atrophy, in diaphragm and sternohyoid muscle. We also elucidated the influence of NAC pre-treatment prior to hypoxia on these proteins in the diaphragm.

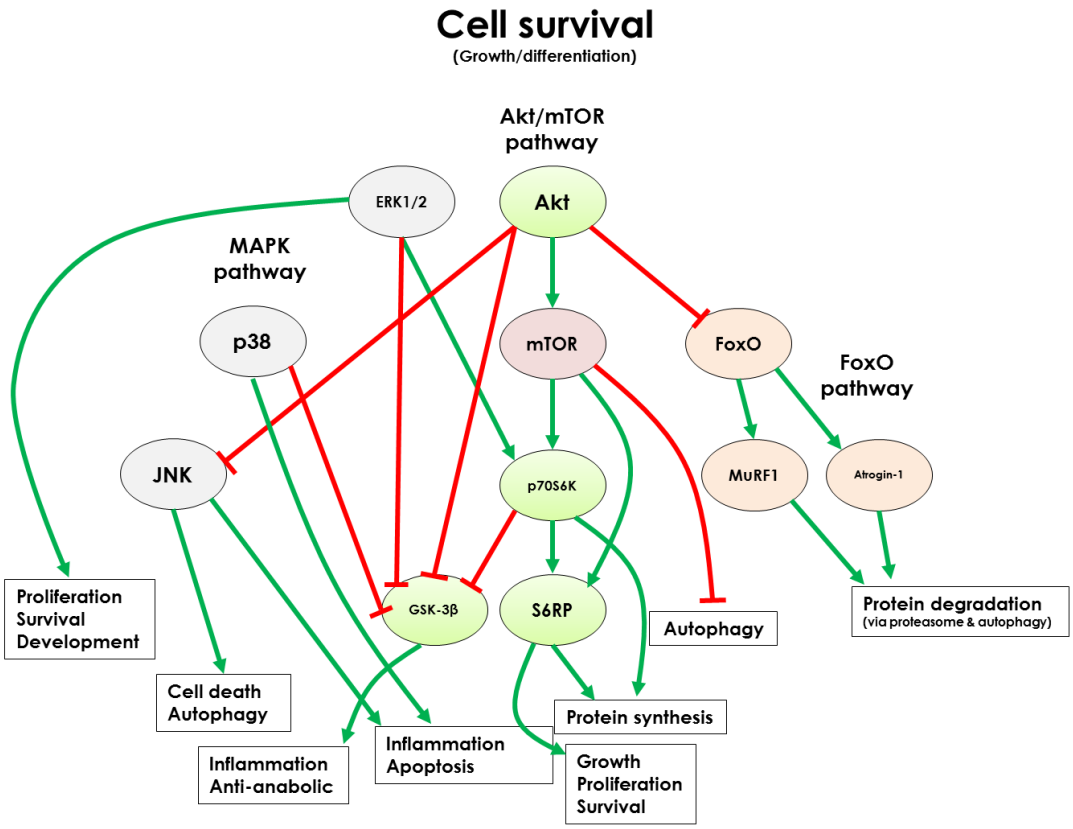

Figure 25: Schematic depicting the various hypertrophy/atrophy signalling pathways examined in this chapter. Green arrows indicate activation, red lines indicate inhibition.

5.3.4.1 Pro-Hypertrophy/Cell Survival Signalling

5.3.4.1.1 Akt Pathway

The Akt signalling pathway is discussed in chapter 1. Akt, particularly the Akt/mTOR pathway, is central to the control of the hypertrophic/atrophic state or balance in muscle, acting in a phosphorylation dependent manner as a key regulator of downstream effectors involved in modulating cell growth and survival. Activated (phosphorylated) Akt is predominantly pro-hypertrophic, via inhibition of atrophic signals and promotion of hypertrophic signals. Here, phosphorylated (active) Akt, or phospho-Akt, protein content is upregulated following acute hypoxia, and upregulated further still following hypoxia + NAC in the diaphragm. It has been previously demonstrated that, under certain conditions, hypoxia can activate Akt and it is

suggested that that hypoxia induced Akt activation may play a role in protection against apoptosis (Alvarez-Tejado et al., 2001; Beitner-Johnson et al., 2001; Dai et al., 2008; Stegeman et al., 2012). Similarly, in this model it would appear that acute hypoxia induced Akt activation is a beneficial compensatory mechanism by the muscle, rather than being a negative consequence of hypoxic damage, attempting to maintain muscle functional integrity. When NAC pre-treatment is administered prior to acute hypoxia, it appears to enhance this endogenous induction of Akt signalling, potentially bolstering the cellular defensive efforts against acute hypoxia. This may be (part of) the mechanism by which NAC rescues diaphragm force in hypoxia. It is also worth noting that Akt/mTOR signalling can regulate HIF1α and may play a role in hypoxia induced HIF1α expression (Kilic-Eren et al., 2013; Land and Tee, 2007; Yang et al., 2009). Akt also exerts pro-hypertrophic effects via inhibition of atrophic signalling, which shall be discussed later on.

In the sternohyoid, hypoxia caused a reduction in phospho-Akt protein content, suggesting a lack of pro-hypertrophy signalling in the hypoxic sternohyoid. Indeed, Akt is activated by hypoxia, as mentioned above, and may play a role in hypoxia induced HIF1α expression. Perhaps a hypoxia induced increase in Akt activation is HIF1α dependent. Therefore, the reduction in HIF1α protein content in the acute hypoxic sternohyoid would lead to this reduced phospho-Akt protein content. Indeed, the relationship between hypoxia and Akt is believed to be HIF1α mediated (Bedogni et al., 2005). This is therefore a likely mechanism for this reduced Akt protein content in the hypoxic sternohyoid.

Phospho-p70S6K, which is downstream of Akt, is slightly but not significantly elevated by acute hypoxia in the diaphragm. Its protein content was, however, significantly elevated by hypoxia + NAC in the diaphragm. p70S6k activation by Akt is mediated via the indirect activation of mTOR by Akt. p70S6K, when activated, promotes translation/protein synthesis and cell survival in muscle (Baar and Esser, 1999; Gran et al., 2014; Zanchi and Lancha, 2008). The fact that the induction of elevated phospho-p70S6K is greater in hypoxia + NAC compared with hypoxia itself is likely due to the greater elevation of phospho-Akt, and phospho-mTOR and phospho-ERK1/2 (see below) in hypoxia + NAC, which both activate phospho-p70S6K (Krolikowski et al., 2006). Again this is indicative of pro-hypertrophy

signalling being induced in hypoxia + NAC, a mechanism which could be beneficial to maintaining diaphragm muscle performance. Indeed, decreased phospho-p70S6K expression occurs in the diaphragm of mechanically ventilated rats prior to decreased protein synthesis (McClung et al., 2008).

There is no difference in phospho-p70S6K protein content between the control and hypoxic sternohyoid muscle, although there is a slight non-significant reduction in phospho-p70S6K protein content, again suggesting a lack of pro-hypertrophy signalling in the acutely hypoxic sternohyoid muscle. The lack of any change in phospho-mTOR in hypoxic sternohyoid is a likely cause of this (see below).

The phosphoprotein content of phospho-S6RP, which is downstream of both Akt/mTOR and p70S6K, is significantly increased by both hypoxia and hypoxia + NAC in the diaphragm. The phosphorylation of S6RP by phospho-p70S6K, driven by Akt/mTOR, drives translation/protein synthesis and growth. Phospho-S6RP protein content is also increased in the hypoxic sternohyoid muscle compared with control. This increase in phospho-S6RP in the sternohyoid must be through activation from another pathway as the phosphoprotein content of its upstream effectors, mTOR and p70S6K, are unaltered. Therefore protein synthesis signalling, via a mechanism other than Akt/mTOR, may be induced in the hypoxic sternohyoid.

Hypoxia, as discussed above, can activate Akt, and this leads to GSK-3 phosphorylation (Beitner-Johnson et al., 2001). Phosphorylation negatively regulates GSK-3β, inhibiting it, resulting in the activation of protein synthesis and a cessation of anti-anabolic signalling from GSK-3β. Here, phospho-GSK-3β protein content is increased significantly by hypoxia, and increased further still by hypoxia + NAC. Again, these data suggest a drive toward a pro-hypertrophic/pro-protein synthesis state in hypoxia that is further augmented by NAC pre-treatment. There is no difference in phospho-GSK-3β protein content between the control and hypoxic sternohyoid muscle, suggesting that the anti-anabolic effects of GSK-3β are unhalted in hypoxic sternohyoid.

5.3.4.1.2 mTOR Pathway

mTOR, as discussed in chapter 1 and in the paragraphs above, is a protein kinase functioning in the regulation of growth, survival and protein synthesis in skeletal muscle. Both mTOR and phospho-mTOR were measured here. mTOR mediates its hypertrophic/cell survival signalling effects via its phosphorylated/activated state. Here, hypoxia significantly increased mTOR protein content while this was not the case in hypoxia + NAC. While both hypoxia and hypoxia + NAC increased phospho-mTOR protein content, expression being augmented furthest in the hypoxia + NAC group. It would appear that hypoxia alone, in the absence of NAC, may induce an increase in mTOR protein expression, or indeed a reduction in mTOR degradation, while phosphorylation of mTOR was upregulated or induced by hypoxia and further still by hypoxia concomitant with NAC. Phospho-p70S6K and phospho-s6RP, discussed above, are also both downstream of, and activated by, mTOR, and so the increase in phospho-mTOR likely contributes to the increases in phospho-p70S6K and phospho-s6RP reported above.

There was no difference in mTOR or phospho-mTOR protein content between the control and hypoxic sternohyoid muscle, likely contributing to the lack of difference in phospho-p70S6K between control and hypoxic sternohyoid.

5.3.4.1.3 MAPK Pathway

ERK1/2 is a member of the MAPK family which positively regulates p70S6K, negatively regulates GSK-3β and itself positively regulates cellular proliferation, survival and development. Through these mechanisms it is pro-cell survival/hypertrophy. Here, acute hypoxia increased diaphragm phospho-ERK1/2 protein content, and NAC pretreatment augmented this acute hypoxia induced phospho-ERK1/2 protein content increase. This, combined with the Akt signalling data above, further supports the theory that NAC pre-treatment bolsters the endogenous cellular signalling mechanisms acting to promote protein synthesis and cell survival in the acutely hypoxic diaphragm. Meanwhile, the phospho-ERK1/2 signal was too low in too many of the sternohyoid muscle samples to obtain any meaningful data on its expression profile in control and hypoxia.

5.3.4.1.4 FoxO3a Pathway

The FoxO pathway is generally associated with atrophy and protein degradation in its dephosphorylated state. However, when phosphorylated, FoxO3a, as discussed in chapter 1, is inhibited from translocation into the nucleus and exerting its atrophic effects. One of the ways in which Akt exerts a hypertrophic effect is by the phosphorylation and thus inhibition of FoxO3a, preventing the atrophic action of MuRF1 and Atrogin-1, which would otherwise be transcriptionally upregulated by FoxO3a. In this chapter, acute hypoxia increased phospho(inhibited)-FoxO3a protein content in the diaphragm and NAC pre-treatment further augmented this acute hypoxia induced increase in protein content, thus enhancing and adding to the pro-hypertrophic/anti-atrophic signalling cascades described above, via the down-regulation of FoxO3a induced proteasomal and autophagy mediated protein degradation. This increase in phosphoprotein content was likely mediated via the increase in phospho-Akt in diaphragm. There was no difference in phospho-FoxO3a protein content between the control and hypoxic sternohyoid muscle.

5.3.4.2 Pro-Atrophy/Cell Death Signalling

5.3.4.1.1 MAPK Pathway

While there appears to be a predominant drive toward protein synthesis in the acutely hypoxic diaphragm, augmented further by NAC, as discussed above, there was also an increase in a certain amount of atrophic signalling via the MAPK pathway. JNK promotes autophagy, apoptosis, inflammation and cell death, and is activated by phosphorylation (Berdichevsky et al., 2010). Here, acute hypoxia elevated levels of phospho-JNK protein, an effect which is further augmented by NAC. This is somewhat surprising given that Akt, which was also activated, negatively regulates the JNK pathway via a cross-talk mechanism (Levresse et al., 2000). JNK phosphorylation in this model is therefore likely induced by some other mechanism/stress affecting the MAPK pathway. There was no difference in phospho-JNK protein content between the control and hypoxic sternohyoid muscle.

p38 can promote inflammation and apoptosis, while also negatively regulating GSK-3β to promote survival (Thornton et al., 2008). Here, acute hypoxia increased phospho-p38 expression to near significant levels in the diaphragm, while NAC concomitant with acute hypoxia significantly augments this increase. This suggests a pro-atrophic effect of hypoxia + NAC in the diaphragm. There is no difference in phospho-p38 protein content between the control and hypoxic sternohyoid muscle.

These signalling pathways are complex. They interact with each other and a host of other signalling mechanism, combining in synergy or antagonistically, to exert a variety of effects (Fey et al., 2012). In this chapter, when attempting to group these data together in order to form conclusions as to the overall direction in which these signalling pathways are converging, we report a general increase in cell survival and pro-hypertrophy/protein synthesis signalling in acute hypoxia, accompanied by a concurrent, albeit less robust, increases in cell death and pro-atrophy/protein degradation signalling in the diaphragm. Most interestingly, both of these signalling programmes are enhanced further still by NAC pre-treatment. Given that NAC improves functional outcome and performance in the diaphragm muscle, this suggests that these signalling initiatives are attempting to drive beneficial responses to acute hypoxia, and they become effective when augmented by NAC pre-treatment. Indeed, NAC appears to bolster, or amplify, these endogenous signalling endeavours in the diaphragm in response to acute hypoxia, rather than abate them, suggesting that NAC may exert its beneficial effects on diaphragm muscle performance, namely mitigating acute hypoxia induced diaphragm weakness, via enhancement of the endogenous signalling responses acting to maintain function and thwart the detrimental effects of acute hypoxia, rather than acting antagonistically against acute hypoxia induced signalling programmes that are inimical to muscle function. While hypoxia signalling through HIF1α was increased by hypoxia in the diaphragm, it was in fact reduced by hypoxia in the sternohyoid highlighting, as mentioned previously, the differential effects that hypoxia can exert on the two muscles, given the different fibre type composition of the two muscles. Another fibre type difference between the two muscles is that the diaphragm is more oxidative than the sternohyoid, and could therefore potential respond differently to changes in oxidative stress, and indeed

experience a different degree of oxidative stress, in response to the same hypoxic insult on the animal as a whole.

5.4 Chapter Conclusions

Acute hypoxia induced diaphragm weakness is ameliorated by NAC pre-treatment, via a mechanism which does not influence the hypometabolic state of the hypoxic mouse. Since this murine hypometabolic strategy is unaffected by NAC pre-treatment, which prevents diaphragm weakness, hypometabolism is not likely a driving force for diaphragm weakness following hypoxic exposure. This is important as humans do not adopt this prominent hypometabolic state, and so in attempting to extrapolate these findings to the human condition it is encouraging that this murine strategy does not appear to play a role in the beneficial potential of NAC to prevent acute hypoxia induced diaphragm dysfunction. NAC pre-treatment bolsters endogenous acute hypoxia induced hypoxic, hypertrophic and atrophic signalling mechanisms. This drive to increase both hypertrophy and atrophy signalling could be a gear change to drive an increase in protein turnover and amino acid dependent ATP generation. Further downstream the atrophic drive may be driving the degradation of non-essential proteins for performance optimisation and amino acid fuel source while the hypertrophic response may be driving the generation of fundamental proteins to muscle performance and cellular optimisation. NAC appears to boost these signalling cascades to further drive this initiative and, potentially through this mechanism, lead to the preservation of diaphragm functionality. These findings further highlight the potentially critical role of hypoxia in the diaphragm muscle dysfunction observed in patients with acute respiratory diseases. NAC may be a beneficial adjunct therapy in these patients, alleviating acute hypoxia induced diaphragm dysfunction, and potentially improving patient outcome.

Chapter 6: Summary and Conclusions

6.1 Summary

The link between hypoxia and respiratory disease is not a new concept. However, while much research in this area has focused on the role of hypoxia in chronic respiratory or cardiac conditions such as COPD or CHF, or indeed the role of intermittent hypoxia in SDB conditions such as OSA and central sleep apnoea, little is known regarding the potential role of acute hypoxia in diaphragm muscle dysfunction in acute respiratory-related conditions and mechanically ventilated patients. This is surprising given the clinical relevance. Indeed, diaphragm muscle weakness is a strong indicator of poor outcome in patients (Supinski and Callahan, 2013), and acute hypoxia can present during airway obstruction, blockage of the alveoli by oedema or infectious exudate, acute haemorrhage, and acute respiratory-related disorders such as VILI/VALI, ARDS and ALI. These conditions are associated with ICUAW, including diaphragm muscle weakness. Chronic and intermittent hypoxia are known to independently affect respiratory muscle performance. It is therefore pertinent to explore whether acute hypoxia alters respiratory muscle contractile performance. In this thesis we aimed to determine whether acute hypoxia would affect: 1) respiratory (diaphragm and sternohyoid) muscle contractile performance; 2) ventilation and metabolism; and 3) the hypertrophy/atrophy balance, mitochondrial function, hypoxic signalling and SR calcium handling in respiratory muscle (and compare some of these to non-respiratory skeletal muscle). Finally, 4) we sought to determine whether a single I.P. injection of NAC immediately prior to hypoxic exposure would alter how the diaphragm responded to acute hypoxia.

A murine model exposed to 1, 4 or 8 hours of hypoxia (10% O_2) or normoxia (21% O_2) was utilised in this study for gene expression analysis in diaphragm sternohyoid, EDL and soleus muscles. Mice exposed to 8 hours of normoxia or hypoxia were used for *in vivo* measurements, *ex vivo* functional analysis, and protein assays.

In chapter three, we demonstrate a 30% reduction in force-generating capacity of the diaphragm, with resultant depression in power output following acute hypoxia, and a similar acute hypoxia induced magnitude of weakness in the sternohyoid. This diaphragm weakness, observed in both mice and rats, could be thought of as

functionally significant, particularly in situations where a patient's ventilation may already be compromised as is often the case in the ICU (assuming a similar response in human diaphragm). This weakness could prove particularly problematic when the diaphragm is required to carry out tasks other than quiet breathing, such as airway clearance manoeuvres and/or ventilation through a narrowed airway (increasing the load on the muscle).

In chapter four, we aimed to uncover some of the molecular mechanisms that may be underpinning acute hypoxia induced respiratory muscle dysfunction, and examine ventilation and metabolism *in vivo* in order to ascertain if ventilation, and therefore diaphragm muscle activity, is increased in acute hypoxia in this mouse model. We also wished to characterise the acute hypoxia induced hypometabolic strategy adopted by the mouse in acute hypoxia so that this could be matched to ventilation in order to explain the ventilatory profile more completely, and to provide a more elaborate picture of oxygen supply and utilisation, providing information such as the RER. In terms of the gene expression data, we profiled gene expression in key areas relating to muscle function (those that may contribute to muscle weakness in an acute hypoxic environment), namely mitochondrial metabolism, atrophy signalling, SR calcium handling and hypoxia signalling. We measured expression of these genes following 1, 4 and 8 hours of hypoxia in order to profile the temporal profile of the expression of these genes over the course of 8 hours of hypoxia. We examined proteasome activity to further assess the atrophy profile of the acutely hypoxic diaphragm. We found that 4-8 hours of hypoxia significantly increases mitochondrial UCP-3 mRNA expression across all 4 muscle types, suggestive of an increased reliance on fatty acid metabolism in skeletal muscle around the body, and potentially reducing ROS production. Differential and dynamic changes in mRNA expression of transcription factors involved in the regulation of mitochondrial biogenesis & energy metabolism are observed in respiratory, but not limb, muscle following 1, 4 & 8 hours of hypoxia. Pro-atrophy signalling mRNA expression is induced by hypoxia across all 4 muscle types, although not with significance in sternohyoid muscle. There was no change in autophagy related gene expression, or proteasome enzymatic activity in the diaphragm. 4 hours of hypoxia caused a certain level of perturbation in SR calcium handling related gene expression in respiratory muscle, the sternohyoid in particular. Hypoxia did not cause any persistent change in ventilation (muscle activity), therefore

muscle weakness and molecular changes are likely hypoxia-dependent. Hypoxia decreased metabolism and body temperature, meaning that although ventilation is unaltered, there is in fact a relative hyperventilation when metabolic rate is considered. The Respiratory Exchange Ratio (RER) was unaffected by hypoxia, suggesting there is no switch in metabolic energy source. An RER of 0.7 suggests that fatty acids are the primary substrate for oxidative metabolism and energy production, over glucose/carbohydrates.

In chapter 5, we tested whether the antioxidant NAC could prevent the acute hypoxia induced diaphragm dysfunction observed in chapter 1, to ascertain whether this NAC pre-treatment would alter the hypoxic hypometablism, and to examine hypoxic and hypertrophy/atrophy signalling pathways in control and 8 hours hypoxic diaphragm and sternohyoid muscle, and determine how NAC pretreatment would alter the way in which hypoxia affects these cascades in the diaphragm. We found that NAC ameliorates acute hypoxia induced diaphragm dysfunction. Acute hypoxia induced both pro-atrophic and pro-hypertrophic signalling pathways and HIF signalling in the diaphragm, and a single I.P. injection of NAC prior to hypoxic exposure appeared to bolster many of these endogenous signalling responses to acute hypoxia, which may be the mechanism by which NAC exerts its beneficial effects on diaphragm muscle function. Alternatively NAC may prevent hypoxia induced redox modulation of contractile function, as observed following chronic exposure to hypoxia (Lewis et al., 2016). NAC may be a beneficial adjunct therapy in patients with acute respiratory diseases, alleviating acute hypoxia induced diaphragm dysfunction, and potentially improving patient outcome.

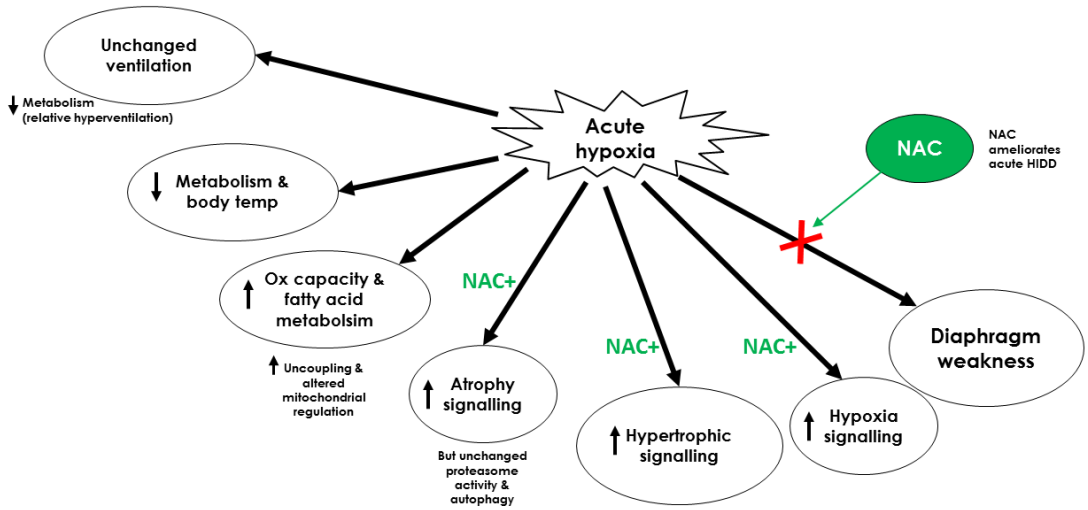

Figure 1: The effects of acute hypoxia on the diaphragm. A summary of the effects of acute hypoxia on diaphragm muscle in mice. NAC pre-treatment ameliorated acute hypoxia-induced diaphragm dysfunction.

6.2 Limitations

As is the case with any scientific study, there are limitations to this study which must be acknowledged. First and foremost, it must be noted that when conducting any research utilising animal models of human conditions one must concede that data or phenotypes observed in the animal, in this instance the mouse, do not always translate directly to the human condition. One primary concern along those lines in this study is the pronounced hypoxic hypometabolic state adopted by the mouse, which is not present in humans. However, it is encouraging that while NAC was effective in preventing acute hypoxia induced diaphragm weakness, it did not alter the hypoxia induced reduction in *post mortem* body temperature, and is therefore unlikely to be altering that hypometabolic state to improve diaphragm performance i.e. acute hypoxia-induced diaphragm dysfunction is unrelated to metabolic consequences of hypoxia. In humans, rather than a reduction in metabolism, as is observed in the mouse, exposure to hypoxia results in an increase in ventilation (diaphragm activity). Meanwhile the rat adopted a strategy of adaptation which lies somewhere in between the human and the mouse, whereby the rat maintains a slightly elevated ventilation while also reducing metabolism, although not to the extent of the mouse

hypometabolic response. Therefore, while the difference in hypoxic strategy between the mouse and the human is an important point of consideration when extrapolating these data to humans, it is encouraging that the same level of diaphragm weakness is observed in both the mouse and the rat, despite the difference in hypoxic ventilatory/metabolic strategy.

The duration of time chosen to represent 'acute hypoxia' is another factor worth consideration. 8 hours or less was chosen because, from review of the literature, mechanical ventilation induced diaphragm maladaptation, weakness and atrophy can manifest within that timeframe in animals and humans (Azuelos et al., 2015; Bruells et al., 2013; Chen et al., 2015; Hooijman et al., 2015; Jaber et al., 2011a; Levine et al., 2008; Picard et al., 2015), demonstrating how quickly these changes can occur in the diaphragm and how quickly the diaphragm can be altered. While disuse or unloading of the diaphragm is obviously a different stimulus to hypoxia alone, the fact that the diaphragm can adapt in this short space of time lead us to believe it was worth looking at hypoxia in this timeframe. Indeed, this fixed time point for measuring muscle function, and other parameters, only gives us a snap shot of how the diaphragm is affected at that time. As evident from the gene expression data at 1, 4 and 8 hours, the expression changes of certain genes under hypoxic conditions is time dependent and differ temporally between those time points. It is also unclear from this study whether, if the mice were reintroduced into a normoxic environment, the diaphragm muscle would recover over time.

Examining muscle contractile performance *ex vivo* has the benefit of allowing us to examine contractile changes intrinsic to the muscle itself. However, the muscle may function differently *in vivo*. There may also be compensatory mechanisms, neural, intercostal muscle assistance, or otherwise, present *in vivo* that allow the diaphragm to perform optimally even with this intrinsic weakness. Performing the functional analysis in hyperoxic conditions allowed for maximum muscle performance to be assessed and gave the best chance to maintain muscle viability, although it is worth noting that this is not physiological and may also have biased results insofar as hypoxic diaphragm may have performed better than control diaphragm under conditions of hypoxic exposure. In other words, the cellular strategy adopted by the

diaphragm in the face of hypoxic stress may be one which confers advantage to the diaphragm in hypoxia (Lewis et al., 2015a), which was not examined in our study.

The method of euthanasia used is another point worth mentioning. Using a rising concentration of CO_2 for euthanasia allowed us to euthanise the animals without re-exposure to a normoxic environment before being euthanised. The concern with this method is that CO_2 can alter gene expression, amongst many other things. However, in this time frame we do not feel that CO_2 would have had any significant effect on our data.

We must also acknowledge certain limitations in extrapolating conclusions from these data. In terms of the fatigue data, as mentioned in chapter 1, it must be noted that what could be perceived as an increased fatigue resistance following hypoxia may well be a bottoming out effect, whereby the hypoxic muscle is already weaker at the beginning of the fatigue protocol and power output at 33% load merely does not fall off to the same extent as does the more powerful normoxic muscle. While we observed some evidence of increased atrophic signalling, we did not see any change in proteasome activity between groups in the diaphragm. We thus cannot say whether or not muscle fibre CSA is being reduced due to muscle atrophy occurring in this model at this time point.

6.3 Future Directions and Studies

The putative contribution of atrophy, if it is occurring in the diaphragm following 8 hours of hypoxia, is something that needs to be determined. We plan on employing immunohistochemical staining of muscle samples taken from diaphragm and sternohyoid muscles from control and hypoxic animals in order to measure fibre CSA in these muscles and determine if muscle fibre atrophy is occurring, which would be consistent with muscle weakness.

The next step in determining how relevant the *ex vivo* diaphragm weakness observed in this study might be to a clinical setting is to determine whether or not this acute

hypoxia induced diaphragm dysfunction also presents *in vivo*. Our group has plans to study this measuring transdiaphragmatic pressure in the anaesthetised mouse and rat following 8 hours of hypoxia and normoxia. Transdiaphragmatic pressure during normal respiration and more importantly during airway obstruction and phrenic nerve stimulation, which elicit maximum transdiaphragmatic pressure changes *in vivo* would provide important information on the effects of acute hypoxia on diaphragm function *in vivo*. This could also be examined in hypoxic rodents pre-treated with NAC.

It would be most interesting to examine *ex vivo* muscle function in EDL and soleus muscle in this model to determine whether muscle weakness induced by acute hypoxia is respiratory muscle specific or whether it elicits a global skeletal muscle phenomenon.

It would also be of interest to determine if acute hypoxia induced diaphragm dysfunction would persist following re-exposure to normoxia following 8 hours of hypoxia. If acute hypoxia induced diaphragmatic dysfunction is perennial, it would have further still implications for patients with acute respiratory diseases.

6.4 Conclusions and Clinical Implications

Acute hypoxia causes diaphragm muscle weakness. Acute hypoxia-induced diaphragm dysfunction (acute HIDD), is prevented by antioxidant pre-treatment immediately prior to hypoxic exposure. As NAC is administered immediately prior to the beginning of the protocol, via a single I.P. injection, as opposed to being given for a number of days prior to hypoxic exposure, its effectiveness in preventing acute HIDD bodes well for an ICU or critical care setting, where a hypoxaemic acute respiratory patient could be given NAC immediately via I.V. infusion/injection upon admission to an ICU. It implies that it is not necessary to preempt hypoxia induced diaphragm dysfunction, widening its utility in the clinical context. NAC is already approved for clinical use for other conditions (discussed in chapter 1) and can be bought as a dietary supplement. It would therefore seem that it would be relatively

simple to implement as an adjunct therapy for hypoxaemic patients with acute respiratory diseases, in comparison to developing a new drug or therapeutic agent from bench to bedside that does not have any prior clinical use. It is, however, important to note that while NAC was beneficial in this model, hypoxaemic patients with acute respiratory diseases often have a whole host of added complications other than solely being hypoxaemic, which may culminate in NAC being less effective in rescuing diaphragm performance. These findings highlight a potentially critical role for hypoxia in the diaphragm muscle dysfunction observed in patients with acute respiratory diseases. NAC may be a beneficial adjunct therapy in these patients.

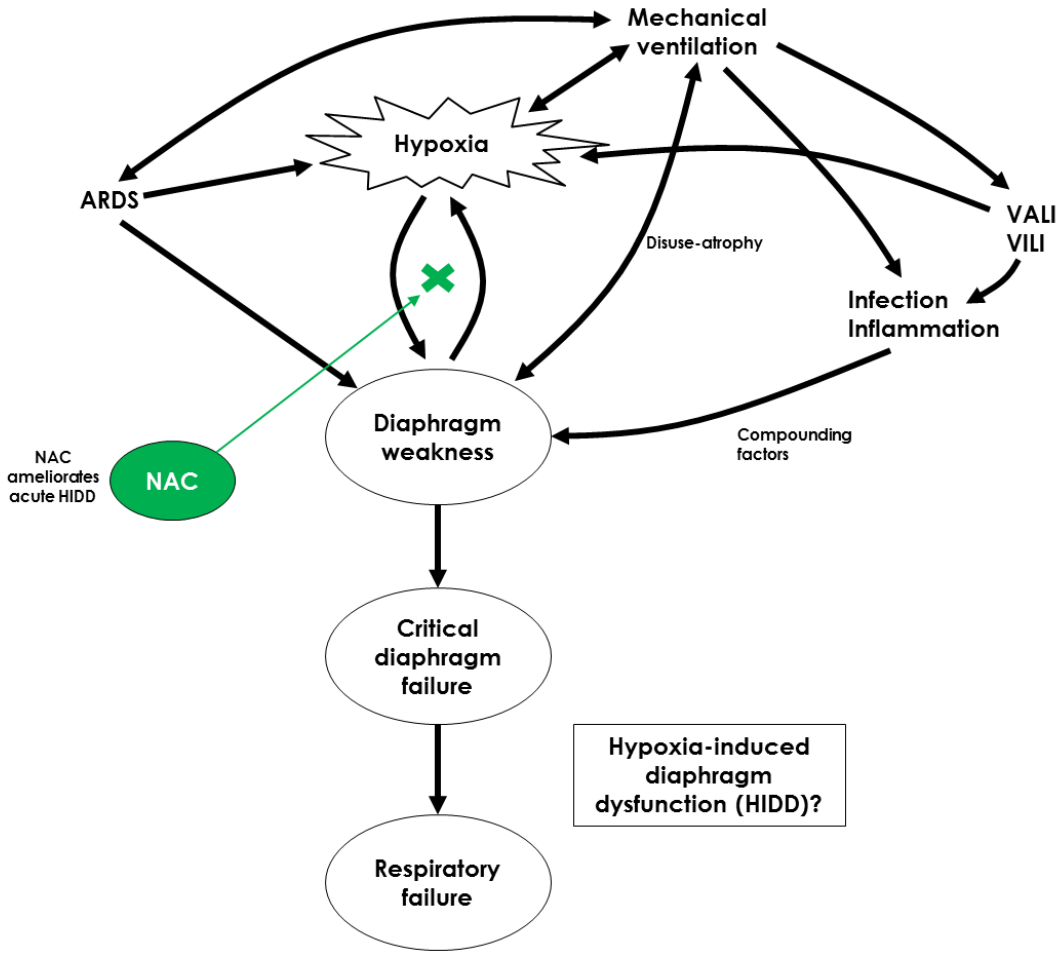

Figure 2: Clinical Relevance. Schematic depicting how acute hypoxia induced diaphragm dysfunction (acute HIDD) may be clinically relevant in acute respiratory conditions, and how NAC may be useful, as an adjunct therapy, in alleviating acute HIDD in respiratory patients.

References

Accili, D., Arden, K.C., 2004. FoxOs at the crossroads of cellular metabolism, differentiation, and transformation. Cell. doi:10.1016/S0092-8674(04)00452-0

Agten, A., Maes, K., Smuder, A., Powers, S.K., Decramer, M., Gayan-Ramirez, G., 2011. N-Acetylcysteine protects the rat diaphragm from the decreased contractility associated with controlled mechanical ventilation. Crit. Care Med. 39, 777–782. doi:10.1097/CCM.0b013e318206cca9

Aguer, C., Fiehn, O., Seifert, E.L., Bézaire, V., Meissen, J.K., Daniels, A., Scott, K., Renaud, J.-M., Padilla, M., Bickel, D.R., Dysart, M., Adams, S.H., Harper, M.-E., 2013. Muscle uncoupling protein 3 overexpression mimics endurance training and reduces circulating biomarkers of incomplete β-oxidation. FASEB J. 27, 4213–25. doi:10.1096/fj.13-234302

Altun, M., Zhao, B., Velasco, K., Liu, H., Hassink, G., Paschke, J., Pereira, T., Lindsten, K., 2012. Ubiquitin-specific protease 19 (USP19) regulates hypoxia-inducible factor 1α (HIF-1α) during hypoxia. J. Biol. Chem. 287, 1962–9. doi:10.1074/jbc.M111.305615

Alvarez-Tejado, M., Naranjo-Suarez, S., Jiménez, C., Carrera, A.C.C., Landázuri, M.O.O., del Peso, L., Naranjo-Suárez, S., Jiménez, C., Carrera, A.C.C., Landázuri, M.O.O., del Peso, L., 2001. Hypoxia induces the activation of the phosphatidylinositol 3-kinase/Akt cell survival pathway in PC12 cells: protective role in apoptosis. J. Biol. Chem. 276, 22368–22374. doi:10.1074/jbc.M011688200

Andrade, F.H., Reid, M.B., Allen, D.G., Westerblad, H., 1998. Effect of hydrogen peroxide and dithiothreitol on contractile function of single skeletal muscle fibres from the mouse. J. Physiol. 509 (Pt 2, 565–75.

Ash, W.H., 1956. Anoxia-Hypoxia - Clinical Considerations. Anesth. Analg. 35, 206–217.

Ayappa, I., Rapoport, D.M., 2003. The upper airway in sleep: physiology of the pharynx. Sleep Med. Rev. 7, 9–33. doi:10.1053/smrv.2002.0238

Azuelos, I., Jung, B., Picard, M., Liang, F., Li, T., Lemaire, C., Giordano, C., Hussain, S., Petrof, B.J., 2015. Relationship between Autophagy and Ventilator-induced Diaphragmatic Dysfunction. Anesthesiology 122, 1349–61. doi:10.1097/ALN.0000000000000656

Baar, K., Esser, K., 1999. Phosphorylation of p70(S6k) correlates with increased skeletal muscle mass following resistance exercise. Am. J. Physiol. 276, C120–C127.

Barbieri, E., Sestili, P., 2012. Reactive Oxygen Species in Skeletal Muscle Signaling. J. Signal Transduct. doi:10.1155/2012/982794

Barreiro, E., de la Puente, B., Minguella, J., Corominas, J.M., Serrano, S., Hussain, S.N. a, Gea, J., 2005. Oxidative stress and respiratory muscle dysfunction in severe chronic obstructive pulmonary disease. Am. J. Respir. Crit. Care Med. 171, 1116–24. doi:10.1164/rccm.200407-887OC

Bassel-Duby, R., Olson, E.N., 2006. Signaling pathways in skeletal muscle remodeling. Annu. Rev. Biochem. 75, 19–37. doi:10.1146/annurev.biochem.75.103004.142622

Batt, J., dos Santos, C.C., Cameron, J.I., Herridge, M.S., 2013. Intensive care unit-acquired weakness: clinical phenotypes and molecular mechanisms. Am. J. Respir. Crit. Care Med. 187, 238–46. doi:10.1164/rccm.201205-0954SO

Bavis, R.W., Powell, F.L., Bradford, A., Hsia, C.C.W., Peltonen, J.E., Soliz, J., Zeis, B., Fergusson, E.K., Fu, Z., Gassmann, M., Kim, C.B., Maurer, J., McGuire, M., Miller, B.M., O'Halloran, K.D., Paul, R.J., Reid, S.G., Rusko, H.K., Tikkanen,

H.O., Wilkinson, K. a, 2007. Respiratory plasticity in response to changes in oxygen supply and demand. Integr. Comp. Biol. 47, 532–551. doi:10.1093/icb/icm070

Beard, N.A., Laver, D.R., Dulhunty, A.F., 2004. Calsequestrin and the calcium release channel of skeletal and cardiac muscle. Prog. Biophys. Mol. Biol. doi:10.1016/j.pbiomolbio.2003.07.001

Bedogni, B., Welford, S.M., Cassarino, D.S., Nickoloff, B.J., Giaccia, A.J., Powell, M.B., 2005. The hypoxic microenvironment of the skin contributes to Akt-mediated melanocyte transformation. Cancer Cell 8, 443–454. doi:10.1016/j.ccr.2005.11.005

Beitner-Johnson, D., Rust, R.T., Hsieh, T.C., Millhorn, D.E., 2001. Hypoxia activates Akt and induces phosphorylation of GSK-3 in PC12 cells. Cell. Signal. 13, 23–27. doi:10.1016/S0898-6568(00)00128-5

Berdichevsky, A., Guarente, L., Bose, A., 2010. Acute oxidative stress can reverse insulin resistance by inactivation of cytoplasmic JNK. J. Biol. Chem. 285, 21581–21589. doi:10.1074/jbc.M109.093633

Bernard, G.R., 2005. Acute respiratory distress syndrome: a historical perspective. Am. J. Respir. Crit. Care Med. 172, 798–806. doi:10.1164/rccm.200504-663OE

Bigard, A.-X., Brunet, A., Serrurier, B., Guezennec, C.-Y., Monod, H., 1992. Effects of endurance training at high altitude on diaphragm muscle properties. Pflugers Arch. Eur. J. Physiol. 422, 239–244. doi:10.1007/BF00376208

Bigard, A.X., Sanchez, H., Birot, O., Serrurier, B., 2000. Myosin heavy chain composition of skeletal muscles in young rats growing under hypobaric hypoxia conditions. J. Appl. Physiol. 88, 479–486.

Biswas, M., Chan, J.Y., 2010. Role of Nrf1 in antioxidant response element-mediated gene expression and beyond. Toxicol. Appl. Pharmacol. 244, 16–20.

doi:10.1016/j.taap.2009.07.034

Bodine, S.C., Stitt, T.N., Gonzalez, M., Kline, W.O., Stover, G.L., Bauerlein, R., Zlotchenko, E., Scrimgeour, A., Lawrence, J.C., Glass, D.J., Yancopoulos, G.D., 2001. Akt/mTOR pathway is a crucial regulator of skeletal muscle hypertrophy and can prevent muscle atrophy in vivo. Nat. Cell Biol. 3, 1014–1019. doi:10.1038/ncb1101-1014

Bodrova, M.E., Dedukhova, V.I., Mokhova, E.N., Skulachev, V.P., 1998. Membrane potential generation coupled to oxidation of external NADH in liver mitochondria. FEBS Lett. 435, 269–274. doi:10.1016/S0014-5793(98)01072-2

Boles, J.-M., Bion, J., Connors, A., Herridge, M., Marsh, B., Melot, C., Pearl, R., Silverman, H., Stanchina, M., Vieillard-Baron, A., Welte, T., 2007. Weaning from mechanical ventilation. Eur. Respir. J. 29, 1033–56. doi:10.1183/09031936.00010206

Bonello, S., Zähringer, C., BelAiba, R.S., Djordjevic, T., Hess, J., Michiels, C., Kietzmann, T., Görlach, A., 2007. Reactive oxygen species activate the HIF-1alpha promoter via a functional NFkappaB site. Arterioscler. Thromb. Vasc. Biol. 27, 755–61. doi:10.1161/01.ATV.0000258979.92828.bc

Bradford, A., McGuire, M., O'Halloran, K.D., 2005. Does episodic hypoxia affect upper airway dilator muscle function? Implications for the pathophysiology of obstructive sleep apnoea. Respir. Physiol. Neurobiol. 147, 223–34. doi:10.1016/j.resp.2005.04.001

Brochard, L., Harf, A., Lorino, H., Lemaire, F., 1989. Inspiratory Pressure Support Prevents Diaphragmatic Fatigue during Weaning from Mechanical Ventilation. Am Rev Respir Dis 139, 513–521. doi:10.1164/ajrccm/139.2.513

Bruells, C.S., Maes, K., Rossaint, R., Thomas, D., Cielen, N., Bleilevens, C., Bergs, I., Loetscher, U., Dreier, A., Gayan-Ramirez, G., Behnke, B.J., Weis, J., 2013. Prolonged mechanical ventilation alters the expression pattern of angio-

neogenetic factors in a pre-clinical rat model. PLoS One 8, e70524. doi:10.1371/journal.pone.0070524

Callahan, L.A., Song, X.-H., Wang, L., Supinski, G., 2015. Prolonged Diaphragm Weakness in Acute Lung Injury UL1TR000117, HL112085, HL113494. FASEB J 29, 947.3-.

Callahan, L.A., Supinski, G.S., 2013. Prevention and treatment of ICU-acquired weakness: is there a stimulating answer? Crit. Care Med. 41, 2457–8. doi:10.1097/CCM.0b013e31829824da

Campos, R., Shimizu, M.H.M., Volpini, R.A., de Bragança, A.C., Andrade, L., Lopes, F.D.T.Q.D.S., Olivo, C., Canale, D., Seguro, A.C., 2012. N-acetylcysteine prevents pulmonary edema and acute kidney injury in rats with sepsis submitted to mechanical ventilation. Am. J. Physiol. Lung Cell. Mol. Physiol. 302, L640-50. doi:10.1152/ajplung.00097.2011

Carberry, J.C., McMorrow, C., Bradford, A., Jones, J.F.X., O'Halloran, K.D., 2014a. Effects of sustained hypoxia on sternohyoid and diaphragm muscle during development. Eur. Respir. J. 43, 1149–58. doi:10.1183/09031936.00139512

Carberry, J.C., McMorrow, C., Bradford, A., Jones, J.F.X., O'Halloran, K.D., 2014b. Effects of sustained hypoxia on sternohyoid and diaphragm muscle during development. Eur. Respir. J. 43, 1149–58. doi:10.1183/09031936.00139512

Carbia-Nagashima, A., Gerez, J., Perez-Castro, C., Paez-Pereda, M., Silberstein, S., Stalla, G.K., Holsboer, F., Arzt, E., 2007. RSUME, a Small RWD-Containing Protein, Enhances SUMO Conjugation and Stabilizes HIF-1α during Hypoxia. Cell 131, 309–323. doi:10.1016/j.cell.2007.07.044

Cazzola, M., Calzetta, L., Page, C., Jardim, J., Chuchalin, A.G., Rogliani, P., Matera, M.G., 2015. Influence of N-acetylcysteine on chronic bronchitis or COPD exacerbations: A meta-analysis. Eur. Respir. Rev. doi:10.1183/16000617.00002215

Chapman, K.R., D'Urzo, A.D., Druck, M.N., Rebuck, A.S., 1989. Cardiovascular response to acute airway obstruction and hypoxia. Am. Rev. Respir. Dis. 140, 1222–1227. doi:10.1164/ajrccm/140.5.1222

Chaudhary, P., Suryakumar, G., Prasad, R., Singh, S.N., Ali, S., Ilavazhagan, G., 2012. Chronic hypobaric hypoxia mediated skeletal muscle atrophy: role of ubiquitin-proteasome pathway and calpains. Mol. Cell. Biochem. 364, 101–13. doi:10.1007/s11010-011-1210-x

Chen, C., Guan, X., Quinn, D.A., Ouyang, B., 2015. N-Acetylcysteine Inhibits Ventilation-Induced Collagen Accumulation in the Rat Lung. Tohoku J. Exp. Med. 236, 255–261. doi:10.1620/tjem.236.255

Chen, Z., Li, Y., Zhang, H., Huang, P., Luthra, R., 2010. Hypoxia-regulated microRNA-210 modulates mitochondrial function and decreases ISCU and COX10 expression. Oncogene 29, 4362–4368. doi:10.1038/onc.2010.193

Chi, J.-T., Wang, Z., Nuyten, D.S. a, Rodriguez, E.H., Schaner, M.E., Salim, A., Wang, Y., Kristensen, G.B., Helland, A., Børresen-Dale, A.-L., Giaccia, A., Longaker, M.T., Hastie, T., Yang, G.P., van de Vijver, M.J., Brown, P.O., 2006. Gene expression programs in response to hypoxia: cell type specificity and prognostic significance in human cancers. PLoS Med. 3, e47. doi:10.1371/journal.pmed.0030047

Chiumello, D., Pristine, G., Slutsky, A.S., 1999. Mechanical ventilation affects local and systemic cytokines in an animal model of acute respiratory distress syndrome. Am. J. Respir. Crit. Care Med. 160, 109–16. doi:10.1164/ajrccm.160.1.9803046

Chung, S.Y., Huang, W.C., Su, C.W., Lee, K.W., Chi, H.C., Lin, C.T., Chen, S.-T., Huang, K.M., Tsai, M.S., Yu, H.P., Chen, S.L., 2013. FoxO6 and PGC-1α form a regulatory loop in myogenic cells. Biosci. Rep. 33, e00045. doi:10.1042/BSR20130031

Cohen, S., Brault, J.J., Gygi, S.P., Glass, D.J., Valenzuela, D.M., Gartner, C., Latres, E., Goldberg, A.L., 2009. During muscle atrophy, thick, but not thin, filament components are degraded by MuRF1-dependent ubiquitylation. J. Cell Biol. 185, 1083–1095. doi:10.1083/jcb.200901052

Cohen, S., Lee, D., Zhai, B., Gygi, S.P., Goldberg, A.L., 2014. Trim32 reduces PI3K-Akt-FoxO signaling in muscle atrophy by promoting plakoglobin-PI3K dissociation. J. Cell Biol. 204, 747–758. doi:10.1083/jcb.201304167

Cohen, S., Zhai, B., Gygi, S.P., Goldberg, A.L., 2012. Ubiquitylation by Trim32 causes coupled loss of desmin, Z-bands, and thin filaments in muscle atrophy. J. Cell Biol. 198, 575–589. doi:10.1083/jcb.201110067

Conrad, C., Lymp, J., Thompson, V., Dunn, C., Davies, Z., Chatfield, B., Nichols, D., Clancy, J., Vender, R., Egan, M.E., Quittell, L., Michelson, P., Antony, V., Spahr, J., Rubenstein, R.C., Moss, R.B., Herzenberg, L.A., Goss, C.H., Tirouvanziam, R., 2015. Long-term treatment with oral N-acetylcysteine: Affects lung function but not sputum inflammation in cystic fibrosis subjects. A phase II randomized placebo-controlled trial. J. Cyst. Fibros. 14, 219–227. doi:10.1016/j.jcf.2014.08.008

Cook, T.M., Macdougall-Davis, S.R., 2012. Complications and failure of airway management. Br. J. Anaesth. 109, i68–i85. doi:10.1093/bja/aes393

Cortopassi, G., Danielson, S., Alemi, M., Zhan, S.S., Tong, W., Carelli, V., Martinuzzi, A., Marzuki, S., Majamaa, K., Wong, A., 2006. Mitochondrial disease activates transcripts of the unfolded protein response and cell cycle and inhibits vesicular secretion and oligodendrocyte-specific transcripts. Mitochondrion 6, 161–175. doi:10.1016/j.mito.2006.05.002

Cummins, E.P., Oliver, K.M., Lenihan, C.R., Fitzpatrick, S.F., Bruning, U., Scholz, C.C., Slattery, C., Leonard, M.O., McLoughlin, P., Taylor, C.T., 2010. NF-κB links CO2 sensing to innate immunity and inflammation in mammalian cells. J.

Immunol. 185, 4439–45. doi:10.4049/jimmunol.1000701

Cummins, E.P., Taylor, C.T., 2005. Hypoxia-responsive transcription factors. Pflugers Arch. 450, 363–71. doi:10.1007/s00424-005-1413-7

D'Hulst, G., Jamart, C., Van Thienen, R., Hespel, P., Francaux, M., Deldicque, L., 2013. Effect of acute environmental hypoxia on protein metabolism in human skeletal muscle. Acta Physiol. (Oxf). 208, 251–64.

Dai, T., Zheng, H., Fu, G., 2008. Hypoxia confers protection against apoptosis via the PI3K/Akt pathway in endothelial progenitor cells. Acta Pharmacol. Sin. 29, 1425–31. doi:10.1111/j.1745-7254.2008.00904.x

Day, B.J., 2008. Antioxidants as potential therapeutics for lung fibrosis. Antioxid. Redox Signal. 10, 355–70. doi:10.1089/ars.2007.1916

Deldicque, L., Francaux, M., 2013. Acute vs chronic hypoxia: what are the consequences for skeletal muscle mass? Cell. Mol. Exerc. Physiol. doi:10.7457/cmep.v2i1.

Deveci, D., Marshall, J.M., Egginton, S., 2002. Chronic hypoxia induces prolonged angiogenesis in skeletal muscles of rat. Exp. Physiol. 87, 287–91.

Diaz-Abad, M., Verceles, A.C., Brown, J.E., Scharf, S.M., 2011. Sleep Disordered Breathing May Be Under-Recognized in Patients Who Wean From Prolonged Mechanical Ventilation. Respir. Care. doi:10.4187/respcare.01260

Dutta, A., Ray, K., Singh, V.K., Vats, P., Singh, S.N., Singh, S.B., 2008. L-carnitine supplementation attenuates intermittent hypoxia-induced oxidative stress and delays muscle fatigue in rats. Exp. Physiol. 93, 1139–1146. doi:10.1113/expphysiol.2008.042465

El-Khoury, R., Bradford, a, O'Halloran, K.D., 2012. Chronic hypobaric hypoxia increases isolated rat fast-twitch and slow-twitch limb muscle force and fatigue.

Physiol. Res. 61, 195–201.

El-Khoury, R., O'Halloran, K.D., Bradford, a, 2003. Effects of chronic hypobaric hypoxia on contractile properties of rat sternohyoid and diaphragm muscles. Clin. Exp. Pharmacol. Physiol. 30, 551–4.

Eskandar, N., Apostolakos, M.J., 2007. Weaning from Mechanical Ventilation. Crit. Care Clin. doi:10.1016/j.ccc.2006.12.002

Faucher, M., Guillot, C., Marqueste, T., Kipson, N., Mayet-Sornay, M.-H., Desplanches, D., Jammes, Y., Badier, M., 2005. Matched adaptations of electrophysiological, physiological, and histological properties of skeletal muscles in response to chronic hypoxia. Pflugers Arch. 450, 45–52. doi:10.1007/s00424-004-1370-6

Favier, F.B., Costes, F., Defour, A., Bonnefoy, R., Lefai, E., Baugé, S., Peinnequin, A., Benoit, H., Freyssenet, D., 2010. Downregulation of Akt/mammalian target of rapamycin pathway in skeletal muscle is associated with increased REDD1 expression in response to chronic hypoxia. Am. J. Physiol. Regul. Integr. Comp. Physiol. 298, R1659–R1666. doi:10.1152/ajpregu.00550.2009

Fey, D., Croucher, D.R., Kolch, W., Kholodenko, B.N., 2012. Crosstalk and signalling switches in mitogen-activated protein kinase cascades. Front. Physiol. 3. doi:10.3389/fphys.2012.00355

Finck, B.N., Kelly, D.P., 2006. PGC-1 coactivators: Inducible regulators of energy metabolism in health and disease. J. Clin. Invest. doi:10.1172/JCI27794

Fink, M.P., 2002. Bench-to-bedside review: Cytopathic hypoxia. Crit. Care 6, 491–9. doi:10.1016/S0749-0704(05)70161-5

Fink, M.P., 2001. Cytopathic hypoxia. Mitochondrial dysfunction as mechanism contributing to organ dysfunction in sepsis. Crit. Care Clin. 17, 219–237. doi:11219231

Fink, M.P., 2001. Cytopathic hypoxia in sepsis: a true problem? Minerva Anestesiol. 67, 290–291. doi:10.1097/PCC.0000000000000299

Fliegel, L., Ohnishi, M., Carpenter, M.R., Khanna, V.K., Reithmeier, R. a, MacLennan, D.H., 1987. Amino acid sequence of rabbit fast-twitch skeletal muscle calsequestrin deduced from cDNA and peptide sequencing. Proc. Natl. Acad. Sci. U. S. A. 84, 1167–71.

Flück, M., Hoppeler, H., 2003. Molecular basis of skeletal muscle plasticity--from gene to form and function. Rev. Physiol. Biochem. Pharmacol. 146, 159–216. doi:10.1007/s10254-002-0004-7

Frappell, P., Lanthier, C., Baudinette, R. V., Mortola, J.P., 1992. Metabolism and ventilation in acute hypoxia: a comparative analysis in small mammalian species. Am J Physiol Regul. Integr. Comp Physiol 262, R1040-1046.

Fuller, B.M., Mohr, N.M., Hotchkiss, R.S., Kollef, M.H., 2014. Reducing the burden of acute respiratory distress syndrome: the case for early intervention and the potential role of the emergency department. Shock 41, 378–87. doi:10.1097/SHK.0000000000000142

Gajic, O., Dara, S.I., Mendez, J.L., Adesanya, A.O., Festic, E., Caples, S.M., Rana, R., St Sauver, J.L., Lymp, J.F., Afessa, B., Hubmayr, R.D., 2004. Ventilator-associated lung injury in patients without acute lung injury at the onset of mechanical ventilation. Crit. Care Med. 32, 1817–24.

Gamboa, J.L., Andrade, F.H., 2012. Muscle endurance and mitochondrial function after chronic normobaric hypoxia: contrast of respiratory and limb muscles. Pflugers Arch. 463, 327–38. doi:10.1007/s00424-011-1057-8

Gamboa, J.L., Andrade, F.H., 2010. Mitochondrial content and distribution changes specific to mouse diaphragm after chronic normobaric hypoxia. Am. J. Physiol. Regul. Integr. Comp. Physiol. 298, R575-83. doi:10.1152/ajpregu.00320.2009

Giacomo, C., Latteri, F., Fichera, C., Sorrenti, V., Campisi, A., Castorina, C., Russo, A., Pinturo, R., Vanella, A., 1993. Effect of acetyl-l-carnitine on lipid peroxidation and xanthine oxidase activity in rat skeletal muscle. Neurochem. Res. 18, 1157–1162. doi:10.1007/BF00978367

Gilbert, D.L., 1983. The first documented report of mountain sickness: the China or Headache Mountain story. Respir. Physiol. 52, 315–26.

Giordano, C., Lemaire, C., Li, T., Kimoff, R.J., Petrof, B.J., 2015. Autophagy-associated atrophy and metabolic remodeling of the mouse diaphragm after short-term intermittent hypoxia. PLoS One 10, e0131068. doi:10.1371/journal.pone.0131068

Glass, D.J., 2010. PI3 kinase regulation of skeletal muscle hypertrophy and atrophy. Curr Top Microbiol Immunol 346, 267–278. doi:10.1007/82_2010_78

Glass, D.J., 2005. Skeletal muscle hypertrophy and atrophy signaling pathways. Int. J. Biochem. Cell Biol. 37, 1974–84. doi:10.1016/j.biocel.2005.04.018

Glass, D.J., 2003. Signalling pathways that mediate skeletal muscle hypertrophy and atrophy. Nat. Cell Biol. 5, 87–90. doi:10.1038/ncb0203-87

Godoy, D.A., Vaz de Mello, L., Masotti, L., Di Napoli, M., 2015. Intensive Care Unit Acquired Weakness (ICU-AW): a brief and practical review. Rev. Heal. Care 6, 9. doi:10.7175/rhc.v6i1.1037

Goldman, M.D., Grassino, A., Mead, J., Sears, T.A., 1978. Mechanics of the human diaphragm during voluntary contraction: dynamics. J Appl Physiol 44, 840–848.

Gong, M.N., Bajwa E.K., Thompson B.T., Christiani D.C., 2010. Body mass index is associated with the development of acute respiratory distress syndrome. 65(1):44-50. doi: 10.1136/thx.

Gordeuk, V.R., Sergueeva, A.I., Miasnikova, G.Y., Okhotin, D., Voloshin, Y., Choyke, P.L., Butman, J.A., Jedlickova, K., Prchal, J.T., Polyakova, L.A., 2004. Congenital disorder of oxygen sensing: association of the homozygous Chuvash polycythemia VHL mutation with thrombosis and vascular abnormalities but not tumors. Blood 103, 3924–32. doi:10.1182/blood-2003-07-2535

Gorman, R.B., McKenzie, D.K., Pride, N.B., Tolman, J.F., Gandevia, S.C., 2002. Diaphragm Length during Tidal Breathing in Patients with Chronic Obstructive Pulmonary Disease. Am. J. Respir. Crit. Care Med. 166, 1461–1469. doi:10.1164/rccm.200111-087OC

Gosker, H.R., Wouters, E.F., van der Vusse, G.J., Schols, a M., 2000. Skeletal muscle dysfunction in chronic obstructive pulmonary disease and chronic heart failure: underlying mechanisms and therapy perspectives. Am. J. Clin. Nutr. 71, 1033–47.

Goyal, M., Houseman, D., Johnson, N.J., Christie, J., Mikkelsen, M.E., Gaieski, D.F., 2012. Prevalence of acute lung injury among medical patients in the emergency department. Acad. Emerg. Med. 19, E1011-8. doi:10.1111/j.1553-2712.2012.01429.x

Gran, P., Larsen, A.E., Bonham, M., Dordevic, A.L., Rupasinghe, T., Silva, C., Nahid, A., Tull, D., Sinclair, A.J., Mitchell, C.J., Cameron-Smith, D., 2014. Muscle p70S6K phosphorylation in response to Soy and dairy rich meals in middle aged Men with metabolic syndrome: a randomised crossover trial. Nutr. Metab. (Lond). 11, 46. doi:10.1186/1743-7075-11-46

Grocott, M.P.W., Martin, D.S., Levett, D.Z.H., McMorrow, R., Windsor, J., Montgomery, H.E., Caudwell Xtreme Everest Research Group, 2009. Arterial blood gases and oxygen content in climbers on Mount Everest. N. Engl. J. Med. 360, 140–9. doi:10.1056/NEJMoa0801581

Gundersen, K., 2011. Excitation-transcription coupling in skeletal muscle: The molecular pathways of exercise. Biol. Rev. 86, 564–600. doi:10.1111/j.1469-

185X.2010.00161.x

Gutierrez, G., Reines, H.D., Wulf-Gutierrez, M.E., 2004. Clinical review: hemorrhagic shock. Crit. Care 8, 373–81. doi:10.1186/cc2851

Gutsaeva, D.R., Carraway, M.S., Suliman, H.B., Demchenko, I.T., Shitara, H., Yonekawa, H., Piantadosi, C.A., 2008. Transient hypoxia stimulates mitochondrial biogenesis in brain subcortex by a neuronal nitric oxide synthase-dependent mechanism. J. Neurosci. 28, 2015–2024. doi:10.1523/JNEUROSCI.5654-07.2008

Hamacher-Brady, A., Brady, N.R., 2016. Mitophagy programs: Mechanisms and physiological implications of mitochondrial targeting by autophagy. Cell. Mol. Life Sci. doi:10.1007/s00018-015-2087-8

Haouzi, P., Bell, H.J., Notet, V., Bihain, B., 2009. Comparison of the metabolic and ventilatory response to hypoxia and H2S in unsedated mice and rats. Respir. Physiol. Neurobiol. 167, 316–322. doi:10.1016/j.resp.2009.06.006

Hellsten, Y., Frandsen, U., Orthenblad, N., Sjodin, B., Richter, E.A., 1997. Xanthine oxidase in human skeletal muscle following eccentric exercise: a role in inflammation. J. Physiol. 498, 239–248.

Heunks, L., 1999. Xanthine oxidase is involved in exercise-induced oxidative stress in chronic obstructive pulmonary disease. Am. J. ….

Heunks, L.M., Dekhuijzen, P.N., 2000. Respiratory muscle function and free radicals: from cell to COPD. Thorax 55, 704–716. doi:10.1136/thorax.55.8.704

Hibbert, K., Rice, M., Malhotra, A., 2012. Obesity and ARDS. Chest 142, 785–790. doi:10.1378/chest.12-0117

Hill, C.A., Thompson, M.W., Ruell, P.A., Thom, J.M., White, M.J., 2001. Sarcoplasmic reticulum function and muscle contractile character following

fatiguing exercise in humans. J. Physiol. 531, 871–8. doi:10.1111/j.1469-7793.2001.0871h.x

Hooijman, P.E., Beishuizen, A., Witt, C.C., de Waard, M.C., Girbes, A.R.J., Spoelstra-de Man, A.M.E., Niessen, H.W.M., Manders, E., van Hees, H.W.H., van den Brom, C.E., Silderhuis, V., Lawlor, M.W., Labeit, S., Stienen, G.J.M., Hartemink, K.J., Paul, M.A., Heunks, L.M.A., Ottenheijm, C.A.C., 2015. Diaphragm muscle fiber weakness and ubiquitin-proteasome activation in critically ill patients. Am. J. Respir. Crit. Care Med. 191, 1126–38. doi:10.1164/rccm.201412-2214OC

Hoppeler, H., Baum, O., Lurman, G., Mueller, M., 2011. Molecular mechanisms of muscle plasticity with exercise. Compr. Physiol. 1, 1383–1412. doi:10.1002/cphy.c100042

Hoppeler, H., Fluck, M., 2003. Plasticity of skeletal muscle mitochondria: structure and function. Med. Sci. Sports Exerc. 35, 95–104. doi:10.1249/01.MSS.0000043292.99104.12

Hoppeler, H., Vogt, M., Weibel, E.R., Flück, M., 2003. Special Review Series – Biogenesis and Physiological Adaptation of Mitochondria Response of skeletal muscle mitochondria to hypoxia Experimental Physiology : Exp. Physiol. 88, 109–119. doi:10.1113/eph8802513

Horowitz, J.F., Leone, T.C., Feng, W., Kelly, D.P., Klein, S., 2000. Effect of endurance training on lipid metabolism in women: a potential role for PPARalpha in the metabolic response to training. Am. J. Physiol. Endocrinol. Metab. 279, E348-55.

Hu, C., Wang, L., Chodosh, L.A., Keith, B., Simon, M.C., 2003. Differential Roles of Hypoxia-Inducible Factor 1 alpha (HIF-1 alpha) and HIF-2 alpha in Hypoxic Gene Regulation. Mol Cell Biol 23, 9361–9374. doi:10.1128/MCB.23.24.9361

Hunter, R.B., Kandarian, S.C., 2004. Disruption of either the Nfkb1 or the Bcl3 gene

inhibits skeletal muscle atrophy. J. Clin. Invest. 114, 1504–1511. doi:10.1172/JCI200421696

Jaber, S., Jung, B., Matecki, S., Petrof, B.J., 2011a. Clinical review: Ventilator-induced diaphragmatic dysfunction - human studies confirm animal model findings! Crit. Care 15, 206. doi:10.1186/cc10023

Jaber, S., Petrof, B.J., Jung, B., Chanques, G., Berthet, J.-P., Rabuel, C., Bouyabrine, H., Courouble, P., Koechlin-Ramonatxo, C., Sebbane, M., Similowski, T., Scheuermann, V., Mebazaa, A., Capdevila, X., Mornet, D., Mercier, J., Lacampagne, A., Philips, A., Matecki, S., 2011b. Rapidly progressive diaphragmatic weakness and injury during mechanical ventilation in humans. Am. J. Respir. Crit. Care Med. 183, 364–71. doi:10.1164/rccm.201004-0670OC

Jackman, R.W., Kandarian, S.C., 2004. The molecular basis of skeletal muscle atrophy. Am. J. Physiol. Cell Physiol. 287, C834-43. doi:10.1152/ajpcell.00579.2003

Ji, M., Katagiri, M., Jagers, J., Easton, P., 2014. Effect of sustained hypoxia on diaphragm length. Eur. Respir. J. 44, P1528-.

Jiang, N., Zhang, G., Bo, H., Qu, J., Ma, G., Cao, D., Wen, L., Liu, S., Ji, L.L., Zhang, Y., 2009. Upregulation of uncoupling protein-3 in skeletal muscle during exercise: a potential antioxidant function. Free Radic. Biol. Med. 46, 138–45. doi:10.1016/j.freeradbiomed.2008.09.026

Jin, W.S., Kong, Z.L., Shen, Z.F., Jin, Y.Z., Zhang, W.K., Chen, G.F., 2011. Regulation of hypoxia inducible factor-1alpha expression by the alteration of redox status in HepG2 cells. J Exp Clin Cancer Res 30, 61. doi:10.1186/1756-9966-30-61

Johnson, D.C., Johnson, K.G., 2012. Obstructive Sleep Apnea and Prolonged Mechanical Ventilation. Respir. Care 57, 326–327. doi:10.4187/respcare.01723

Johnson, E.R., Matthay, M.A., 2010. Acute lung injury: epidemiology, pathogenesis, and treatment. J. Aerosol Med. Pulm. Drug Deliv. 23, 243–52. doi:10.1089/jamp.2009.0775

Jubran, A., 2006. Critical Illness and Mechanical Ventilation: Effects on the Diaphragm. Respir Care 51, 1054–1064.

Jurynec, M.J., Xia, R., Mackrill, J.J., Gunther, D., Crawford, T., Flanigan, K.M., Abramson, J.J., Howard, M.T., Grunwald, D.J., 2008. Selenoprotein N is required for ryanodine receptor calcium release channel activity in human and zebrafish muscle. Proc. Natl. Acad. Sci. U. S. A. 105, 12485–90. doi:10.1073/pnas.0806015105

Jusman, S.W., Halim, A., Wanandi, S.I., Sadikin, M., 2010. Expression of hypoxia-inducible factor-1alpha (HIF-1alpha) related to oxidative stress in liver of rat-induced by systemic chronic normobaric hypoxia. Acta Med. Indones. 42, 17–23. doi:040579197 [pii]

Kacmarek, R.M., 2011. The mechanical ventilator: past, present, and future. Respir. Care 56, 1170–80. doi:10.4187/respcare.01420

Kallet, R.H., 2011. Patient-ventilator interaction during acute lung injury, and the role of spontaneous breathing: part 1: respiratory muscle function during critical illness. Respir. Care 56, 181–9. doi:10.4187/respcare.00964

Karnatovskaia, L. V, Lee, A.S., Bender, S.P., Talmor, D., Festic, E., US Critical Illness and Injury Trials Group: Lung Injury Prevention Study Investigators (USCIITG–LIPS), 2014. Obstructive sleep apnea, obesity, and the development of acute respiratory distress syndrome. J. Clin. Sleep Med. 10, 657–62. doi:10.5664/jcsm.3794

Kasaikina, M. V, Hatfield, D.L., Gladyshev, V.N., 2012. Understanding selenoprotein function and regulation through the use of rodent models. Biochim. Biophys. Acta 1823, 1633–42. doi:10.1016/j.bbamcr.2012.02.018

Ke, Q., Costa, M., 2006. Hypoxia-Inducible Factor-1 (HIF-1). Mol. Pharmacol. 70, 1469–1480. doi:10.1124/mol.106.027029.ABBREVIATIONS

Kelly, G.S., 1998. Clinical applications of N-acetylcysteine. Altern. Med. Rev. 3, 114–127.

Kerksick, C., Willoughby, D., 2005. The antioxidant role of glutathione and N-acetyl-cysteine supplements and exercise-induced oxidative stress. J. Int. Soc. Sports Nutr. 2, 38–44. doi:10.1186/1550-2783-2-2-38

Kilic-Eren, M., Boylu, T., Tabor, V., 2013. Targeting PI3K/Akt represses Hypoxia inducible factor-1α activation and sensitizes Rhabdomyosarcoma and Ewing's sarcoma cells for apoptosis. Cancer Cell Int. 13, 36. doi:10.1186/1475-2867-13-36

Kim, J.W., Tchernyshyov, I., Semenza, G.L., Dang, C. V, 2006. HIF-1-mediated expression of pyruvate dehydrogenase kinase: A metabolic switch required for cellular adaptation to hypoxia. Cell Metab. 3, 177–185. doi:10.1016/j.cmet.2006.02.002

Koenig, S.M., Truwit, J.D., 2006. Ventilator-associated pneumonia: diagnosis, treatment, and prevention. Clin. Microbiol. Rev. 19, 637–57. doi:10.1128/CMR.00051-05

Koritzinsky, M., Magagnin, M.G., van den Beucken, T., Seigneuric, R., Savelkouls, K., Dostie, J., Pyronnet, S., Kaufman, R.J., Weppler, S.A., Voncken, J.W., Lambin, P., Koumenis, C., Sonenberg, N., Wouters, B.G., 2006. Gene expression during acute and prolonged hypoxia is regulated by distinct mechanisms of translational control. EMBO J. 25, 1114–1125. doi:10.1038/sj.emboj.7600998

Krolikowski, J.G., Weihrauch, D., Bienengraeber, M., Kersten, J.R., Warltier, D.C., Pagel, P.S., 2006. Role of Erk1/2, p70s6K, and eNOS in isoflurane-induced

cardioprotection during early reperfusion in vivo. Can. J. Anesth. 53, 174–182. doi:10.1007/BF03021824

Kuchnicka, K., Maciejewski, D., 2013. Ventilator-associated lung injury. Anaesthesiol. Intensive Ther. 45, 164–70. doi:10.5603/AIT.2013.0034

Kulshreshtha, R., Davuluri, R. V, Calin, G.A., Ivan, M., 2008. A microRNA component of the hypoxic response. Cell Death Differ. 15, 667–671. doi:10.1038/sj.cdd.4402310

Laghi, F., Cattapan, S.E., Jubran, A., Parthasarathy, S., Warshawsky, P., Choi, Y.S.A., Tobin, M.J., 2003. Is weaning failure caused by low-frequency fatigue of the diaphragm? Am. J. Respir. Crit. Care Med. 167, 120–127. doi:10.1164/rccm.200210-1246OC

Land, S.C., Tee, A.R., 2007. Hypoxia-inducible factor 1α is regulated by the mammalian target of rapamycin (mTOR) via an mTOR signaling motif. J. Biol. Chem. 282, 20534–20543. doi:10.1074/jbc.M611782200

Le Moan, N., Houslay, D.M., Christian, F., Houslay, M.D., Akassoglou, K., 2011. Oxygen-dependent cleavage of the p75 neurotrophin receptor triggers stabilization of HIF-1α. Mol. Cell 44, 476–90. doi:10.1016/j.molcel.2011.08.033

Lecker, S.H., Jagoe, R.T., Gilbert, A., Gomes, M., Baracos, V., Bailey, J., Price, S.R., Mitch, W.E., Goldberg, A.L., 2004. Multiple types of skeletal muscle atrophy involve a common program of changes in gene expression. FASEB J. 18, 39–51. doi:10.1096/fj.03-0610com

Léger, B., Cartoni, R., Praz, M., Lamon, S., Dériaz, O., Crettenand, A., Gobelet, C., Rohmer, P., Konzelmann, M., Luthi, F., Russell, A.P., 2006. Akt signalling through GSK-3beta, mTOR and Foxo1 is involved in human skeletal muscle hypertrophy and atrophy. J. Physiol. 576, 923–33. doi:10.1113/jphysiol.2006.116715

Levett, D.Z., Radford, E.J., Menassa, D. a, Graber, E.F., Morash, A.J., Hoppeler, H., Clarke, K., Martin, D.S., Ferguson-Smith, A.C., Montgomery, H.E., Grocott, M.P.W., Murray, A.J., 2012. Acclimatization of skeletal muscle mitochondria to high-altitude hypoxia during an ascent of Everest. FASEB J. 26, 1431–41. doi:10.1096/fj.11-197772

Levine, S., Nguyen, T., Taylor, N., Friscia, M.E., Budak, M.T., Rothenberg, P., Zhu, J., Sachdeva, R., Sonnad, S., Kaiser, L.R., Rubinstein, N.A., Powers, S.K., Shrager, J.B., 2008. Rapid disuse atrophy of diaphragm fibers in mechanically ventilated humans. N. Engl. J. Med. 358, 1327–1335. doi:10.1097/SA.0b013e3181925bed

Levresse, V., Butterfield, L., Zentrich, E., Heasley, L.E., 2000. Akt negatively regulates the cJun N-terminal kinase pathway in PC12 cells. J.Neurosci.Res. 62, 799–808. doi:10.1002/1097-4547(20001215)62:6<799::AID-JNR6>3.0.CO;2-1

Lewis, P., McMorrow, C., Bradford, A., O'Halloran, K.D., 2015a. Improved tolerance of acute severe hypoxic stress in chronic hypoxic diaphragm is nitric oxide-dependent. J. Physiol. Sci. doi:10.1007/s12576-015-0381-8

Lewis, P., O'Halloran, K.D., 2016. Diaphragm Muscle Adaptation to Sustained Hypoxia: Lessons from Animal Models with Relevance to High Altitude and Chronic Respiratory Diseases. Front. Physiol. 7, 623. doi:10.3389/FPHYS.2016.00623

Lewis, P., Sheehan, D., O'Halloran, K., 2014. Chronic sustained hypoxia induces temporal redox and metabolic remodelling and atrophy signalling in mouse diaphragm muscle. Proc. Physiol. Soc.

Lewis, P., Sheehan, D., Soares, R., Coelho, A.V., O'Halloran, K.D., 2016. Redox Remodeling Is Pivotal in Murine Diaphragm Muscle Adaptation to Chronic Sustained Hypoxia. Am. J. Respir. Cell Mol. Biol. 55, 12–23. doi:10.1165/rcmb.2015-0272OC

Lewis, P., Sheehan, D., Soares, R., Coelho, A.V., O'Halloran, K.D., 2015b. Redox Remodelling is Pivotal in Murine Diaphragm Muscle Adaptation to Chronic Sustained Hypoxia. Am. J. Respir. Cell Mol. Biol. doi:10.1165/rcmb.2015-0272OC

Lewis, P., Sheehan, D., Soares, R., Varela Coelho, A., O'Halloran, K.D., 2015c. Chronic sustained hypoxia-induced redox remodeling causes contractile dysfunction in mouse sternohyoid muscle. Front. Physiol. 6, 122. doi:10.3389/fphys.2015.00122

Lewis, P., Sheehan, D., Soares, R., Varela Coelho, A., O'Halloran, K.D., 2015d. Chronic sustained hypoxia-induced redox remodeling causes contractile dysfunction in mouse sternohyoid muscle. Front. Physiol. 6, 122. doi:10.3389/fphys.2015.00122

Liang, H., Ward, W.F., 2006. PGC-1alpha: a key regulator of energy metabolism. Adv. Physiol. Educ. 30, 145–51. doi:10.1152/advan.00052.2006

Lundby, C., Calbet, J. a L., Robach, P., 2009. The response of human skeletal muscle tissue to hypoxia. Cell. Mol. Life Sci. 66, 3615–23. doi:10.1007/s00018-009-0146-8

M. J. Tobin, A. Jubran, F.L., 1998. Respiratory Muscle Fatigue and Weaning, in: Acute Lung Injury. Springer Berlin Heidelberg. doi:10.1016/B978-0-7216-8706-3.50014-1

Mador, M.J., Bozkanat, E., 2001. Skeletal muscle dysfunction in chronic obstructive pulmonary disease. Respir. Res. 2, 216–224.

Magalhães, J., Ascensão, A., Soares, J.M.C., Ferreira, R., Neuparth, M.J., Marques, F., Duarte, J.A., 2005. Acute and severe hypobaric hypoxia increases oxidative stress and impairs mitochondrial function in mouse skeletal muscle. J. Appl. Physiol. 99, 1247–53. doi:10.1152/japplphysiol.01324.2004

Mammucari, C., Milan, G., Romanello, V., Masiero, E., Rudolf, R., Del Piccolo, P., Burden, S.J., Di Lisi, R., Sandri, C., Zhao, J., Goldberg, A.L., Schiaffino, S., Sandri, M., 2007. FoxO3 Controls Autophagy in Skeletal Muscle In Vivo. Cell Metab. 6, 458–471. doi:10.1016/j.cmet.2007.11.001

Martin, U.J., Hincapie, L., Nimchuk, M., Gaughan, J., Criner, G.J., 2005. Impact of whole-body rehabilitation in patients receiving chronic mechanical ventilation. Crit. Care Med. 33, 2259–2265. doi:10.1097/01.CCM.0000181730.02238.9B

Marvyn, P.M., Bradley, R.M., Mardian, E.B., Marks, K.A., Duncan, R.E., 2016. Data on oxygen consumption rate, respiratory exchange ratio, and movement in C57BL/6J female mice on the third day of consuming a high-fat diet. Data Br. 7, 472–475. doi:10.1016/j.dib.2016.02.066

Matthay, M.A., Zimmerman, G.A., Esmon, C., Bhattacharya, J., Coller, B., Doerschuk, C.M., Floros, J., Gimbrone, M.A., Hoffman, E., Hubmayr, R.D., Leppert, M., Matalon, S., Munford, R., Parsons, P., Slutsky, A.S., Tracey, K.J., Ward, P., Gail, D.B., Harabin, A.L., 2003. Future research directions in acute lung injury: summary of a National Heart, Lung, and Blood Institute working group. Am. J. Respir. Crit. Care Med. 167, 1027–35. doi:10.1164/rccm.200208-966WS

McClung, J.M., Whidden, M.A., Kavazis, A.N., Falk, D.J., Deruisseau, K.C., Powers, S.K., 2008. Redox regulation of diaphragm proteolysis during mechanical ventilation. Am. J. Physiol. Regul. Integr. Comp. Physiol. 294, R1608-17. doi:10.1152/ajpregu.00044.2008

McGuire, M., MacDermott, M., Bradford, A., 2002. The effects of chronic episodic hypercapnic hypoxia on rat upper airway muscle contractile properties and fiber-type distribution. Chest 122, 1400–1406. doi:10.1378/chest.122.4.1400

McLellan, S.A., Walsh, T.S., 2004. Oxygen delivery and haemoglobin. Contin. Educ. Anaesthesia, Crit. Care Pain 4, 123–126. doi:10.1093/bjaceaccp/mkh033

McMorrow, C., Fredsted, A., Carberry, J., O'Connell, R. a., Bradford, A., Jones, J.F.X., O'Halloran, K.D., 2011. Chronic hypoxia increases rat diaphragm muscle endurance and sodium-potassium ATPase pump content. Eur. Respir. J. 37, 1474–1481. doi:10.1183/09031936.00079810

Milan, G., Romanello, V., Pescatore, F., Armani, A., Paik, J.-H., Frasson, L., Seydel, A., Zhao, J., Abraham, R., Goldberg, A.L., Blaauw, B., DePinho, R.A., Sandri, M., 2015a. Regulation of autophagy and the ubiquitin-proteasome system by the FoxO transcriptional network during muscle atrophy. Nat. Commun. 6, 6670. doi:10.1038/ncomms7670

Milan, G., Romanello, V., Pescatore, F., Armani, A., Paik, J.-H., Frasson, L., Seydel, A., Zhao, J., Abraham, R., Goldberg, A.L., Blaauw, B., DePinho, R.A., Sandri, M., 2015b. Regulation of autophagy and the ubiquitin-proteasome system by the FoxO transcriptional network during muscle atrophy. Nat. Commun. 6, 6670. doi:10.1038/ncomms7670

Mourkioti, F., Rosenthal, N., 2008. NF-kappaB signaling in skeletal muscle: prospects for intervention in muscle diseases. J. Mol. Med. (Berl). 86, 747–59. doi:10.1007/s00109-008-0308-4

Mrozek, S., Jung, B., Petrof, B.J., Pauly, M., Roberge, S., Lacampagne, A., Cassan, C., Thireau, J., Molinari, N., Futier, E., Scheuermann, V., Constantin, J.M., Matecki, S., Jaber, S., 2012. Rapid onset of specific diaphragm weakness in a healthy murine model of ventilator-induced diaphragmatic dysfunction. Anesthesiology 117, 560–7. doi:10.1097/ALN.0b013e318261e7f8

Muller, F.L., Song, W., Jang, Y.C., Liu, Y., Sabia, M., Richardson, A., Van Remmen, H., 2007. Denervation-induced skeletal muscle atrophy is associated with increased mitochondrial ROS production. Am. J. Physiol. Regul. Integr. Comp. Physiol. 293, R1159–R1168. doi:10.1152/ajpregu.00767.2006

Murphy, M.P., 2009. How mitochondria produce reactive oxygen species. Biochem. J. 417, 1–13. doi:10.1042/BJ20081386

Murray, A.J., 2009. Metabolic adaptation of skeletal muscle to high altitude hypoxia: how new technologies could resolve the controversies. Genome Med. 1(12), 117. doi: 10.1186/gm117.

Nanduri, J., Yuan, G., Kumar, G.K., Semenza, G.L., Prabhakar, N.R., 2008. Transcriptional responses to intermittent hypoxia. Respir. Physiol. Neurobiol. 164, 277–281. doi:10.1016/j.resp.2008.07.006

Neary, M.T., Breckenridge, R.A., 2013. Hypoxia at the heart of sudden infant death syndrome? Pediatr. Res. 74, 375–9. doi:10.1038/pr.2013.122

Nguyen, T., Rubinstein, N.A., Vijayasarathy, C., Rome, L.C., Kaiser, L.R., Shrager, J.B., Levine, S., 2005. Effect of chronic obstructive pulmonary disease on calcium pump ATPase expression in human diaphragm. J. Appl. Physiol. 98, 2004–10. doi:10.1152/japplphysiol.00767.2004

Niecknig, H., Tug, S., Reyes, B.D., Kirsch, M., Fandrey, J., Berchner-Pfannschmidt, U., 2012. Role of reactive oxygen species in the regulation of HIF-1 by prolyl hydroxylase 2 under mild hypoxia. Free Radic. Res. 46, 705–717. doi:10.3109/10715762.2012.669041

Nikinmaa, M., Pursiheimo, S., Soitamo, A.J., 2004. Redox state regulates HIF-1alpha and its DNA binding and phosphorylation in salmonid cells. J. Cell Sci. 117, 3201–3206. doi:10.1242/jcs.01192

O'Hagan, K.A., Cocchiglia, S., Zhdanov, A. V, Tambuwala, M.M., Tambawala, M.M., Cummins, E.P., Monfared, M., Agbor, T.A., Garvey, J.F., Papkovsky, D.B., Taylor, C.T., Allan, B.B., 2009. PGC-1alpha is coupled to HIF-1alpha-dependent gene expression by increasing mitochondrial oxygen consumption in skeletal muscle cells. Proc. Natl. Acad. Sci. U. S. A. 106, 2188–93. doi:10.1073/pnas.0808801106

O'Halloran, K.D., 2016. Chronic intermittent hypoxia creates the perfect storm with

calamitous consequences for respiratory control. Respir. Physiol. Neurobiol. 226, 63–67. doi:10.1016/j.resp.2015.10.013

O'Halloran, K.D., McGuire, M., O'Hare, T., Bradford, A., 2002. Chronic intermittent asphyxia impairs rat upper airway muscle responses to acute hypoxia and asphyxia. Chest 122, 269–275. doi:10.1378/chest.122.1.269

O'Halloran, K.D., McGuire, M., O'Hare, T., MacDermott, M., Bradford, a., 2003. Upper airway EMG responses to acute hypoxia and asphyxia are impaired in streptozotocin-induced diabetic rats. Respir. Physiol. Neurobiol. 138, 301–308. doi:10.1016/j.resp.2003.09.001

O 'Halloran, K.D., Lewis, P., Mcdonald, F., 2016. Title: Sex, stress and sleep apnoea: Decreased susceptibility to upper airway muscle dysfunction following intermittent hypoxia in females. Respir. Physiol. Neurobiol. doi:10.1016/j.resp.2016.11.009

Ohtsuji, M., Katsuoka, F., Kobayashi, A., Aburatani, H., Hayes, J.D., Yamamoto, M., 2008. Nrf1 and Nrf2 play distinct roles in activation of antioxidant response element-dependent genes. J. Biol. Chem. 283, 33554–33562. doi:10.1074/jbc.M804597200

Ottenheijm, C. a C., Heunks, L.M. a, Dekhuijzen, R.P.N., 2008. Diaphragm adaptations in patients with COPD. Respir. Res. 9, 12. doi:10.1186/1465-9921-9-12

Palma, S. De, Ripamonti, M., 2007. Metabolic modulation induced by chronic hypoxia in rats using a comparative proteomic analysis of skeletal muscle tissue. J. proteome … 1974–1984.

Palmer, L.A., May, W.J., deRonde, K., Brown-Steinke, K., Gaston, B., Lewis, S.J., 2013. Hypoxia-induced ventilatory responses in conscious mice: gender differences in ventilatory roll-off and facilitation. Respir. Physiol. Neurobiol. 185, 497–505. doi:10.1016/j.resp.2012.11.010

Parekh, D., Dancer, R.C., Thickett, D.R., 2011. Acute lung injury. Clin. Med. (Northfield. Il). 11, 615–618. doi:10.7861/clinmedicine.11-6-615

Peng, Y.-J., Nanduri, J., Khan, S.A., Yuan, G., Wang, N., Kinsman, B., Vaddi, D.R., Kumar, G.K., Garcia, J.A., Semenza, G.L., Prabhakar, N.R., 2011. Hypoxia-inducible factor 2α (HIF-2α) heterozygous-null mice exhibit exaggerated carotid body sensitivity to hypoxia, breathing instability, and hypertension. Proc. Natl. Acad. Sci. U. S. A. 108, 3065–3070. doi:10.1073/pnas.1100064108

Pengelly, L.D., Alderson, A.M., Milic-Emili, J., 1971. Mechanics of the diaphragm. J. Appl. Physiol. 30, 797–805.

Petrof, B.J., Hussain, S.N., 2016. Ventilator-induced diaphragmatic dysfunction: what have we learned? Curr. Opin. Crit. Care 22, 67–72. doi:10.1097/MCC.0000000000000272

Petrof, B.J., Jaber, S., Matecki, S., 2010. Ventilator-induced diaphragmatic dysfunction. Curr. Opin. Crit. Care 16, 19–25. doi:10.1097/MCC.0b013e328334b166

Pette, D., Staron, R.S., 1997. Mammalian skeletal muscle fiber type transitions. Int. Rev. Cytol. 170, 143–223.

Piantadosi, C.A., Carraway, M.S., Babiker, A., Suliman, H.B., 2008. Heme oxygenase-1 regulates cardiac mitochondrial biogenesis via nrf2-mediated transcriptional control of nuclear respiratory factor-1. Circ. Res. 103, 1232–1240. doi:10.1161/01.RES.0000338597.71702.ad

Picard, M., Azuelos, I., Jung, B., Giordano, C., Matecki, S., Hussain, S., White, K., Li, T., Liang, F., Benedetti, A., Gentil, B.J., Burelle, Y., Petrof, B.J., 2015. Mechanical ventilation triggers abnormal mitochondrial dynamics and morphology in the diaphragm. J. Appl. Physiol. 118, 1161–71. doi:10.1152/japplphysiol.00873.2014

Pisani, D.F., Dechesne, C.A., 2005. Skeletal muscle HIF-1alpha expression is dependent on muscle fiber type. J. Gen. Physiol. 126, 173–8. doi:10.1085/jgp.200509265

Plant, D., Gregorevic, P., 2001. Redox modulation of maximum force production of fast- and slow-twitch skeletal muscles of rats and mice. J. Appl. … 832–838.

Polkey, M.I., Kyroussis, D., Hamnegard, C.H., Mills, G.H., Green, M., Moxham, J., 1996. Diaphragm strength in chronic obstructive pulmonary disease. Am. J. Respir. Crit. Care Med. 154, 1310–7. doi:10.1164/ajrccm.154.5.8912741

Powell, F.., Milsom, W.., Mitchell, G.., 1998. Time domains of the hypoxic ventilatory response. Respir. Physiol. 112, 123–134. doi:10.1016/S0034-5687(98)00026-7

Powers, J., 2007. The five P's spell positive outcomes for ARDS patients [WWW Document]. Am. Nurse Today. URL https://www.americannursetoday.com/the-five-ps-spell-positive-outcomes-for-ards-patients/

Powers, S.K., Hudson, M.B., Nelson, W.B., Talbert, E.E., Min, K., Szeto, H.H., Kavazis, A.N., Smuder, A.J., 2011. Mitochondria-targeted antioxidants protect against mechanical ventilation-induced diaphragm weakness. Crit. Care Med. 39, 1749–59. doi:10.1097/CCM.0b013e3182190b62

Powers, S.K., Kavazis, A.N., Levine, S., 2009. Prolonged mechanical ventilation alters diaphragmatic structure and function. Crit. Care Med. 37, S347-53. doi:10.1097/CCM.0b013e3181b6e760

Powers, S.K., Wiggs, M.P., Sollanek, K.J., Smuder, A.J., 2013. Ventilator-induced diaphragm dysfunction: cause and effect. Am. J. Physiol. Regul. Integr. Comp. Physiol. 305, R464-77. doi:10.1152/ajpregu.00231.2013

Prabhakar, N.R., Kumar, G.K., Nanduri, J., 2009. Intermittent hypoxia-mediated

plasticity of acute O2 sensing requires altered red-ox regulation by HIF-1 and HIF-2, in: Annals of the New York Academy of Sciences. pp. 162–168. doi:10.1111/j.1749-6632.2009.05034.x

Prabhakar, N.R., Semenza, G.L., 2012. Adaptive and maladaptive cardiorespiratory responses to continuous and intermittent hypoxia mediated by hypoxia-inducible factors 1 and 2. Physiol. Rev. 92, 967–1003. doi:10.1152/physrev.00030.2011

Quadrilatero, J., Hoffman-Goetz, L., 2005. N-acetyl-L-cysteine inhibits exercise-induced lymphocyte apoptotic protein alterations. Med. Sci. Sports Exerc. 37, 53–56. doi:10.1249/01.MSS.0000149809.95484.3D

Quadrilatero, J., Hoffman-Goetz, L., 2004. N-Acetyl-L-cysteine prevents exercise-induced intestinal lymphocyte apoptosis by maintaining intracellular glutathione levels and reducing mitochondrial membrane depolarization. Biochem. Biophys. Res. Commun. 319, 894–901. doi:10.1016/j.bbrc.2004.05.068

Ramirez, J.-M., Folkow, L.P., Blix, A.S., 2007. Hypoxia tolerance in mammals and birds: from the wilderness to the clinic. Annu. Rev. Physiol. 69, 113–43. doi:10.1146/annurev.physiol.69.031905.163111

Ranatunga, K.W., Wylie, S.R., 1983. Temperature-dependent transitions in isometric contractions of rat muscle. J. Physiol. 339, 87–95.

Ranieri, V.M., Suter, P.M., Tortorella, C., De Tullio, R., Dayer, J.M., Brienza, A., Bruno, F., Slutsky, A.S., 1999. Effect of Mechanical Ventilation on Inflammatory Mediators in Patients With Acute Respiratory Distress Syndrome. JAMA 282, 54. doi:10.1001/jama.282.1.54

Rasbach, K.A., Gupta, R.K., Ruas, J.L., Wu, J., Naseri, E., Estall, J.L., Spiegelman, B.M., 2010. PGC-1alpha regulates a HIF2alpha-dependent switch in skeletal muscle fiber types. Proc. Natl. Acad. Sci. U. S. A. 107, 21866–21871. doi:10.1073/pnas.1016089107

Reid, M.B., Stokić, D.S., Koch, S.M., Khawli, F.A., Leis, A.A., 1994. N-acetylcysteine inhibits muscle fatigue in humans. J. Clin. Invest. 94, 2468–2474. doi:10.1172/JCI117615

Rello, J., Lisboa, T., Koulenti, D., 2014. Respiratory infections in patients undergoing mechanical ventilation. Lancet. Respir. Med. 2, 764–74. doi:10.1016/S2213-2600(14)70171-7

Rius, J., Guma, M., Schachtrup, C., Akassoglou, K., Zinkernagel, A.S., Nizet, V., Johnson, R.S., Haddad, G.G., Karin, M., 2008. NF-kappaB links innate immunity to the hypoxic response through transcriptional regulation of HIF-1alpha. Nature 453, 807–11. doi:10.1038/nature06905

Rommel, C., Bodine, S.C., Clarke, B.A., Rossman, R., Nunez, L., Stitt, T.N., Yancopoulos, G.D., Glass, D.J., 2001. Mediation of IGF-1-induced skeletal myotube hypertrophy by PI(3)K/Akt/mTOR and PI(3)K/Akt/GSK3 pathways. Nat. Cell Biol. 3, 1009–1013. doi:10.1038/ncb1101-1009

Roseguini, B.T., Silva, L.M., Polotow, T.G., Barros, M.P., Souccar, C., Han, S.W., 2015. Effects of N-acetylcysteine on skeletal muscle structure and function in a mouse model of peripheral arterial insufficiency, in: Journal of Vascular Surgery. pp. 777–786. doi:10.1016/j.jvs.2013.10.098

Roux, P.P., Blenis, J., 2004. ERK and p38 MAPK-Activated Protein Kinases: a Family of Protein Kinases with Diverse Biological Functions. Microbiol. Mol. Biol. Rev. 68, 320–344. doi:10.1128/mmbr.68.2.320-344.2004

Rowley, K.L., Mantilla, C.B., Sieck, G.C., 2005. Respiratory muscle plasticity. Respir. Physiol. Neurobiol. 147, 235–51. doi:10.1016/j.resp.2005.03.003

Rubenfeld, G.D., Herridge, M.S., 2007. Epidemiology and outcomes of acute lung injury. Chest 131, 554–62. doi:10.1378/chest.06-1976

Sacchetto, R., Turcato, F., Damiani, E., Margreth, A., 1999. Interaction of triadin with

histidine-rich Ca(2+)-binding protein at the triadic junction in skeletal muscle fibers. J. Muscle Res. Cell Motil. 20, 403–15.

Safar, P., 1969. Recognition and Management of Airway Obstruction. JAMA J. Am. Med. Assoc. 208, 1008. doi:10.1001/jama.1969.03160060078010

Safdar, A., Little, J.P., Stokl, A.J., Hettinga, B.P., Akhtar, M., Tarnopolsky, M.A., 2011. Exercise increases mitochondrial PGC-1α content and promotes nuclear-mitochondrial cross-talk to coordinate mitochondrial biogenesis. J. Biol. Chem. 286, 10605–10617. doi:10.1074/jbc.M110.211466

Saguil, A., Fargo, M., 2012. Acute respiratory distress syndrome: diagnosis and management. Am. Fam. Physician 85, 352–8.

Saito, T., Sadoshima, J., 2016. The Molecular Mechanisms of Mitochondrial Autophagy/ Mitophagy in the Heart. Circ. Res. 116, 1477–1490. doi:10.1161/CIRCRESAHA.116.303790.The

Salman, D., Finney, S.J., Griffiths, M.J.D., 2013. Strategies to reduce ventilator-associated lung injury (VALI). Burns 39, 200–11. doi:10.1016/j.burns.2012.10.013

Sanchez, A.M.J., Candau, R.B., Bernardi, H., 2014. FoxO transcription factors: Their roles in the maintenance of skeletal muscle homeostasis. Cell. Mol. Life Sci. doi:10.1007/s00018-013-1513-z

Sandow, A., 1952. Excitation-contraction coupling in muscular response. Yale J. Biol. Med. 25, 176–201.

Sandri, M., Sandri, C., Gilbert, A., Skurk, C., Calabria, E., Picard, A., Walsh, K., Schiaffino, S., Lecker, S.H., Goldberg, A.L., 2004. Foxo transcription factors induce the atrophy-related ubiquitin ligase atrogin-1 and cause skeletal muscle atrophy. Cell 117, 399–412. doi:10.1016/S0092-8674(04)00400-3

Sang, N., Stiehl, D.P., Bohensky, J., Leshchinsky, I., Srinivas, V., Caro, J., 2003. MAPK signaling up-regulates the activity of hypoxia-inducible factors by its effects on p300. J. Biol. Chem. 278, 14013–14019. doi:10.1074/jbc.M209702200

Sastre, J., Pallardó, F. V., Viña, J., 2003. The role of mitochondrial oxidative stress in aging. Free Radic. Biol. Med. doi:10.1016/S0891-5849(03)00184-9

Sceneay, J., Liu, M.C.P., Chen, A., Wong, C.S.F., Bowtell, D.D.L., Möller, A., 2013. The Antioxidant N-Acetylcysteine Prevents HIF-1 Stabilization under Hypoxia In Vitro but Does Not Affect Tumorigenesis in Multiple Breast Cancer Models In Vivo. PLoS One 8, e66388. doi:10.1371/journal.pone.0066388

Schaible, B., Schaffer, K., Taylor, C.T., 2010. Hypoxia, innate immunity and infection in the lung. Respir. Physiol. Neurobiol. doi:10.1016/j.resp.2010.08.006

Schiaffino, S., Gorza, L., Sartore, S., Saggin, L., Ausoni, S., Vianello, M., Gundersen, K., LØmo, T., 1989. Three myosin heavy chain isoforms in type 2 skeletal muscle fibres. J. Muscle Res. Cell Motil. 10, 197–205. doi:10.1007/BF01739810

Schiaffino, S., Reggiani, C., 2011. Fiber types in mammalian skeletal muscles. Physiol. Rev. 91, 1447–531. doi:10.1152/physrev.00031.2010

Schieber, M., Chandel, N.S., 2014. ROS function in redox signaling and oxidative stress. Curr. Biol. doi:10.1016/j.cub.2014.03.034

Schwartz, D.R., Malhotra, A., Fink, M.P., 1998. Cytopathic Hypoxia in Sepsis : An Overview. Sepsis 2, 279–289. doi:10.1023/A:1009830318674

Semenza, G.L., 2004. Hydroxylation of HIF-1: oxygen sensing at the molecular level. Physiology (Bethesda). 19, 176–182. doi:10.1152/physiol.00001.2004

Semenza, G.L., Roth, P.H., Fang, H.M., Wang, G.L., 1994. Transcriptional regulation of genes encoding glycolytic enzymes by hypoxia-inducible factor 1. J. Biol.

Chem. 269, 23757–63.

Serpa Neto, A., Filho, R.R., Rocha, L.L., Schultz, M.J., 2014. Recent advances in mechanical ventilation in patients without acute respiratory distress syndrome. F1000Prime Rep. 6, 115. doi:10.12703/P6-115

Severinghaus, J.W., 2016. HIGH LIFE: High altitude fatalities led to pulse oximetry. J. Appl. Physiol. 120, 236–43. doi:10.1152/japplphysiol.00476.2015

Shchedrina, V.A., Zhang, Y., Labunskyy, V.M., Hatfield, D.L., Gladyshev, V.N., 2010. Structure-function relations, physiological roles, and evolution of mammalian ER-resident selenoproteins. Antioxid. Redox Signal. 12, 839–849. doi:10.1089/ars.2009.2865

Shee, C.D., Cameron, I.R., 1990. The effect of pH and hypoxia on function and intracellular pH of the rat diaphragm. Respir. Physiol. 79, 57–68. doi:10.1016/0034-5687(90)90060-C

Shen, G., Li, X., Jia, Y., Piazza, G. a, Xi, Y., 2013. Hypoxia-regulated microRNAs in human cancer. Acta Pharmacol. Sin. 34, 336–41. doi:10.1038/aps.2012.195

Shindoh, C., DiMarco, A., Thomas, A., Manubay, P., Supinski, G., 1990. Effect of N-acetylcysteine on diaphragm fatigue. J Appl Physiol 68, 2107–2113.

Shortt, C.M., Fredsted, A., Chow, H.B., Williams, R., Skelly, J.R., Edge, D., Bradford, A., O'Halloran, K.D., 2014. Reactive oxygen species mediated diaphragm fatigue in a rat model of chronic intermittent hypoxia. Exp. Physiol. 99, 688–700. doi:10.1113/expphysiol.2013.076828

Sieck, G.C., 2015. Muscle weakness in critical illness. Am. J. Respir. Crit. Care Med. 191, 1094–6. doi:10.1164/rccm.201503-0478ED

Sieck, G.C., Mantilla, C.B., 2013. CrossTalk opposing view: The diaphragm muscle does not atrophy as a result of inactivity. J. Physiol. 591, 5259–62.

doi:10.1113/jphysiol.2013.254698

Siren, P.M.A., 2016. SIDS-CDF hypothesis revisited: explaining hypoxia in SIDS. Ups. J. Med. Sci. 121, 199–201. doi:10.1080/03009734.2016.1176972

Siren, P.M.A., Siren, M.J., 2011. Critical diaphragm failure in sudden infant death syndrome. Ups. J. Med. Sci. 116, 115–23. doi:10.3109/03009734.2010.548011

Skelly, J.R., Bradford, A., Jones, J.F.X., O'Halloran, K.D., 2010. Superoxide scavengers improve rat pharyngeal dilator muscle performance. Am. J. Respir. Cell Mol. Biol. 42, 725–31. doi:10.1165/rcmb.2009-0160OC

Skelly, J.R., Edge, D., Shortt, C.M., Jones, J.F.X., Bradford, A., O'Halloran, K.D., 2012a. Respiratory control and sternohyoid muscle structure and function in aged male rats: decreased susceptibility to chronic intermittent hypoxia. Respir. Physiol. Neurobiol. 180, 175–82. doi:10.1016/j.resp.2011.11.004

Skelly, J.R., Edge, D., Shortt, C.M., Jones, J.F.X., Bradford, A., O'Halloran, K.D., 2012b. Tempol ameliorates pharyngeal dilator muscle dysfunction in a rodent model of chronic intermittent hypoxia. Am. J. Respir. Cell Mol. Biol. 46, 139–48. doi:10.1165/rcmb.2011-0084OC

Skelly, J.R., Edge, D., Shortt, C.M., Jones, J.F.X., Bradford, A., O'Halloran, K.D., 2012c. Respiratory control and sternohyoid muscle structure and function in aged male rats: decreased susceptibility to chronic intermittent hypoxia. Respir. Physiol. Neurobiol. 180, 175–82. doi:10.1016/j.resp.2011.11.004

Skelly, J.R., O'Connell, R. a, Jones, J.F.X., O'Halloran, K.D., 2011. Structural and functional properties of an upper airway dilator muscle in aged obese male rats. Respiration. 82, 539–49. doi:10.1159/000332348

Skov, M., Pressler, T., Lykkesfeldt, J., Poulsen, H.E., Jensen, P.Ø., Johansen, H.K., Qvist, T., Kræmer, D., Høiby, N., Ciofu, O., 2015. The effect of short-term, high-dose oral N-acetylcysteine treatment on oxidative stress markers in cystic

fibrosis patients with chronic P. aeruginosa infection - A pilot study. J. Cyst. Fibros. 14, 211–218. doi:10.1016/j.jcf.2014.09.015

Smith, M. a, Reid, M.B., 2006. Redox modulation of contractile function in respiratory and limb skeletal muscle. Respir. Physiol. Neurobiol. 151, 229–41. doi:10.1016/j.resp.2005.12.011

Smuder, A.J., Hudson, M.B., Nelson, W.B., Kavazis, A.N., Powers, S.K., 2012. Nuclear factor-κB signaling contributes to mechanical ventilation-induced diaphragm weakness*. Crit. Care Med. 40, 927–34. doi:10.1097/CCM.0b013e3182374a84

Smuder, A.J., Sollanek, K.J., Min, K., Nelson, W.B., Powers, S.K., 2015. Inhibition of forkhead boxO-specific transcription prevents mechanical ventilation-induced diaphragm dysfunction. Crit. Care Med. 43, e133-42. doi:10.1097/CCM.0000000000000928

Soltan-Sharifi, M.S., Mojtahedzadeh, M., Najafi, A., Reza Khajavi, M., Reza Rouini, M., Moradi, M., Mohammadirad, A., Abdollahi, M., 2007. Improvement by N-acetylcysteine of acute respiratory distress syndrome through increasing intracellular glutathione, and extracellular thiol molecules and anti-oxidant power: evidence for underlying toxicological mechanisms. Hum. Exp. Toxicol. 26, 697–703. doi:10.1177/0960327107083452

Sonoda, J., Mehl, I.R., Chong, L.-W., Nofsinger, R.R., Evans, R.M., 2007. PGC-1beta controls mitochondrial metabolism to modulate circadian activity, adaptive thermogenesis, and hepatic steatosis. Proc. Natl. Acad. Sci. U. S. A. 104, 5223–5228. doi:10.1073/pnas.0611623104

Soukup, T., Zachařová, G., Smerdu, V., 2002. Fibre type composition of soleus and extensor digitorum longus muscles in normal female inbred Lewis rats. Acta Histochem. 104, 399–405. doi:10.1078/0065-1281-00660

Stegeman, H., Kaanders, J.H., Wheeler, D.L., van der Kogel, A.J., Verheijen, M.M.,

Waaijer, S.J., Iida, M., Grénman, R., Span, P.N., Bussink, J., 2012. Activation of AKT by hypoxia: a potential target for hypoxic tumors of the head and neck. BMC Cancer 12, 463. doi:10.1186/1471-2407-12-463

St-Pierre, J., Tattersall, G.J., Boutilier, R.G., 2000. Metabolic depression and enhanced O(2) affinity of mitochondria in hypoxic hypometabolism. Am. J. Physiol. Regul. Integr. Comp. Physiol. 279, R1205-14.

Supinski, G.S., Callahan, L.A., 2013. Diaphragm weakness in mechanically ventilated critically ill patients. Crit. Care 17, R120. doi:10.1186/cc12792

Supinski, G.S., Stofan, D., Ciufo, R., DiMarco, A., 1997. N-acetylcysteine administration alters the response to inspiratory loading in oxygen-supplemented rats. J Appl Physiol 82, 1119–1125. doi:10.1139/y91-043

Suter, P.M., Domenighetti, G., Schaller, M.-D., Laverrière, M.-C., Ritz, R., Perret, C., 1994. N-Acetylcysteine Enhances Recovery From Acute Lung Injury in Man. Chest 105, 190–194. doi:10.1378/chest.105.1.190

Tavi, P., Westerblad, H., 2011. The role of in vivo Ca^{2+} signals acting on Ca^{2+}-calmodulin-dependent proteins for skeletal muscle plasticity. J. Physiol. 589, 5021–31. doi:10.1113/jphysiol.2011.212860

Terada, L.S., Leff, J.A., Repine, E., 1990. Oxygen Radicals in Biological Systems Part B: Oxygen Radicals and Antioxidants, null, Methods in Enzymology. Elsevier. doi:10.1016/0076-6879(90)86161-N

Testelmans, D., Crul, T., Maes, K., Agten, a, Crombach, M., Decramer, M., Gayan-Ramirez, G., 2010. Atrophy and hypertrophy signalling in the diaphragm of patients with COPD. Eur. Respir. J. 35, 549–56. doi:10.1183/09031936.00091108

Thornton, T.M., Pedraza-Alva, G., Deng, B., Wood, C.D., Aronshtam, A., Clements, J.L., Sabio, G., Davis, R.J., Matthews, D.E., Doble, B., Rincon, M., 2008.

Phosphorylation by p38 MAPK as an alternative pathway for GSK3beta inactivation. Science 320, 667–70. doi:10.1126/science.1156037

Tobin, M.J., Laghi, F., Jubran, A., 1998. Respiratory muscle dysfunction in mechanically-ventilated patients. Mol. Cell. Biochem. doi:10.1023/A:1006807904036

Udobi, K.F., Childs, E., Touijer, K., 2003. Acute respiratory distress syndrome. Am. Fam. Physician 67, 315–22.

van boxel, G.I., Doherty, W.L., Parmar, M., 2012. Cellular oxygen utilization in health and sepsis. Contin. Educ. Anaesthesia, Crit. Care Pain 12, 207–212. doi:10.1093/bjaceaccp/mks023

van der Horst, A., Burgering, B.M.T., 2007. Stressing the role of FoxO proteins in lifespan and disease. Nat. Rev. Mol. Cell Biol. 8, 440–450. doi:10.1038/nrm2190

van Lunteren, E., Moyer, M., 2013. Gene expression of sternohyoid and diaphragm muscles in type 2 diabetic rats. BMC Endocr. Disord. 13, 43. doi:10.1186/1472-6823-13-43

van Lunteren, E., Spiegler, S., Moyer, M., 2010. Differential expression of lipid and carbohydrate metabolism genes in upper airway versus diaphragm muscle. Sleep 33, 363–70.

Varney, N.R., Ju, D., Shepherd, J.S., Kealey, G.P., 1998. Long-Term Neuropsychological Sequelae of Severe Burns. Arch. Clin. Neuropsychol. 13, 737–749. doi:10.1016/S0887-6177(98)00011-0

Vassilakopoulos, T., Zakynthinos, S., Roussos, C., 2006. Bench-to-bedside review: weaning failure--should we rest the respiratory muscles with controlled mechanical ventilation? Crit. Care 10, 204. doi:10.1186/cc3917

Verges, S., Bachasson, D., Wuyam, B., 2010. Effect of acute hypoxia on respiratory

muscle fatigue in healthy humans. Respir. Res. 11, 109. doi:10.1186/1465-9921-11-109

Víctor, V.M., Espulgues, J. V, Hernández-Mijares, A., Rocha, M., 2009. Oxidative stress and mitochondrial dysfunction in sepsis: a potential therapy with mitochondria-targeted antioxidants. Infect. Disord. Drug Targets 9, 376–89.

Vogt, M., Puntschart, A., Geiser, J., Zuleger, C., Billeter, R., Hoppeler, H., 2001. Molecular adaptations in human skeletal muscle to endurance training under simulated hypoxic conditions. J. Appl. Physiol. 91.

Volek, J.S., Kraemer, W.J., Rubin, M.R., Gómez, A.L., Ratamess, N. a, Gaynor, P., 2002. L-Carnitine L-tartrate supplementation favorably affects markers of recovery from exercise stress. Am. J. Physiol. Endocrinol. Metab. 282, E474-82. doi:10.1152/ajpendo.00277.2001

Vomhof-DeKrey, E.E., Picklo, M.J., 2012. The Nrf2-antioxidant response element pathway: A target for regulating energy metabolism. J. Nutr. Biochem. doi:10.1016/j.jnutbio.2012.03.005

Ward, J., 2006. Oxygen delivery and demand. Surgery. doi:10.1053/j.mpsur.2006.08.010

Watson, A.C., Hughes, P.D., Louise Harris, M., Hart, N., Ware, R.J., Wendon, J., Green, M., Moxham, J., 2001. Measurement of twitch transdiaphragmatic, esophageal, and endotracheal tube pressure with bilateral anterolateral magnetic phrenic nerve stimulation in patients in the intensive care unit. Critical Care Med. 9(7), 1325-31.

Wei, L., Gallant, E.M., Dulhunty, A.F., Beard, N.A., 2009. Junctin and triadin each activate skeletal ryanodine receptors but junctin alone mediates functional interactions with calsequestrin. Int. J. Biochem. Cell Biol. 41, 2214–2224. doi:10.1016/j.biocel.2009.04.017

West, J.B., Hackett, P.H., Maret, K.H., Milledge, J.S., Peters, R.M., Pizzo, C.J., Winslow, R.M., 1983. Pulmonary gas exchange on the summit of Mount Everest. J. Appl. Physiol. 55, 678–87.

Wheeler, A.P., Bernard, G.R., 1999. Treating patients with severe sepsis. N. Engl. J. Med. 340, 207–14. doi:10.1056/NEJM199901213400307

Wheeler, D.S., 2011. Oxidative Stress in Critically Ill Children with Sepsis. Open Inflamm. J. 4, 74–81. doi:10.2174/1875041901104010074

Williams, R.Ms., Lemaire, P.Bs., Lewis, P.P., McDonald, F.B.P., Lucking, E.P., Hogan, S.Bs., Sheehan, D.P., Healy, V.P., O'Halloran, K.D.P., 2015. Chronic Intermittent Hypoxia Increases Rat Sternohyoid Muscle NADPH Oxidase Expression with Attendant Modest Oxidative Stress. Front. Physiol. 6. doi:10.3389/fphys.2015.00015

Woods, S.J., Waite, A.A.C., O'Dea, K.P., Halford, P., Takata, M., Wilson, M.R., 2015. Kinetic profiling of in vivo lung cellular inflammatory responses to mechanical ventilation. Am. J. Physiol. Lung Cell. Mol. Physiol. 308, L912-21. doi:10.1152/ajplung.00048.2015

Wunsch, H., Linde-Zwirble, W.T., Angus, D.C., Hartman, M.E., Milbrandt, E.B., Kahn, J.M., 2010. The epidemiology of mechanical ventilation use in the United States. Crit. Care Med. 38, 1. doi:10.1097/CCM.0b013e3181ef4460

Yang, X.M., Wang, Y.S., Zhang, J., Li, Y., Xu, J.F., Zhu, J., Zhao, W., Chu, D.K., Wiedemann, P., 2009. Role of PI3K/Akt and MEK/ERK in mediating hypoxia-induced expression of HIF-1α and VEGF in laser-induced rat choroidal neovascularization. Investig. Ophthalmol. Vis. Sci. 50, 1873–1879. doi:10.1167/iovs.08-2591

Yoshida, M., Minamisawa, S., Shimura, M., Komazaki, S., Kume, H., Zhang, M., Matsumura, K., Nishi, M., Saito, M., Saeki, Y., Ishikawa, Y., Yanagisawa, T., Takeshima, H., 2005. Impaired Ca2+ store functions in skeletal and cardiac

muscle cells from sarcalumenin-deficient mice. J. Biol. Chem. 280, 3500–6. doi:10.1074/jbc.M406618200

Zanchi, N.E., Lancha, A.H., 2008. Mechanical stimuli of skeletal muscle: Implications on mTOR/p70s6k and protein synthesis. Eur. J. Appl. Physiol. doi:10.1007/s00421-007-0588-3

Zhang, Y.L., Dong, C., 2005. MAP kinases in immune responses. Cell Mol Immunol 2, 20–27.

Zhang, Z., Yan, J., Taheri, S., Liu, K.J., Shi, H., 2014. Hypoxia-inducible factor 1 contributes to N-acetylcysteine's protection in stroke. Free Radic. Biol. Med. 68, 8–21. doi:10.1016/j.freeradbiomed.2013.11.007

Zhou, M., Lin, B., 2000. UCP-3 expression in skeletal muscle: effects of exercise, hypoxia, and AMP-activated protein kinase. Am. J. ….

Zhou, M., Lin, B.-Z., Coughlin, S., Vallega, G., Pilch, P.F., 2000. UCP-3 expression in skeletal muscle: effects of exercise, hypoxia, and AMP-activated protein kinase. Am J Physiol Endocrinol Metab 279, E622-629.

Zolfaghari, P.S., Carré, J.E., Parker, N., Curtin, N.A., Duchen, M.R., Singer, M., 2015a. Skeletal muscle dysfunction is associated with derangements in mitochondrial bioenergetics (but not UCP3) in a rodent model of sepsis. Am. J. Physiol. Endocrinol. Metab. 308, E713-25. doi:10.1152/ajpendo.00562.2014

Zolfaghari, P.S., Carré, J.E., Parker, N., Curtin, N.A., Duchen, M.R., Singer, M., 2015b. Skeletal muscle dysfunction is associated with derangements in mitochondrial bioenergetics (but not UCP3) in a rodent model of sepsis. Am. J. Physiol. Endocrinol. Metab. 308, E713-25. doi:10.1152/ajpendo.00562.2014

Zorov, D.B., Juhaszova, M., Sollott, S.J., 2014. Mitochondrial Reactive Oxygen Species (ROS) and ROS-Induced ROS Release. Physiol. Rev. 94, 909–950. doi:10.1152/physrev.00026.2013